ABSTRACT

BUCKLING OF COMPOSITE CONICAL SHELLS UNDER COMBINED AXIAL COMPRESSION, EXTERNAL PRESSURE, AND BENDING

by
Youngjin Chung

Conical shells are extensively used in space crafts, robots, shelters, domes, tanks, and in machinery or devices (e.g. as Belleville washers). Thus, the design of minimum weight, maximum strength, stiffened conical (and cylindrical) shells under combined loads has long been of interest to designers. The objective of this study is to improve the strength of conical shells and reduce the weight of the structure. Buckling of composite conical shells subjected to combined axial loading, external pressure, and bending is investigated **using energy and finite element methods**. The conical shells have single and multiple layers, different cone angle, length, and radius. These parameters are considered to determine optimal condition against loads. It shall be demonstrated that these layers will improve buckling values of compression, external pressure, and bending of the composite shell. The applied loading is resisted primarily by in-plane stresses of the conical shell.

Donnell-type shell theory and Minimum Potential Energy Methods are presented for linear bending analysis of composite laminated conical shells with isotropic and orthotropic stretching-bending coupling under combined loading. The buckling equations for the shells are expressed in terms of displacements. The solution is developed in the form of a power series in terms of a particularly convenient coordinate system. The energy method is used to develop the recurrence relations to calculate coefficients of the series. A set of typical boundary conditions, thicknesses, the direction of layers axes of

orthotropy, number of them, the circumferential wave number, and different materials are considered to analyze the buckling.

The energy solution is extended to include the buckling of composite cones subjected to combined loads. This step shows clearly what type of load contributes more than other loads for buckling. The parameters for the cones are also investigated to find the interesting values for strong structures. Finite Element Analysis is extensively used to verify the results. The numerical solutions obtained are also compared with those of cylinders.

BUCKLING OF COMPOSITE CONICAL SHELLS UNDER COMBINED AXIAL COMPRESSION, EXTERNAL PRESSURE, AND BENDING

by
Youngjin Chung

A Dissertation
Submitted to the Faculty of
New Jersey Institute of Technology
in Partial Fulfillment of the Requirements for the Degree of
Doctor of Philosophy in Mechanical Engineering

Department of Mechanical Engineering

August 2001

APPROVAL PAGE

BUCKLING OF COMPOSITE CONICAL SHELLS UNDERCOMBINED AXIAL COMPRESSION, EXTERNAL PRESSURE, AND BENDING

Youngjin Chung

Dr. Ansel C. Ugural, Dissertation Advisor Research Professor of Mechanical Engineering, NJIT	Date
Dr. Bernard Koplik, Committee Member Professor of Mechanical Engineering, NJIT	Date
Dr. Rong-Yaw Chen, Committee Member Professor of Mechanical Engineering, NJIT	Date
Dr. Benedict C. Sun, Committee Member Associate Professor of Engineering Technology, NJIT	Date
Dr. C. T. Thomas Hsu, Committee Member Professor of Civil Engineering, NJIT	Date

BIOGRAPHICAL SKETCH

Author: Youngjin Chung

Degree: Doctor of Philosophy

Date: August, 2001

Undergraduate and Graduate Education:

- Doctor of Philosophy in Mechanical Engineering
  New Jersey Institute of Technology, Newark, NJ, USA, 2001

- Master of Science in Mechanical Engineering
  Fairleigh Dickinson University, Teaneck, NJ, USA, 1990

- Bachelor of Science in Mechanical Engineering
  Inha University, Inchun, Korea, 1985

Major: Mechanical Engineering

To my family who give me their love, courage and support

ACKNOWLEDGEMENT

I would like to express my appreciation and sincere gratitude to my research advisor, Dr. Ansel C. Ugural, for his valuable guidance, and counsel throughout this research.

I am very grateful to Dr. Rong-Yaw Chen for his good advice. I also express my special thanks to my committee Dr. Bernard Koplik, Dr. Rong-Yaw Chen, Dr. Benedict C. Sun, and Dr. C. T. Thomas Hsu for their suggestions to improve the dissertation. I am also thankful to the Mechanical Engineering Department, New Jersey Institute of Technology for providing me financial support during my Doctoral program.

I would especially like to thank my parents for their support all these years of my life. I also thank to my wife, Jungmi, for her patience, comfort and support.

Finally, I extend my thanks to God.

TABLE OF CONTENTS

TABLE OF CONTENTS
(Continued)

Chapter **page**

TABLE OF CONTENTS
(Continued)

Chapter **page**

TABLE OF CONTENTS
(Continued)

Chapter **page**

TABLE OF CONTENTS
(Continued)

Chapter **page**

TABLE OF CONTENTS
(Continued)

Chapter **page**

TABLE OF CONTENTS
(Continued)

Chapter **page**

LIST OF TABLES

Table **page**

LIST OF FIGURES

LIST OF FIGURES
(Continued)

Figure **page**

LIST OF FIGURES
(Continued)

Figure **page**

LIST OF FIGURES
(Continued)

Figure **page**

LIST OF FIGURES
(Continued)

Figure **page**

LIST OF SYMBOLS

a_m, b_m, c_m	coefficients in the power series
A_{ij}	stretching stiffness matrix
B_{ij}	stretching-bending coupling stiffness matrix
D_{ij}	bending stiffness matrix
$[Q_{ij}^*]_k$	lamina rigidity matrix in any θ direction of kth layer
E	modulus of elasticity
G	modulus of elasticity in shear
$G_{i,j}$	coefficients in the recurrence relations
h	laminate thickness
L	slant length of the cone
$L_{ij}, L_N, L_{ij}^*, L_N^*$	partial differential operator
m	terms of power series
M_a	bending moment load
$M_x, M_\phi, M_{x\phi}$	resultant moments
n	circumferential wave number
$\overline{N}$	number of arbitrarily oriented orthotropic layers
$N_{x0}, N_{\phi 0}$	membrane forces per unit width at critical state
$N_x, N_\phi, N_{x\phi}$	resultant forces
P, P_a, P_b	total axial load, axial compressive load, axial load from bending

LIST OF SYMBOLS
(Continued)

P_{cl}, P_{cr}	critical cone buckling load from classical and power series methods, respectively
q	external pressure
Q_x, Q_ϕ	transverse shear stress resultants
$R_1, R_2, R_0, R(x)$	radii of the cone at small end, large end, middle, arbitrary point x
U, V, W	displacement functions in the x, ϕ, z directions, respectively
u, v, w	displacements
U_b, U_m	bending strain energy and membrane strain energy, respectively
U_s, Ω	strain energy and potential energy, respectively
x	cone's generator coordinate
α	semivertex cone angle
$\gamma_{x\phi}$	shear strain in the $x\phi$ plane
$\varepsilon_x, \varepsilon_\phi$	normal strains in x, and ϕ directions
θ, ϕ	laminate orientation angle and cone's circumferential coordinate
$\kappa_x, \kappa_y, \kappa_{xy}$	curvatures of planes
$\chi_x, \chi_\phi, \chi_{x\phi}$	variation of curvatures
ν	Poisson's ratio
Π	total potential energy
σ_x, σ_ϕ	normal stresses on the x, and ϕ planes
$\sigma_{x\phi}$	shear stress on the x plane to the ϕ direction

CHAPTER 1

INTRODUCTION

1.1 Background and Outlines

The demands of conical shells used in space crafts, robots, shelters, domes, tanks, and in machinery or devices (Belleville washers) are extensive. Thus, the design of minimum weight, maximum strength, stiffened conical and cylindrical shells under combined load has long been of interest to designers. The advent of high strength, light weight, composite materials has resulted in broad use of multi-layered shells. Many distinctive researchers have improved the strength of the shells changing the thicknesses, the direction of layer axes of orthotropy, and number of them, or introducing fiber reinforcements. These changes improve the resistance of buckling, under bending and axial loads of the cone or cylinder.

The general case of buckling analysis of conical shells by the "equilibrium method" represents a very complicated mathematical problem [28]. Only a few solutions for simplified particular cases have been obtained. These involve considerable difficulty and subtlety. The energy methods are usually more efficient than the equilibrium approaches and lead to move accurate results [35].

In the following development, a procedure for buckling analysis of single layer isotropic, orthotropic and laminated shells under axial compression, external pressure, and bending is considered. For these shells, the combinations of the geometrical symmetry, length, thickness, and material property characteristics are important factors.

Energy method is used to develop the recurrence relations for pure bending and combined loads. The effects of boundary conditions and elastic coefficients on buckling of loads are studied. The procedure consists of the following steps:

1) The buckling equations for isotropic and orthotropic conical shells under combined loads are expressed in terms of displacements.
2) Item (1) is repeated for multilayered composite conical shells with more complicate form.
3) Displacements developed in series form. Then, governing equations for the cases described in item (1) and (2) are solved for the critical buckling loads of axial compression P_{cr}, outer pressure q_{cr}, and pure bending M_{cr} satisfying the set of boundary conditions.
4) Results of item (3) are extended to different thickness, different length, and different materials.
5) Results of combined analysis for pre-loading with axial compression, outer pressure, and pure bending.
6) An independent, extensive, Finite Element Analysis will be made to verify the results of item (3).
7) Results and conclusions.

1.2 Objective

To make strong structure with light weight material, thickness, material properties, the direction of material, and number of layers for composite structure are considered. The demands of conical shells show the importance of the applications, such as space ships,

connections with two different diameter cylinders, Belleville washers and even cola can (Appendix B.1). Those conical shells exposed to various loads. The loads are not single direction but multiple directions. To resist the multiple loads, combined loads analysis is necessary. Typical buckling loads are axial compression and outer pressure. The buckling loads of conical shell with pure bending is developed using minimum potential energy method and power series method [31]. This research is concentrated on the combination of loads and what combination is more effective with these combined loads.

CHAPTER 2

LITERATURE SURVEY

Donnell [9] shows a theory for the buckling of thin cylinder with moderately *large deformation*, which permits initial eccentricities or deviations *from cylindrical shape*. Donnell [10] and Timoshenko [28] also shows the range of the relation between the half wave length of the deflection and the radius. The stability of circular cylindrical shells under pure bending is investigated by Seide and Weingarten [25]. Analyses are presented for solving the buckling problems of laminated, with the linear problem of hetrogeneous anisotropic long cylindrical shells under axial compression and bending by Ugural [33, 36] and Flügge [11] derived nonuniform axial compression introducing dimensionless load parameters.

The buckling analysis of *conical shells* has been extensively studied by the areonautical industry. A simple formula was developed for the buckling of isotropic conical shells under axial compression for long cone of constant thickness compared with cylinder of equal thickness by Seide [23]. Seide [24] also made an attempt to prove the developed formula for the critical value of cylinder and cone. For orthotropic shells there have been fewer studies. By using the expressions for middle-surface displacement strain relations given by Seide [22], Singer [26] derived a set of equations for the buckling of orthotropic conical shells using the stress-strain relations for a homogeneous orthotropic material in generalized plane stress and four independent elastic constants. Baruch [5] explained the essential difference between cylinder and cone with boundary conditions.

Chang and Katz [7] studied buckling of axially compressed conical shells with proper boundary condition.

The derivation procedures of general shells are explained using minimum potential energy criterion by Brush [6]. An energy procedure in series form of a particularly convenient coordinate system was developed by Liyong Tong et al [31] for buckling analysis of isotropic conical shells. Liyong Tong and T. K. Wang [29, 32] developed a procedure for buckling analysis of laminated conical shells, with stretching-bending coupling, under axial compression and external pressure. And Liyong Tong et al [30] presented for bending analysis of orthotropic conical shells.

The *combined* loads, axial compression, external pressure, and pure bending of composite laminated conical shells, with which this thesis is concerned, may be practical importance. It appears that there is no significant publication in the literature which covers the buckling problem of laminated composite cones under axial compression, external pressure and pure bending or *nonuniform axial compression.*

CHAPTER 3

THEORY OF ORTHOTROPIC CONICAL SHELLS UNDER COMBINED LOADS

3.1 Introduction

The definition of buckling can be a sudden large, lateral deflection of a structure due to a small increase in an existing compression load [34]. To understand the conical shells, the theory of plates and shells is necessary. Plates and shells are initially flat and curved surface structures, respectively, where thicknesses are slight compared to their other dimensions. Shells are often defined as thin when the ratio of thickness h to radius curvature r is equal to or less than 1/20.

This work analyzes the buckling of orthotropic conical shells under axial compression, external pressure, and bending. The treatment is based upon Donnell-type 'shallow shell theory' (Appendix B.3) governing equations for conical shells. The parameters such as thickness, angle, radius of the cone, and material properties are considered to determine optimal condition against loads.

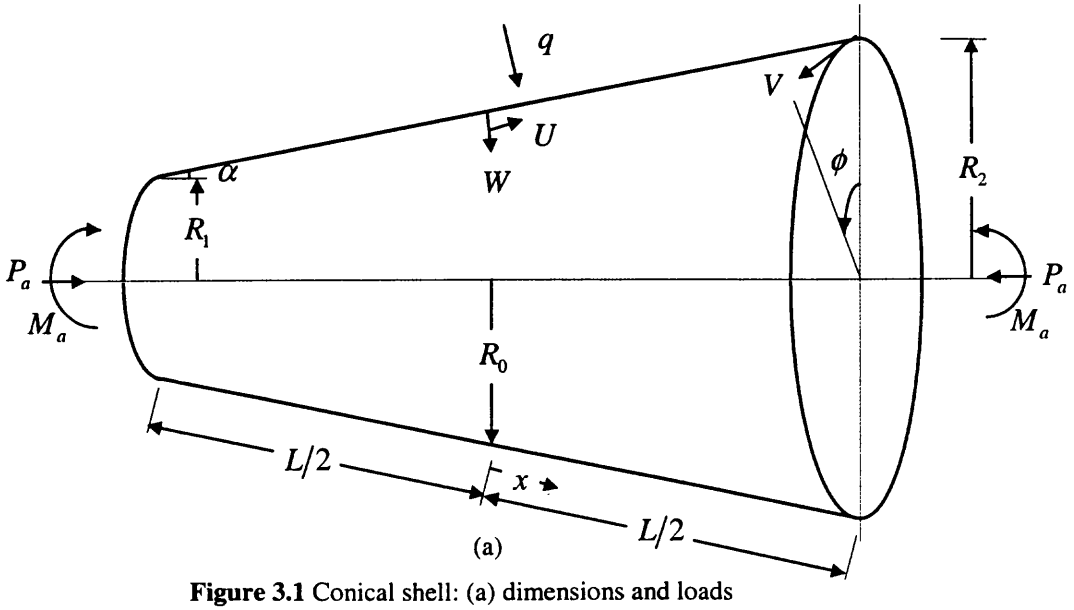

Figure 3.1 Conical shell: (a) dimensions and loads

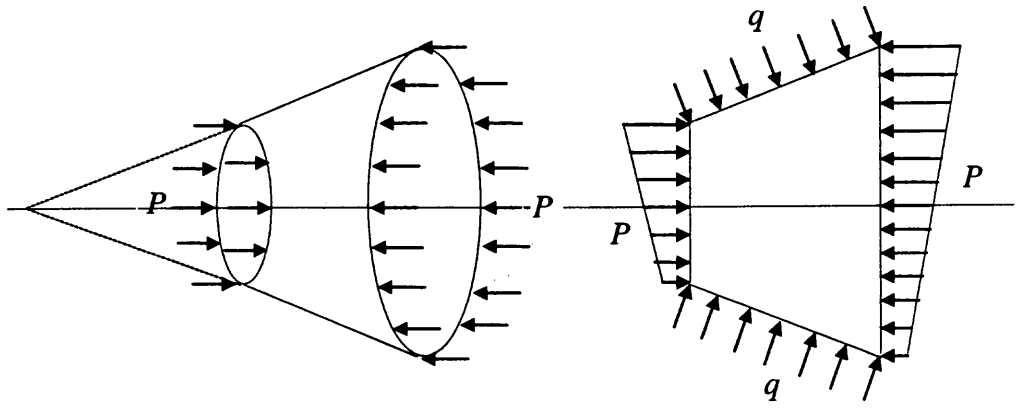

Figure 3.1 (Cont'd) Conical shell
(b) Uniform axial loading (c) Nonuniform axial loading and external pressure

The cone geometry, dimensions, and loading are in Figure 3.1 and force resultants [37] are in Figure 3.2.

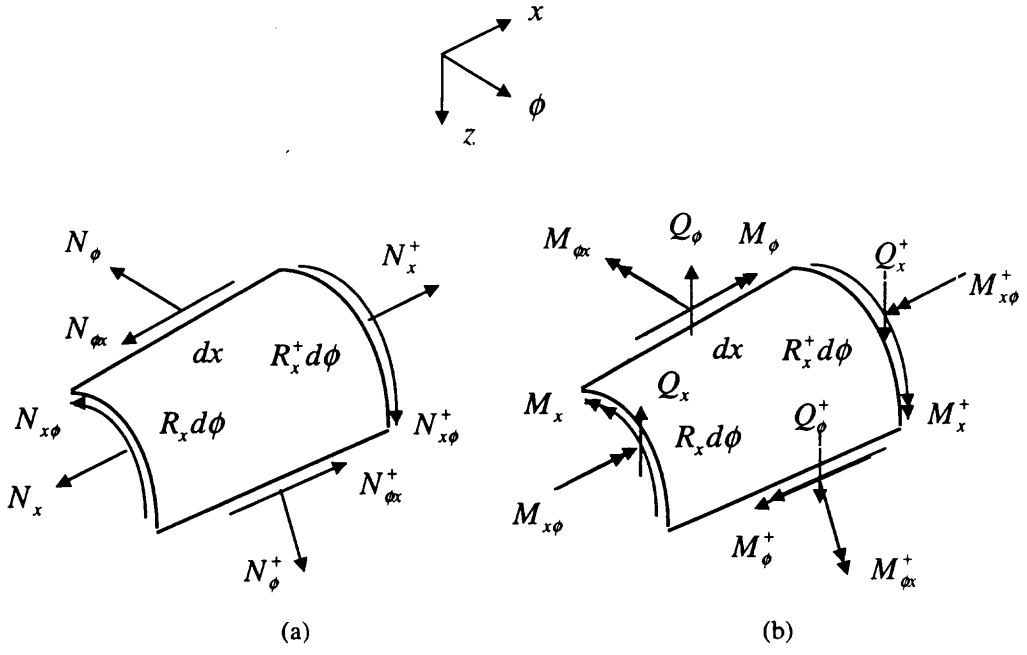

Figure 3.2 Shell elements: (a) under force resultants ;
(b) under moment and shear force resultants.

* The notation N_x^+ is employed to denote $N_x + (\partial N_x / \partial x)dx$ etc.

3.2 Strain - Displacement Relations

The radius of the conical shell at an arbitrary distance x, referring to Figure 3.1 may be conveniently expressed as follows

$$R(x) = R_0 + x\sin\alpha. \tag{3.1}$$

The strains and curvature changes in the middle surface of the conical shell are expressed as follows [32].

$$\begin{aligned}
\varepsilon_x &= \frac{\partial U}{\partial x} + \frac{1}{2}\left(\frac{\partial W}{\partial x}\right)^2 \\
\varepsilon_\phi &= \frac{U\sin\alpha - W\cos\alpha}{R(x)} + \frac{1}{R(x)}\frac{\partial V}{\partial \phi} + \frac{1}{2}\left(\frac{1}{R(x)}\frac{\partial W}{\partial \phi}\right)^2 \\
\gamma_{x\phi} &= 2\varepsilon_{x\phi} = \frac{1}{R(x)}\frac{\partial U}{\partial \phi} - \frac{V\sin\alpha}{R(x)} + \frac{\partial V}{\partial x} + \frac{1}{R(x)}\frac{\partial W}{\partial x}\frac{\partial W}{\partial \phi} \\
\chi_x &= -\frac{\partial^2 W}{\partial x^2} \\
\chi_\phi &= -\frac{\sin\alpha}{R(x)}\frac{\partial W}{\partial x} - \frac{1}{R^2(x)}\frac{\partial^2 W}{\partial \phi^2} \\
\chi_{x\phi} &= -\frac{\partial}{\partial x}\left(\frac{1}{R(x)}\frac{\partial W}{\partial \phi}\right)
\end{aligned} \tag{3.2a-f}$$

3.3 Stress Resultant - Strain Relations

Resultant force obtained by Hooke's Law for orthotropic layer is expressed $\{\sigma\} = [Q^*]\{\varepsilon\}$ and considering thickness $\{N\} = \{\sigma\} \cdot h$. More details are in chapter 4.

$$\begin{Bmatrix} N_x \\ N_\phi \\ N_{x\phi} \\ M_x \\ M_\phi \\ M_{x\phi} \end{Bmatrix} = \begin{bmatrix} A_{11} & A_{12} & 0 & 0 & 0 & 0 \\ A_{21} & A_{22} & 0 & 0 & 0 & 0 \\ 0 & 0 & A_{66} & 0 & 0 & 0 \\ 0 & 0 & 0 & D_{11} & D_{12} & 0 \\ 0 & 0 & 0 & D_{21} & D_{22} & 0 \\ 0 & 0 & 0 & 0 & 0 & D_{66} \end{bmatrix} \begin{Bmatrix} \varepsilon_x \\ \varepsilon_\phi \\ 2\varepsilon_{x\phi} \\ \chi_x \\ \chi_\phi \\ 2\chi_{x\phi} \end{Bmatrix} \tag{3.3}$$

The material rigidities A_{ij} and D_{ij} $(i, j = 1,2,6)$ for a typical orthotropic layer are calculated from the following equations:

$$
\begin{aligned}
A_{11} &= \frac{E_x h}{1 - \nu_{x\phi}\nu_{\phi x}}, \quad A_{12} = \frac{\nu_{\phi x} E_x h}{1 - \nu_{x\phi}\nu_{\phi x}} \\
A_{21} &= \frac{\nu_{x\phi} E_\phi h}{1 - \nu_{x\phi}\nu_{\phi x}}, \quad A_{22} = \frac{E_\phi h}{1 - \nu_{x\phi}\nu_{\phi x}}, \quad A_{66} = G_{x\phi} h \\
D_{11} &= \frac{E_x h^3}{12(1 - \nu_{x\phi}\nu_{\phi x})}, \quad D_{12} = \frac{\nu_{\phi x} E_x h^3}{12(1 - \nu_{x\phi}\nu_{\phi x})} \\
D_{21} &= \frac{\nu_{x\phi} E_\phi h^3}{12(1 - \nu_{x\phi}\nu_{\phi x})}, \quad D_{22} = \frac{E_\phi h^3}{12(1 - \nu_{x\phi}\nu_{\phi x})}, \quad D_{66} = \frac{G_{x\phi} h^3}{12}
\end{aligned}
\tag{3.4}
$$

where h is the thickness of the shell. If the layer is isotropic, $E_x = E_\phi = E$, $\nu_{x\phi} = \nu_{\phi x} = \nu$, and $\nu_{x\phi} E_\phi = \nu_{\phi x} E_x$.

The cone is subjected to an axially compressive load P_a per unit width, external pressure q, and bending moment load M_a. Let

$$N_x = P_a + P_b \cos\phi \tag{3.5}$$

It can be verified that [2 and 3] :

$$P_b = \sigma_b t = \frac{M_a c}{I} t = \frac{M_a R(x)}{\pi R^3(x) t} t = \frac{M_a}{\pi R^2(x)} \tag{3.6}$$

Under this loading, we have

$$N_{x0} = \frac{P + 2q\pi(R_0 + x\sin\alpha)x\sin\alpha}{2\pi R(x)\cos\alpha} + \frac{M_a}{\pi R^2(x)\cos\alpha}\cos\phi \tag{3.7}$$

$$N_{\phi 0} = \frac{qR(x)}{\cos\alpha} \tag{3.8}$$

where $N_{x0}, N_{\phi 0}$ are membrane forces per unit width at critical state [31].

3.4 Application of the Principle of Minimum Potential Energy

For linear buckling analysis of conical shells with isotropic and orthotropic single layer under axial compression and bending, adopting the **shallow shell theory** [10] of Donnell-type in Appendix B.3 and the **minimum total potential energy principle** [6] :

$$\frac{\partial N_x}{\partial x}+(N_x-N_\phi)\frac{\sin\alpha}{R(x)}+\frac{1}{R(x)}\frac{\partial N_{x\phi}}{\partial\phi}=0$$

$$\frac{\partial N_{x\phi}}{\partial x}+\frac{2\sin\alpha}{R(x)}N_{x\phi}+\frac{1}{R(x)}\frac{\partial N_\phi}{\partial\phi}=0 \qquad \text{(3.9a-c)}$$

$$\frac{\partial^2}{\partial x^2}[R(x)M_x]-\sin\alpha\frac{\partial M_\phi}{\partial x}+\frac{1}{R(x)}\frac{\partial^2 M_\phi}{\partial\phi^2}+\frac{2}{R(x)}\frac{\partial^2}{\partial x\partial\phi}[R(x)M_{x\phi}]$$
$$+\cos\alpha N_\phi+\frac{1}{R(x)}\frac{\partial}{\partial x}[N_{x0}R(x)\frac{\partial W}{\partial x}]+\frac{1}{R^2(x)}\frac{\partial}{\partial\phi}[N_{\phi 0}\frac{\partial W}{\partial\phi}]=0$$

In the foregoing equations, we have the potential energy function is $\Pi=U_s-\Omega$. Here U_s, and Ω represent the strain energy and work, respectively from Appendix A.

3.5 Governing Differential Equations

Let the differential operators $L_{ij}(i,j=1,2,3)$ and L_N are expressed using reference [31] given in the Appendix A (A.13-15). Substituting $N_x, N_\phi, N_{x\phi}, M_x, M_\phi,$ and $M_{x\phi}$ from Eq. (3.3) into Eq. (3.9a-c), we have

$$\begin{aligned} &L_{11}U+L_{12}V+L_{13}W=0\\ &L_{21}U+L_{22}V+L_{23}W=0\\ &L_{31}U+L_{32}V+L_{33}W+L_NW=0 \end{aligned} \qquad \text{(3.10a-c)}$$

The quantities $L_{11}, L_{12}, \cdots,$ are defined in Appendix A (A.16 through A.24)

3.6 Stress Resultant - Displacement Relations

We now substitute Eqs. (3.2) into (3.3) to obtain the force and moment stress resultants for an orthotropic conical shell. In so doing, we have

$$\begin{Bmatrix} N_x \\ N_\phi \\ N_{x\phi} \\ M_x \\ M_\phi \\ M_{x\phi} \end{Bmatrix} = \begin{bmatrix} l_{11} & l_{12} & l_{13} \\ l_{21} & l_{22} & l_{23} \\ l_{31} & l_{32} & 0 \\ 0 & 0 & l_{43} \\ 0 & 0 & l_{53} \\ 0 & 0 & l_{63} \end{bmatrix} \begin{Bmatrix} U \\ V \\ W \end{Bmatrix} \tag{3.11}$$

Here
$$l_{i1} = A_{i1}\frac{\partial}{\partial x} + \frac{A_{i2}\sin\alpha}{R(x)}, \quad l_{i2} = \frac{A_{i2}}{R(x)}\frac{\partial}{\partial\phi}, \quad l_{i3} = -\frac{A_{i2}\cos\alpha}{R(x)}$$
$$l_{31} = \frac{A_{66}}{R(x)}\frac{\partial}{\partial\phi}, \quad l_{32} = A_{66}\left(\frac{\partial}{\partial x} - \frac{\sin\alpha}{R(x)}\right) \tag{3.12}$$
$$l_{j3} = -D_{1i}\frac{\partial^2}{\partial x^2} - \frac{D_{i2}\sin\alpha}{R(x)}\frac{\partial}{\partial x} - \frac{D_{i2}}{R^2(x)}\frac{\partial^2}{\partial\phi^2}, \quad l_{63} = -\frac{D_{66}}{R(x)}\frac{\partial}{\partial x}\left(\frac{1}{R(x)}\frac{\partial}{\partial\phi}\right)$$

where $i = 1,2$ *and* $j = 3+i$.

The transverse shear force resultants are from Reference [31]

$$Q_x = \frac{1}{R(x)}\frac{\partial}{\partial x}[R(x)M_x] - \frac{M_\phi\sin\alpha}{R(x)} + \frac{1}{R(x)}\frac{\partial M_{x\phi}}{\partial\phi}$$
$$Q_\phi = \frac{1}{R(x)}\frac{\partial}{\partial x}[R(x)M_{x\phi}] + \frac{M_{x\phi}\sin\alpha}{R(x)} + \frac{1}{R(x)}\frac{\partial M_\phi}{\partial\phi}. \tag{3.13}$$

3.7 Boundary Conditions

For the conical shell loaded as shown in Figure 3.1, the conditions at ends $x = \pm L/2$ may be expressed as follows :

Case 1: **Simply-supported boundary conditions** at $x = \pm L/2$.

SS1: $N_{x\phi} = N_x = M_x = W = 0$
SS2: $N_{x\phi} = U = M_x = W = 0$

$$\text{SS3}: V = N_x = M_x = W = 0 \qquad (3.14)$$
$$\text{SS4}: V = U = M_x = W = 0$$

Case 2: **Clamped or built-in boundary conditions** at $x = \pm L/2$.

$$\text{CC1}: N_{x\phi} = N_x = \frac{\partial W}{\partial x} = W = 0$$
$$\text{CC2}: N_{x\phi} = U = \frac{\partial W}{\partial x} = W = 0$$
$$\text{CC3}: V = N_x = \frac{\partial W}{\partial x} = W = 0 \qquad (3.15)$$
$$\text{CC4}: V = U = \frac{\partial W}{\partial x} = W = 0$$

3.8 Special Cases of Orthotropic Conical Shells

Donnell-Type Governing Equation for orthotropic conical shells developed in Sec.3.5, degenerate to those of **cylindrical shells when** α is set equal to zero (Figure 3.3(a)). When α is 90^o (Figure 3.3(b)) the differential operators L_{13}, L_{23}, L_{31} and L_{32} approach zero and the three equilibrium equations become independent, that is the first two equations will then describe the in-plane problem and the third, the **buckling problem of circular plates** under axially symmetric in-plane loading.

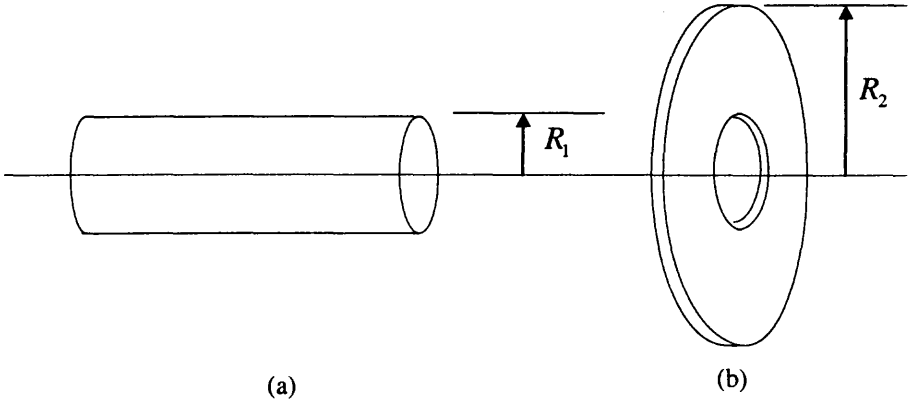

Figure 3.3 Special cases of composite conical shells (a) $\alpha = 0$ (b) $\alpha = \pi/2$

3.9 Modified Governing Differential Equations

To change equations more convenient form, multiply for the first two and the third of equations of Eqs. (3.10) by $R^2(x)$ and $R^4(x)$, respectively.

In so doing, we have

$$\begin{aligned} &L_{11}^* U + L_{12}^* V + L_{13}^* W = 0 \\ &L_{21}^* U + L_{22}^* V + L_{23}^* W = 0 \\ &L_{31}^* U + L_{32}^* V + L_{33}^* W + L_N^* W = 0 \end{aligned} \tag{3.16a-c}$$

Here

$$L_{11}^* = R^2(x)L_{11}, \cdots\cdots, L_{21}^* = R^2(x)L_{21}, \cdots\cdots, L_{31}^* = R^4(x)L_{31}, \cdots\cdots, \text{ and}$$
$$L_N^* = R^4(x)L_N^*$$

3.10 Displacement Functions for Axial and Outer Pressure Loading

We shell assume solutions of the following series :

$$U = u(x)\cos n\phi, \quad V = v(x)\sin n\phi, \quad W = w(x)\cos n\phi \tag{3.17}$$

where

$$u(x) = \sum_{m=0}^{\infty} a_m x^m, \quad v(x) = \sum_{m=0}^{\infty} b_m x^m, \quad w(x) = \sum_{m=0}^{\infty} c_m x^m \tag{3.18}$$

n is an integer representing the circumferential wave number of the buckled shell and m is the terms of power series.

Using Eq. (3.11), resultant forces and moments can be obtained to apply boundary conditions.

$$N_{x\phi} = -\frac{A_{66}n}{R(x)}\sum_{m=0}^{\infty} a_m x^m \sin n\phi + A_{66}\sum_{m=1}^{\infty} m b_m x^{m-1} \sin n\phi$$

$$- A_{66}\frac{\sin\alpha}{R(x)}\sum_{m=0}^{\infty} b_m x^m \sin n\phi$$

$$N_x = A_{11}\sum_{m=1}^{\infty} m a_m x^{m-1} \cos n\phi + A_{12}\frac{\sin\alpha}{R(x)}\sum_{m=0}^{\infty} a_m x^m \cos n\phi$$

$$+\frac{A_{12}n}{R(x)}\sum_{m=0}^{\infty}b_m x^m\cos n\phi-\frac{A_{12}\cos\alpha}{R(x)}\sum_{m=0}^{\infty}c_m x^m\cos n\phi \tag{3.19}$$

$$M_x=-D_{11}\sum m(m-1)c_m x^{m-2}\cos n\phi-\frac{D_{12}\sin\alpha}{R(x)}\sum_{m=1}^{\infty}mc_m x^{m-1}\cos n\phi$$

$$+\frac{D_{12}n^2}{R^2(x)}\sum_{m=0}^{\infty}c_m x^m\cos n\phi$$

$$U=\sum_{m=0}^{\infty}a_m x^m\cos n\phi \qquad V=\sum_{m=0}^{\infty}b_m x^m\sin n\phi$$

$$W=\sum_{m=0}^{\infty}c_m x^m\cos n\phi \qquad \frac{\partial W}{\partial x}=\sum_{m=1}^{\infty}mc_m x^{m-1}\cos n\phi$$

Recurrence Relations:

Eqs. (3.17) and (3.18) into Eq. (3.16) and using Eqs. (3.1) and L_{ij}^{*} to obtain the following recurrence relations:

$$\begin{aligned}
a_{m+2} &= G_{1,1}a_{m+1}+G_{1,2}a_m+G_{1,3}b_{m+1}+G_{1,4}b_m+G_{1,5}c_{m+1}+G_{1,6}c_m\\
b_{m+2} &= G_{2,1}a_{m+1}+G_{2,2}a_m+G_{2,3}b_{m+1}+G_{2,4}b_m+G_{2,5}c_m\\
c_{m+4} &= G_{3,1}a_{m+1}+G_{3,2}a_m+G_{3,3}a_{m-1}+G_{3,4}a_{m-2}+G_{3,5}b_m+G_{3,6}b_{m-1}+G_{3,7}b_{m-2}\\
&\quad +G_{3,8}c_{m+3}+G_{3,9}c_{m+2}+G_{3,10}c_{m+1}+G_{3,11}c_m+G_{3,12}c_{m-1}+G_{3,13}c_{m-2}+G_{3,14}c_{m-3}\\
&\qquad\qquad (m=0,1,2,\ldots)
\end{aligned} \tag{3.20}$$

where the coefficients $G_{i,j}$ [$(i,j)=(1,6)$, $(2,5)$, *and* $(3,14)$] are given in the Appendix C (C.1 through C.25). The above recurrence relations allow one to express the unknown constants $a_m, b_m\,(m\geq 2)$ and $c_m\,(m\geq 4)$ in terms of $a_0, a_1, b_0, b_1, c_0, c_1, c_2$ and c_3. Therefore the general form of $u(x), v(x)$ and $w(x)$ may be written [31] as

$$\begin{aligned}
u(x) &= u_1(x)a_0+u_2(x)a_1+u_3(x)b_0+u_4(x)b_1\\
&\quad +u_5(x)c_0+u_6(x)c_1+u_7(x)c_2+u_8(x)c_3\\
v(x) &= v_1(x)a_0+v_2(x)a_1+v_3(x)b_0+v_4(x)b_1\\
&\quad +v_5(x)c_0+v_6(x)c_1+v_7(x)c_2+v_8(x)c_3\\
w(x) &= w_1(x)a_0+w_2(x)a_1+w_3(x)b_0+w_4(x)b_1\\
&\quad +w_5(x)c_0+w_6(x)c_1+w_7(x)c_2+w_8(x)c_3
\end{aligned} \tag{3.21}$$

Here $u_i(x), v_i(x)$ and $w_i(x)$, $(i = 1,2,\ldots,8)$, are the *base functions* of $u(x), v(x)$ and $w(x)$, respectively and $a_0, a_1, b_0, b_1, c_0, c_1, c_2$ and c_3 are the unknowns to be determined by imposing the boundary conditions at both ends of the cone. When m becomes large enough using Eqs. (3.20) with Appendix C (C.1 through C.25), we have the condition for convergence [31]

$$R_1 \geq 0. \tag{3.22}$$

3.11 Displacement Functions for Pure Bending

We shell assume solutions of the following series for bending analysis:

$$U = \sum_{n=1}^{\infty} u(x)\cos n\phi, \quad V = \sum_{n=1}^{\infty} v(x)\sin n\phi, \quad W = \sum_{n=1}^{\infty} w(x)\cos n\phi \tag{3.23}$$

Using Eq. (3.18)

$$U = \sum_{n=1}^{\infty}\sum_{m=0}^{\infty} a_{mn}x^m \cos n\phi, \quad V = \sum_{n=1}^{\infty}\sum_{m=0}^{\infty} b_{mn}x^m \sin n\phi, \quad W = \sum_{n=1}^{\infty}\sum_{m=0}^{\infty} c_{mn}x^m \cos n\phi \tag{3.24}$$

n is an integer representing the circumferential wave number of the buckled shell and m is terms of power series.

Recurrence Relations:

Eqs. (3.24) into Eq. (3.16) and using Eqs. (3.1) and L_{ij}^* to obtain the following recurrence relations with Flügge's [11] derive way using additional coefficients in Appendix C (C.26 through C.31):

$$\begin{aligned}
a_{m+2\,n} &= G_{1,1}a_{m+1\,n} + G_{1,2}a_{m\,n} + G_{1,3}b_{m+1\,n} + G_{1,4}b_{m\,n} + G_{1,5}c_{m+1\,n} + G_{1,6}c_{m\,n} \\
b_{m+2\,n} &= G_{2,1}a_{m+1\,n} + G_{2,2}a_{m\,n} + G_{2,3}b_{m+1\,n} + G_{2,4}b_{m\,n} + G_{2,5}c_{m\,n} \\
c_{m+4\,n} &= G_{3,1}a_{m+1\,n} + G_{3,2}a_{m\,n} + G_{3,3}a_{m-1\,n} + G_{3,4}a_{m-2\,n} + G_{3,5}b_{m\,n} + G_{3,6}b_{m-1\,n} \\
&\quad + G_{3,7}b_{m-2\,n} + G_{3,8}c_{m+3\,n} + G'_{3,9}c_{m+2\,n} + G''_{3,9}c_{m+2\,n-1} + G''_{3,9}c_{m+2\,n+1} \\
&\quad + G'_{3,10}c_{m+1\,n} + G''_{3,10}c_{m+1\,n-1} + G''_{3,10}c_{m+1\,n+1} + G'_{3,11}c_{m\,n} + G''_{3,11}c_{m\,n-1} + G''_{3,11}c_{m\,n+1}
\end{aligned} \tag{3.25}$$

$$+G_{3,12}c_{m-1\,n}+G_{3,13}c_{m-2\,n}+G_{3,14}c_{m-3\,n}$$

$$(m=0,1,2,\cdots)$$
$$(n=1,2,\cdots\cdots)$$

The first equations (n=0, n=1) have some irregularities, they are usually little importance [6].

3.12 Determination of Stress Resultants

The three displacements U, V and W can be obtained from the buckling of cones under axial compressive loads, outer pressure, and pure bending. Then the three displacements may be used to calculate the membrane forces N_x, N_ϕ and $N_{x\phi}$, the bending moments M_x, M_ϕ and $M_{x\phi}$ in Eqs(3.19). Equations (3.13) now yields the transverse shear force Q_x and Q_ϕ may be obtained to find the critical buckling load.

The critical buckling loads and the corresponding buckling patterns can finally be obtained by equating the determinants of the coefficients matrix obtained after the imposition of the eight boundary conditions to zero. This determinant is the buckling condition of the shell.

CHAPTER 4

THEORY OF MULTILAYERED COMPOSITE CONICAL SHELLS UNDER COMBINED LOADS

4.1 Introduction

This work is to analyze composite conical shells under axial compression, external pressure, and bending. The treatment is based upon Donnell-type governing equations for conical shells. A laminate is two or more laminae bonded together to act as an integral structural element. The laminae principal material directions are oriented to produce a structural element capable of resisting load in several directions. The stiffness of such a composite material [21] configuration is obtained from the properties of the constituent laminae by procedures showed in this chapter. Classical lamination theory is used to understand multilayered composite conical shells through the chapter.

The procedures enable the analysis of laminates that have individual laminae with principal material directions oriented at cross-ply to the to the chosen axes of laminate. Multilayered shells are fabricated such that act as single layer materials. The layers can not slip over each other, and the displacements remain continuous across the bond. The parameters such as thickness, angle, radius of the cone, and material properties are considered to determine optimal condition against loads. The cone geometry, and dimensions are in Figure 3.1.

4.2 Classical Lamination Theory

Classical lamination theory shows a collection of stress and deformation theories that are described in this section. Because of the stress and deformation hypotheses that are an

inseparable part of classical lamination theory, it would be classical thin lamination theory. The common simplification classical lamination theory will be used. First, the stress-strain relation of an individual lamina is mentioned, and expressed in equation form for the k-th lamina of a laminate. Then, the variations of stress and strain through the thickness of the laminate are determined. The laminate stiffnesses, including the stiffnesses that are used to relate coupling between bending and extension.

4.2.1 Lamina Stress - Strain Relations

The stress-strain relation for the k-th layer of a multilayered laminate are [35] and [1]:

$$\begin{Bmatrix} \sigma_x \\ \sigma_y \\ \sigma_{xy} \end{Bmatrix}_k = [Q_{ij}^*]_k \begin{Bmatrix} \varepsilon_x \\ \varepsilon_y \\ \varepsilon_{xy} \end{Bmatrix}_k \tag{4.1}$$

The term Q_{ij}^* $(i, j = 1,2,6)$ of the lamina rigidity matrix $[Q_{ij}^*]$ are determined in Appendix B.2. The stress-strain relations in arbitrary coordinates, Eq. (4.1), are useful in the definition of the laminate stiffnesses because of the arbitrary orientation of the constituent laminae.

4.2.2 Strain and Stress Properties in a Laminate

The concept of the variation of stress and strain through the laminate thickness is essential to the definition of the extensional, compressive and bending stiffnesses of a laminate. The laminate is considered to consist of perfectly bonded laminae. In addition, the bonds are considered to be thin as well as non-shear-deformable. That is, the displacements are continuous across lamina boundaries so that no lamina can slip relative

to another. Thus the laminate acts as a single layer with very special properties, but nevertheless acts as a single layer of material.

Therefore, if the laminate is thin, a line originally straight and perpendicular to the middle surface of the laminate is assumed to remain straight and perpendicular to the middle surface when the laminate is extended, compressed, and bent. Requiring the normal to the middle surface to remain straight and normal under deformation is equivalent to ignoring the shearing strains in planes perpendicular to the middle surface, that is, $\gamma_{xz} = \gamma_{yz} = 0$ where is the direction of the normal to the middle surface. In addition, the normals are presumed to have constant length so that the strain perpendicular to the middle surface is ignored, that is $\varepsilon_z = 0$.

4.2.3 Stress Resultant - Strain Relations

The strains can be expressed in the form of middle surface strains ε_x^0, ε_y^0, γ_{xy}^0 and middle surface curvatures κ_x, κ_y, κ_{xy} in xy plane are

$$\begin{Bmatrix} \varepsilon_x \\ \varepsilon_y \\ \gamma_{xy} \end{Bmatrix} = \begin{Bmatrix} \varepsilon_x^0 \\ \varepsilon_y^0 \\ \gamma_{xy}^0 \end{Bmatrix} + z \begin{Bmatrix} \kappa_x \\ \kappa_y \\ \kappa_{xy} \end{Bmatrix} \tag{4.2}$$

Using the strain variation through the thickness, Eq. (4.2), in the stress-strain the relations, the stresses in k-th layer can be expressed in terms of the laminate middle surface strains and curvatures as

$$\begin{Bmatrix} \sigma_x \\ \sigma_y \\ \tau_{xy} \end{Bmatrix}_k = \left[Q_{ij}^*\right]_k \left\{ \begin{Bmatrix} \varepsilon_x^0 \\ \varepsilon_y^0 \\ \gamma_{xy}^0 \end{Bmatrix} + z \begin{Bmatrix} \kappa_x \\ \kappa_y \\ \kappa_{xy} \end{Bmatrix} \right\} \tag{4.3}$$

The strain-displacement relations in Eq. (3.2) are same as section 3.2 . Resultant forces and moments acting on a laminate are obtained by integration of the corresponding stresses in each layer or lamina through the laminate thickness, h:

$$\begin{Bmatrix} N_x \\ N_y \\ N_{xy} \end{Bmatrix} = \int_{-h/2}^{h/2} \begin{Bmatrix} \sigma_x \\ \sigma_y \\ \sigma_{xy} \end{Bmatrix} dz = \sum_{k=1}^{\overline{N}} \int_{h_{k-1}}^{h_k} \begin{Bmatrix} \sigma_x \\ \sigma_y \\ \sigma_{xy} \end{Bmatrix} dz \tag{4.4}$$

$$\begin{Bmatrix} M_x \\ M_y \\ M_{xy} \end{Bmatrix} = \int_{-h/2}^{h/2} \begin{Bmatrix} \sigma_x \\ \sigma_y \\ \sigma_{xy} \end{Bmatrix} z dz = \sum_{k=1}^{\overline{N}} \int_{h_{k-1}}^{h_k} \begin{Bmatrix} \sigma_x \\ \sigma_y \\ \sigma_{xy} \end{Bmatrix} z dz \tag{4.5}$$

where $\overline{N}$ represents number of layers.

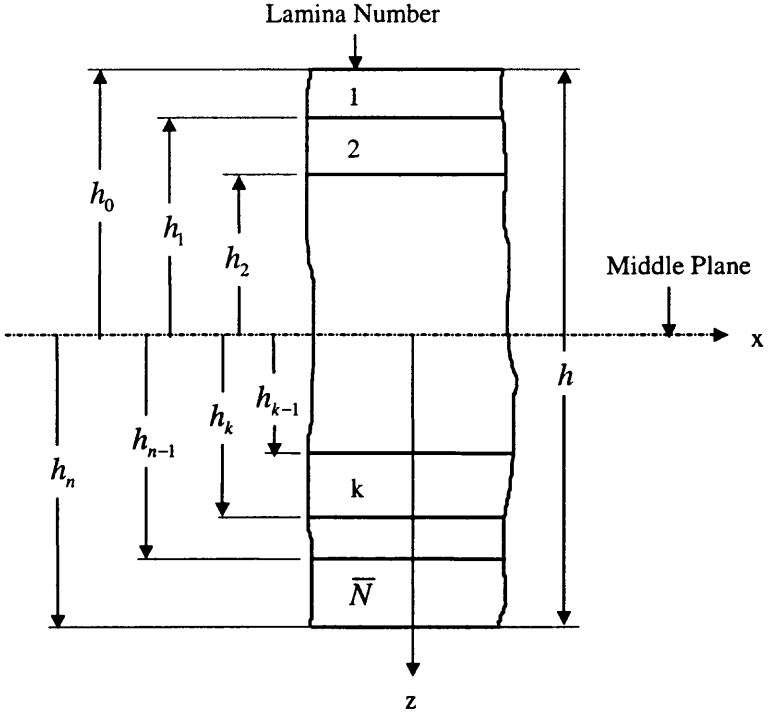

Figure 4.1 Multilayered laminate of a conical shell

N_x is a force per unit length of the cross section of the laminate as shown in Figure 4.2(a). Similarly, M_x is a moment per unit length as shown in Figure 4.2(b). These force and moment resultants do not depend on z after integration, but are functions of x and y, the coordinates in the plane of the laminate middle surface.

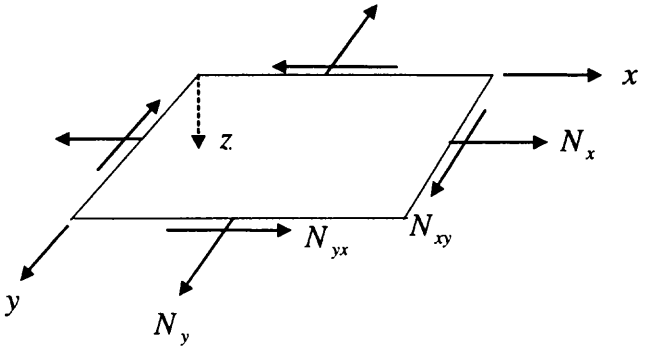

(a)

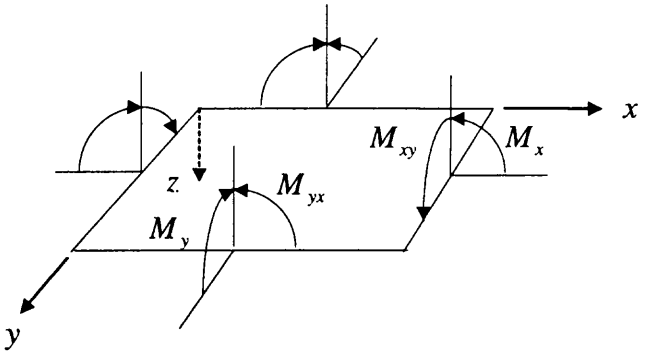

(b)

Figure 4.2 (a) In-plane forces and (b) Moments on a laminate element.

The integration indicated in Eqs. (4.4) and (4.5) can be rearranged to take advantage of the fact that the stiffness matrix for a lamina is constant within the lamina. Thus, the stiffness matrix goes outside the integration over each layer, but is within summation of force and moment resultants for each layer. If the lamina stress-strain relations, Eq. (4.3), are substituted, stress resultant-strain relations for shell expression are

$$\begin{Bmatrix} N_x \\ N_\phi \\ N_{x\phi} \\ M_x \\ M_\phi \\ M_{x\phi} \end{Bmatrix} = \begin{bmatrix} A_{11} & A_{12} & A_{16} & B_{11} & B_{12} & B_{16} \\ A_{12} & A_{22} & A_{26} & B_{12} & B_{22} & B_{26} \\ A_{16} & A_{26} & A_{66} & B_{16} & B_{26} & B_{66} \\ B_{11} & B_{12} & B_{16} & D_{11} & D_{12} & D_{16} \\ B_{12} & B_{22} & B_{26} & D_{12} & D_{22} & D_{26} \\ B_{16} & B_{26} & B_{66} & D_{16} & D_{26} & D_{66} \end{bmatrix} \begin{Bmatrix} \varepsilon_x \\ \varepsilon_\phi \\ 2\varepsilon_{x\phi} \\ \chi_x \\ \chi_\phi \\ 2\chi_{x\phi} \end{Bmatrix} \tag{4.6}$$

In this equations A_{ij}, B_{ij} and D_{ij} $(i, j = 1,2,6)$ are given in the forms :

$$\begin{aligned} A_{ij} &= \sum_{k=1}^{\overline{N}} (Q_{ij}^*)_k (h_{(k)} - h_{(k-1)}) \\ B_{ij} &= \sum_{k=1}^{\overline{N}} (Q_{ij}^*)_k (h_{(k)}^2 - h_{(k-1)}^2)/2 \\ D_{ij} &= \sum_{k=1}^{\overline{N}} (Q_{ij}^*)_k (h_{(k)}^3 - h_{(k-1)}^3)/3 \end{aligned} \tag{4.7}$$

Here $(Q_{ij}^*)_k$ are lamina rigidity of kth layer Jones [12] consisting of $\overline{N}$ orthotropic laminae as shown in Figure 4.1. The matrices A, B, and D are called *stretching stiffness* matrix, *stretching-bending* coupling matrix, and *bending stiffness* matrix, respectively. The matrix B implies coupling between bending and extension of a laminate. Thus, it is impossible to pull on laminate that has the matrix B without at the same time bending and/or twisting the laminate. That is, an extensional force results in not only extensional deformations, but also twisting and/or bending of the laminate. Also, such a laminate cannot be subjected to bending without at the same time including extension of the middle surface.

4.3 Simplification of Laminate Stiffnesses

Some special case of laminates for which the stiffnesses take on certain simplified values as different from the general form in Eq. (4.7). Some of the cases are almost trivial, other

cases are more specialized, but all are contributions to the understanding of the idea of laminate stiffnesses. Many of the cases result from the common practice of constructing laminates from laminae that have the same material properties and thickness, but have different orientations of their orthotropy directions relative to one another and relative to the laminate axes.

According to the types of layer, A_{ij}, B_{ij}, D_{ij} can be simplified. The symmetry of midplane also affects the three stiffness matrices, A, B, and D. For the matrix B can be zero if laminates in which for each ply above the midplane there is an identical ply placed an equal distance bellow the midplane. A set of laminated layer ply that no twisting coupling terms imply that

$$A_{i6} = B_{i6} = D_{i6} = 0 \qquad (i = 1,2)$$

Among various kind of layer cases, antisymmetric laminates is studied for their physical applications of laminated composites required nonsymmetric laminates to achieve design requirement.

4.3.1 Antisymmetric Laminates

Symmetry of a laminate about the middle surface is often effective to avoid coupling between bending and extension. However, to achieve practical applications, the study of nonsymmetric laminates is interesting field. For instance, laminate coupling is necessary to make jet turbine fan blade with pre-twist. As a further example, if the shear stiffness of a laminate made of laminae with unidirectional fibers must be increased, one way to achieve this requirement is to position layers at some angle to the laminate axes. To stay within weight and cost requirements, an even number of such layers may be necessary at

orientations that alternate from layer to layer, e.g. $+\theta/-\theta/+\theta/-\theta$. Therefore, symmetry about the middle surface is changed and the behavioral characteristics of the laminate can be changed from the symmetric case. Even though the example laminate is not symmetric, it is antisymmetric about the middle surface and certain stiffness simplifications are possible.

The general case of antisymmetric laminates must have an even number of layers if adjacent laminae have alternating signs of the principal material property directions with respect to the laminate axes. Each pair of layers must have the same thickness. The only exceptions to the above stipulations occur when the angle of orientation is 0^o or 90^o. As a consequence of antisymmetry of material properties of generally orthotropic laminae, but symmetry of their thickness, the extensional coupling stiffness A_{16}

$$A_{16} = \sum_{k=1}^{\bar{N}} (Q_{ij}^*)_k (h_{(k)} - h_{(k-1)})$$

is easily seen to be zero since

$$(Q_{ij}^*)_{+\theta} = -(Q_{ij}^*)_{-\theta} \tag{4.8}$$

and layers symmetric about the middle surface have equal thickness and hence the same value of the geometric term multiplying $(Q_{16}^*)_k$. Similarly, A_{26} is zero as is the bending twist coupling stiffness D_{16},

$$D_{16} = \sum_{k=1}^{\bar{N}} (Q_{16}^*)_k (h_{(k)}^3 - h_{(k-1)}^3)/3$$

since again Eq. (4.8) holds and the geometric term multiplying $(Q_{16}^*)_k$ is the same for two layers symmetric about the middle surface. The preceding result applies also for D_{26}.

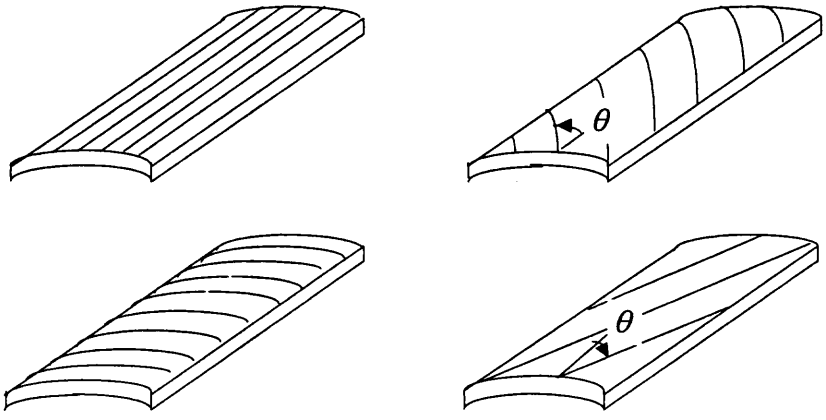

Figure 4.3 (a) Cross-ply laminate (b) Angle-ply laminate

There are two important class of antisymmetric laminates, the antisymmetric cross-ply laminate and the antisymmetric angle-ply laminate in Figure 4.3. The antisymmetric cross-ply laminate of an even number of orthotropic laminae is studied.

4.3.2 Antisymmetric Cross-ply Laminates

An antisymmetric cross-ply laminate consists of an even number of orthotropic laminae laid on each other with principal material directions alternating at 0^o and 90^o to the laminate axes as in the simple example of Figure 4.4. This case laminates do not have A_{16}, A_{26}, D_{16}, and D_{26}, but do have coupling between bending and extension. The regular antisymmetric cross-ply laminate is defined to have laminae all of equal thickness and is common because of simplicity of fabrication. As the number of layers increases, the coupling stiffness B_{11} can be shown to approach zero. The stiffnesses of antisymmetric cross-ply laminates can be expressed Tong [32] as;

$$A_{11} = A_{22} = \tfrac{1}{2}(Q_{11} + Q_{22})h \qquad A_{12} = Q_{12}h, \qquad A_{66} = Q_{66}h$$

$$B_{11} = -B_{22} = \pm\tfrac{1}{4N}(Q_{11} - Q_{22})h^2 \qquad B_{12} = 0, \qquad B_{66} = 0$$

$$D_{11} = D_{22} = \tfrac{1}{24}(Q_{11} + Q_{22})h^3 \qquad D_{12} = \tfrac{1}{12}Q_{12}h^3, \qquad D_{66} = \tfrac{1}{12}Q_{66}h^3$$

The expression Q_{ij} are in Appendix B.2.

The membrane forces at critical state $N_{x0}, N_{\phi 0}$ are same as Eq. (3.7) and Eq. (3.8) in section 3.3.

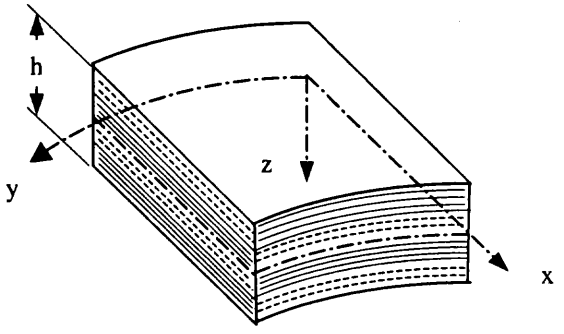

Figure 4.4 Element of a four layer cross-ply composite shell

4.4 Application of the Principle of Minimum Potential Energy

For linear buckling analysis of multilayered composite conical shells under axial compression and bending, adopting the **shallow shell theory** [10] of Donnell-type and the **minimum total potential energy principle** [6] :

$$\frac{\partial N_x}{\partial x} + (N_x - N_\phi)\frac{\sin\alpha}{R(x)} + \frac{1}{R(x)}\frac{\partial N_{x\phi}}{\partial \phi} = 0$$

$$\frac{\partial N_{x\phi}}{\partial x} + \frac{2\sin\alpha}{R(x)}N_{x\phi} + \frac{1}{R(x)}\frac{\partial N_\phi}{\partial \phi} = 0 \qquad \text{(4.9a-c)}$$

$$\frac{\partial^2}{\partial x^2}[R(x)M_x] - \sin\alpha\frac{\partial M_\phi}{\partial x} + \frac{1}{R(x)}\frac{\partial^2 M_\phi}{\partial \phi^2} + \frac{2}{R(x)}\frac{\partial^2}{\partial x \partial \phi}[R(x)M_{x\phi}]$$

$$+\cos\alpha N_\phi + \frac{1}{R(x)}\frac{\partial}{\partial x}[N_{x0}R(x)\frac{\partial W}{\partial x}] + \frac{1}{R^2(x)}\frac{\partial}{\partial \phi}[N_{\phi 0}\frac{\partial W}{\partial \phi}] = 0$$

In the foregoing equations, we have the total potential energy is $\Pi = U_s - \Omega$. Here U_s, and Ω represent the strain energy and the potential energy, respectively from Appendix A.

4.5 Governing Differential Equations

Let the differential operators $L_{ij}(i, j = 1,2,3)$ *and* L_N are expressed using reference [32] given in the Appendix A (A.13-15). Substituting $N_x, N_\phi, N_{x\phi}, M_x, M_\phi,$ and $M_{x\phi}$ from Eq. (4.6) into Eq. (4.9a-c), we have

$$\begin{aligned} &L_{11}U + L_{12}V + L_{13}W = 0 \\ &L_{21}U + L_{22}V + L_{23}W = 0 \\ &L_{31}U + L_{32}V + L_{33}W + L_N W = 0 \end{aligned} \tag{4.10}$$

The quantities $L_{11}, L_{12}, \cdots,$ are defined in Appendix A (A.25 through A.34).

4.6 Stress Resultant - Displacement Relations

Upon following a procedure similar to that of chapter 3, we obtain the governing differential equations. For laminated case, the differential operators $L_{ij}(i, j = 1,2,3)$, which are more complicated than single layer are developed.

As in the case of shells orthotropic case, substitute Eqs. (3.2) into (4.6) to obtain the force and moment stress resultants for laminated conical shells. In so doing, we have

$$\begin{Bmatrix} N_x \\ N_\phi \\ N_{x\phi} \\ M_x \\ M_\phi \\ M_{x\phi} \end{Bmatrix} = \begin{bmatrix} l_{11} & l_{12} & l_{13} \\ l_{21} & l_{22} & l_{23} \\ l_{31} & l_{32} & l_{33} \\ l_{41} & l_{42} & l_{43} \\ l_{51} & l_{52} & l_{53} \\ l_{61} & l_{62} & l_{63} \end{bmatrix} \begin{Bmatrix} U \\ V \\ W \end{Bmatrix} \tag{4.11}$$

In this equation, we have

$$\begin{aligned}
l_{i1} &= A_{i1}\frac{\partial}{\partial x} + \frac{A_{i2}\sin\alpha}{R(x)}\ ,\ l_{i2} = \frac{A_{i2}}{R(x)}\frac{\partial}{\partial\phi} \\
l_{i3} &= -\frac{A_{i2}\cos\alpha}{R(x)} - B_{1i}\frac{\partial^2}{\partial x^2} - \frac{B_{i2}\sin\alpha}{R(x)}\frac{\partial}{\partial x} - \frac{B_{i2}}{R^2(x)}\frac{\partial^2}{\partial\phi^2} \\
l_{31} &= \frac{A_{66}}{R(x)}\frac{\partial}{\partial\phi}\ ,\ \ l_{32} = A_{66}\left(\frac{\partial}{\partial x} - \frac{\sin\alpha}{R(x)}\right) \\
l_{33} &= -2B_{66}\frac{\partial}{\partial x}\left(\frac{1}{R(x)}\frac{\partial}{\partial\phi}\right) \\
l_{j1} &= B_{1i}\frac{\partial}{\partial x} + \frac{B_{i2}\sin\alpha}{R(x)}\ ,\ l_{j2} = \frac{B_{i2}}{R(x)}\frac{\partial}{\partial\phi} \\
l_{j3} &= -D_{1i}\frac{\partial^2}{\partial x^2} - \frac{D_{i2}\sin\alpha}{R(x)}\frac{\partial}{\partial x} - \frac{D_{i2}}{R^2(x)}\frac{\partial^2}{\partial\phi^2} - \frac{B_{i2}\cos\alpha}{R(x)} \\
l_{61} &= \frac{B_{66}}{R(x)}\frac{\partial}{\partial\phi}\ ,\ \ l_{62} = B_{66}\left(\frac{\partial}{\partial x} - \frac{\sin\alpha}{R(x)}\right) \\
l_{63} &= -2D_{66}\frac{\partial}{\partial x}\left(\frac{1}{R(x)}\frac{\partial}{\partial\phi}\right)
\end{aligned} \tag{4.12}$$

where $i = 1,2\ and\ j = 3+i$. The stiffness A_{ij}, B_{ij}, and D_{ij} are defined by Eq. (4.7).

The transverse shear force resultants are same as in section 3.6

4.7 Boundary Conditions

For the conical shell loaded as shown in Figure 3.1, the conditions at ends $x = \pm L/2$ may be expressed as follows as discussed in Sec. 3.6:

Case 1: **Simply-supported boundary conditions** at $x = \pm L/2$.

$$\begin{aligned} &\text{SS1}: N_{x\phi} = N_x = M_x = W = 0 \\ &\text{SS2}: N_{x\phi} = U = M_x = W = 0 \\ &\text{SS3}: V = N_x = M_x = W = 0 \\ &\text{SS4}: V = U = M_x = W = 0 \end{aligned} \tag{3.14}$$

Case 2: **Clamped or built-in boundary conditions** at $x = \pm L/2$.

$$\begin{aligned} &\text{CC1}: N_{x\phi} = N_x = \frac{\partial W}{\partial x} = W = 0 \\ &\text{CC2}: N_{x\phi} = U = \frac{\partial W}{\partial x} = W = 0 \\ &\text{CC3}: V = N_x = \frac{\partial W}{\partial x} = W = 0 \\ &\text{CC4}: V = U = \frac{\partial W}{\partial x} = W = 0 \end{aligned} \tag{3.15}$$

4.8 Modified Governing Differential Equations

To change equations more convenient form, multiply for the first two and the third of equations of Eqs. (4.10) by $R^3(x)$ and $R^4(x)$, respectively.

In so doing, we have

$$\begin{aligned} &L_{11}^* U + L_{12}^* V + L_{13}^* W = 0 \\ &L_{21}^* U + L_{22}^* V + L_{23}^* W = 0 \\ &L_{31}^* U + L_{32}^* V + L_{33}^* W + L_N^* W = 0 \end{aligned} \tag{4.13}$$

Here

$L_{11}^* = R^3(x)L_{11}, \cdots\cdots, L_{21}^* = R^3(x)L_{21}, \cdots\cdots, L_{31}^* = R^4(x)L_{31}, \cdots\cdots$, and
$L_N^* = R^4(x)L_N^*$

4.9 Displacement Functions for Axial and Outer Pressure Loading

We shell assume solutions of the following series :

$$U = u(x)\cos n\phi, \quad V = v(x)\sin n\phi, \quad W = w(x)\cos n\phi \tag{4.14}$$

where

$$u(x)=\sum_{m=0}^{\infty}a_m x^m,\quad v(x)=\sum_{m=0}^{\infty}b_m x^m,\quad w(x)=\sum_{m=0}^{\infty}c_m x^m \tag{4.15}$$

n is an integer representing the circumferential wave number of the buckled shell and m is the terms of power series.

Using Eq. (4.11), resultant forces and moments can be obtained to apply boundary conditions.

$$\begin{aligned}N_{x\phi}=&-\frac{A_{66}n}{R(x)}\sum_{m=0}^{\infty}a_m x^m\sin n\phi+A_{66}\sum_{m=1}^{\infty}mb_m x^{m-1}\sin n\phi\\&-A_{66}\frac{\sin\alpha}{R(x)}\sum_{m=0}^{\infty}b_m x^m\sin n\phi-2B_{66}\frac{\sin\alpha n}{R^2(x)}\sum_{m=0}^{\infty}c_m x^m\sin n\phi\\&+\frac{2B_{66}n}{R(x)}\sum_{m=1}^{\infty}c_m m x^{m-1}\sin n\phi\end{aligned}$$

$$\begin{aligned}N_x=&A_{11}\sum_{m=1}^{\infty}ma_m x^{m-1}\cos n\phi+A_{12}\frac{\sin\alpha}{R(x)}\sum_{m=0}^{\infty}a_m x^m\cos n\phi\\&+\frac{A_{12}n}{R(x)}\sum_{m=0}^{\infty}b_m x^m\cos n\phi-\frac{A_{12}\cos\alpha}{R(x)}\sum_{m=0}^{\infty}c_m x^m\cos n\phi\\&-B_{11}\sum_{m=2}^{\infty}c_m m(m-1)x^{m-2}\cos n\phi-\frac{B_{12}\sin\alpha}{R(x)}\sum_{m=1}^{\infty}c_m m x^{m-1}\cos n\phi\\&+\frac{B_{12}n^2}{R^2(x)}\sum_{m=0}^{\infty}c_m x^m\cos n\phi\end{aligned} \tag{4.16}$$

$$\begin{aligned}M_x=&-B_{11}\sum_{m=1}^{\infty}a_m m x^{m-1}\cos n\phi-\frac{B_{12}\sin\alpha}{R(x)}\sum_{m=0}^{\infty}a_m m x^m\cos n\phi\\&+\frac{B_{12}n}{R(x)}\sum_{m=0}^{\infty}b_m x^m\cos n\phi\\&-D_{11}\sum_{m=2}^{\infty}m(m-1)c_m x^{m-2}\cos n\phi-\frac{D_{12}\sin\alpha}{R(x)}\sum_{m=1}^{\infty}mc_m x^{m-1}\cos n\phi\\&+\frac{D_{12}n^2}{R^2(x)}\sum_{m=0}^{\infty}c_m x^m\cos n\phi-\frac{B_{12}\cos\alpha}{R(x)}\sum_{m=0}^{\infty}c_m x^m\cos n\phi\end{aligned}$$

$$U=\sum_{m=0}^{\infty}a_m x^m\cos n\phi\qquad V=\sum_{m=0}^{\infty}b_m x^m\sin n\phi$$

$$W = \sum_{m=0}^{\infty} c_m x^m \cos n\phi \qquad \frac{\partial W}{\partial x} = \sum_{m=1}^{\infty} m c_m x^{m-1} \cos n\phi$$

Recurrence Relations:

Eqs. (4.14) and (4.15) into Eq. (4.13) and using Eq. (3.1) and L_{ij}^{*} to obtain the following recurrence relations:

$$\begin{aligned} b_{m+2} &= G_{2,1}a_{m+1} + G_{2,2}a_m + G_{2,3}a_{m-1} + G_{2,4}b_{m+1} + G_{2,5}b_m \\ &\quad + G_{2,6}b_{m-1} + G_{2,7}c_{m+2} + G_{2,8}c_{m+1} + G_{2,9}c_m + G_{2,10}c_{m-1} \end{aligned}$$

$$\begin{aligned} a_{m+2} &= G_{1,1}a_{m+1} + G_{1,2}a_m + G_{1,3}a_{m-1} + G_{1,4}b_{m+1} + G_{1,5}b_m \\ &\quad + G_{1,6}b_{m-1} + G_{1,7}c_{m+3} + G_{1,8}c_{m+2} + G_{1,9}c_{m+1} + G_{1,10}c_m + G_{1,11}c_{m-1} \end{aligned} \tag{4.17}$$

$$\begin{aligned} c_{m+4} &= G_{3,1}a_{m+3} + G_{3,2}a_{m+2} + G_{3,3}a_{m+1} + G_{3,4}a_m + G_{3,5}a_{m-1} + G_{3,6}a_{m-2} + G_{3,7}b_{m+2} \\ &\quad + G_{3,8}b_{m+1} + G_{3,9}b_m + G_{3,10}b_{m-1} + G_{3,11}b_{m-2} + G_{3,12}c_{m+3} + G_{3,13}c_{m+2} + G_{3,14}c_{m+1} \\ &\quad + G_{3,15}c_m + G_{3,16}c_{m-1} + G_{3,17}c_{m-2} + G_{3,18}c_{m-3} \qquad (m = 0,1,2,\ldots) \end{aligned}$$

where the coefficients $G_{i,j}$ [$(i, j) = (1,6)$, $(2,5)$, *and* $(3,14)$] are given in the Appendix C (C.32 through C.70). From the above recurrence relations, one cannot directly obtain c_{m+4} because the term a_{m+3} is involved in the last equation. However, combining the first two equations with $m+1$ with the last equation with m and rearranging them, we have the following explicit recurrence relations:

$$\begin{aligned} b_{m+3} &= G_{2,1}(m+1)a_{m+2} + G_{2,2}(m+1)a_{m+1} + G_{2,3}(m+1)a_m \\ &\quad + G_{2,4}(m+1)b_{m+2} + G_{2,5}(m+1)b_{m+1} + G_{2,6}(m+1)b_m \\ &\quad + G_{2,7}(m+1)c_{m+3} + G_{2,8}(m+1)c_{m+2} + G_{2,9}(m+1)c_{m+1} \\ &\quad + G_{2,10}(m+1)c_m \qquad (m = 1,2,\ldots) \end{aligned}$$

$$\begin{aligned} c_{m+4} &= G_{3,2}^{p}a_{m+2} + G_{3,3}^{p}a_{m+1} + G_{3,4}^{p}a_m + G_{3,5}^{p}a_{m-1} \\ &\quad + G_{3,6}^{p}a_{m-2} + G_{3,7}^{p}b_{m+2} + G_{3,8}^{p}b_{m+1} + G_{3,9}^{p}b_m + G_{3,10}^{p}b_{m-1} \\ &\quad + G_{3,11}^{p}b_{m-2} + G_{3,12}^{p}c_{m+3} + G_{3,13}^{p}c_{m+2} + G_{3,14}^{p}c_{m+1} + G_{3,15}^{p}c_m \end{aligned} \tag{4.18}$$

$$+ G^p_{3,16}c_{m-1} + G^p_{3,17}c_{m-2} + G^p_{3,18}c_{m-3} \qquad (m = 0,1,2,\ldots)$$

$$\begin{aligned} a_{m+3} = {} & G_{1,1}(m+1)a_{m+2} + G_{1,2}(m+1)a_{m+1} + G_{1,3}(m+1)a_m \\ & + G_{1,4}(m+1)b_{m+2} + G_{1,5}(m+1)b_{m+1} + G_{1,6}(m+1)b_m \\ & + G_{1,7}(m+1)c_{m+4} + G_{1,8}(m+1)c_{m+3} + G_{1,9}(m+1)c_{m+2} \\ & + G_{1,10}(m+1)c_{m+1} + G_{1,11}(m+1)c_m \qquad (m=1,2,\ldots) \end{aligned}$$

where

$$\begin{aligned} b_2 = {} & G_{2,1}(0)a_1 + G_{2,2}(0)a_0 + G_{2,4}(0)b_1 + G_{2,5}(0)b_0 \\ & + G_{2,7}(0)c_2 + G_{2,8}(0)c_1 + G_{2,9}(0)c_0 \end{aligned}$$

$$\begin{aligned} a_2 = {} & G_{1,1}(0)a_1 + G_{1,2}(0)a_0 + G_{1,4}(0)b_1 + G_{1,5}(0)b_0 \\ & + G_{1,7}(0)c_3 + G_{1,8}(0)c_2 + G_{1,9}(0)c_1 + G_{1,10}(0)c_0 \end{aligned} \qquad (4.19)$$

and

$$\begin{aligned} G_0 &= 1 - G_{3,1}(m)G_{1,7}(m+1) \\ G^p_{3,2} &= [G_{3,2}(m) + G_{3,1}(m)G_{1,1}(m+1)]/G_0 \\ G^p_{3,3} &= [G_{3,3}(m) + G_{3,1}(m)G_{1,2}(m+1)]/G_0 \\ G^p_{3,4} &= [G_{3,4}(m) + G_{3,1}(m)G_{1,3}(m+1)]/G_0 \\ G^p_{3,5} &= G_{3,5}(m)/G_0 \\ G^p_{3,6} &= G_{3,6}(m)/G_0 \\ G^p_{3,7} &= [G_{3,7}(m) + G_{3,1}(m)G_{1,4}(m+1)]/G_0 \\ G^p_{3,8} &= [G_{3,8}(m) + G_{3,1}(m)G_{1,5}(m+1)]/G_0 \\ G^p_{3,9} &= [G_{3,9}(m) + G_{3,1}(m)G_{1,6}(m+1)]/G_0 \\ G^p_{3,10} &= G_{3,10}(m)/G_0 \\ G^p_{3,11} &= G_{3,11}(m)/G_0 \\ G^p_{3,12} &= [G_{3,12}(m) + G_{3,1}(m)G_{1,8}(m+1)]/G_0 \\ G^p_{3,13} &= [G_{3,13}(m) + G_{3,1}(m)G_{1,9}(m+1)]/G_0 \\ G^p_{3,14} &= [G_{3,14}(m) + G_{3,1}(m)G_{1,10}(m+1)]/G_0 \\ G^p_{3,15} &= [G_{3,15}(m) + G_{3,1}(m)G_{1,11}(m+1)]/G_0 \\ G^p_{3,16} &= G_{3,16}(m)/G_0 \\ G^p_{3,17} &= G_{3,17}(m)/G_0 \\ G^p_{3,18} &= G_{3,18}(m)/G_0 \end{aligned} \qquad (4.20)$$

The above recurrence relations allow one to express the unknown constants $a_m, b_m\,(m \geq 2)$ and $c_m\,(m \geq 4)$ in terms of $a_0, a_1, b_0, b_1, c_0, c_1, c_2$ and c_3. Therefore the general form of $u(x), v(x)$ and $w(x)$ may be written Tong [31] as

$$\begin{aligned} u(x) &= u_1(x)a_0 + u_2(x)a_1 + u_3(x)b_0 + u_4(x)b_1 \\ &\quad + u_5(x)c_0 + u_6(x)c_1 + u_7(x)c_2 + u_8(x)c_3 \\ v(x) &= v_1(x)a_0 + v_2(x)a_1 + v_3(x)b_0 + v_4(x)b_1 \\ &\quad + v_5(x)c_0 + v_6(x)c_1 + v_7(x)c_2 + v_8(x)c_3 \\ w(x) &= w_1(x)a_0 + w_2(x)a_1 + w_3(x)b_0 + w_4(x)b_1 \\ &\quad + w_5(x)c_0 + w_6(x)c_1 + w_7(x)c_2 + w_8(x)c_3 \end{aligned} \tag{4.21}$$

Here $u_i(x), v_i(x)$ and $w_i(x)$, $(i = 1,2,\ldots,8)$, are the *base functions* of $u(x), v(x)$ and $w(x)$, respectively and $a_0, a_1, b_0, b_1, c_0, c_1, c_2$ and c_3 are the unknowns to be determined by imposing the boundary conditions at both ends of the cone. When m becomes large enough using Eqs. (4.18), (4.19) and (4.20) with Appendix C (C.32 through C.70), we have the condition for convergence in Eq. (3.22) $R_1 \geq 0$.

4.10 Displacement Functions for Pure Bending

We shell assume solutions of the following series :

$$U = \sum_{n=1}^{\infty} u(x)\cos n\phi, \quad V = \sum_{n=1}^{\infty} v(x)\sin n\phi, \quad W = \sum_{n=1}^{\infty} w(x)\cos n\phi \tag{4.22}$$

Using Eq. (4.15);

$$U = \sum_{n=1}^{\infty}\sum_{m=0}^{\infty} a_{mn}x^m \cos n\phi, \quad V = \sum_{n=1}^{\infty}\sum_{m=0}^{\infty} b_{mn}x^m \sin n\phi, \quad W = \sum_{n=1}^{\infty}\sum_{m=0}^{\infty} c_{mn}x^m \cos n\phi \tag{4.23}$$

n is an integer representing the circumferential wave number of the buckled shell and m is the terms of power series.

Eqs. (4.23) into Eq. (4.13) and using Eqs. (3.1) and L_{ij}^{*} to obtain the following recurrence relations with Flügge's [11] derive way using additional coefficients in Appendix C (C.71 through C.76):

$$\begin{aligned} b_{m+3\,n} &= G_{2,1}(m+1)a_{m+2\,n} + G_{2,2}(m+1)a_{m+1\,n} + G_{2,3}(m+1)a_{m\,n} \\ &+ G_{2,4}(m+1)b_{m+2\,n} + G_{2,5}(m+1)b_{m+1\,n} + G_{2,6}(m+1)b_{m\,n} \\ &+ G_{2,7}(m+1)c_{m+3\,n} + G_{2,8}(m+1)c_{m+2\,n} + G_{2,9}(m+1)c_{m+1\,n} \\ &+ G_{2,10}(m+1)c_{m\,n} \qquad (m=1,2,\ldots) \end{aligned}$$

$$\begin{aligned} c_{m+4\,n} &= G_{3,2}^{p}a_{m+2\,n} + G_{3,3}^{p}a_{m+1\,n} + G_{3,4}^{p}a_{m\,n} + G_{3,5}^{p}a_{m-1\,n} \\ &+ G_{3,6}^{p}a_{m-2\,n} + G_{3,7}^{p}b_{m+2\,n} + G_{3,8}^{p}b_{m+1\,n} + G_{3,9}^{p}b_{m\,n} + G_{3,10}^{p}b_{m-1\,n} \\ &+ G_{3,11}^{p}b_{m-2\,n} + G_{3,12}^{p}c_{m+3\,n} \\ &+ G_{3,13}^{p'}c_{m+2\,n} + G_{3,13}^{p''}c_{m+2\,n-1} + G_{3,13}^{p''}c_{m+2\,n+1} \\ &+ G_{3,14}^{p'}c_{m+1\,n} + G_{3,14}^{p''}c_{m+1\,n-1} + G_{3,14}^{p''}c_{m+1\,n+1} \\ &+ G_{3,15}^{p'}c_{m\,n} + G_{3,15}^{p''}c_{m\,n-1} + G_{3,15}^{p''}c_{m\,n+1} \\ &+ G_{3,16}^{p}c_{m-1\,n} + G_{3,17}^{p}c_{m-2\,n} + G_{3,18}^{p}c_{m-3\,n} \qquad (m=0,1,2,\cdots) \\ &\qquad\qquad\qquad\qquad\qquad\qquad\qquad\qquad (n=1,2,\cdots\cdots) \end{aligned} \tag{4.24}$$

$$\begin{aligned} a_{m+3\,n} &= G_{1,1}(m+1)a_{m+2\,n} + G_{1,2}(m+1)a_{m+1\,n} + G_{1,3}(m+1)a_{m\,n} \\ &+ G_{1,4}(m+1)b_{m+2\,n} + G_{1,5}(m+1)b_{m+1\,n} + G_{1,6}(m+1)b_{m\,n} \\ &+ G_{1,7}(m+1)c_{m+4\,n} + G_{1,8}(m+1)c_{m+3\,n} + G_{1,9}(m+1)c_{m+2\,n} \\ &+ G_{1,10}(m+1)c_{m+1\,n} + G_{1,11}(m+1)c_{m\,n} \qquad (m=1,2,\cdots) \end{aligned}$$

$$\begin{aligned} G_{3,13}^{p'} &= [G_{3,13}^{'}(m) + G_{3,1}(m)G_{1,9}(m+1)]/G_0 \\ G_{3,13}^{p''} &= [G_{3,13}^{''}(m)]/G_0 \\ G_{3,14}^{p'} &= [G_{3,14}^{'}(m) + G_{3,1}(m)G_{1,10}(m+1)]/G_0 \\ G_{3,14}^{p''} &= [G_{3,14}^{''}(m)]/G_0 \\ G_{3,15}^{p'} &= [G_{3,15}^{'}(m) + G_{3,1}(m)G_{1,11}(m+1)]/G_0 \\ G_{3,15}^{p''} &= [G_{3,15}^{''}(m)]/G_0 \end{aligned} \tag{4.25}$$

The first equations (n=0, n=1) have some irregularities, they are usually little importance [11].

4.11 Solution of Multilayered Composite Conical Shells

All conditions and steps are similar as orthotropic single layer case. The recurrence relations of composite case are more complicate than orthotropic case. The three displacements, U, V and W can be obtained from the buckling of cones under axial compressive loads, outer pressure, and pure bending. Then, the three displacements may be used to calculate the membrane forces N_x, N_ϕ and $N_{x\phi}$, the bending moments M_x, M_ϕ and $M_{x\phi}$ in Eqs. (4.16).

The critical buckling loads and the corresponding buckling patterns can finally be obtained by equating the determinants of the coefficients matrix obtained after the imposition of the eight boundary conditions to zero. This determinant is the buckling condition of the shell.

CHAPTER 5

CONICAL SHELLS UNDER COMBINED LOADS

For linear buckling analysis of isotropic and orthotropic single layer and multi layer conical shell, under axial compression, outer pressure, and pure bending, adopting the minimum total potential energy method, numerical buckling solutions are obtained. The solutions are consist of two groups: First, three types of loading are studied separately. second, three loads are combined each other. This analysis is available not only single layer but also multi layer.

5.1 Classical Value of the Buckling Load under Axial Load

The notation of solution is introduced Baruch [5] and Tong [31 and 32].

$$\rho_{cr} = \frac{P_{cr}}{P_{cl}} \tag{5.1}$$

where P_{cr} is the critical buckling load obtained from the present power series method. **The classical value of the critical buckling load** P_{cl} for axisymmetrical long *isotropic cones*, suggested by Seide [23].

$$P_{cl} = P_{conical} = P_{cylindrical} \cos^2 \alpha$$

$$P_{cl} = \frac{2\pi E h^2 \cos^2 \alpha}{\sqrt{3(1-\nu^2)}} \tag{5.2}$$

The formula disregards the effect of boundary conditions. The long cylinder means that the edge conditions only a minor influence on the magnitude of the buckling load provided that the shell length is not small (L > 2a; a: radius) from Ugural [35]. The

critical values depends upon the material properties, thickness, and radius, while it is independent of cylinder length.

5.2 Solution Procedure and Material Property

Solution procedure:

C-language program COMBINED1 and COMBINED2 have been developed (see Appendix D). The program steps are:

1) Enter dimensions and materials parameters.
2) Determine a_m, b_m, c_m in terms of $a_0, a_1, b_0, b_1, c_0, c_1, c_2, c_3$ using recurrence relationships Eqs. (3.20, 3.25) and Eqs. (4.18, 4.24).
3) Calculate $U, V, W, \partial W/\partial x, N_x, N_{x\phi}$ and M_x for applying boundary conditions.
4) Calculate P_{cr}, q_{cr}, M_{cr} and combined P_{cr} with q, M_{cr} with P, and M_{cr} with q from the condition that the determinant of each set of boundary conditions is equal to zero. There are eight sets of boundary conditions given by Eq. (3.14) and Eq. (3.15).
5) Check the convergence in the critical buckling loads by increasing m from 0 to 35.

Material property :

The property of single layer isotropic material is steel, $E = 30 \times 10^6 psi$, $\nu = 0.3$. For multi layer, the material is used graphite/epoxy composite with from Jones [12]:

$E_1 = 30 \times 10^6 \ psi$, $E_1/E_2 = 40$

$G_{12}/E_2 = 0.5$, $\nu_{12} = 0.25$

Subscript 1 is primary direction and 2 is secondary direction.

5.3 Numerical Solutions for Isotropic Conical Shells

Buckling of isotropic material single layer is the simplest case for this research. For all the equation, the orthotropic material reduce to simple isotropic expression. The buckling loads are axial compression, P_{cr}, outer pressure, q_{cr}, and pure bending M_{cr}. Combined buckling loads are obtained from combination of q and P_{cr}, q and M_{cr}, and P and M_{cr}.

5.3.1 Isotropic Conical Shells under Axial Compression

Buckling of conical shell under axial compression in series form is developed by Tong et al. [31]. For extremely short cones with $L/R_1 = 0.2$, ρ_{cr} becomes large as α increases and ρ_{cr} tends to constant independent of α for cones with L/R_1 larger than 0.5 under axial compressive loads for boundary conditions SS3 and SS4 in Figure 5.1 from Appendix E.3. This expression is done by Tong et al. [31].

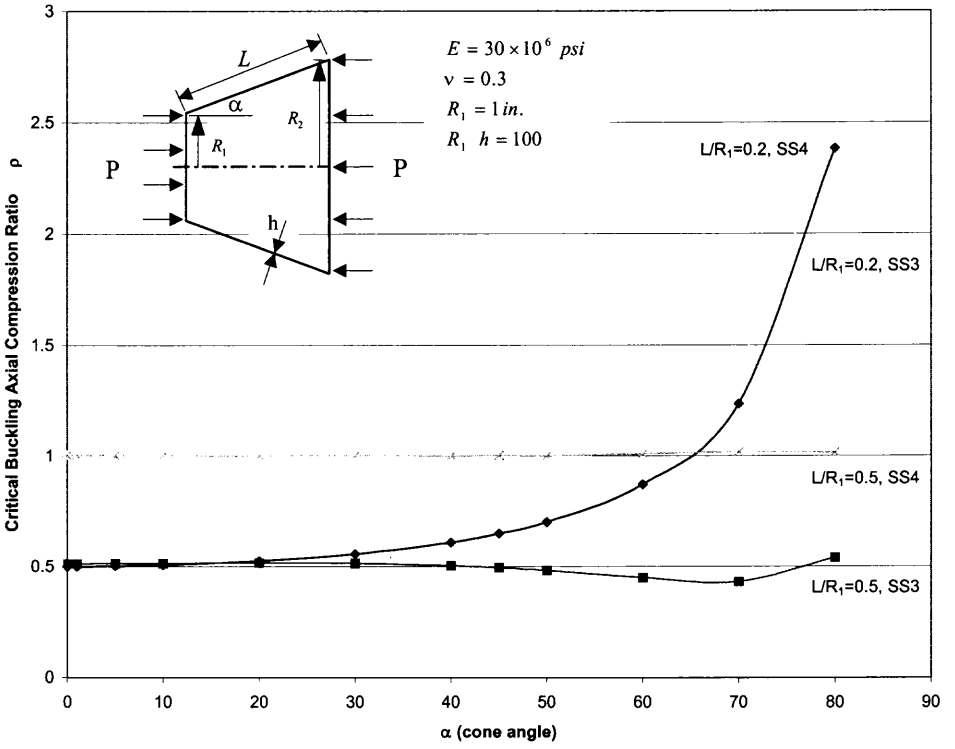

Figure 5.1 Buckling ratio of single layer isotropic conical shell under axial compression boundary condition SS3, SS4 and different length ratio $L/R_1 = 0.2, 0.5$ about cone angle α

For extremely short cone with length ratio $L/R_1 = 0.2$, the buckling load ratio ρ_{cr} becomes larger as α increases and it becomes abrupt changes near 80 degree. ρ_{cr} tends to be constant values independent of α and for cone with L/R_1 larger than 0.5. The properties of boundary condition show that SS4 is almost as twice as SS3 for both length for the small cone angle α .

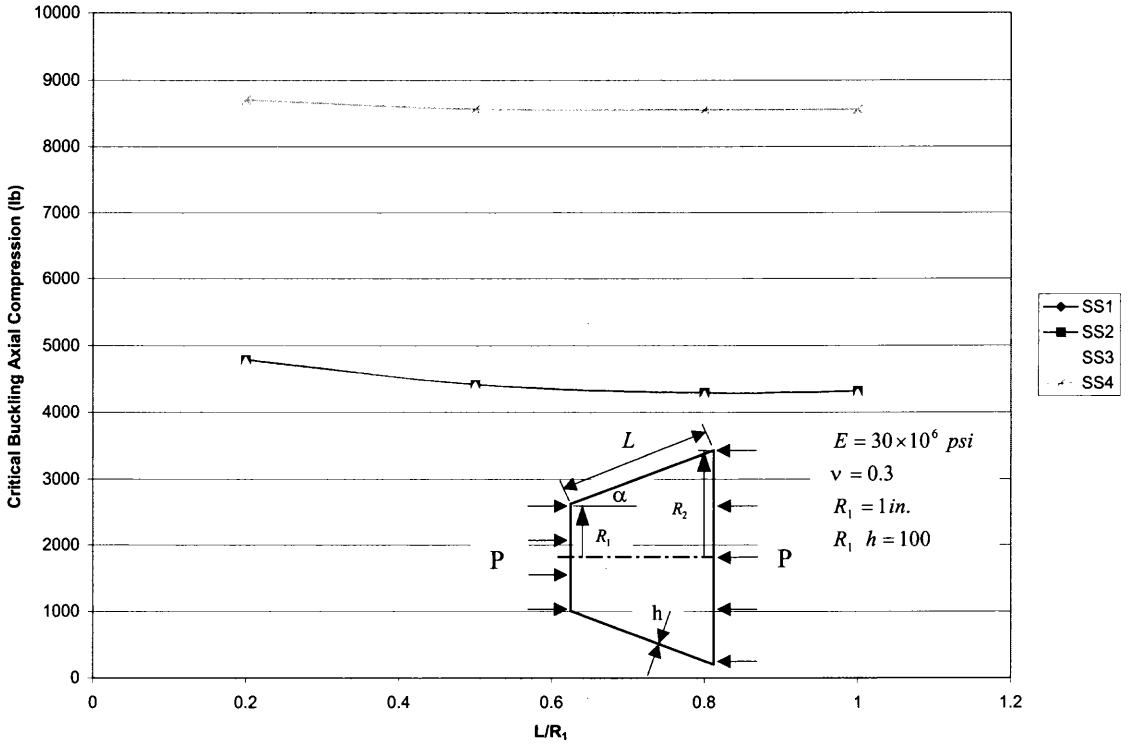

Figure 5.2 Buckling values of single layer isotropic conical shell under axial compression for $\alpha = 30^o$ and different boundary condition

The buckling values of single conical shells under axial compression at cone angle $\alpha = 30^o$ are different buckling loads for different boundary conditions. For simply supported boundary conditions, SS1, SS2, and SS3 are similar trends comparing with SS4. Through the length ratio $L/R1$ from 0.2 to 1, boundary condition SS4 is almost twice stronger than the rest three boundary conditions in Figure 5.2 from Appendix E.1.

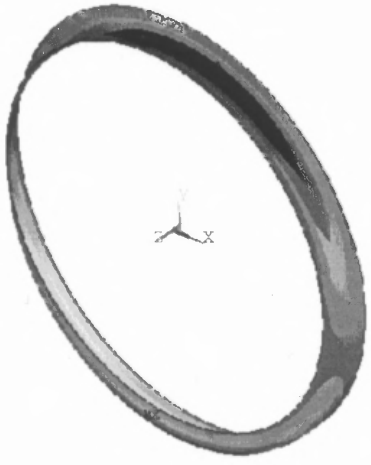

Figure 5.3(a) Deformed shape for L/R_1=0.2, $\alpha = 30^o$, SS2 under axial compression

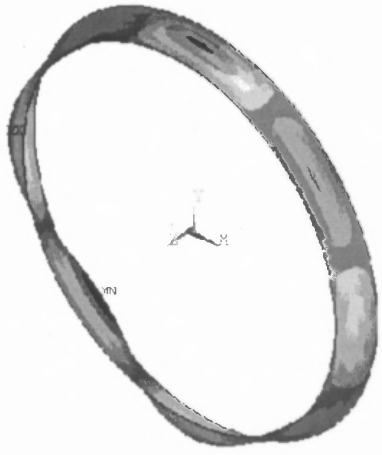

Figure 5.3(b) Deformed shape for L/R_1=0.2, $\alpha = 30^o$, SS4 under axial compression

Figure 5.4(a) Deformed shape for L/R_1=0.5 $\alpha = 30^o$, SS2 under outer pressure

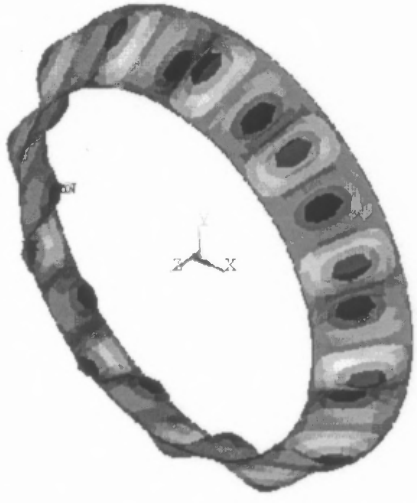

Figure 5.4(b) Deformed shape for L/R_1=0.5 $\alpha = 30^o$, SS4 under outer pressure

There are some deformed shapes using analysis software ANSYS 5.4. Detailed Finite Element Analysis will be in Chapter 6. Simple deformed shapes are introduced to understand buckling problem. The deformed shapes of cone under axial compression in Figure 5.3(a) and 5.3(b) has different circumferential wave number. Because the buckling

load of the cone with boundary condition SS4 needs more compression than with SS2, the cone with boundary condition SS4 has more wave number than with SS2. The outer pressure also affects similar to axial compression. The cone with boundary condition SS4 under outer pressure in Figure 5.4(b) has more waves than that with SS2 in Figure 5.4(a).

The circumferential wave number n can be obtained when the buckling value is decided on simulation. For the single layer isotropic conical shell under axial compression with $\alpha = 30^o$ and $L/R_1 = 0.5$, the circumferential wave number n and buckling value P_{cr} can be decided in Figure 5.5 from Appendix E.23. When the buckling value reaches minimum value of first mode, the wave number n is obtained.

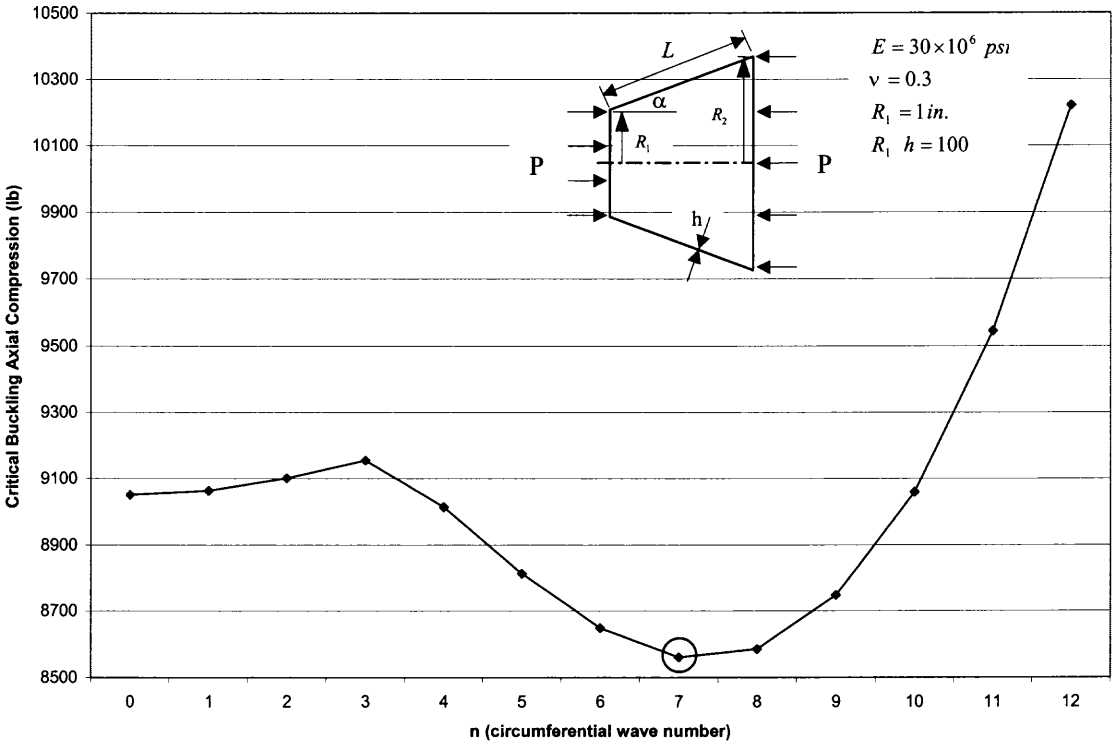

Figure 5.5 Buckling values of single layer isotropic conical shell under axial compression to decide circumferential wave number n and critical value P_{cr} for $\alpha = 30^o$ and L/R_1=0.5, SS4

When the terms of power series m become large enough in Eq. (3.18) and Eq. (3.20), the convergent condition is obtained by Tong [31]. The buckling value of single isotropic conical shell under axial compression for length ratio $L/R_1 = 1.0$ and $\alpha = 30^o$ about the term of power series m is an example in Figure 5.6. from Appendix E.27. For small m, the buckling values are diverging. The buckling values converge as m becomes large enough. For different conditions of buckling need different number of terms m. For this simulation, all calculations used 35 terms to get accurate buckling values as Figure 5.6.

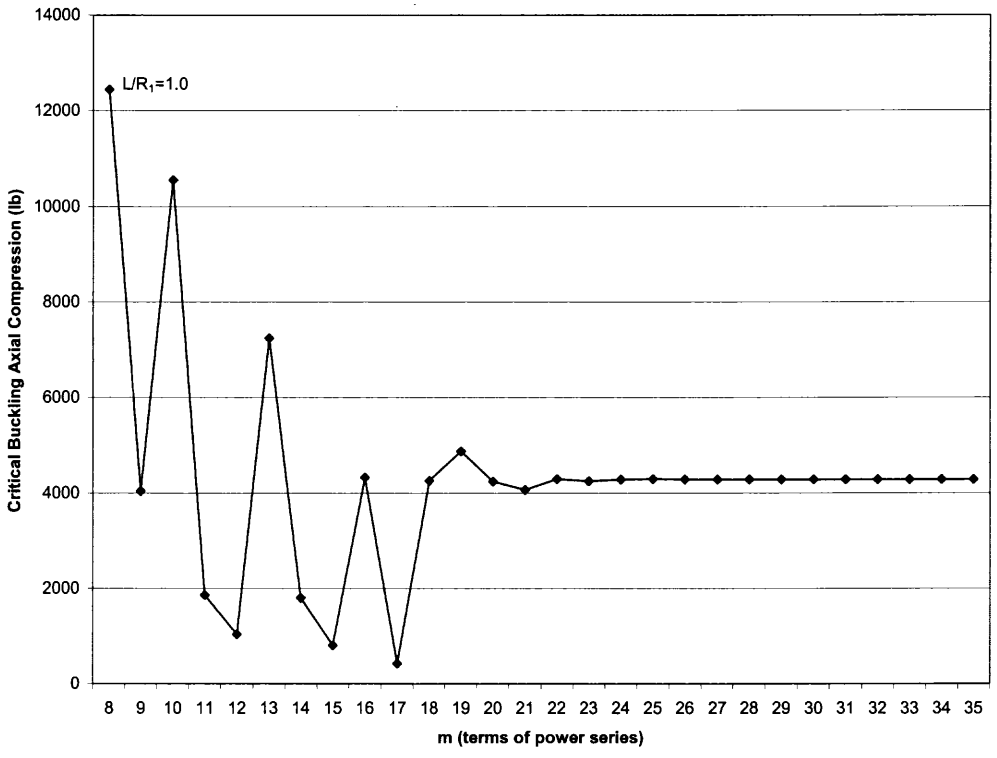

Figure 5.6 Check convergence of buckling value of single isotropic conical shell under axial compression for L/R_1=1.0 and $\alpha = 30^o$ about terms of power series m, SS1

5.3.2 Isotropic Conical Shells under Outer Pressure

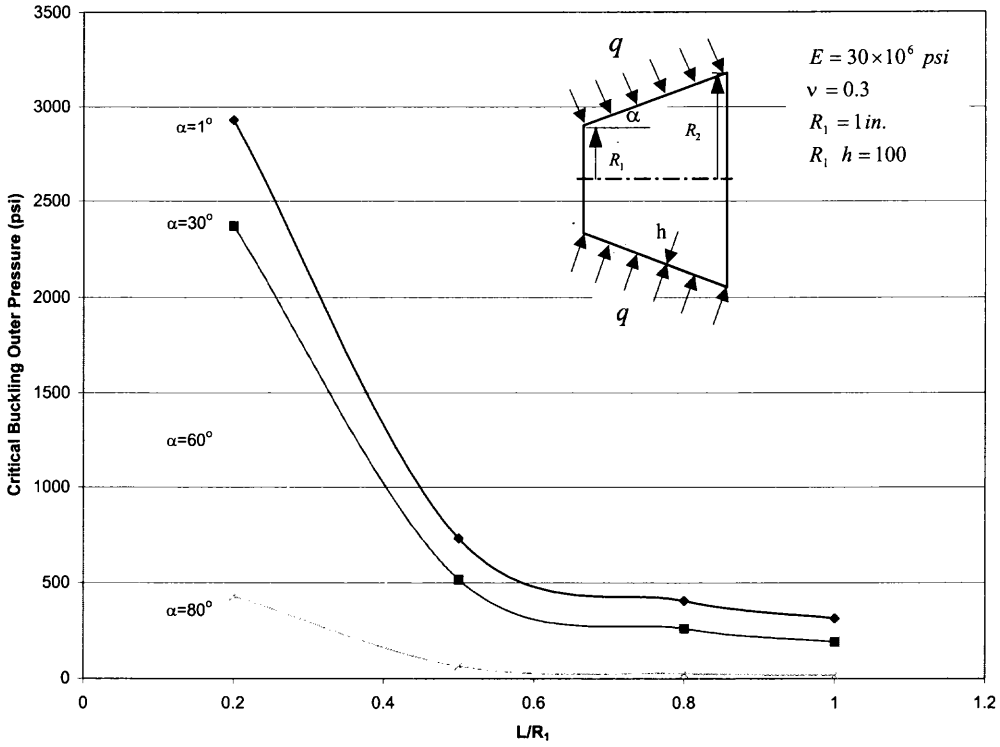

Figure 5.7 Buckling values of single layer isotropic conical shell under outer pressure for cone angles about length ratio

The buckling values of single layer isotropic conical shell under outer pressure are different according to the cone angle α in Figure 5.7 from Appendix E.2. As cone angle α increases, the buckling pressure becomes smaller. The buckling pressure tends to be constant as length ratio L/R_1 gets longer. If the length ratio is same value, sharp angle cone ($\alpha \approx 0$) is stronger than dull angle cone for outer pressure loading.

The circumferential wave number n can be obtained when the buckling value is decided with similar way as axial compression case. For the single layer isotropic conical shell under outer pressure with $\alpha = 30^o$ and $L/R_1 = 0.2$, the circumferential wave number n and buckling value q_{cr} can be decided in Figure 5.8 from Appendix E.25. When the buckling value reaches minimum value, the wave number n is decided.

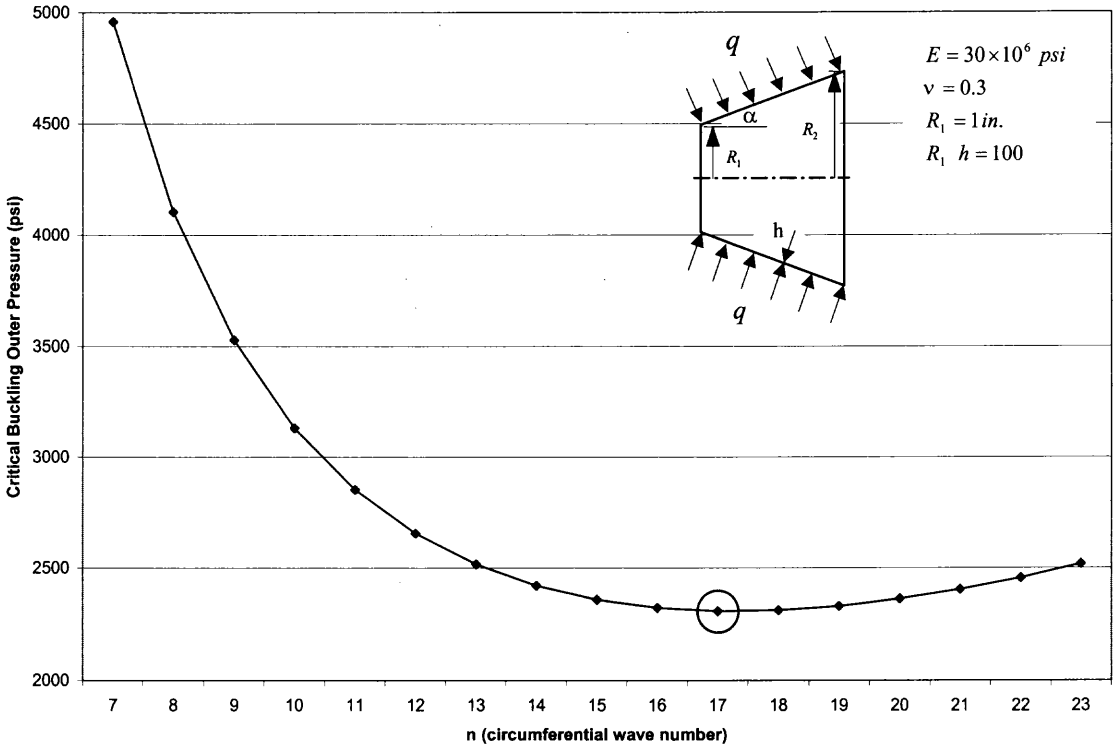

Figure 5.8 Buckling values of single layer isotropic conical shell under outer pressure to decide circumferential wave number n and critical value q_{cr} for $\alpha = 30^{o}$ and L/R_1=0.2, SS1

5.3.3 Isotropic Conical Shells in Pure Bending

The buckling values of single layer isotropic conical shells in pure bending for different length ratio are interesting. For short cone, the buckling values become small as cone angle α increases. As the length ratio becomes longer, the buckling shows unstable values for small angle region in Figure 5.9 from Appendix E.4. This trends are somewhat related to the thickness of the cone. Thinner cones with relatively long length are not so strong as short cones. The short cones, with $L/R_1 = 0.2$ and 0.5, are stable through the cone angle α in Figure 5.9. There are unstable cone angle region of $L/R_1 = 1.0$ for the thickness ratio $R_1/h = 100$. More details of long cone shows later section.

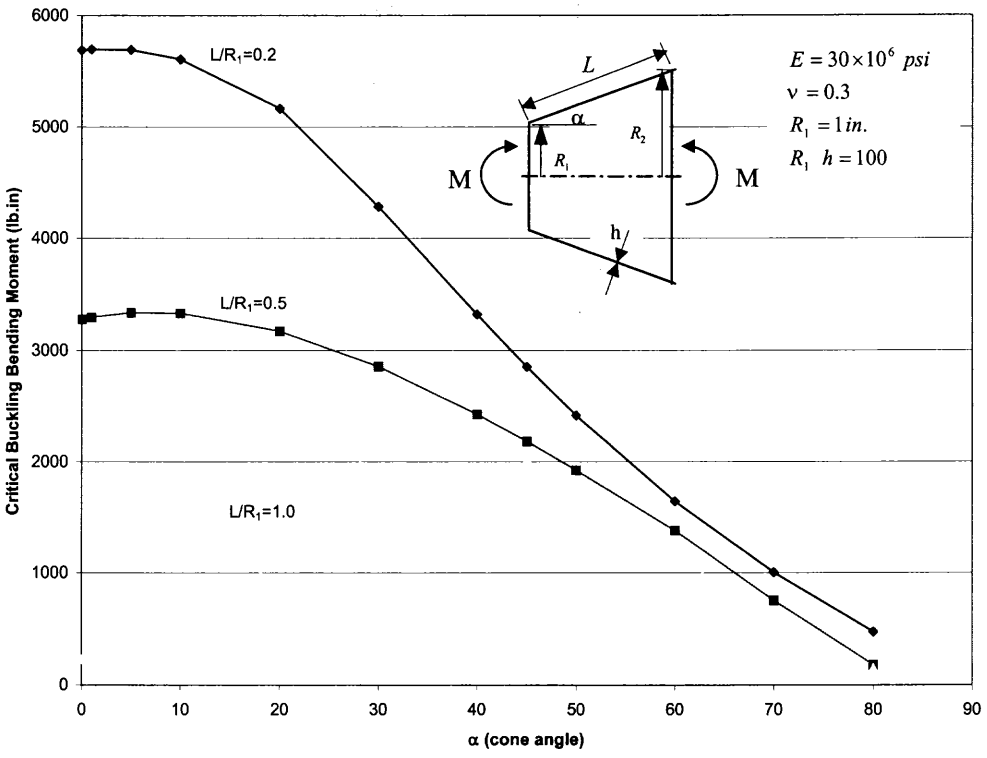

Figure 5.9 Buckling values of single layer isotropic conical shell in pure bending for different length ratio about cone angle, SS3

5.3.4 Long Isotropic Conical Shells

The length ratio (L/R_1) of a cone is an important factor for its buckling value. Short cone is usually strong but long cone needs other factors to be strong. The thickness is one of the important factor to make long cone strong. Shells of technical significance are often defined as thin when the ratio of thickness h to radius r is equal to or less then $1/20$. The buckling effects of length ratio (L/R_1) are different to the loads, axial compression, outer pressure, and pure bending. Buckling values of long cone with different Young's modulus are available in Appendix E (E.20-24). This changes do not affect much more than thickness changes.

Case A. Long Isotropic Conical Shells under Axial Compression

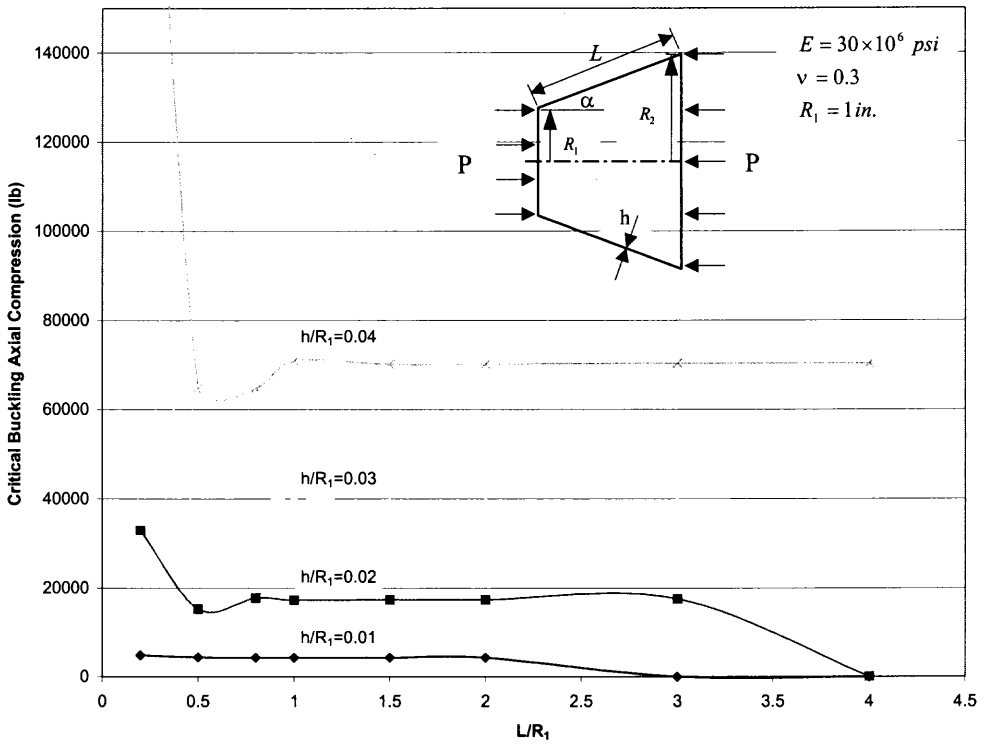

Figure 5.10 Buckling values of long single layer isotropic conical shell under axial compression for different thickness $\alpha = 30^{o}$ about length ratio L/R_1, SS2

The buckling values of single layer isotropic cone shell under axial compression in Figure 5.10 from Appendix E.18. are different for each thickness ratio (h/R_1). When the thickness ratios are 0.01 and 0.02, the buckling values are falling down to zero for certain length. The relatively thicker cones such as $h/R_1 = 0.03$ and $h/R_2 = 0.04$ have steady buckling values for the length. The values are independent of the length as cones become longer if the thickness is properly increased under axial compression. The deformed shape examples are in Figure 5.11(a) and 5.12(a) for thin shell, and Figure 5.11(b) and 5.12(b) for relatively thicker shells.

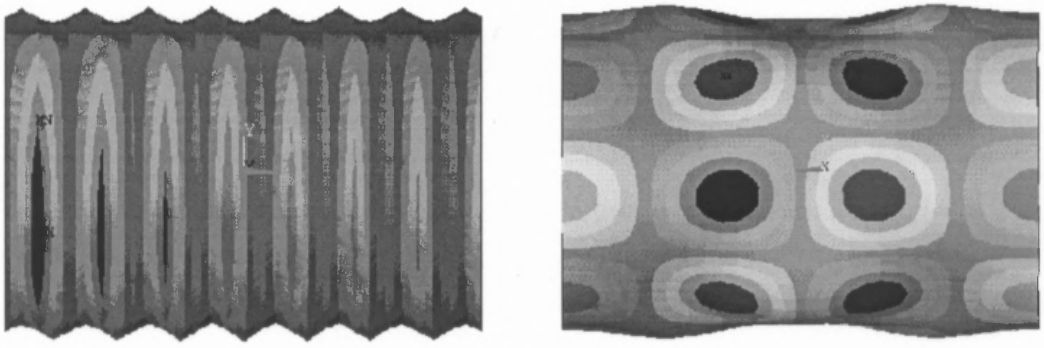

(a) (b)

Figure 5.11 Deformed shapes for relatively long cylinder L/R_1=3.0, E_x=30E6 under axial compression. (a) h/R_1=0.01, B.C(SS1) (b) h/R_1=0.05, B.C(CC3)

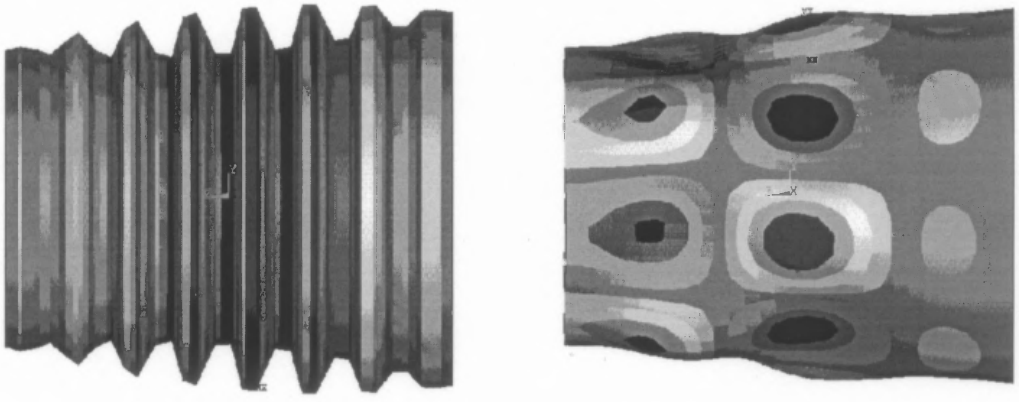

(a) (b)

Figure 5.12 Deformed shapes for relatively long cone L/R_1=3.0, E_x=30E6 under axial compression. (a) h/R_1=0.01, B.C. (SS1) (b) h/R_1=0.05, B.C. (CC3)

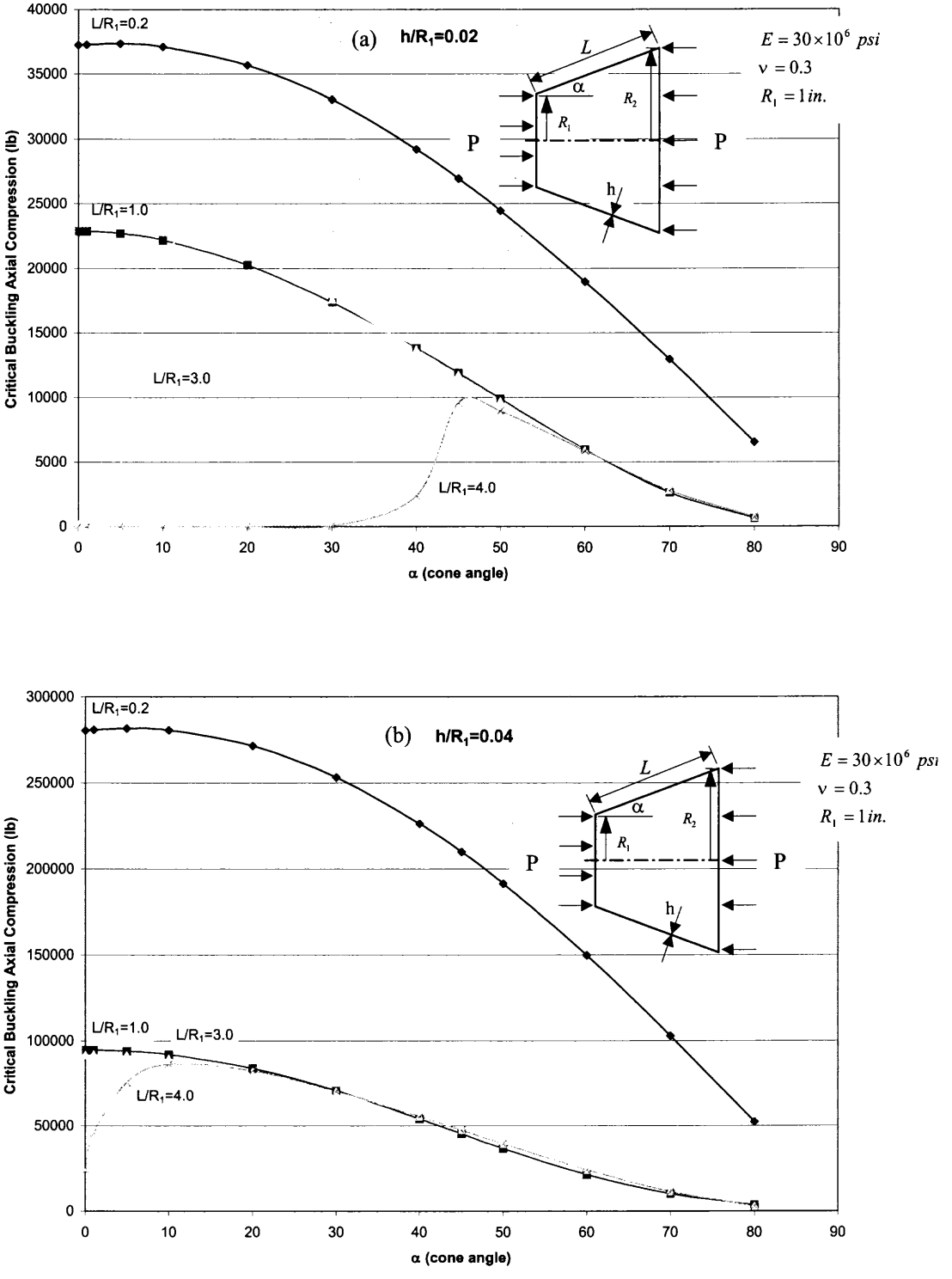

Figure 5.13 Buckling values of long single layer isotropic conical shell under axial compression for different thickness (a) h/R_1=0.02 (b) h/R_1=0.04 and length ratio L/R_1 about cone angle α ,SS2

The cone angle α is also an important parameter of different thickness ratio for buckling. For relatively thinner cone, $h/R_1 = 0.02$ in Figure 5.13(a), has different buckling values according to different length ratio L/R_1. Although there are stable conditions for $L/R_1 = 0.2$ and 1.0, the longer cones, $L/R_1 = 3.0$ and 4.0 show unstable status for some cone angle region. The longer cones can be more stable if thicker cones are used as in Figure 5.13(b). For cone shells with $L/R_1 = 3.0$ and 4.0, buckling values became stable and increased respectively in Figure 5.13(b). Therefore, the thickness is one of the important parameters for buckling values of long cones.

Case B. Long Isotropic Conical Shells under Outer Pressure

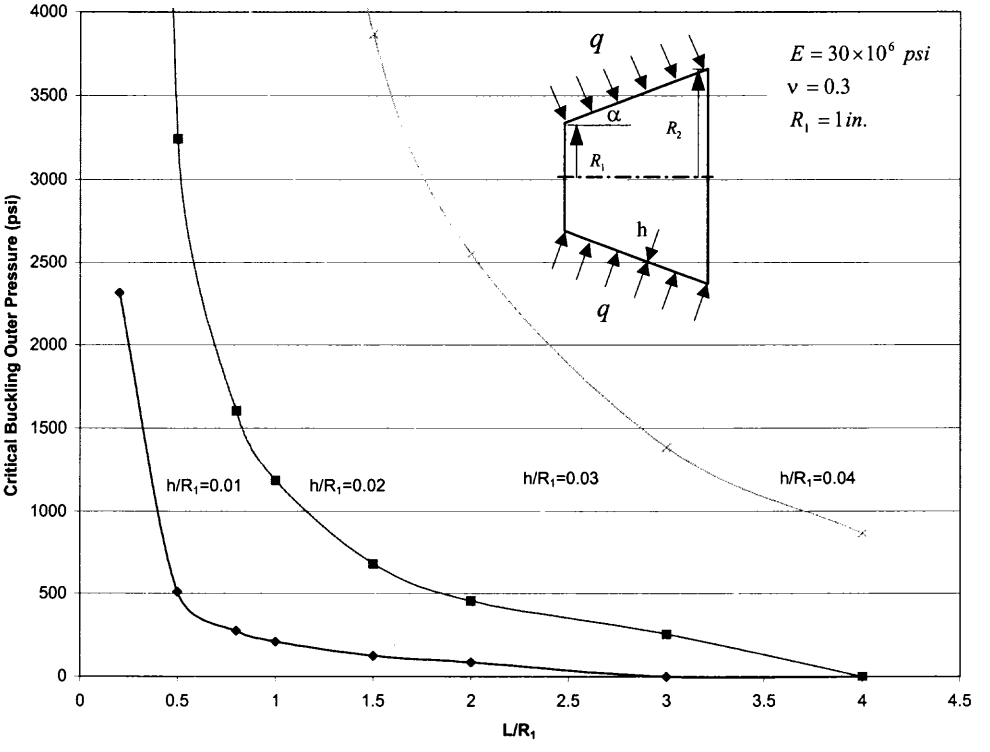

Figure 5.14 Buckling values of long single layer conical shell under outer pressure for different thickness $\alpha = 30^o$ about length ratio, SS2

The buckling values of single layer isotropic cone shell under outer pressure in Figure 5.14 from Appendix E.19 are similar as axial compression case. When the thickness ratios are thin (h/R_1 = 0.01, 0.02), the buckling values are falling down to zero for certain length. The thicker cones (h/R_1 =0.03, 0.04) have some values but with slope to down. If the buckling values under outer pressure are necessary, the thickness should be considered for the length. The deformed shape examples are in Figure 5.16(a) for thin shell, and Figure 5.16(b) for relatively thicker shell.

The buckling of outer pressure for long cone is similar as axial compression case. The cone angle α is also an important parameter of different thickness ratio for buckling. For relatively thinner cone, $h/R_1 = 0.02$ in Figure 5.15(a), has different buckling values according to different length ratio L/R_1. Although there are stable conditions for $L/R_1 = 0.2$ and 1.0, the longer cone, $L/R_1 = 3.0$ shows unstable status for some cone angle region. The buckling values for $L/R_1 = 4.0$ are near zero and unstable of whole cone angle region for this thinner ratio. The longer cones can be more stable if thicker cones are used as in Figure 5.15(b). For cone shells with $L/R_1 = 3.0$ and 4.0, buckling values became stable and increased respectively in Figure 5.15(b). Therefore, the thickness is one of the important parameters for buckling values of long cones.

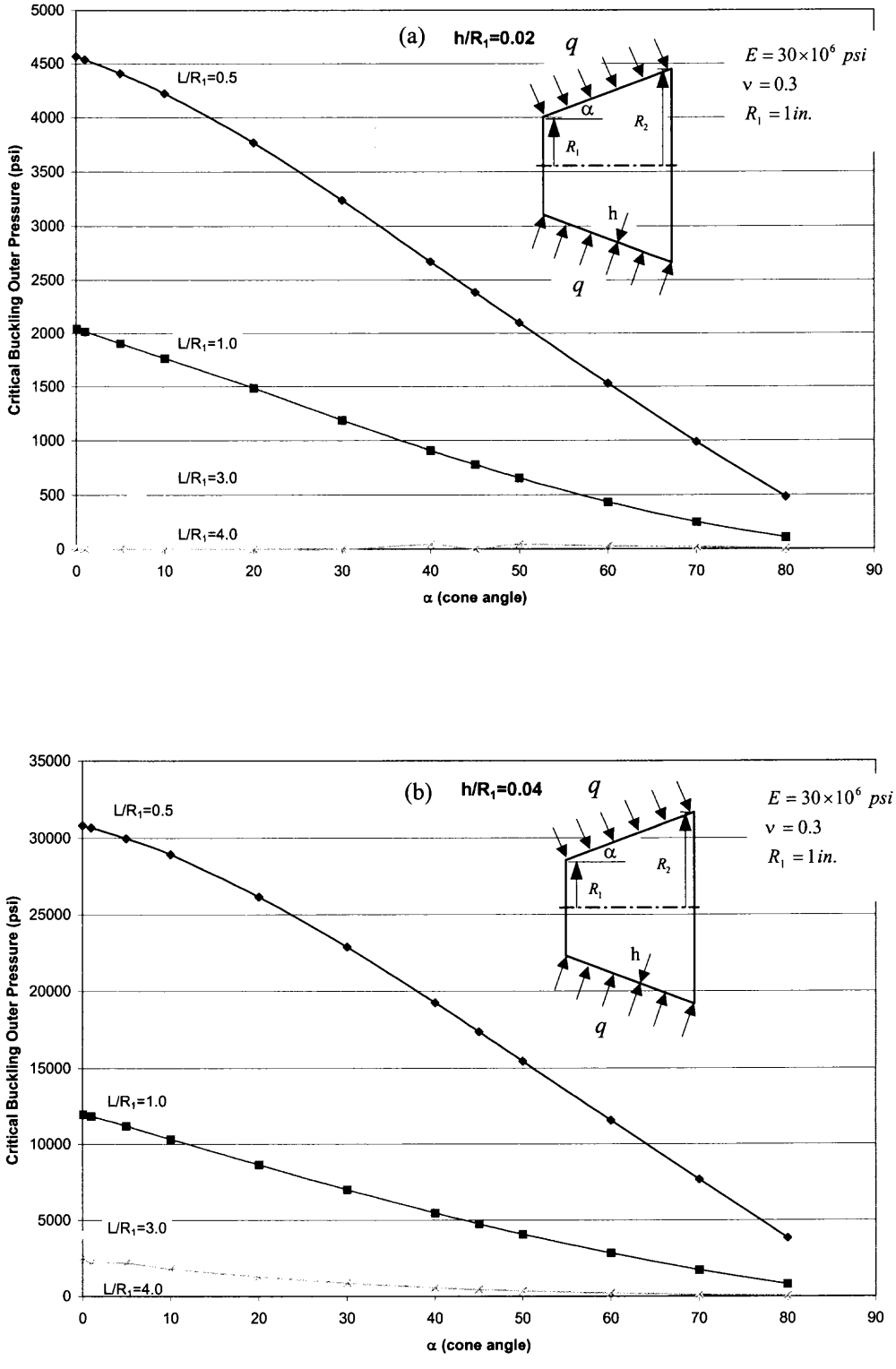

Figure 5.15 Buckling values of long single layer conical shell under outer pressure for different thickness (a) h/R_1=0.02 (b) h/R_1=0.04 and length ratio L/R_1 about cone angleα , SS2

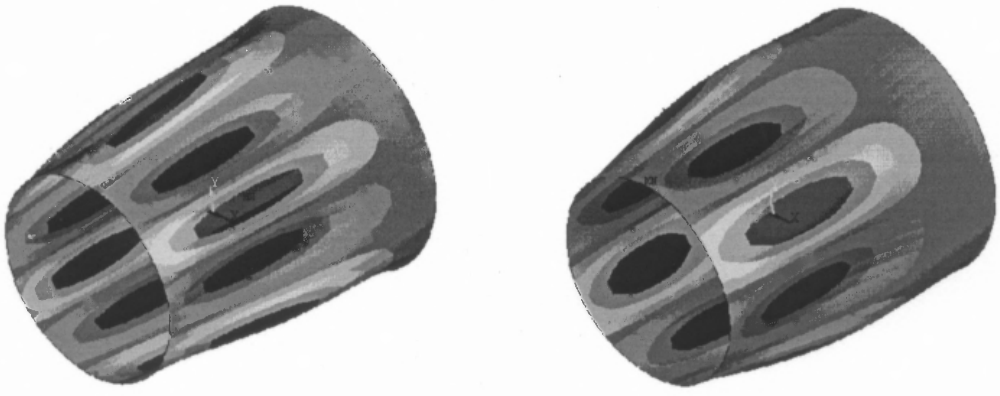

(a) (b)

Figure 5.16 Deformed shapes for relatively long cone L/R_1=3.0, E_x=30E6 under outer pressure. (a) h/R_1=0.01, B.C. (SS1) (b) h/R_1=0.05, B.C. (CC3)

Case C. Long Isotropic Conical Shells in Pure Bending

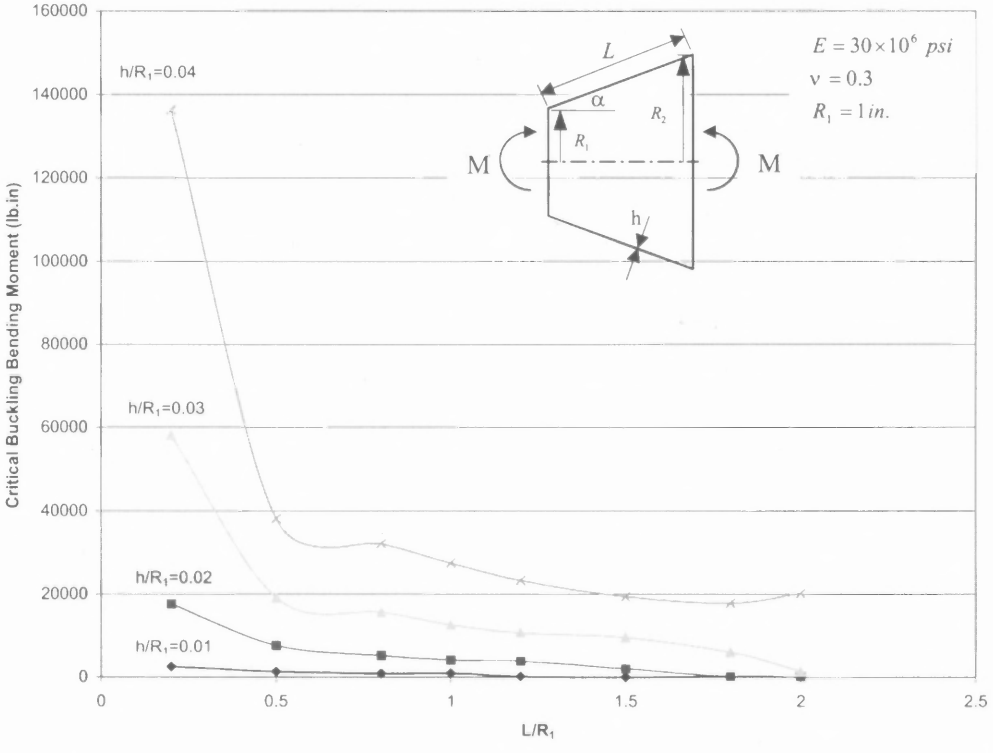

Figure 5.17 Buckling values of long single layer isotropic conical shell in pure bending for different thickness and $\alpha = 30^o$ about length ratio, SS2

For pure bending in Figure 5.17 from Appendix E.20, the buckling values of long single layer isotropic conical shell are similar to axial compression case with some differences. The buckling values of pure bending for short cone, $L/R_1 = 0.2$, are larger than other values for fixed thickness and decrease smoothly as length ratio increases. For thinner shell, $h/R_1 = 0.01$, the buckling values become near or almost zero as length ratio increases. As shell becomes thick, $h/R_1 = 0.04$, the buckling values become larger than other thickness throughout the length reaches L/R_1 =2.0 in Figure 5.17. For considering buckling values in pure bending, the thickness is one of the important factor for the length.

The buckling of pure bending for long cone is similar as axial compression and outer cases. The cone angle α is also an important parameter of different thickness ratio for buckling. In comparing with pervious two loading, the buckling of pure bending is small. Therefore a little shorter cones are used for this case. For relatively thinner cone, $h/R_1 = 0.02$ in Figure 5.18(a), has different buckling values according to different length ratio L/R_1. Although there are stable conditions for $L/R_1 = 0.2$, 0.5, and 1.0, the longer cone, $L/R_1 = 1.8$ shows unstable status for some cone angle region. The buckling values for $L/R_1 = 1.8$ are near zero and unstable of some cone angle region for this thinner ratio. The longer cones can be more stable if thicker cones are used as in Figure 5.18(b). For cone shells with $L/R_1 = 1.8$, buckling values increase stability but still unstable cone angle region is exist in Figure 5.18(b). To obtain buckling values of pure bending for long cones, the thickness is more important than other two loads.

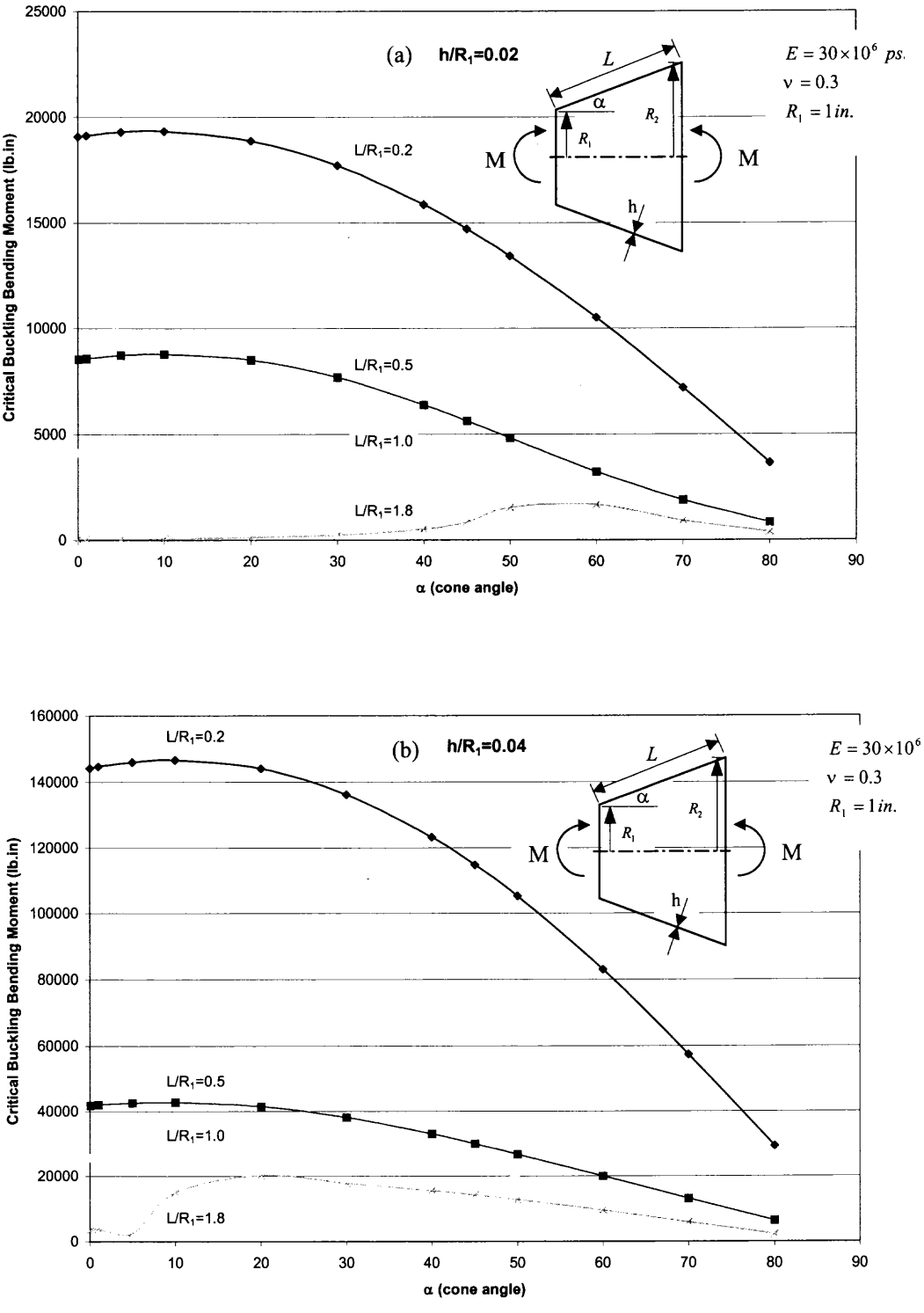

Figure 5.18 Buckling values of long single layer isotropic conical shell in pure bending for different thickness (a) h/R_1=0.02 (b) h/R_1=0.04 and length ratio L/R_1 about cone angle α , SS2

5.3.5 Isotropic Conical Shells under Combined Loads

The way of applying combined load is consist of two parts. First, apply pre-load for some different rates of buckling load for each cone angle α , length ratio L/R_1 and other cases. Second, calculate the buckling loads using simulation program for each case of pre-load. The loading coupled axial compression with outer pressure, pure bending moment with axial compression, and pure bending moment with outer pressure.

Case A. Combined Loads for Outer Pressure and Axial Compression

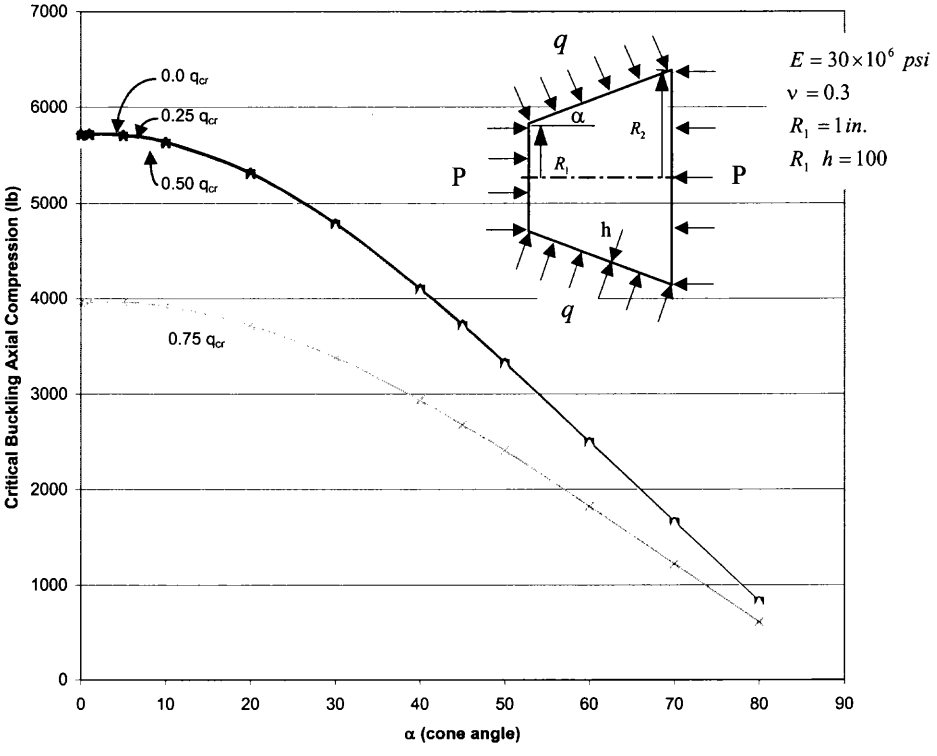

Figure 5.19 Buckling values of single isotropic conical shell under axial compression with different rate outer pressure for L/R_1=0.2 about cone angle, SS2

The buckling values of single isotropic conical shell under axial compression combined with outer pressure are in Figure 5.19 from Appendix E.6. The pre-applied pressure

doesn't make big change for the 25% and 50% of its own buckling values (q_{cr}) for the cone angle α. After 50% of buckling pressure (q_{cr}), the axial compression buckling values (P_{cr}) are decreased more than other pre-pressure loading. Therefore axial compression buckling values are not sensitive to outer pre-pressure of lower percentage.

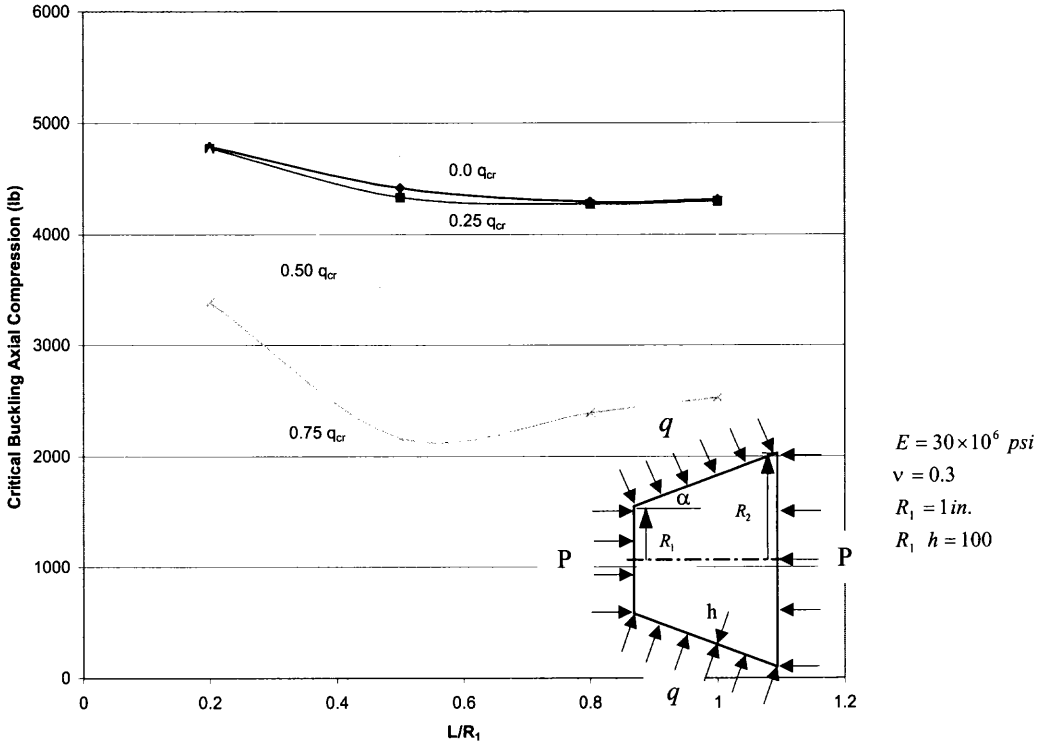

Figure 5.20 Buckling values of single layer isotropic conical shell in pure bending with different axial pre-compression for $\alpha = 30^{o}$ about length ratio, SS2

For buckling values of single layer isotropic conical shell in pure bending with different axial pre-compression, the trend is similar to previous case in Figure 5.20 from Appendix E.6. The pre-applied pressure shows little change for the 25% of its own buckling values (q_{cr}) for the length ratio L/R_1. After that percentage, axial compression values become sensitive to outer pre-pressure.

Case B. Combined Loads for Axial Compression and Pure Bending

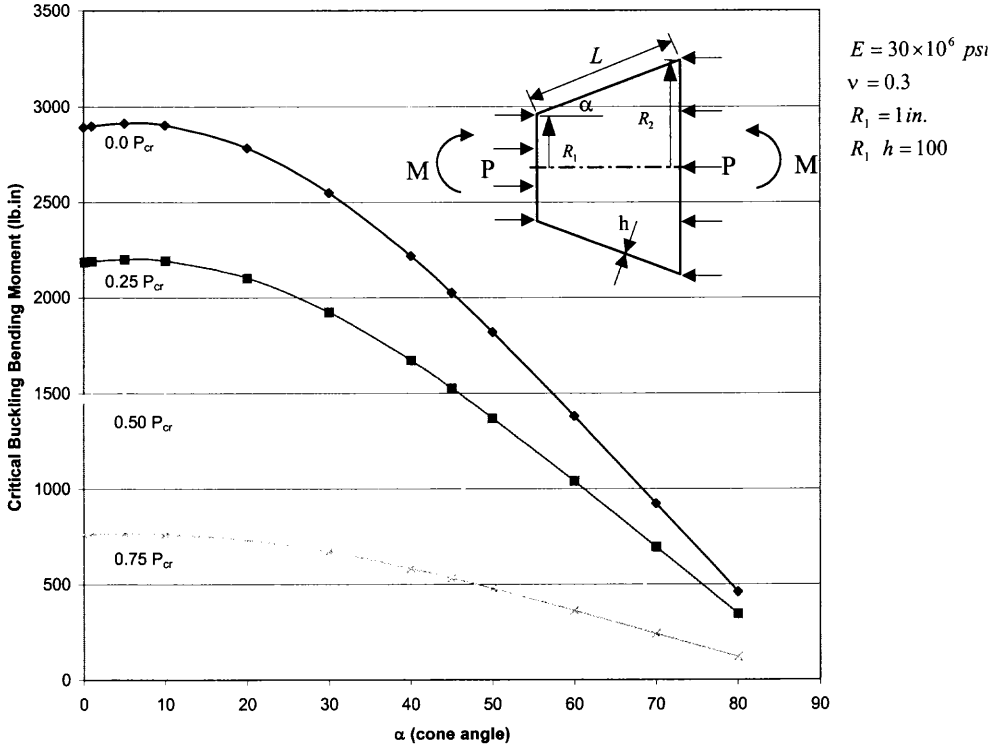

Figure 5.21 Buckling values of single layer isotropic conical shell in pure bending with axial pre-compression for length ratio, L/R_1=0.2 about cone angle α , SS2

The buckling values of single layer isotropic conical shell in pure bending with axial pre-compression are somewhat different from previous case in Figure 5.21 from Appendix E.7. For the previous outer pressure and axial compression case, there are sensitive and insensitive regions about outer pre-pressure. The pre-applied loads and buckling values are changed similar pattern to axial pre-compression and pure bending. This means that the effect of axial pre-compression changes the buckling values of bending moment almost linearly.

Case C. Combined Loads for Outer Pressure and Pure Bending

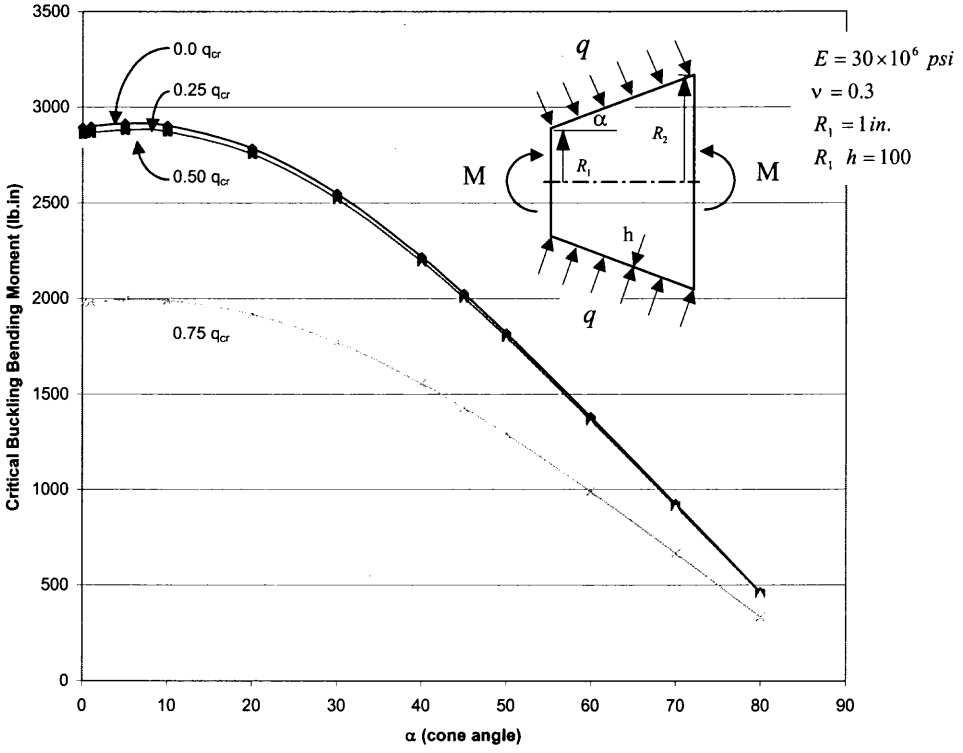

Figure 5.22 Buckling values of single layer isotropic conical shell in pure bending with outer pre-pressure for length ratio, L/R_1=0.2 about α , SS2

The buckling values of single layer isotropic conical shell in pure bending with outer pre-pressure are similar to outer pre-pressure and axial compression in Figure 5.22 from Appendix E.8. For the 25% and 50% of outer pre-pressure of (q_{cr}), the buckling values of bending are insensitive. After 50% of pre-pressure of it, the pure bending buckling values (M_{cr}) are decreased more and more. This means that the buckling values of pure bending are not sensitive to outer pre-pressure at the lower percentage of it.

5.3.6 Isotropic Conical Shells Compare with Cylinder Case

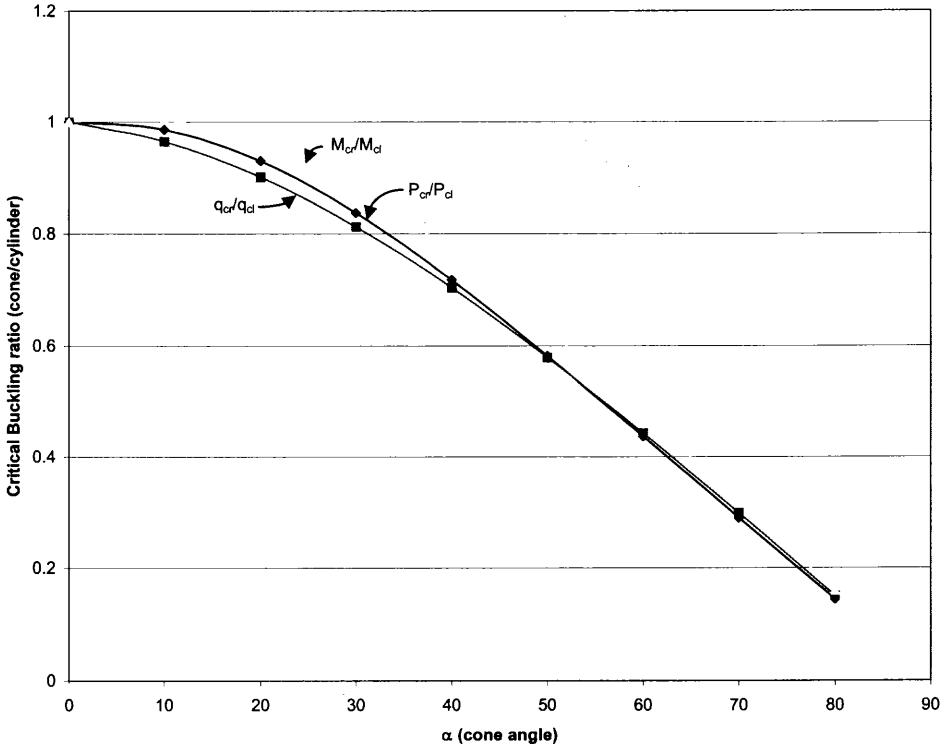

Figure 5.23 Buckling ratio of single layer isotropic conical and cylindrical shell under axial compression, outer pressure, and pure bending for length ratio, L/R_1=0.2 about angle, SS2

The buckling ratios of single layer isotropic conical to cylindrical shell under axial compression, outer pressure, and pure bending show in Figure 5.23 from Appendix E.5. The ratios of three loading decreases almost similar trend about cone angle α . For axial compression, the ratios are higher than outer pressure ratios as cone angle α increases to around 50 degrees. From that angle, the ratios of axial compression are smaller than that of outer pressure. The ratios of pure bending are usually higher than that of other loadings. For the three cases of ratios, pure bending case is the most effective, and axial compression case is better than outer pressure before 50 degree cone angle. After 50 degrees, outer pressure case is more effective than axial compression case.

5.3.7 Isotropic Conical Shells for Different Radius with Same R_1/h

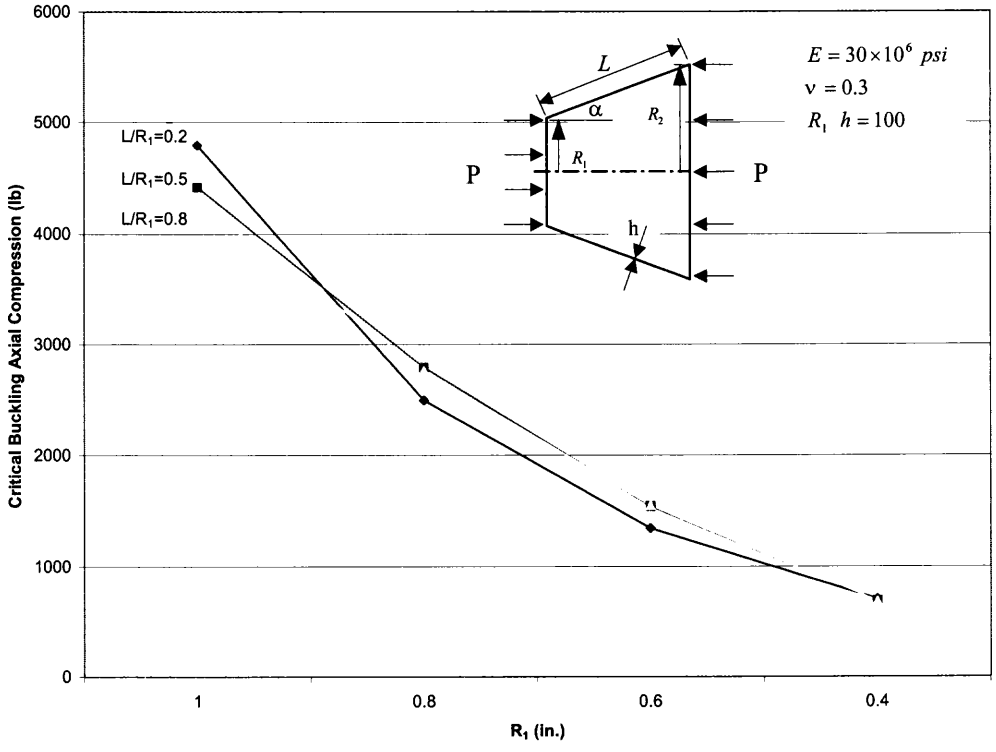

Figure 5.24 Buckling values of single layer isotropic conical shell under axial compression for L/R_1 and cone angle $\alpha = 30^o$ with same R_1/h=100 ratio about different radius R_1, SS2

For the buckling values of single layer isotropic conical shell under axial compression, the radius also a parameter. The buckling values are different for radius R_1 with keeping the ratio $R_1/h = 100$. If R_1 is decreased, the thickness h also becomes smaller in Figure 5.24 from Appendix E.26. The absolute buckling values of cone are dependent on the size of radius R_1. Although the cone with same R_1/h ratio, the buckling values can be extremely large or small for different radius. For the shorter cone, the buckling values decrease nonlinearly as radius R_1 decreases. As cones become longer, the buckling values decrease near linear.

5.4 Numerical Solutions for Orthotropic Shells

The buckling of orthotropic material is the same way as previous procedure. For orthotropic material, the direction of strength should be considered. Graphite/epoxy is used and orthotropy ratio range E_ϕ / E_x (1/40 ~ 1) is adopted.

5.4.1 Orthotropic Shells under Axial Compression

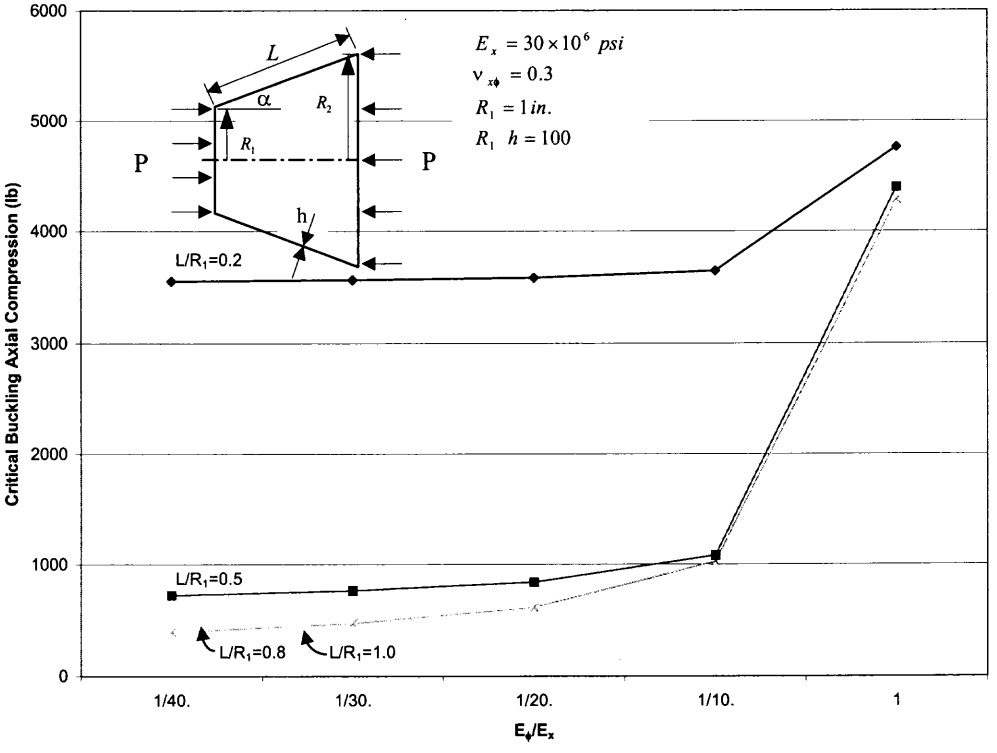

Figure 5.25 Buckling values of single layer orthotropic conical shells under axial compression for length ratio at $\alpha = 30^\circ$ about E_ϕ / E_x ratio, SS1

Orthotropic material is also important for buckling. Buckling values of single layer orthotropic cone shells under axial compression at $L/R_1 = 0.2$ are steady and longer cones ($L/R_1 = 0.5, 0.8, 1.0$) are similar trends as short cone for the orthotropy ratio range E_ϕ / E_x (1/40 ~ 1/10). For the range E_ϕ / E_x (1/10 ~ 1), the buckling values increase all

length ratio in Figure 5.25 from Appendix E.9. The buckling values of longer cones increase abruptly even though the absolute values are not so large as short cones.

5.4.2 Orthotropic Shells under Outer Pressure

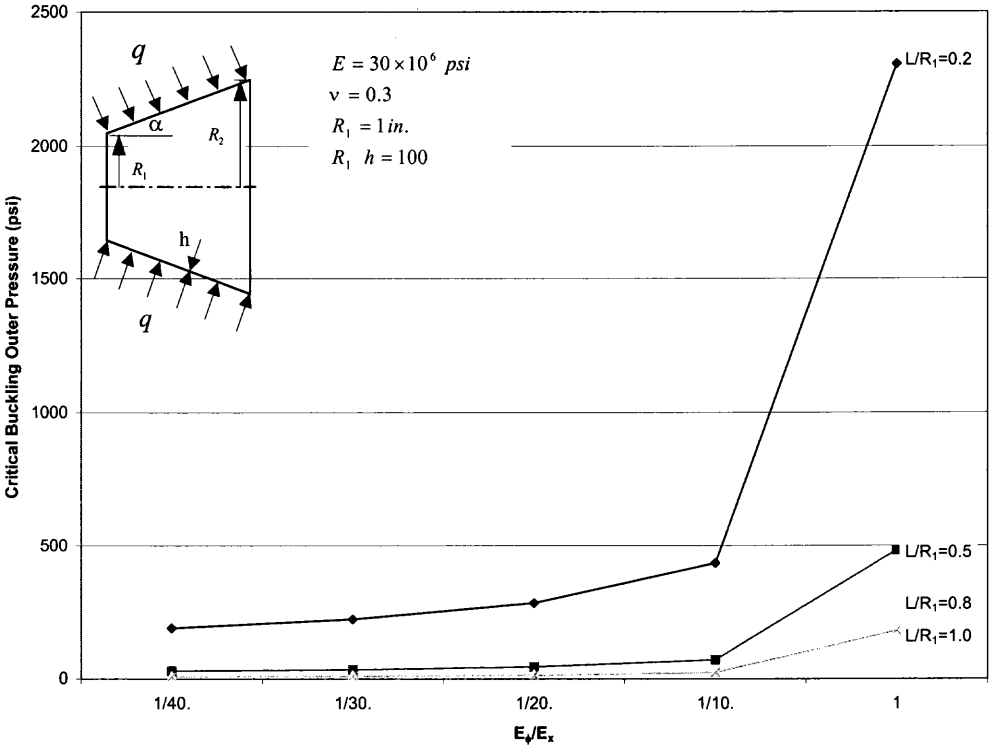

Figure 5.26 Buckling values of single layer orthotropic conical shells under outer pressure for length ratio at $\alpha = 30^{o}$ about E_{ϕ}/E_{x} ratio, SS1

Buckling values of single layer orthotropic cone shells under outer pressure at $L/R_1 = 0.2$ are not increasing much and longer cones ($L/R_1 = 0.5, 0.8, 1.0$) are almost constant for the orthotropy ratio E_{ϕ}/E_{x} (1/40 ~ 1/10). For the range E_{ϕ}/E_{x} (1/10 ~ 1), the buckling values increase for all length ratio. Although the buckling values of longer cones increase little, the values of short cone increase dramatically in Figure 5.26 from Appendix E.10. Comparing with axial loading, the length ratio acts sensitively, especially for short cone.

5.4.3 Orthotropic Shells in Pure Bending

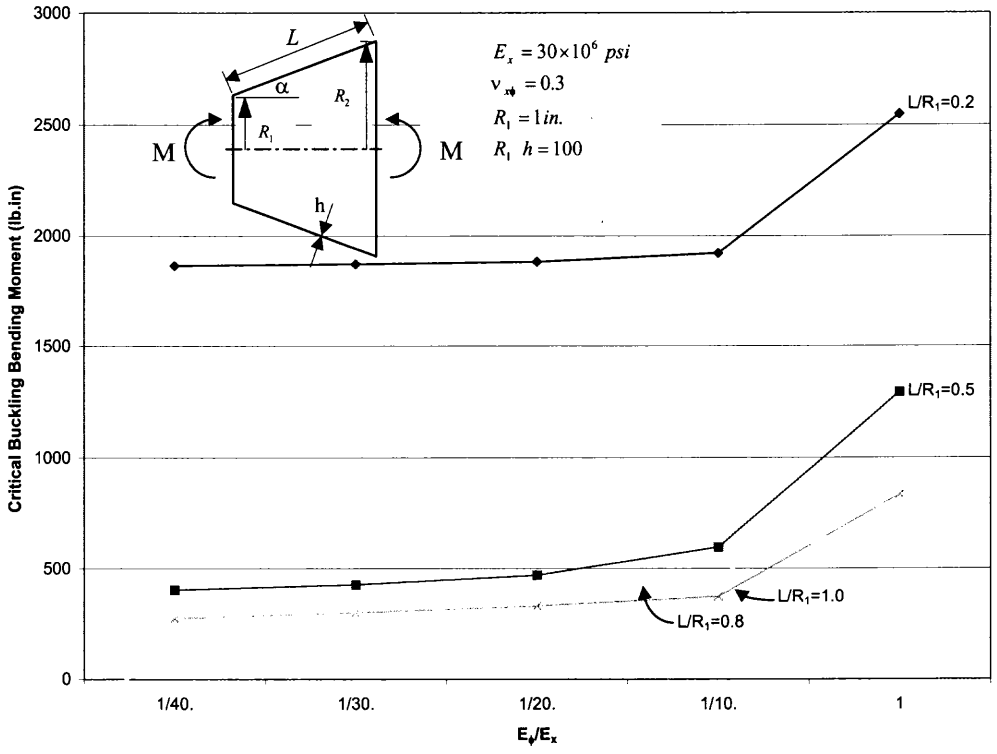

Figure 5.27 Buckling values of single layer orthotropic conical shell in pure bending for different length ratio, and $\alpha = 30^o$ about E_ϕ / E_x, SS1

The buckling values of single layer orthotropic conical shell in pure bending for different length ratio about orthotropy ratio, E_ϕ / E_x are in Figure 5.27 from Appendix E.11. The orthotropic cone shells under pure bending at $L/R_1 = 0.2$ are steady with large values and longer cones ($L/R_1 = 0.5, 0.8, 1.0$) are similar trends with small values for the orthotropy ratio range E_ϕ / E_x (1/40 ~ 1/10). For the range E_ϕ / E_x (1/10 ~ 1), the buckling values increase all length ratio.

5.5 Numerical Solutions for Multilayered Composite Conical Shells

A set of laminated cone with antisymmetric even number cross-ply cones in Figure 4.1 and 4.4 (or $\overline{N}$ layered conical shell) are numerically studied. The laminae oriented angles 0^o and 90^o are also considered in Figure 4.3 (a). The coefficients, A_{ij}, B_{ij}, and D_{ij}, in the constitutive Eq. (4.6) for this lamination are partly different according to the layers conditions.

5.5.1 Multilayered Composite Conical Shells under Axial Compression

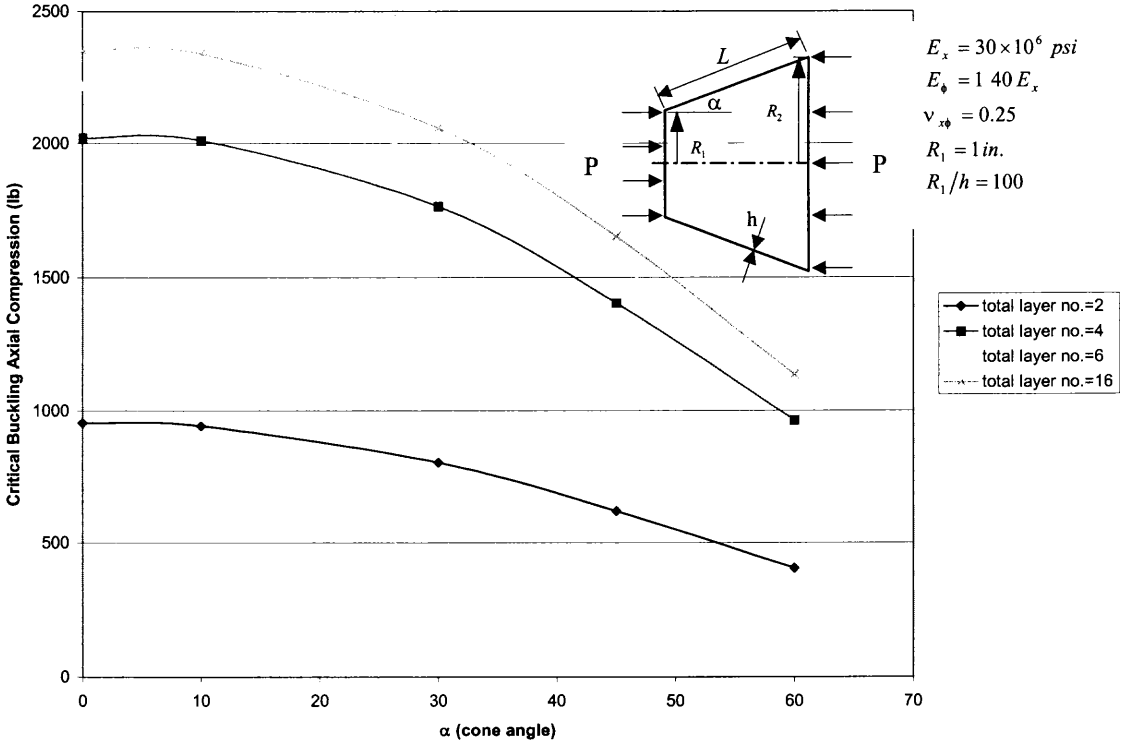

Figure 5.28 Buckling value of multi layer orthotropic conical shell under axial compression for layers about cone angle, SS1

The buckling values of multi layer orthotropic conical shells under axial compression are affected by the number of layers. The buckling values increase as the number of layers

increase in Figure 5.28 from Appendix E.12. In comparing with other increment of layer number, the buckling values increase large as layer number changes from 2 to 4. All the buckling values decrease as cone angle α increases.

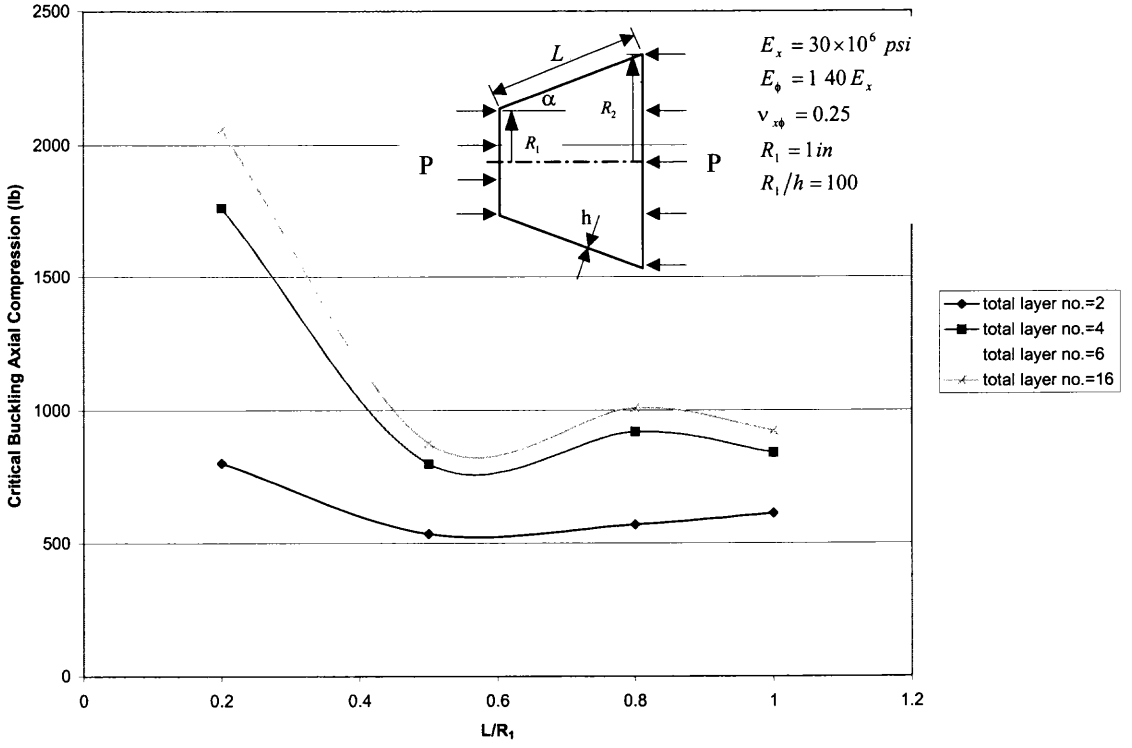

Figure 5.29 Buckling values of multi layer orthotropic conical shell under axial compression for layer no. and α = 30° about length ratio, SS1

The buckling values of multi layer orthotropic conical shell under axial compression are affected by length ratio L/R_1. The buckling values increase as the number of layers increase in Figure 5.29 from Appendix E.12. In comparing with other increment of layer number, the buckling values increase largest as layer number changes from 2 to 4. The trends of buckling values for length ratio $L/R1$ are similar as single layer. For short length ratio region, the buckling values become large. The buckling values tend to be constant as the length ratios become longer.

5.5.2 Multilayered Composite Conical Shells under Outer Pressure

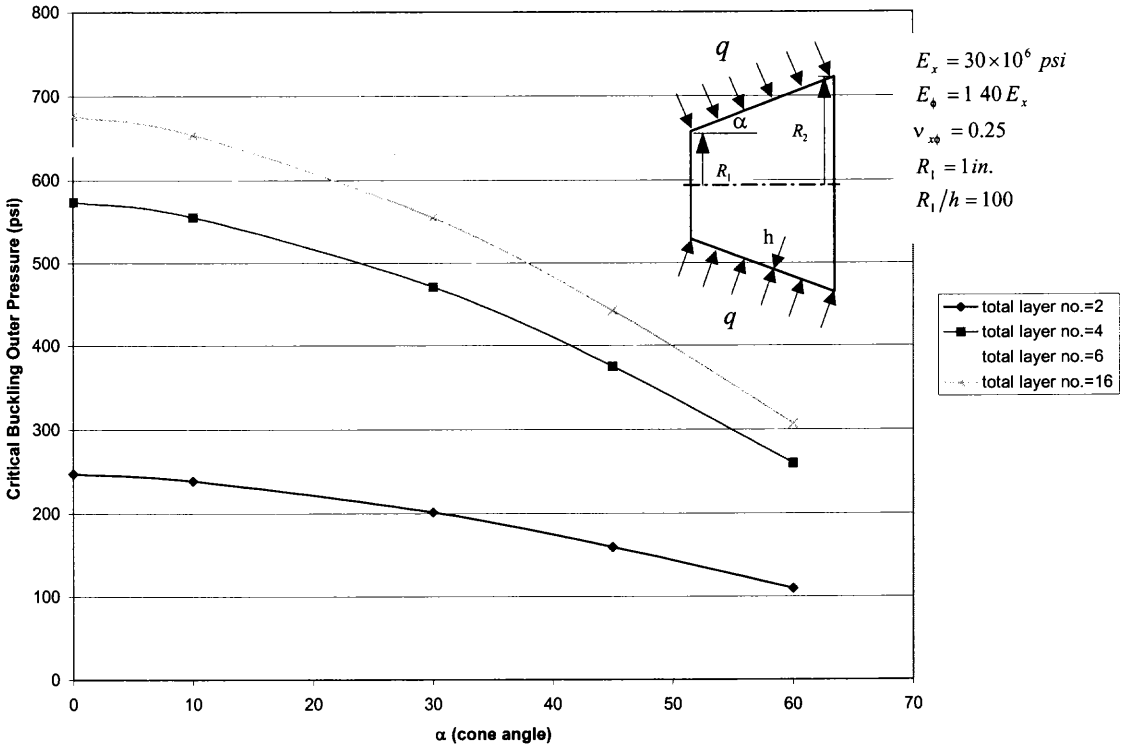

Figure 5.30 Buckling values of multi layer orthotropic conical shell under outer pressure for layer no. about cone angle, SS1

The buckling values of multi layer orthotropic conical shells under outer pressure are affected by the number of layers. The buckling values increase as the number of layers increase. The coupling of two layers in the cone reduces the buckling load. In comparing with other increments of layer number, the buckling values increase large as layer number changes from 2 to 4. All the buckling values decrease as cone angle α increases in Figure 5.30 from Appendix E.13.

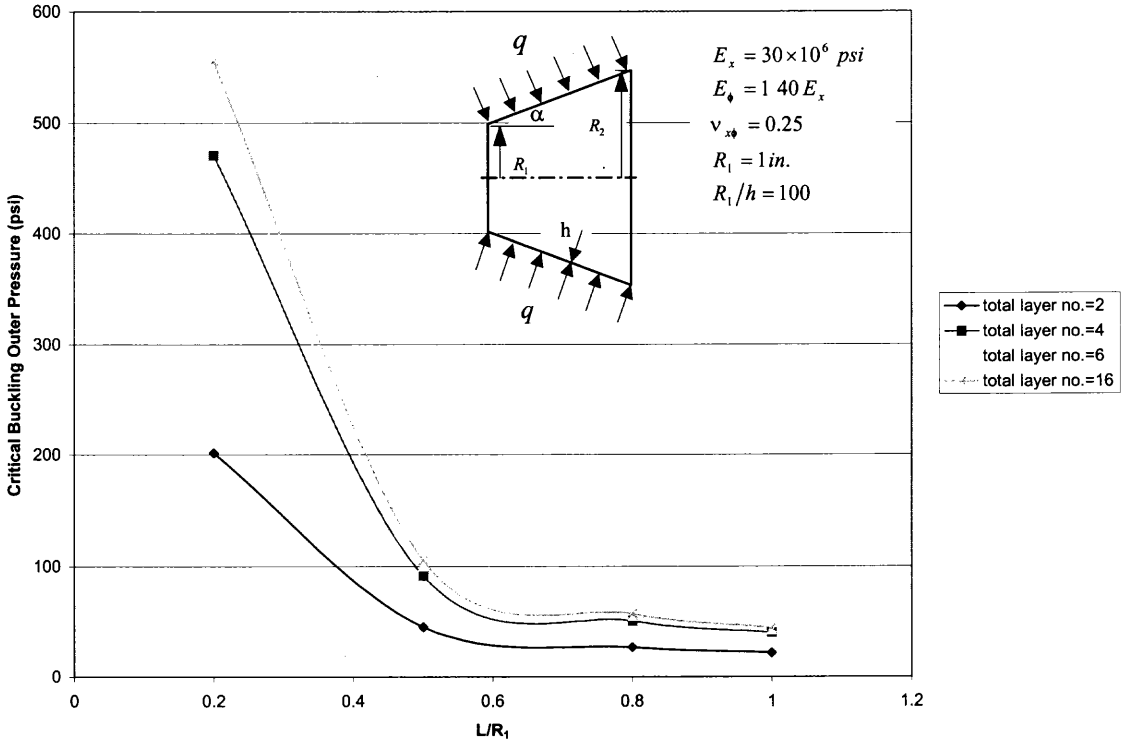

Figure 5.31 Buckling values of multi layer orthotropic conical shell under outer pressure for layer no. and $\alpha = 30^o$ about length ratio, SS1

The buckling values of multi layer orthotropic conical shell under outer pressure are affected by length ratio L/R_1. The buckling values increase as the number of layers increase. In comparing with other increment of layer number, the buckling values increase largest as layer number changes from 2 to 4. The trends of buckling values for length ratio $L/R1$ are similar as single layer. For short length ratio regions, the buckling values become large. The buckling values tend to be constant as the length ratios become longer in Figure 5.31 from Appendix E.13.

5.5.3 Multilayered Composite Conical Shells in Pure Bending

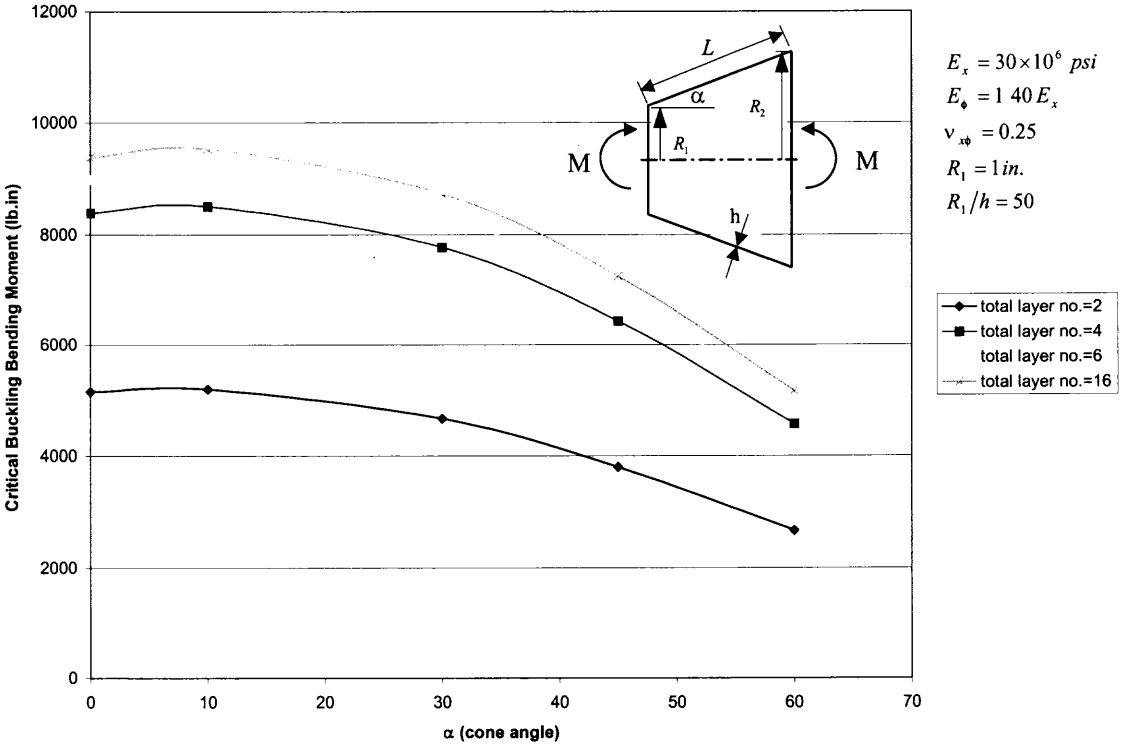

Figure 5.32 Buckling values of multi layer orthotropic conical shell in pure bending for layers about cone angle, SS1

Buckling values of multi layer orthotropic conical shell in pure bending increase as the number of layers become larger in Figure 5.32 from Appendix E.14. The buckling values are changed largest for layer number from 2 to 4. The trends are similar to outer pressure loading case as cone angle changes.

Buckling values of multi layer orthotropic conical shell in pure bending are interesting for different length ratio. The influence of bending-extension coupling is to reduce for the buckling load for two-layer cone. The maximum buckling values occur around length ratio, $L/R_1 = 0.8$ in Figure 5.33 from Appendix E.14. The largest change occurs for the layer number from 2 to 4 like other loads.

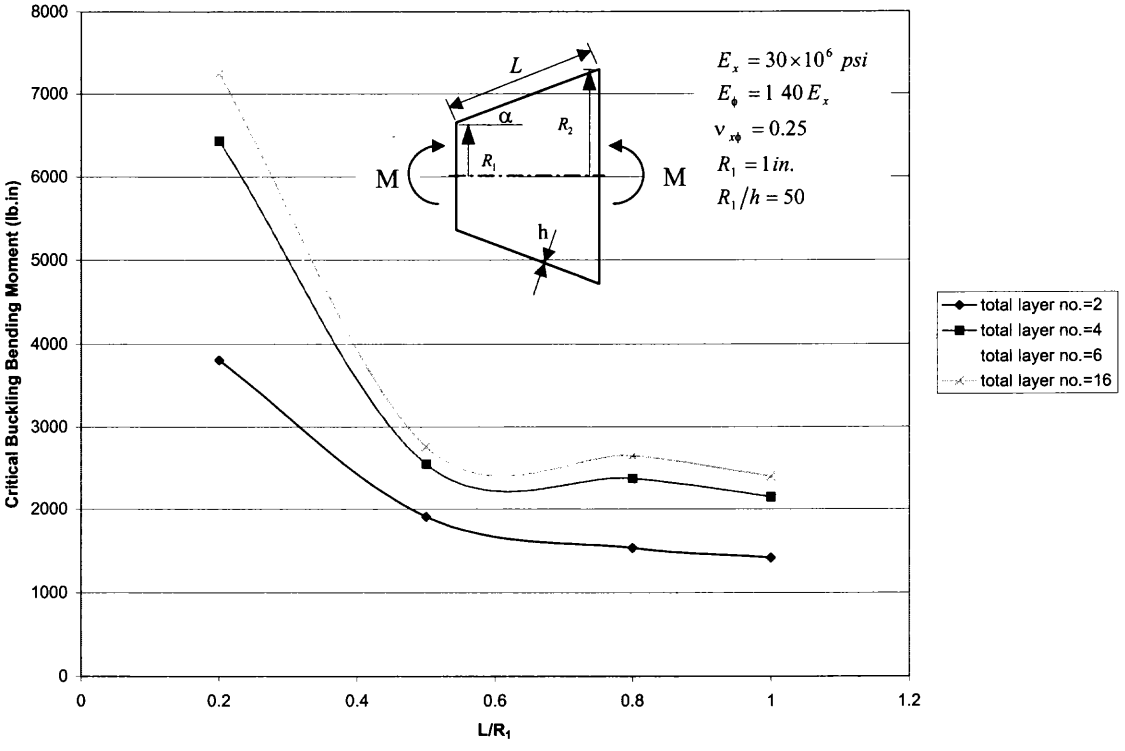

Figure 5.33 Buckling values of multi layer orthotropic conical shell in pure bending for layer numbers and $\alpha = 45^o$ about length ratio, SS1

5.5.4 Multilayered Composite Conical Shells under Combined Loads

Like single layer case, the way of applying combined load is consist of two parts. First, apply pre-load for several different rates of buckling load for each cone angle α , length ratio L/R_1 , different number of layers and other cases. Second, calculate the buckling loads using simulation program for each case of pre-load. The loading coupled axial compression with outer pressure, pure bending moment with axial compression, and pure bending moment with outer pressure.

Case A. Combined Loads for Outer Pressure and Axial Compression

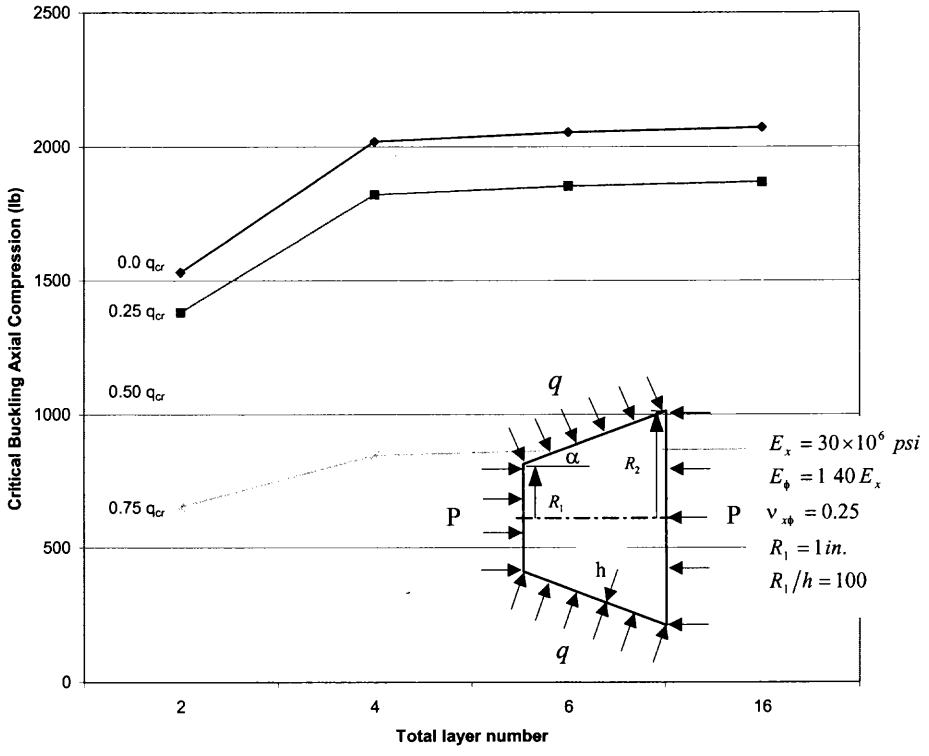

Figure 5.34 Buckling values of multi layer orthotropic conical shell under axial compression with outer pre-pressure about number of layers at $\alpha = 30^{o}$, SS2

The buckling of multi layer orthotropic conical shell under combined loading with axial compression and outer pressure shows in Figure 5.34 from Appendix E.15. An axial compressive load P, in pounds, and uniform outer pressure q, in pounds per square inch. The external pressure is applied for each rate of critical pressure q_{cr} for number of layer. For 25% of q_{cr}, the buckling values of axial compression P_{cr} are similar to the values without any pre-pressure. For the pre-load of outer pressure, the second half of q_{cr} is more sensitive than that of first half. In comparing with other increments of layer number, the buckling values are increased large as layer number changes from 2 to 4.

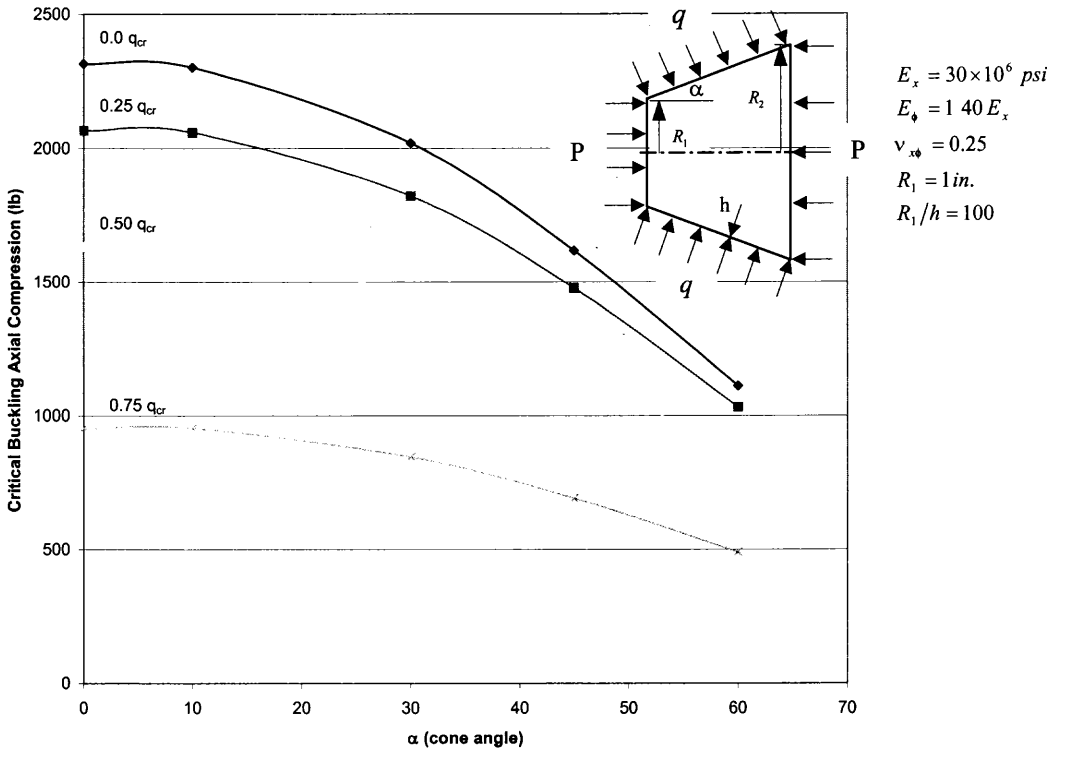

Figure 5.35 Buckling values of multi layer orthotropic conical shell under axial compression with outer pre-pressure for number of layer=4 and L/R_1=0.2 about cone angle, SS2

The combined buckling values of multi layer conical shells with axial compression and outer pressure for the fixed number of layer show in Figure 5.35 from Appendix E.15. For the total layer number 4, length ratio $L/R_1 = 0.2$, the buckling values are similar trends to single layer case about cone angle α. When pre-applied outer pressure rate is 25%, the axial compression buckling values are not so much changed as that of without pre-load. After the first 25% of pre-applied outer pressure, every 25% increment affects more and more. This means that the effect of outer pressure is little at the lower pre-pressure. The outer pre-pressure is sensitive to higher pre-pressure for combined with axial compression.

Case B. Combined Loads for Axial Compression and Pure Bending

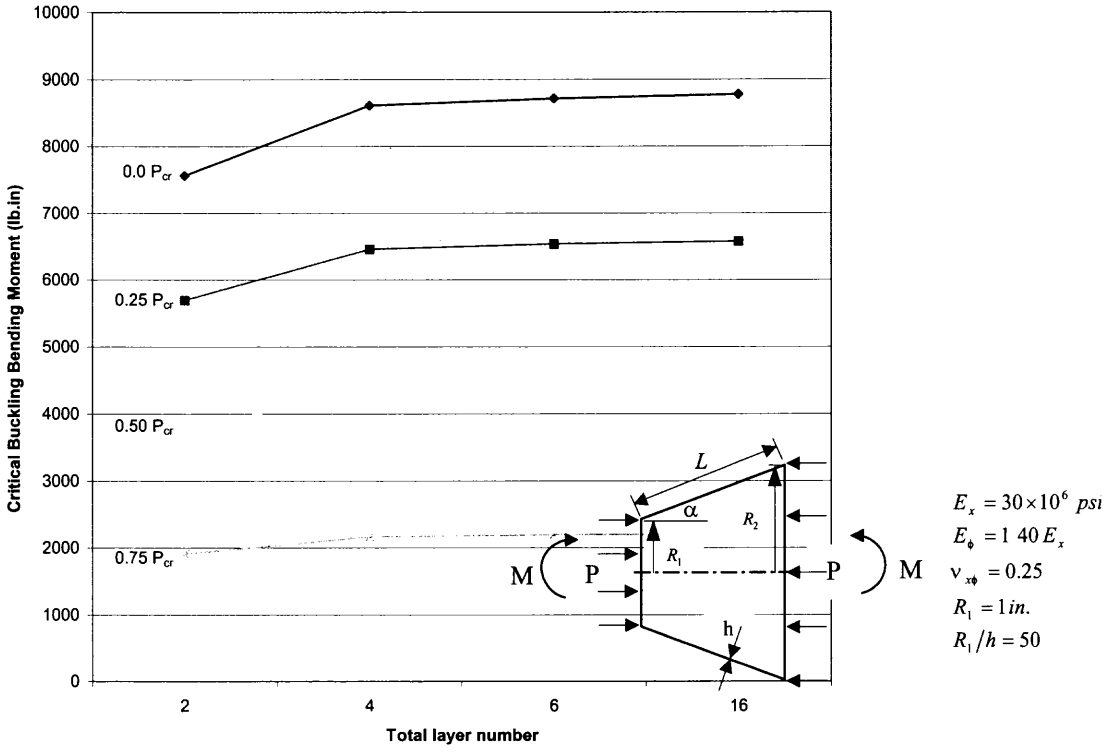

Figure 5.36 Buckling values of multi layer orthotropic conical shell in pure bending with axial pre-compression for L/R_1=0.2 and $\alpha = 30^{o}$ about number of layer, SS2

The buckling of multi layer orthotropic conical shell under combined loading with axial compression and pure bending is in Figure 5.36 from Appendix E.16. An axial compressive load P, in pounds, and bending moment M, in pounds inch. The axial compression is applied for each rate of critical buckling values P_{cr} for different cone angle α and number of layer. Every 25% increment affects similar rate change to buckling value of pure bending. This means that the effect of pre-axial compression changes the buckling values of bending moment almost linearly. This trend is different from combined axial compression with outer pressure case in Figure 5.33. In comparing

with other increment of layer number, the buckling values also increase large as layer number changes from 2 to 4.

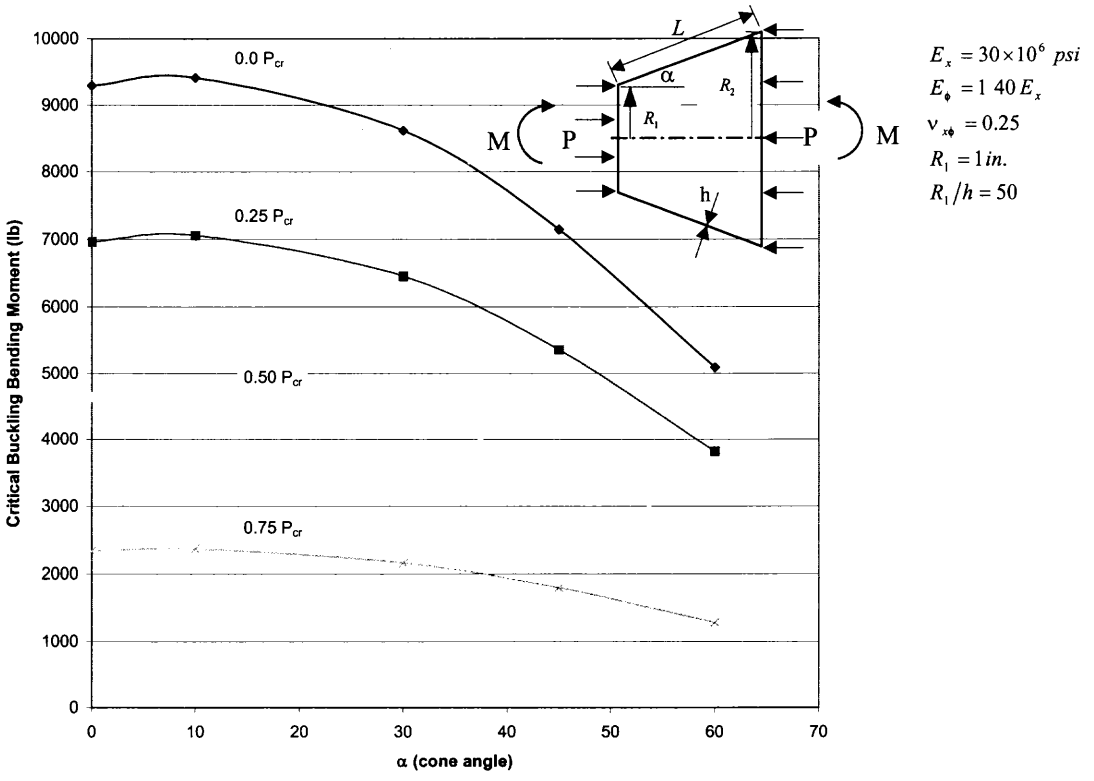

Figure 5.37 Buckling values of multi layer orthotropic conical shell in pure bending with axial pre-compression for number of layer=4 and L/R_1=0.2 about cone angle, SS2

The combined buckling values of multi layer conical shells with pure bending and axial pre-compression for fixed number of layer is in Figure 5.37 from Appendix E.16. With the total number 4 and length ratio $L/R_1 = 0.2$, the buckling values are similar trends to single layer case for cone angle α. Each rate of increment of pre-axial compression, the buckling value of pure bending is similar rate of it.

Case C. Combined Loads for Outer Pressure and Pure Bending

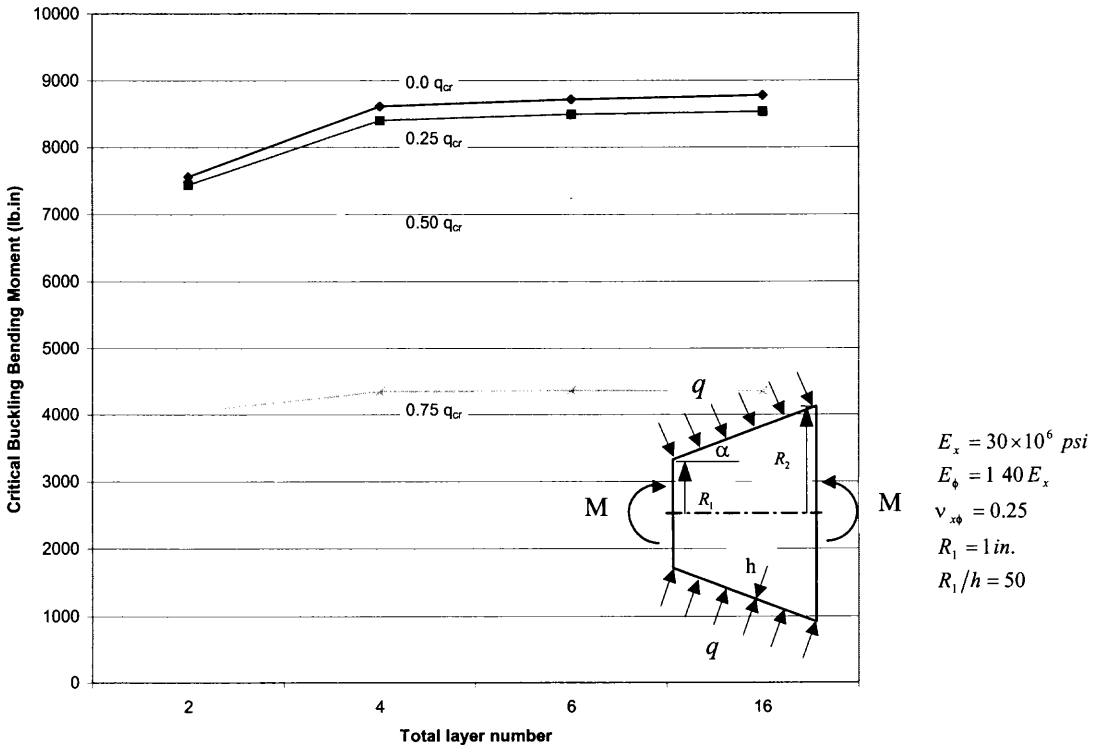

Figure 5.38 Buckling values of multi layer orthotropic conical shell in pure bending with outer pre-pressure for L/R_1=0.2 and $\alpha = 30^o$ about number of layer, SS2

The buckling values of multi layer orthotropic conical shell under outer pressure and pure bending are in Figure 5.38 from Appendix E.17. The uniform outer pressure q, in pounds per square inch. The outer pressure is applied for each rate of critical pressure q_{cr} for each number of layer. For 25% of q_{cr}, the buckling values of pure bending M_{cr} are not much changed in comparing with other rate of q_{cr}. The buckling values are increased large as the number of layer changes from 2 to 4 comparing with other increment of layer number.

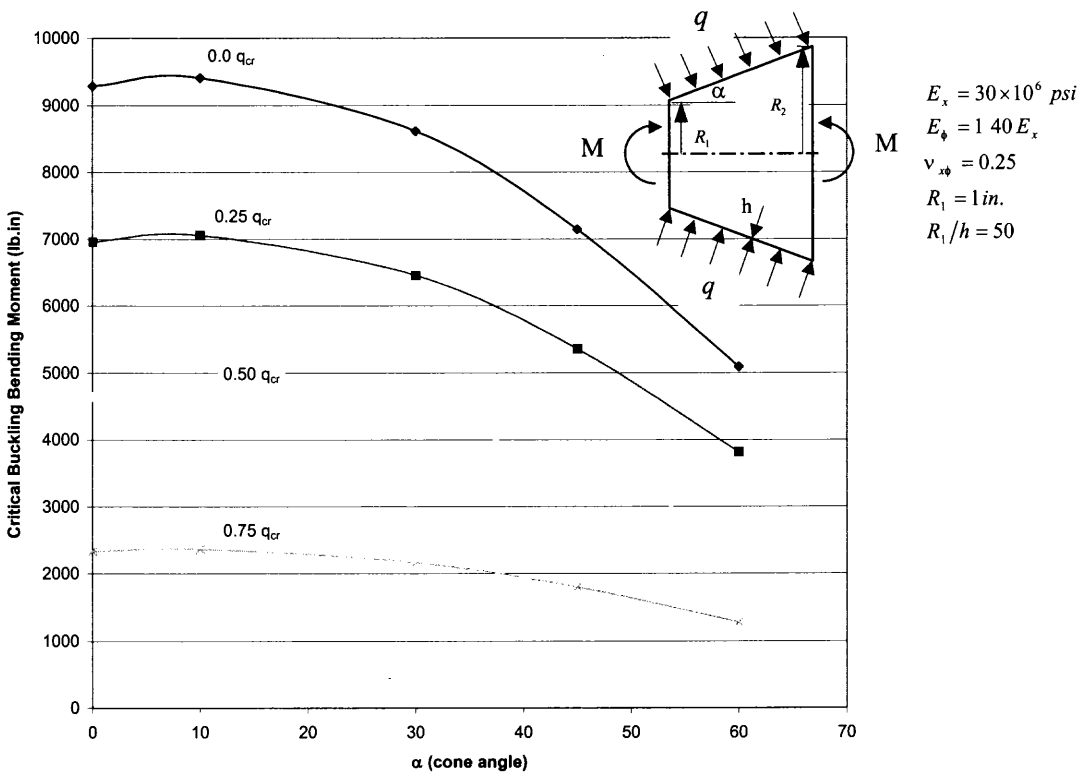

Figure 5.39 Buckling values of multi layer orthotropic conical shell in pure bending with outer pre-pressure for number of layer=4 and L/R_1=0.2 about cone angle, SS2

Buckling values of multi layer orthotropic conical shell in pure bending with outer pressure for fixed number of layer are in Figure 5.39 from Appendix E.17. This shows similar trends to combined outer pressure and axial compression case. When pre-outer pressure rate is 25%, the buckling values of pure bending are not so much changed as that of without pre-outer pressure. After the first 25% of pre-applied outer pressure, every 25% increment affects more and more for the buckling values. This means that the outer pre-pressure is sensitive to higher pre-pressure for buckling value of combined with pure bending.

CHAPTER 6

FINITE ELEMENT ANALYSIS (FEA)

6.1 Introduction

Numerical methods enables the engineer to expend his or her ability to solve practical design problems. The engineer may now treat real shapes as distinct from the somewhat limited variety of shapes amenable to simple analytic solution. Similarly, the engineer need no longer force a complicate loading system to fit a more regular load configuration to conform to the dictates of a purely academic situation. Numerical analysis thus provides a good tool with which the engineer may feel free to deal with the solution of problems as they are found in practice. Numerical analyses lead often to a system of linear algebraic equations. The most appropriate method of solution then depends on the nature and the number of such equations, as well as the type of high level computing equipment available.

The powerful finite element method had its beginnings in the 1950s, and with the widespread us of the digital computer it has since gained considerable favor relative to other numerical approaches. The finite element approach deals with an assembly of elements that replaces the continuous structure, and it is the replaced structure that is then the subject of analysis. The general procedures of the finite element and conventional structural matrix methods are similar. In the latter approach, the structure is idealized as an assembly of structural members connected to one another at joints or nodes at which the resultants of the applied forces are assumed to be concentrated. The basic concept of FEM is shown in Reddy [18]. Throughout the FEM analysis, the ANSYS 5.4, software

program, is used. Theoretical buckling values are compared with FEM results for single layer and multi layer structure under load. ANSYS 5.4 doesn't include buckling of pure bending function. Therefore, FEM analyses are done mainly on axial compression and outer pressure.

6.2 Definition of Buckling Analysis

Buckling analysis is a technique used to determine buckling loads-critical loads at which a structure becomes unstable-and buckled mode shape-the characteristic shape associated with a structure's buckled response. The general **procedure for buckling problem by the finite element method** is summarized as follows [19]:

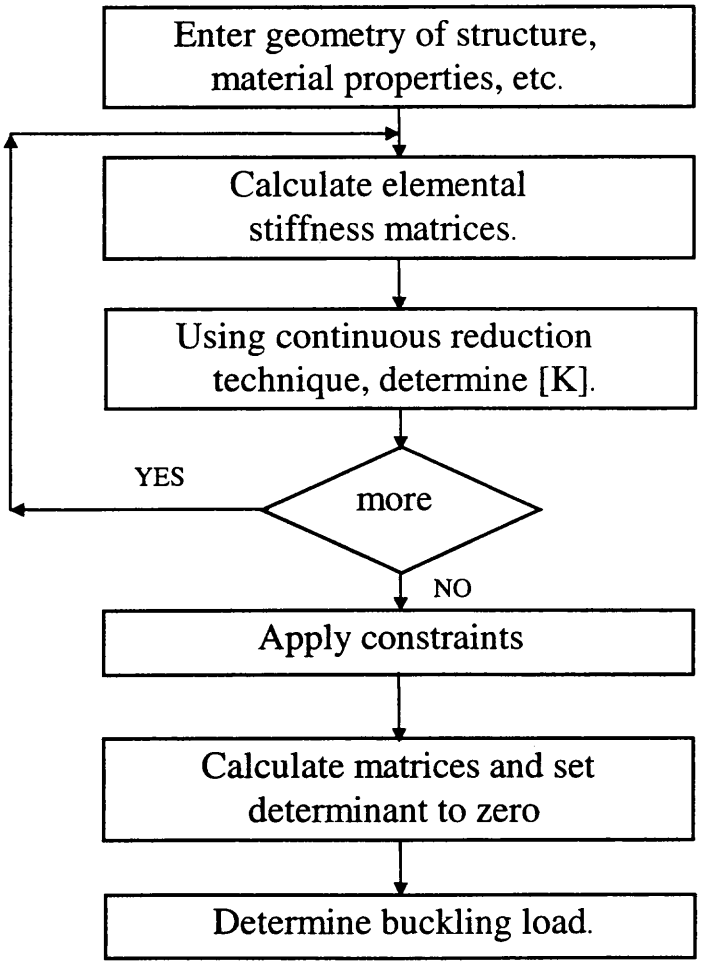

6.2.1 Types of Buckling Analyses

Two techniques are available in the ANSYS/Multiphysics, ANSYS/Mechanical, ANSYS/Structural, and ANSYS/LinearPlus programs for predicting the buckling load and buckling mode shape of a structure: nonlinear buckling analysis, and eigenvalue (or linear) buckling analysis. Eigenvalue (or linear) buckling analysis is used to compare with theoretical results [3]. Procedure of eigenvalue buckling analysis is given Appendix F.

6.2.2 Eigenvalue Buckling Analysis

Eigenvalue buckling analysis predicts the theoretical buckling strength of an ideal linear elastic structure. This method corresponds to the textbook approach to elastic buckling analysis: for instance an eigenvalue buckling analysis of a column will match the classical Euler solution. However, imperfections and nonlinearities prevent most real structures from achieving their theoretical elastic buckling strength.

6.2.3 Commands Used in a Buckling Analysis

There are two types of way to build a model and perform a buckling analysis. First, use sets of commands that are used to do any other type of finite element analysis. Second, choose similar options from the graphical user interface (GUI) to build and solve models.

6.2.4 Procedure for Eigenvalue Buckling Analysis

Eigenvalue buckling analysis for five-step procedure (see Appendix F for details):

1.Build the model. 2.Obtain the static solution.

3.Obtain the eigenvalue buckling solution.

4.Expand the solution. 5.Review the results.

6.3 The FEA of Isotropic Conical Shells

Finite Element Analysis, using ANSYS 5.4 software programs, is used to verify the results of present method outlined in item 3) of Chapter1.

Element Type:

To analyze isotropic case, SHELL63, an element type, is used in ANSYS. SHELL63 has both bending and membrane capabilities. Both in-plane and normal loads are permitted [2].

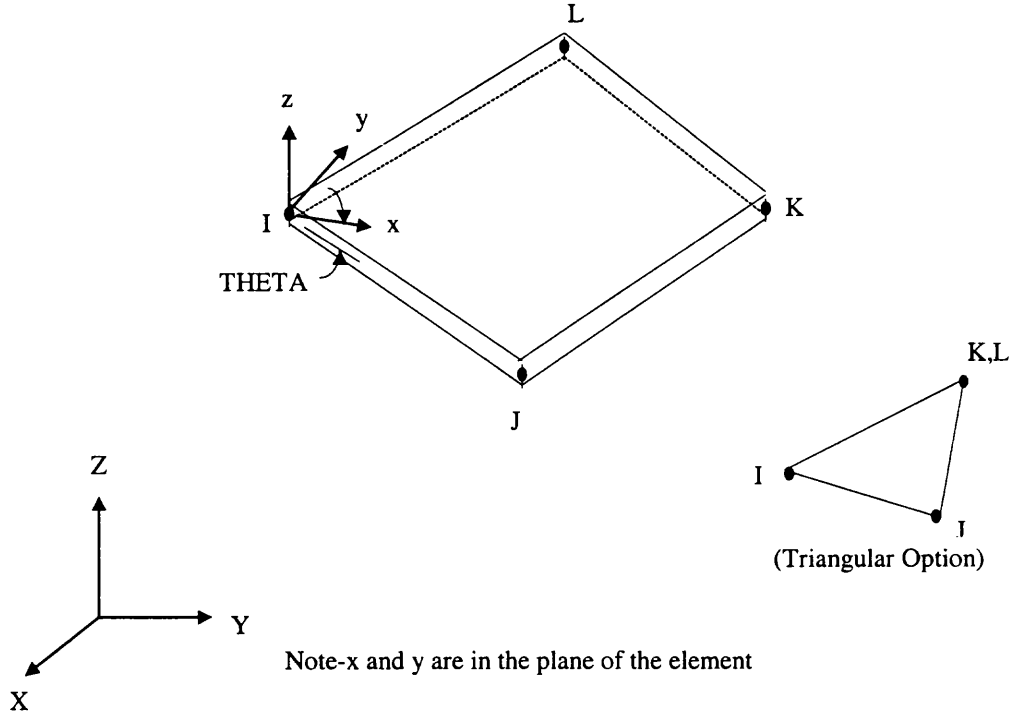

Element Name	SHELL63
Nodes	I, J, K, L
Degree of Freedom	UX, UY, UZ, ROTX, ROTY, ROTZ
Real Constants	TK(I), TK(J), TK(K), TK(L), THETA
Material Properties	EX, EY, PRXY or NUXY, GXY

Figure 6.1 SHELL63 Elastic Shell

The element has six degree of freedom at each node: translations in the nodal x, y, and z directions and rotations about the nodal x, y, and z axes. Stress stiffening and large

deflection capabilities are included. A consistent tangent stiffness matrix option is available for use in large deflection analyses.

The geometry, node locations, and the coordinate system for this element are shown in Figure 6.1 and SHELL63. The element is defined by four nodes, four thickness, an elastic foundation stiffness, and the orthotropic material properties. Orthotropic material directions correspond to the element coordinate directions. The elements of this analysis are depend on the size of cones. The geometry and the coordinate system for this cone are followed by theoretical data. For single layer, the number of elements are: the length ratio $L/R_1 = 0.2(180\times6)$, $L/R_1 = 0.5(120\times10)$, $L/R_1 = 0.8(120\times12)$, and $L/R_1 = 1.0(100\times16)$ with radius $R_1 = 1$ in. in Figure 6.2.

The thickness is assumed to vary smoothly over the area of the element with the thickness input at the four nodes. If the element has a constant thickness, only TK(I) need be input. If the thickness is not constant, all four thicknesses must be input.

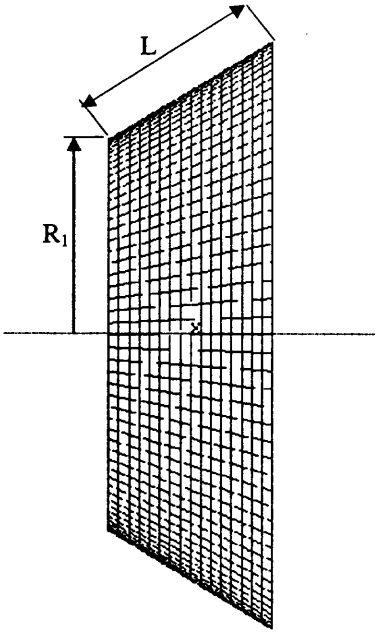

Figure 6.2 The elements of L/R_1=1.0 (100x16) at $\alpha = 30^o$

6.3.1 Comparison with Theoretical Results under Axial Compression

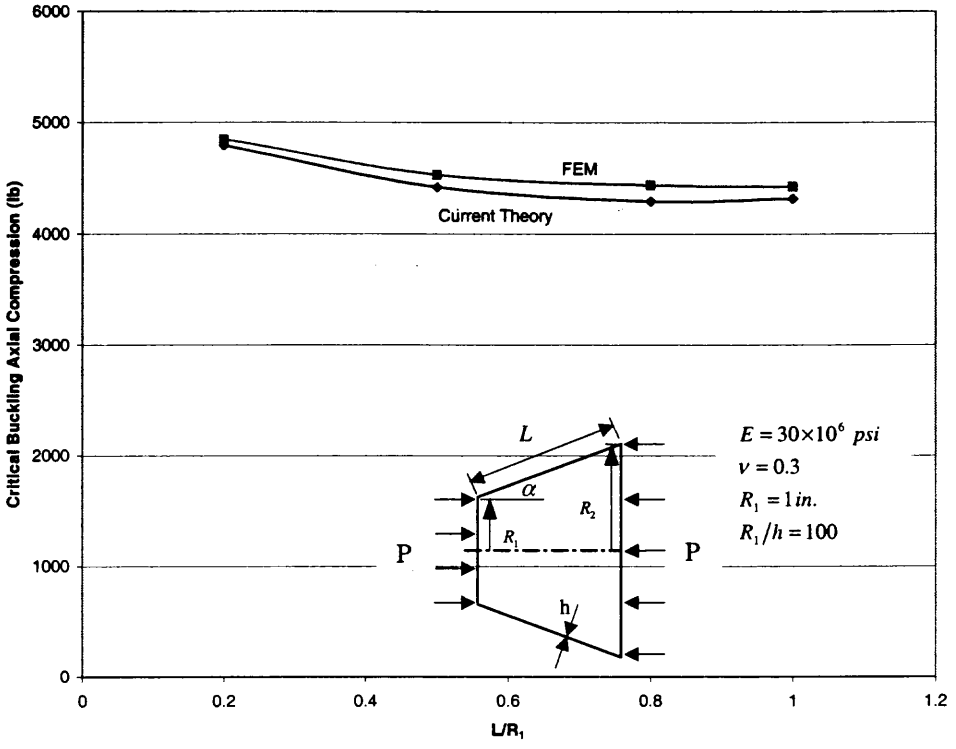

Figure 6.3 Buckling values of single layer isotropic conical shell under axial compression comparing with FEM for $\alpha = 30^o$ about length ratio, SS2

The comparison theoretical results with FEM results for single layer isotropic cone under axial compression is in Figure 6.3. At cone angle $\alpha = 30^o$ and boundary condition SS2, two values are almost identical profiles and results. For the shorter length ratio $L/R_1 = 0.2$, the difference is the smallest among other length because of the most stable condition for short cone. Table 6.1 shows the values and error percentage.

Table 6.1 Buckling values of single layer isotropic conical shell under axial compression comparing with FEM for $\alpha = 30^o$ about length ratio, SS2

L/R_1	Current Theory (lb)	FEM (lb)	Difference
0.2	4791.70	4844.51	1.10 %
0.5	4418.81	4727.00	6.97 %
0.8	4291.79	4436.76	3.38 %
1.0	4315.75	4420.46	2.43 %

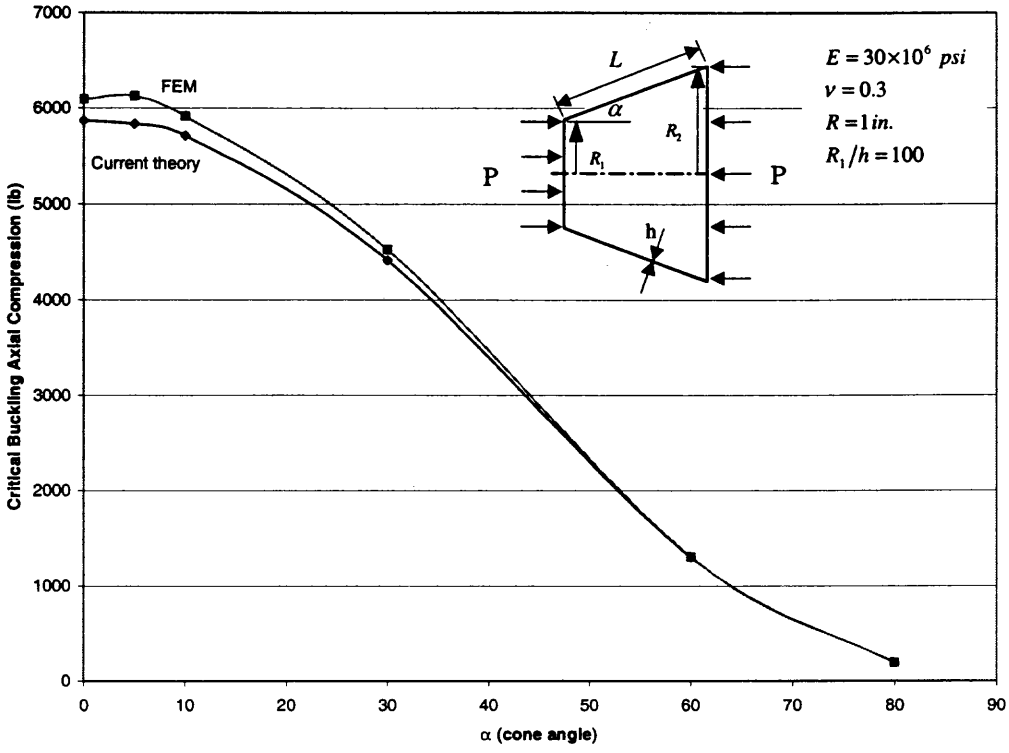

Figure 6.4 Buckling values of single layer isotropic conical shell under axial compression comparing theory data with FEM for $L/R_1 = 0.5$ about cone angle, SS2

The comparison theoretical results with FEM results for single layer isotropic cone under axial compression is in Figure 6.4. For length ratio $L/R_1 = 0.5$ and boundary condition SS2, the theory and FEM values are almost identical profiles and results for large cone angle region. The differences are small among other cone angles because of the stable condition for large cone angle region in Table 6.2.

Table 6.2 Buckling values of single layer isotropic conical shell under axial compression comparing theory data with FEM for $L/R_1 = 0.5$ about cone angle, SS2

α	Current Theory (lb)	FEM(lb)	Difference
0	5868.08	6095.38	3.88 %
5	5832.42	6127.23	5.05 %
10	5710.26	5917.44	3.63 %
30	4418.81	4527.00	2.45 %
60	1303.43	1305.42	0.15 %
80	191.78	192.35	0.29 %

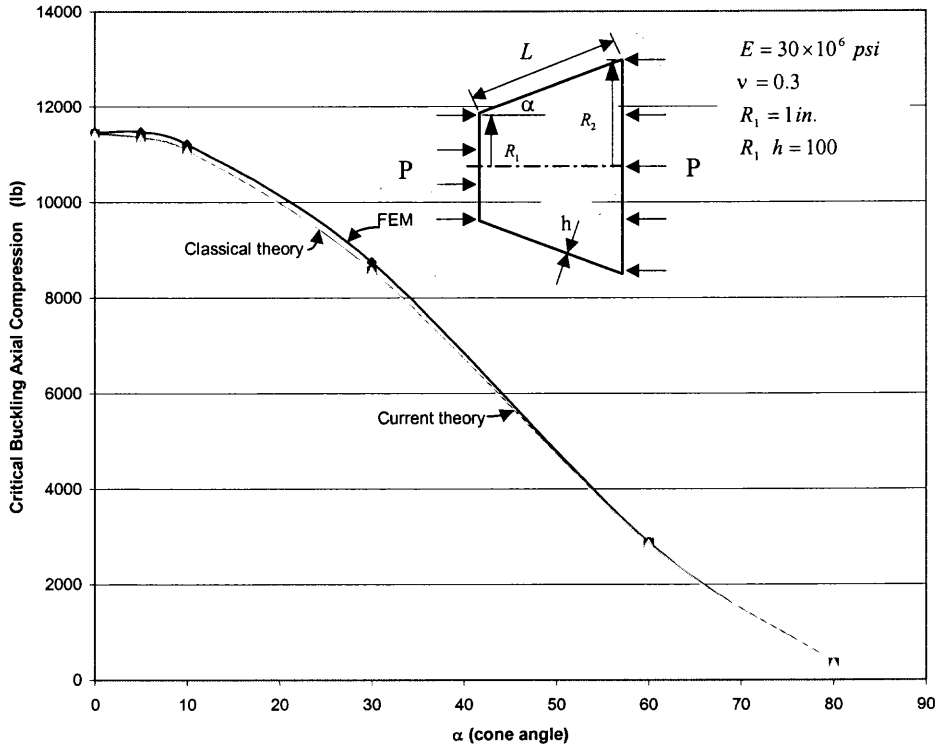

Figure 6.5 Buckling values of single layer isotropic conical shell under axial compression comparing theory, FEM and classical theory for $L/R_1 = 0.5$ about cone angle, SS4

The comparison theoretical results with FEM and classical results for single layer isotropic cone under axial compression is in Figure 6.5. For length ratio $L/R_1 = 0.5$ and boundary condition SS4, the theory and FEM values are almost similar profiles as boundary condition SS2. Table 6.3 shows the values and difference.

Table 6.3 Buckling values of single layer isotropic conical shell under axial compression comparing theory, FEM and classical theory for $L/R_1 = 0.5$ about cone angle, SS4

α	Current Theory (lb)	Classical Theory (lb)	Difference	FEM (lb)	Difference
0	11434.46	11408.27	-0.23 %	11465.04	0.27 %
5	11344.97	11321.61	-0.21 %	11471.97	1.12 %
10	11080.13	11064.27	-0.14 %	11213.67	1.21 %
30	8561.41	8556.20	-0.06 %	8745.92	2.16 %
70	2878.30	2852.07	-0.91 %	2881.96	0.13 %
80	349.13	344.00	-1.47 %	341.18	-2.27 %

6.3.2 Comparison with Theoretical Results under Outer Pressure

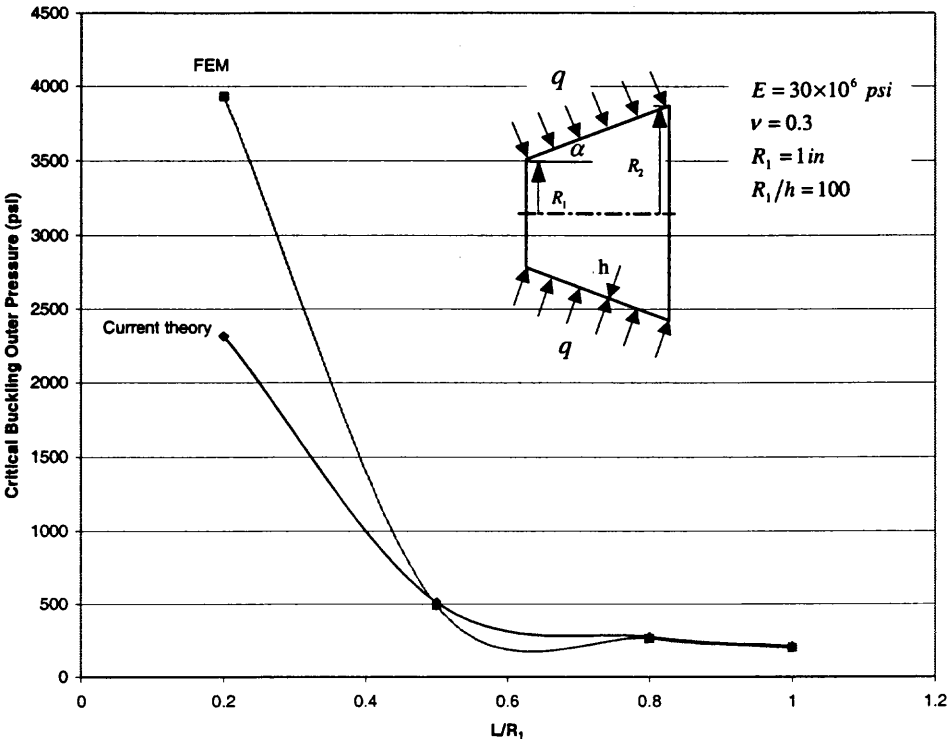

Figure 6.6 Buckling values of single layer isotropic conical shell under outer pressure comparing theory data with FEM for $\alpha = 30^o$ about length ratio, SS2

The comparison theoretical results with FEM and classical results for single layer isotropic cone under outer pressure is in Figure 6.6. For cone angle $\alpha = 30^o$ and boundary condition SS2, the theory and FEM values are almost similar profiles except extremely short cone. At the length ratio $L/R_1 = 0.2$, the boundary region may increase the buckling values during FEM analysis. Smaller elements may increase the accuracy. Table 6.3 shows the values and difference percentage.

Table 6.4 Buckling values of single layer isotropic conical shell under outer pressure comparing theory data with FEM for $\alpha = 30^o$ about length ratio, SS2

L/R_1	Current Theory (lb)	FEM (lb)	Difference
0.2	2315.08	3931.41	69.81 %
0.5	509.64	489.21	-4.01 %
0.8	276.00	262.75	-4.80 %
1.0	208.81	200.19	-4.22 %

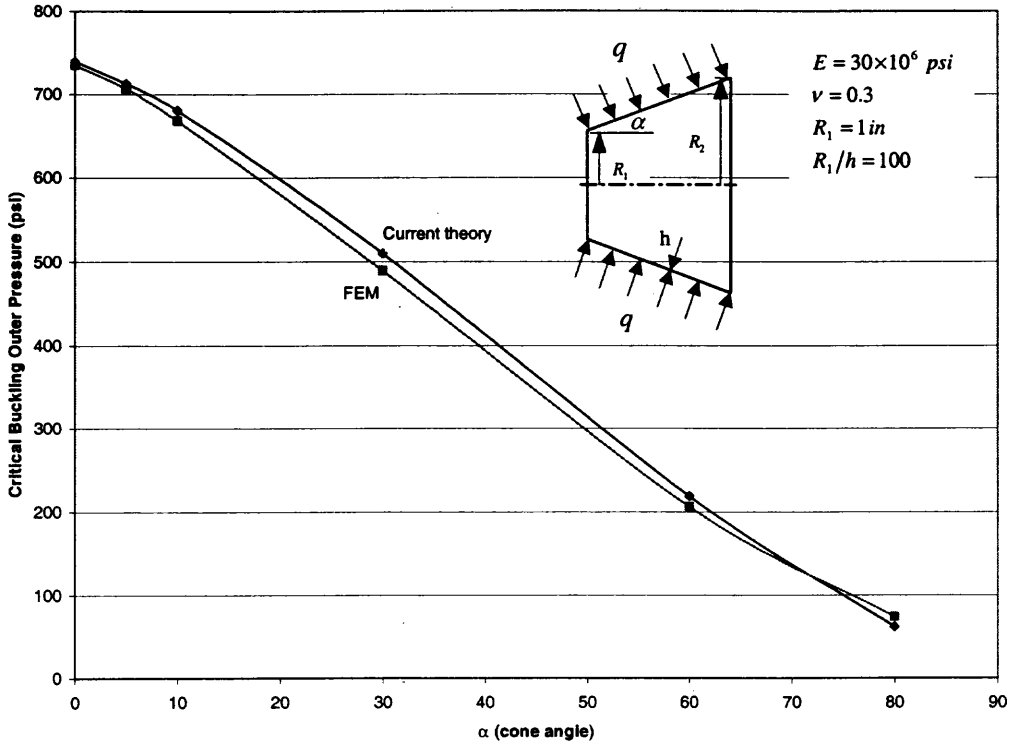

Figure 6.7 Buckling values of single layer isotropic conical shell under outer pressure comparing theory data with FEM for $L/R_1 = 0.5$ about cone angle, SS2

Under outer pressure, the comparison theoretical results with FEM results for single layer isotropic cone is in Figure 6.7. For length ratio $L/R_1 = 0.5$ and boundary condition SS2, the theory and FEM values are similar profiles and results for cone angle α. The differences are small for near zero degree cone angle. Table 6.5 shows the values and difference percentages.

Table 6.5 Buckling values of single layer isotropic conical shell under outer pressure comparing theory data with FEM for $L/R_1 = 0.5$ about cone angle, SS2

α	Current Theory (lb)	FEM (lb)	Difference
0	739.19	734.57	-0.63 %
5	712.45	706.65	-0.81 %
10	680.19	667.58	-1.85 %
30	509.64	489.21	-4.01 %
60	218.89	206.30	-5.75 %
80	62.02	74.36	19.9 %

6.4 The FEA of Orthotropic Conical Shells

6.4.1 Comparison with Theoretical Results under Axial Compression

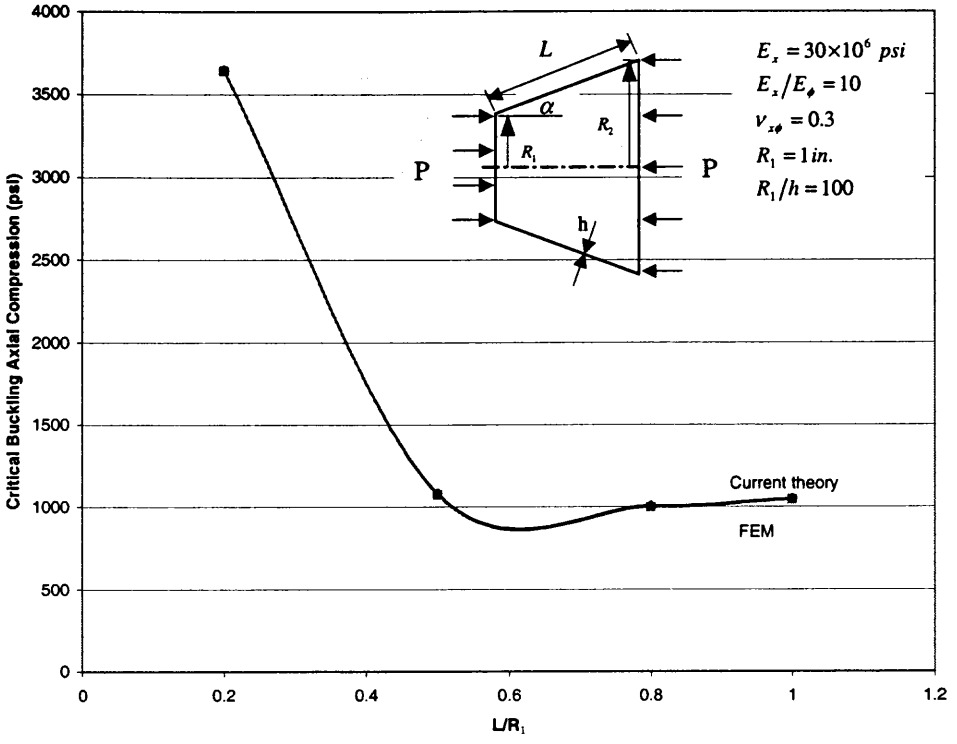

Figure 6.8 Buckling values single layer orthotropic conical shell under axial compression comparing theory data with FEM for $E_x/E_\phi = 10$ and $\alpha = 30^o$ about length ratio, SS2

Under outer pressure the comparison theoretical results with FEM and classical results for single layer isotropic cone is in Figure 6.8. For $E_x/E_\phi = 10$, cone angle $\alpha = 30^o$ and boundary condition SS2, the theory and FEM values are almost identical profile through the length ratio. Table 6.6 shows the values and difference percentage.

Table 6.6 Buckling values single layer orthotropic conical shell under axial compression comparing theory data with FEM for $E_x/E_\phi = 10$ and $\alpha = 30^o$ about length ratio, SS2

L/R_1	Current Theory (lb)	FEM (lb)	Difference
0.2	3647.44	3643.27	-0.11 %
0.5	1084.97	1075.47	-0.88 %
0.8	1009.19	999.15	-0.99 %
1.0	1050.89	1045.54	-0.51 %

6.4.2 Comparison with Theoretical Results under Outer Pressure

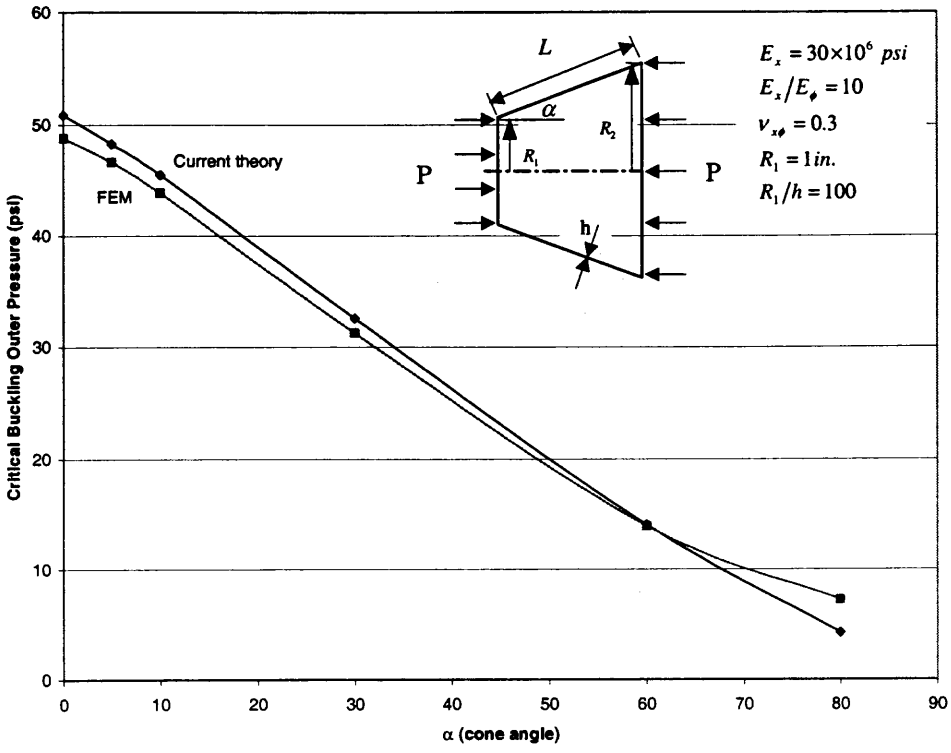

Figure 6.9 Buckling values of single layer orthotropic conical shell under outer pressure comparing theory data with FEM for $E_x/E_\phi = 10$ and L/R$_1$=0.8 about cone angle, SS2

The comparison theoretical results with FEM results for single layer orthotropic cone under outer pressure is in Figure 6.7. For $E_x/E_\phi = 10$, length ratio $L/R_1 = 0.5$ and SS2, the theory and FEM values are similar profiles and results for cone angle α. The differences are a little larger for cone angle approaches to 80 degree. Table 6.7 shows the values and difference percentages.

Table 6.7 Buckling values of single layer orthotropic conical shell under outer pressure comparing theory data with FEM for $E_x/E_\phi = 10$ and L/R$_1$=0.8 about cone angle, SS2

α	Current Theory (psi)	FEM (psi)	Difference
0	50.87	48.79	-4.09 %
5	48.31	46.66	-3.42 %
10	45.52	43.88	-3.60 %
30	32.53	31.21	-4.06 %
60	14.06	13.93	-0.92 %
80	4.22	7.24	71.56 %

6.5 The FEA of Multi Layer Composite Conical Shells

Element Type:

SHELL91 [2] is used for layered applications of a structural shell model or for modeling thick sandwich structures. Up to 16 different layers are permitted for applications with the sandwich option turned off. The element has six degree of freedom at each node: translations in the nodal x, y, and z directions and rotations about the nodal x, y, and z axes.

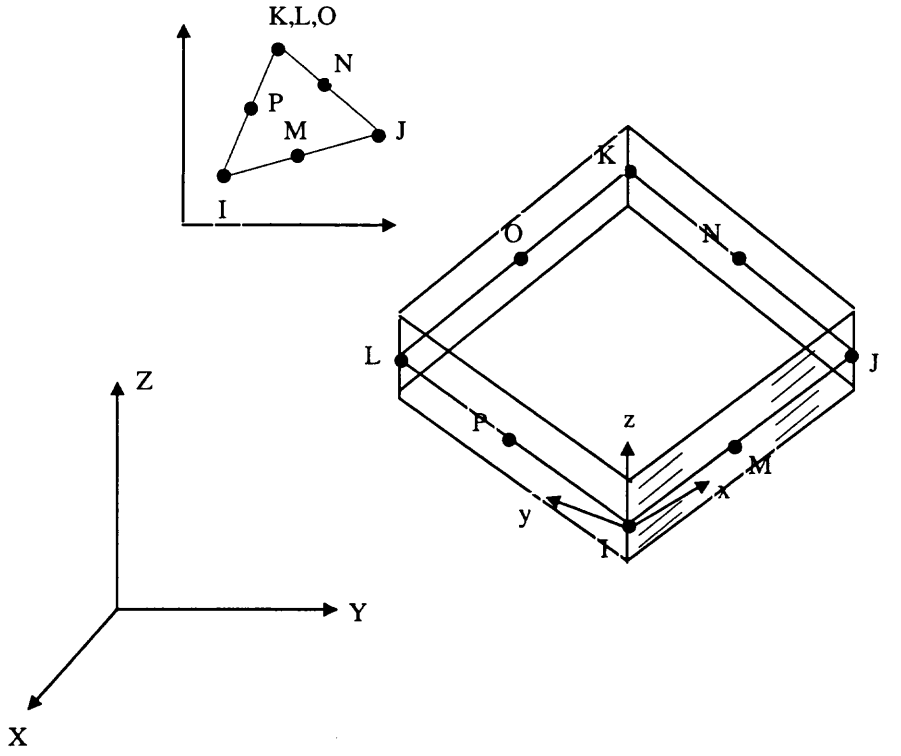

Element Name	SHELL91
Nodes	I, J, K, L
Degree of Freedom	UX, UY, UZ, ROTX, ROTY, ROTZ
Real Constants	NL, LSYM, MAT, TK(I), TK(J), TK(K), TK(L), NL
Material Properties	EX, EY, EZ, PRXY, PRYZ, PRXZ, GXY, GYZ, GXZ

Figure 6.10 SHELL91 16-Layer Structure Shell

Input Data:

The geometry, node locations, and the coordinate system for this element are shown in Figure 6.10. The element is defined by eight nodes, layer thickness, layer material direction angles, and orthotropic material properties. Midside nodes may not be removed (with a zero node number) from this element. The elements of this analysis are depend on the size of cones. The geometry and the coordinate system for this cone are followed by theoretical data. For multi layer, the number of elements are: the length ratio $L/R_1 = 0.2(40\times5)$, $L/R_1 = 0.5(40\times8)$, $L/R_1 = 0.8(40\times10)$,and $L/R_1 = 1.0(40\times12)$ with radius $R_1 = 1$ in. in Figure 6.2. Because SHELL91 has eight nodes for each rectangular element, it makes more equation than SHELL63. A triangular element may be formed by defining the same node number for nodes K, L and O.

The total number of layers (NL; up to 16) must be specified. Layer of 2, 4, 6, 16 are calculated. If the properties of the layers are symmetric about the mid-thickness of element (layer symmetry, LSYM=1), only half the properties, up to and including those of the middle layer (if any), need to be entered. Otherwise (LSYM=0), the properties of all layers should be entered.

6.5.1 Comparison with Theoretical Results under Axial Compression

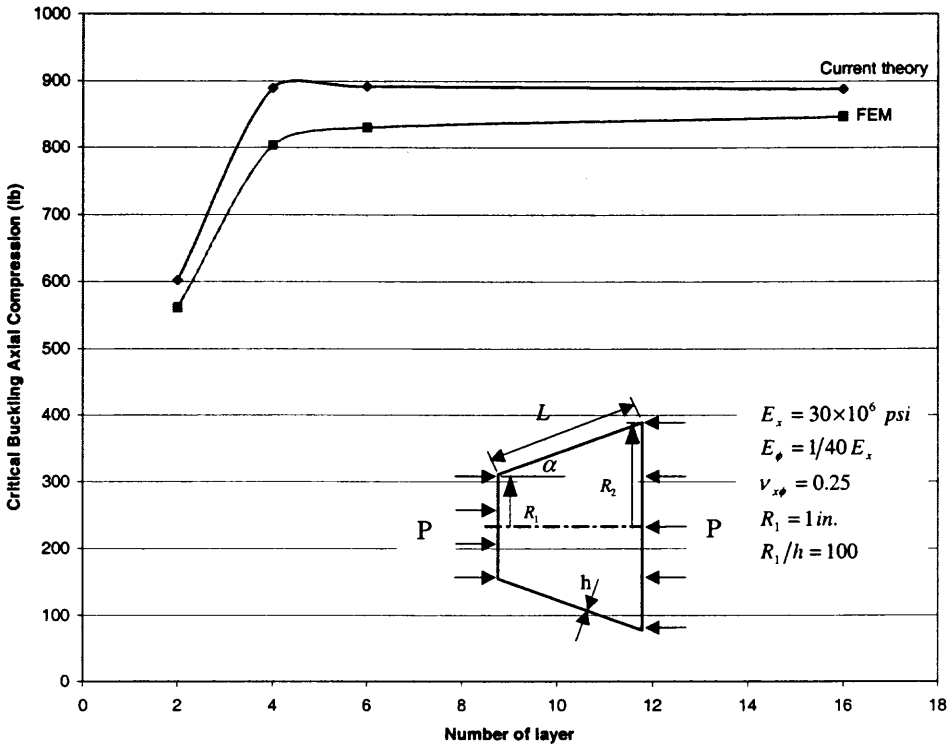

Figure 6.11 Buckling values of multi layer orthotropic conical shell under axial compression comparing with theory and FEM for L/R_1=0.8, and $\alpha = 30^o$ about length ratio, SS2

Under axial compression, the comparison theoretical results with FEM results for multi layer orthotripic cone is in Figure 6.11. For cone angle $\alpha = 30^o$, $L/R_1 = 0.8$, and boundary condition SS2, two values are similar profiles and results. The differences between theory and FEM values decrease as layer numbers increase. Fine mesh may improve the accuracy. Table 6.8 shows the values and difference percentage.

Table 6.8 Buckling values of multi layer orthotropic conical shell under axial compression comparing theory data with FEM for L/R_1=0.8, $\alpha = 30^o$ about number of layer, SS2

$\bar{N}$	Current Theory (lb)	FEM (lb)	Difference
2	601.89	561.06	-6.78 %
4	888.99	802.81	-9.69 %
6	891.28	830.03	-6.87 %
16	887.69	846.18	-4.67 %

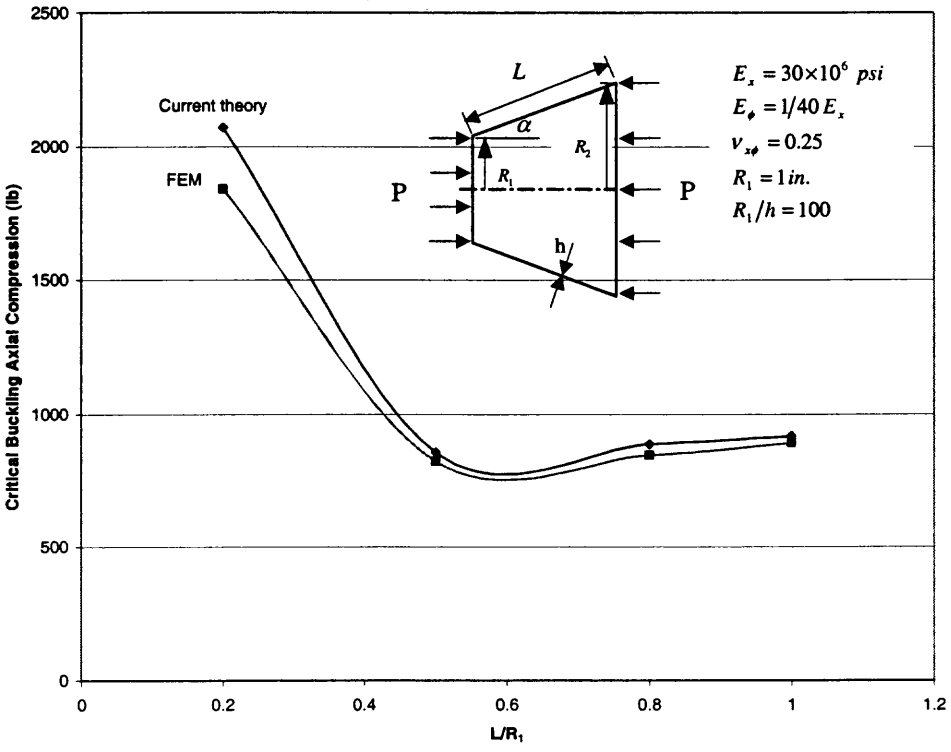

Figure 6.12 Buckling values of multi layer orthotropic conical shell under axial compression comparing with theory and FEM for $\alpha = 30^o$ and number of layer=16 about length ratio, SS2

The comparison theoretical results with FEM results for multi layer orthotropic cone under axial compression is in Figure 6.12. For cone angle $\alpha = 30^o$, number of layer=16, and boundary condition SS2, two values are similar profiles and results. For shorter length ratio $L/R_1 = 0.2$, the difference is a little larger among other length cones. Table 6.9 shows the values and difference percentage.

Table 6.9 Buckling values of multi layer orthotropic conical shell under axial compression comparing with theory and FEM for $\alpha = 30^o$ and number of layer=16 about length ratio, SS2

L/R_1	Current Theory (lb)	FEM (lb)	Difference
0.2	2073.16	1841.90	-11.15 %
0.5	856.91	823.56	-3.89 %
0.8	887.69	846.18	-4.68 %
1.0	918.33	891.56	-2.92 %

6.5.2 Comparison with Theoretical Results under Outer Pressure

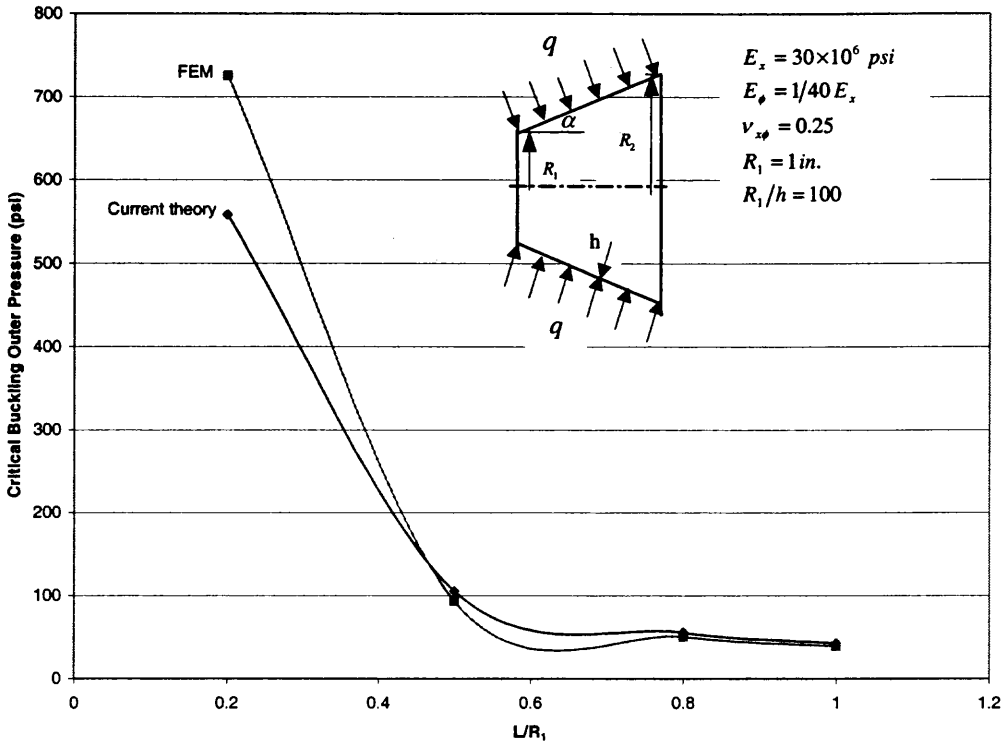

Figure 6.13 Buckling values of multi layer orthotropic conical shell under outer pressure comparing with theory and FEM for $\alpha = 30^{o}$, and number of layer=16 about length ratio, SS2

The comparison theoretical results with FEM and classical results for multi layer isotropic cone under outer pressure is in Figure 6.13. For cone angle $\alpha = 30^{o}$ and boundary condition SS2, the theory and FEM values are almost similar profiles except extremely short cone like single layer case. Fine elements may increase the accuracy. Table 6.10 shows the values and difference percentage.

Table 6.10 Buckling values of multi layer orthotropic conical shell under outer pressure comparing with theory and FEM for $\alpha = 30^{o}$, and number of layer=16 about length ratio, SS2

L/R_1	Current Theory (lb)	FEM (lb)	Difference
0.2	558.30	725.52	29.95 %
0.5	105.30	93.09	-11.59 %
0.8	55.47	50.18	-9.54 %
1.0	42.28	38.91	-7.97 %

CHAPTER 7

RESULTS AND CONCLUSIONS

1. Using developed C-language program COMBINED1, COMBINED2, results of the two simulation outputs are in Appendix E. MS VISUAL C++ 6.0 is used as a compiler.
2. The buckling values are affected by boundary conditions, length ratio L/R_1, cone angle α, thickness ratio h/R_1 etc. For axial compression, boundary condition SS1, SS2, and SS3 have similar trends but SS4 is larger. In Figure 5.4 and 5.5, different boundary condition has different wave number. More wave number needs more compression. For the buckling values of outer pressure, the length ratio and cone angle are important factors. As cone angle α increases the buckling pressure becomes smaller. For pure bending, thickness ratio and length ratio are important. As the length ratio becomes longer, the buckling shows unstable values for small cone angle region in Figure 5.9. Buckling values are related to the thickness of the cone.
3. For combined loads, outer pressure and axial compression act differently. Axial compression buckling values are not sensitive to outer pre-pressure of lower percentage, while axial compression and pure bending do not have similar patterns. This means that the effect of axial pre-compression changes the buckling values of bending moment almost linearly. The combined load pattern of outer pressure and axial compression are identical to that of outer pressure and pure bending. The buckling values of pure bending are not sensitive to outer pre-pressure at the lower percentage of it.

4. Orthotropic material has two different strengths in each direction. Regardless of length ratio and loads, buckling values increase as orthotropy ratio E_ϕ/E_x reaches 1. Shorter cones have large buckling loads comparing with other long cone.
5. For a multi-layered cone, a set of laminated cone with antisymmetric even number cross-ply cones (or $\overline{N}$ layered conical shell) are used. The laminae oriented angles 0^o and 90^o are also considered. The buckling values increase as the number of layers increase. The increment of layer from 2 to 4 is larger than other increments. The buckling values of each loading have similar trends as single layer.
6. For axial compression of single layer cone, comparison theoretical and FEM values matches well. Boundary conditions also affect FEM solution. The three types of solutions, current solution, classical solution, and FEM solution are almost same profiles with boundary condition SS4 in Figure 6.4. For outer pressure, the theory and FEM results are almost similar profile except extremely short cone. The buckling values of multilayered cones have similar trends as single layer cones. The buckling values increase as number of layer increases. The difference between theoretical and FEM buckling values are also reduced as number of layer increases.

The buckling of conical shell under pure bending is developed using minimum potential energy method and power series method. Relatively long cones are studied to find the stability conditions about thickness ratio. Three types of loads, axial compression, outer pressure, and pure bending are used to obtain the effects of combined loads. Multilayered cone shells increase the buckling loads as the number of layers increase. Generally, the results of finite element method matches well with theoretical values. To avoid the buckling conditions from various loads and to lessen the weight, combination of the layer

symmetry, length, and material properties are important. To make good structure, new material needs to be developed stronger and light weight material to economize energy.

APPENDIX A

ENERGY METHODS AND COEFFICIENTS

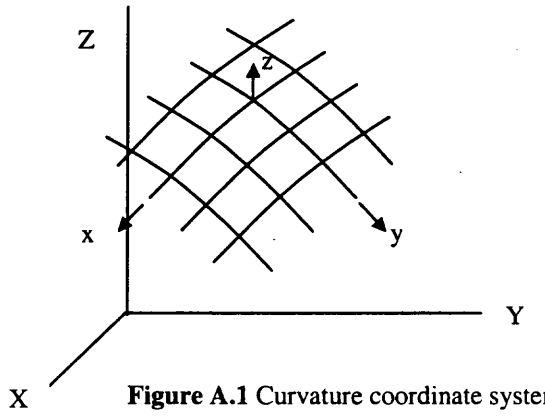

Figure A.1 Curvature coordinate system

The lines of curvature coordinates are denoted by the symbols x and y, and the principal radii of curvature by R_x and R_y. Along the coordinates lines, distances ds_x and ds_y can be expressed as $ds_x = A_L\, dx \qquad ds_y = B_L\, dy$

Where A_L, B_L are the Lamé coefficients for the X, Y, Z rectangular coordinates.

A point can be expressed on the surface (Figure A.1), then X=X(x,y), Y=Y(x,y), Z=Z(x,y).

$$A_L = \left[\left(\frac{\partial X}{\partial x}\right)^2 + \left(\frac{\partial Y}{\partial x}\right)^2 + \left(\frac{\partial Z}{\partial x}\right)^2\right]^{1/2}$$

$$B_L = \left[\left(\frac{\partial X}{\partial y}\right)^2 + \left(\frac{\partial Y}{\partial y}\right)^2 + \left(\frac{\partial Z}{\partial y}\right)^2\right]^{1/2}$$

The sign of z for convex shells is taken to be negative inward. The coordinates x, y, z are orthogonal coordinate system.

The method is based on a strain energy expression derived in terms of the following three simplifying assumptions developed by Koiter [13] and [14]:

1. The shell is thin, h/R << 1, where is the smallest principal radius of curvature of the undeformed middle surface.
2. The strains are small compared with unity, and the strain energy per unit volume of the undeformed body is given by quadratic function of strain for an isotropic solid.
3. The effect of transverse shearing and normal stresses may be neglected in strain

   energy density.

In terms of these Koiter's assumptions, the strain energy of a thin elastic shell equations [13]

$$U_s = U_m + U_b \tag{A.1}$$

$$U_m = \frac{C}{2}\iint\left(\varepsilon_x^2 + \varepsilon_y^2 + 2\nu\varepsilon_x\varepsilon_y + \frac{1-\nu}{2}\gamma_{xy}^2\right)A_L B_L dxdy \tag{A.2}$$

$$U_b = \frac{D}{2}\iint\left[\kappa_x^2 + \kappa_y^2 + 2\nu\kappa_x\kappa_y + 2(1-\nu)\gamma_{xy}^2\right]A_L B_L dxdy \tag{A.3}$$

$$C \equiv \frac{Eh}{1-\nu^2}, \qquad D \equiv \frac{Eh^3}{12(1-\nu^2)}$$

U_m, U_b are membrane strain energy and bending strain energy, respectively.

where $\varepsilon_x, \varepsilon_y$ and γ_{xy} are middle surface normal and shear strain components and κ_x, κ_y and κ_{xy} are curvature changes.

$$\Pi = U_s + \Omega \tag{A.4}$$

$$\Omega = -\iint(P_x U + P_y v + P_z W)A_L B_L dxdy \tag{A.5}$$

The total potential energy Π is consists of strain energy and the potential energy Ω of the applied loads. For Ω, P_x, P_y, P_z are the distributed load on the surface of the shell element, and u, v, w represent the displacements of a point on the shell middle surface of x, y, and z components. Equations (A.1) through (A.5) need a set of kinematic relations of general potential energy expression for an arbitrary shape shell.

The equations developed here start from nonlinear middle surface kinematic relations of simple form.

$$\begin{aligned} \varepsilon_x &= e_{xx} + \tfrac{1}{2}\beta_x^2 \qquad \kappa_x = \chi_{xx} \\ \varepsilon_y &= e_{yy} + \tfrac{1}{2}\beta_y^2 \qquad \kappa_y = \chi_{yy} \\ \gamma_{xy} &= e_{xy} + \tfrac{1}{2}\beta_x\beta_y \qquad \kappa_{xy} = \chi_{xy} \end{aligned} \tag{A.6}$$

where e_{ij}, β_{ij} and χ_{ij} are linear functions of the displacement components U, V, W. The relations of this form are derived by Sanders [20].

$$e_{xx} = \frac{u_{,x}}{A_L} + \frac{A_{L,y}\, v}{A_L B_L} + \frac{w}{R_x} \qquad e_{yy} = \frac{v_{,y}}{B_L} + \frac{B_{L,x}\, u}{A_L B_L} + \frac{w}{R_y} \tag{A.7}$$

$$e_{xy} = \frac{v_{,x}}{A_L} + \frac{u_{,y}}{B_L} - \frac{B_{L,x}\, v + A_{L,y}\, u}{A_L B_L}$$

$$\beta_x = -\frac{w_{,x}}{A_L} + \frac{u}{R_x} \qquad \beta_y = -\frac{w_{,y}}{B_L} + \frac{v}{R_y} \tag{A.8}$$

$$\chi_{xx} = \frac{\beta_{x,x}}{A_L} + \frac{A_{L,y}\, \beta_y}{A_L B_L} \qquad \chi_{yy} = \frac{\beta_{y,y}}{B_L} + \frac{B_{L,x}\, \beta_x}{A_L B_L} \tag{A.9}$$

$$2\chi_{xy} = \frac{\beta_{x,y}}{A_L} + \frac{\beta_{x,y}}{B_L} - \frac{A_{L,y}\, \beta_x + B_{L,x}\, \beta_x}{A_L B_L}$$

The minimum potential energy criterion is used to derive an expression for the second variation of the potential energy of a shell of general shape in terms of the linear displacement parameters $e_{ij}, \beta_i, \chi_{ij}$.

$$\delta^2\Pi = \delta^2 U_s + \delta^2\Omega \tag{A.10}$$

Thus the final expression for the second variation may be written

$$\delta^2\Pi = C\iint F dxdy \tag{A.11}$$

For a functional of the form, the Euler equations are given;

$$\begin{aligned}
&\frac{\partial F}{\partial u} - \frac{\partial}{\partial x}\frac{\partial F}{\partial u_x} - \frac{\partial}{\partial y}\frac{\partial F}{\partial u_y} = 0 \\
&\frac{\partial F}{\partial v} - \frac{\partial}{\partial x}\frac{\partial F}{\partial v_x} - \frac{\partial}{\partial y}\frac{\partial F}{\partial v_y} = 0 \\
&\frac{\partial F}{\partial w} - \frac{\partial}{\partial x}\frac{\partial F}{\partial w_x} - \frac{\partial}{\partial y}\frac{\partial F}{\partial w_y} + \frac{\partial^2}{\partial x^2}\frac{\partial F}{\partial w_{xx}} + \frac{\partial^2}{\partial x\partial y}\frac{\partial F}{\partial w_{xy}} + \frac{\partial^2}{\partial y^2}\frac{\partial F}{\partial w_{yy}} = 0
\end{aligned} \tag{A.12}$$

This leads to, after dropping the terms involving the squares of the derivatives in Eq. (A.12)

$$L_{11}U + L_{12}V + L_{13}W = 0 \tag{A.13}$$

Similarly

$$L_{21}U + L_{22}V + L_{23}W = 0 \tag{A.14}$$

$$L_{31}U + L_{32}V + L_{33}W + L_N W = 0 \tag{A.15}$$

where

For single layer :

$$L_{11} = A_{11}\frac{\partial^2}{\partial x^2} + \frac{A_{11}\sin\alpha}{R(x)}\frac{\partial}{\partial x} - \frac{A_{22}\sin^2\alpha}{R^2(x)} + \frac{A_{66}}{R^2(x)}\frac{\partial^2}{\partial\phi^2} \tag{A.16}$$

$$L_{12} = \frac{(A_{12}+A_{66})}{R(x)}\frac{\partial^2}{\partial x\partial\phi} - \frac{(A_{22}+A_{66})\sin\alpha}{R^2(x)}\frac{\partial}{\partial\phi} \tag{A.17}$$

$$L_{21} = \frac{(A_{12}+A_{66})}{R(x)}\frac{\partial^2}{\partial x\partial\phi} + \frac{(A_{22}+A_{66})\sin\alpha}{R^2(x)}\frac{\partial}{\partial\phi} \tag{A.18}$$

$$L_{22} = A_{66}\left[\frac{\partial^2}{\partial x^2} + \frac{\sin\alpha}{R(x)}\frac{\partial}{\partial x} - \frac{\sin^2\alpha}{R^2(x)}\right] + \frac{A_{22}}{R^2(x)}\frac{\partial^2}{\partial\phi^2} \tag{A.19}$$

$$L_{13} = -\frac{A_{12}\cos\alpha}{R(x)}\frac{\partial}{\partial x} + \frac{A_{22}\sin\alpha\cos\alpha}{R^2(x)} \tag{A.20}$$

$$L_{23} = L_{32} = \frac{A_{22}\cos\alpha}{R^2(x)}\frac{\partial}{\partial\phi} \tag{A.21}$$

$$L_{31} = -\frac{A_{12}\cos\alpha}{R(x)}\frac{\partial}{\partial x} - \frac{A_{22}\sin\alpha\cos\alpha}{R^2(x)} \tag{A.22}$$

$$\begin{aligned} L_{33} = {} & \frac{A_{22}\cos^2\alpha}{R^2(x)} + D_{11}\frac{\partial^4}{\partial x^4} + \frac{2(D_{12}+2D_{66})}{R^2(x)}\frac{\partial^4}{\partial x^2\partial\phi^2} + \frac{D_{22}}{R^4(x)}\frac{\partial^4}{\partial\phi^4} \\ & + \frac{2D_{11}\sin\alpha}{R(x)}\frac{\partial^3}{\partial x^3} - \frac{2(D_{12}+2D_{66})\sin\alpha}{R^3(x)}\frac{\partial^3}{\partial x\partial\phi^2} - \frac{D_{22}\sin^2\alpha}{R^2(x)}\frac{\partial^2}{\partial x^2} \\ & + \frac{2(D_{12}+D_{22}+2D_{66})\sin^2\alpha}{R^4(x)}\frac{\partial^2}{\partial\phi^2} + \frac{D_{22}\sin^3\alpha}{R^3(x)}\frac{\partial}{\partial x} \end{aligned} \tag{A.23}$$

$$L_N = \frac{1}{R(x)}\frac{\partial}{\partial x}\left[R(x)N_{x0}\frac{\partial}{\partial x}\right] + \frac{1}{R^2(x)}\frac{\partial}{\partial\phi}\left(N_{\phi 0}\frac{\partial}{\partial\phi}\right) \tag{A.24}$$

where

For multi layer :

$$L_{11} = A_{11}\frac{\partial^2}{\partial x^2} + \frac{A_{11}\sin\alpha}{R(x)}\frac{\partial}{\partial x} - \frac{A_{22}\sin^2\alpha}{R^2(x)} + \frac{A_{66}}{R^2(x)}\frac{\partial^2}{\partial\phi^2} \tag{A.25}$$

$$L_{12} = \frac{(A_{12}+A_{66})}{R(x)}\frac{\partial^2}{\partial x\partial\phi} - \frac{(A_{22}+A_{66})\sin\alpha}{R^2(x)}\frac{\partial}{\partial\phi} \tag{A.26}$$

$$L_{21} = \frac{(A_{12}+A_{66})}{R(x)}\frac{\partial^2}{\partial x\partial\phi} + \frac{(A_{22}+A_{66})\sin\alpha}{R^2(x)}\frac{\partial}{\partial\phi} \tag{A.27}$$

$$L_{22} = A_{66}\left[\frac{\partial^2}{\partial x^2} + \frac{\sin\alpha}{R(x)}\frac{\partial}{\partial x} - \frac{\sin^2\alpha}{R^2(x)}\right] + \frac{A_{22}}{R^2(x)}\frac{\partial^2}{\partial\phi^2} \tag{A.28}$$

$$\begin{aligned} L_{13} = {} & -\frac{A_{12}\cos\alpha}{R(x)}\frac{\partial}{\partial x} + \frac{A_{22}\sin\alpha\cos\alpha}{R^2(x)} \\ & - B_{11}\frac{\partial^3}{\partial x^3} - \frac{(B_{12}+2B_{66})}{R^2(x)}\frac{\partial^3}{\partial x\partial\phi^2} - \frac{B_{11}\sin\alpha}{R(x)}\frac{\partial^2}{\partial x^2} \\ & - \frac{(B_{12}+B_{22}+2B_{66})\sin\alpha}{R^3(x)}\frac{\partial^2}{\partial\phi^2} + \frac{B_{22}\sin^2\alpha}{R^2(x)}\frac{\partial}{\partial x} \end{aligned} \tag{A.29}$$

$$\begin{aligned} L_{23} = {} & \frac{A_{22}\cos\alpha}{R^2(x)}\frac{\partial}{\partial\phi} - \frac{(B_{12}+2B_{66})}{R(x)}\frac{\partial^3}{\partial x^2\partial\phi} - \frac{B_{22}}{R^3(x)}\frac{\partial^3}{\partial\phi^3} \\ & - \frac{B_{22}\sin\alpha}{R^2(x)}\frac{\partial^2}{\partial x\partial\phi} \end{aligned} \tag{A.30}$$

$$L_{31} = -\frac{A_{12}\cos\alpha}{R(x)}\frac{\partial}{\partial x} - \frac{A_{22}\sin\alpha\cos\alpha}{R^2(x)} - B_{11}\frac{\partial^3}{\partial x^3} - \frac{(B_{12}+2B_{66})}{R^2(x)}\frac{\partial^3}{\partial x\partial\phi^2} - \frac{2B_{11}\sin\alpha}{R(x)}\frac{\partial^2}{\partial x^2} + \frac{B_{22}\sin^2\alpha}{R^2(x)}\frac{\partial}{\partial x} - \frac{B_{22}\sin\alpha}{R^3(x)}\frac{\partial^2}{\partial\phi^2} - \frac{B_{22}\sin^3\alpha}{R^3(x)} \tag{A.31}$$

$$L_{32} = \frac{A_{22}\cos\alpha}{R^2(x)}\frac{\partial}{\partial\phi} - \frac{(B_{12}+2B_{66})}{R(x)}\frac{\partial^3}{\partial x^2\partial\phi} - \frac{B_{22}}{R^3(x)}\frac{\partial^3}{\partial\phi^3} + \frac{B_{22}\sin\alpha}{R^2(x)}\frac{\partial^2}{\partial x\partial\phi} - \frac{B_{22}\sin^2\alpha}{R^3(x)}\frac{\partial}{\partial\phi} \tag{A.32}$$

$$L_{33} = \frac{A_{22}\cos^2\alpha}{R^2(x)} + \frac{2B_{12}\cos}{R(x)}\frac{\partial^2}{\partial x^2} + \frac{2B_{22}\cos\alpha}{R^3(x)}\frac{\partial^2}{\partial\phi^2} + \frac{B_{22}\cos\alpha\sin^2\alpha}{R^3(x)} + D_{11}\frac{\partial^4}{\partial x^4} + \frac{2(D_{12}+2D_{66})}{R^2(x)}\frac{\partial^4}{\partial x^2\partial\phi^2} + \frac{D_{22}}{R^4(x)}\frac{\partial^4}{\partial\phi^4} + \frac{2D_{11}\sin\alpha}{R(x)}\frac{\partial^3}{\partial x^3} - \frac{2(D_{12}+2D_{66})\sin\alpha}{R^3(x)}\frac{\partial^3}{\partial x\partial\phi^2} - \frac{D_{22}\sin^2\alpha}{R^2(x)}\frac{\partial^2}{\partial x^2} + \frac{2(D_{12}+D_{22}+2D_{66})\sin^2\alpha}{R^4(x)}\frac{\partial^2}{\partial\phi^2} + \frac{D_{22}\sin^3\alpha}{R^3(x)}\frac{\partial}{\partial x} \tag{A.33}$$

$$L_N = \frac{1}{R(x)}\frac{\partial}{\partial x}\left[R(x)N_{x0}\frac{\partial}{\partial x}\right] + \frac{1}{R^2(x)}\frac{\partial}{\partial\phi}\left(N_{\phi 0}\frac{\partial}{\partial\phi}\right) \tag{A.34}$$

APPENDIX B

APPLICATION, TRANSFORMATION, AND SHELL THEORY

B.1 Applications for Conical Shells

The applications of cone shape structure; (a) upper and lower part of can have cone shapes, Belleville spring washers[16, 17] are popular cone structure, (c) space ship [8] is consist of many cone shapes, (d) space station [15] has large cone structures.

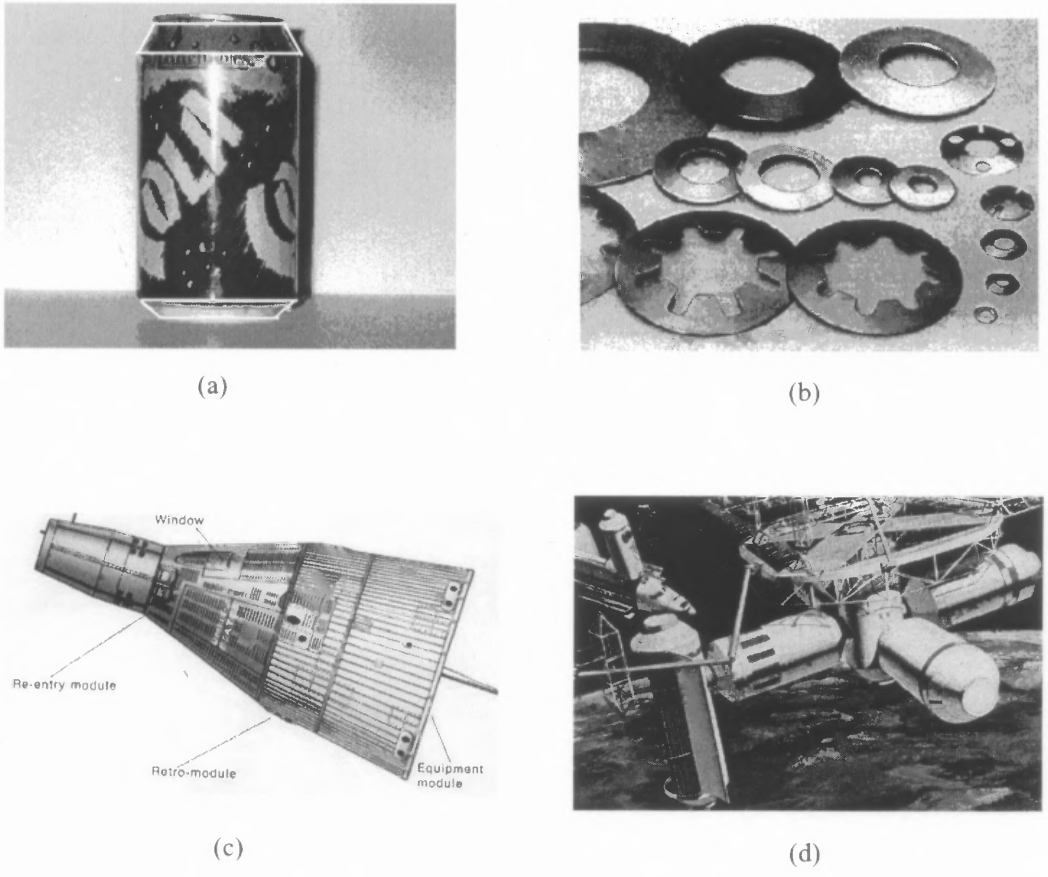

Figure B.1 Applications for conical shells: (a) cola can
(b) belleville washers (c) space ship, Gemini (d) space station

B.2 Transformed Reduced Stiffness Matrix

$$Q_{11} = \frac{E_1}{1-\nu_{12}\nu_{21}}, \qquad Q_{22} = \frac{E_2}{1-\nu_{12}\nu_{21}}$$

$$Q_{12} = \frac{E_1\nu_{21}}{1-\nu_{12}\nu_{21}}, \qquad Q_{21} = \frac{E_2\nu_{12}}{1-\nu_{12}\nu_{21}} \qquad Q_{12} = Q_{21} \quad (\because E_1\nu_{21} = E_2\nu_{12})$$

$$Q_{66} = \frac{E_1}{2(1+\nu_{12})}$$

$$Q_{11}^* = Q_{11}\cos^4\theta + Q_{22}\sin^4\theta + 2(Q_{12}+2Q_{66})\sin^2\theta\cos^2\theta$$
$$Q_{12}^* = (Q_{11}+Q_{22}-4Q_{66})\sin^2\theta\cos^2\theta + Q_{12}(\sin^4\theta+\cos^4\theta)$$
$$Q_{22}^* = Q_{11}\sin^4\theta + Q_{22}\cos^4\theta + 2(Q_{12}+2Q_{66})\sin^2\theta\cos^2\theta$$
$$Q_{16}^* = (Q_{11}-Q_{12}-2Q_{66})\sin\theta\cos^3\theta - (Q_{12}-Q_{22}+2Q_{66})\sin^3\theta\cos\theta$$
$$Q_{26}^* = (Q_{11}-Q_{12}-2Q_{66})\sin^3\theta\cos\theta - (Q_{12}-Q_{22}+2Q_{66})\sin\theta\cos^3\theta$$
$$Q_{66}^* = (Q_{11}+Q_{22}-2Q_{12}-2Q_{66})\sin^2\theta\cos^2\theta + Q_{66}(\sin^4\theta+\cos^4\theta)$$

Here Q_{11}, Q_{22}, and Q_{12} are referred to the principal direction (x, y) of the material. The θ is the angle between these axes and the reference coordinates (x^*, y^*) lamina in Figure B.2.

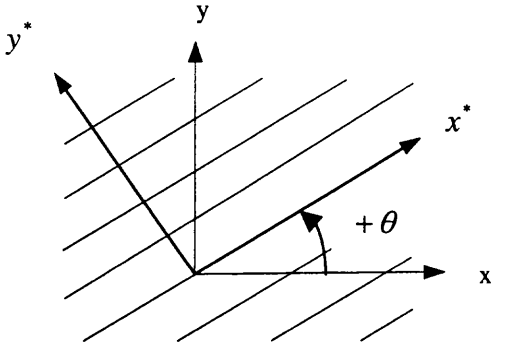

Figure B.2 Positive rotation of principal material axes from xy axes.

B.3 Shallow Shell Theory

Figure B.3 shows Donnell-type [10] 'shallow shell theory' out of general shell theory. When n is very large so that the half wave length of the deformation is small compared to the radius, the flat plate developed should give a fair approximation. The complete general shell theory is applicable over the whole span, but a modification of it which has come to be known as 'shallow shell theory' has been found to be very useful, giving good approximation in the upper range of values of n, for values down to three or four (and acceptable approximation for values as low as two).

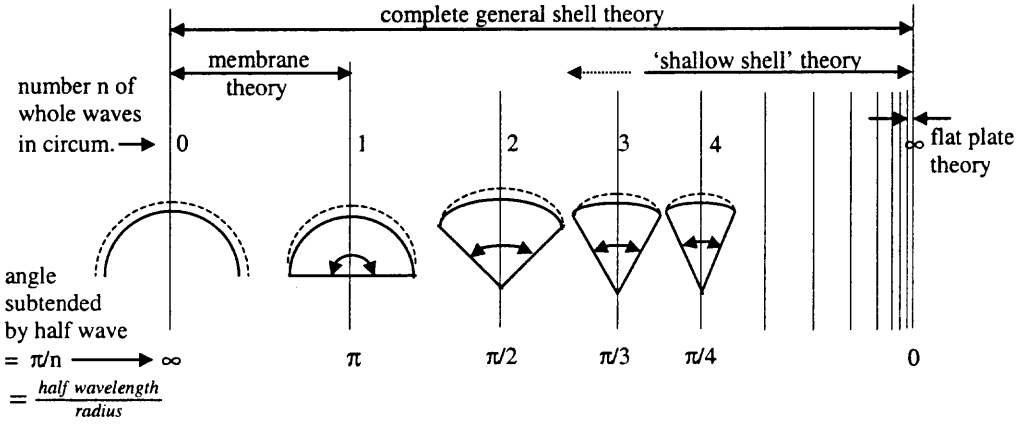

Figure B.3 Range of applicability of shell

APPENDIX C

RECURRENCE RELATION COEFFICIENTS

For single layer :

The coefficients $G_{i,j}$ in Eqs.(3.20) $G'_{i,j}$, $G''_{i,j}$ in Eqs.(3.25) are

$$G_{1,1} = -\frac{(2m+1)\sin\alpha}{(m+2)R_0} \tag{C.1}$$

$$G_{1,2} = -\frac{m^2\sin^2\alpha}{(m+2)(m+1)R_0^2} + \frac{A_{22}\sin^2\alpha + A_{66}n^2}{A_{11}R_0^2(m+2)(m+1)} \tag{C.2}$$

$$G_{1,3} = -\frac{(A_{12}+A_{66})n}{A_{11}R_0(m+2)} \tag{C.3}$$

$$G_{1,4} = -\frac{[(A_{12}+A_{66})m-(A_{22}+A_{66})]n\sin\alpha}{A_{11}R_0^2(m+2)(m+1)} \tag{C.4}$$

$$G_{1,5} = \frac{A_{12}\cos\alpha}{A_{11}R_0(m+2)} \tag{C.5}$$

$$G_{1,6} = \frac{(A_{12}m-A_{22})\sin\alpha\cos\alpha}{A_{11}R_0^2(m+2)(m+1)} \tag{C.6}$$

$$G_{2,1} = \frac{(A_{12}+A_{66})n}{A_{66}R_0(m+2)} \tag{C.7}$$

$$G_{2,2} = \frac{[(A_{12}+A_{66})m+(A_{22}+A_{66})n\sin\alpha}{A_{66}R_0^2(m+2)(m+1)} \tag{C.8}$$

$$G_{2,3} = -\frac{(2m+1)\sin\alpha}{(m+2)R_0} \tag{C.9}$$

$$G_{2,4} = -\frac{m^2\sin^2\alpha}{(m+2)(m+1)R_0^2} + \frac{A_{66}\sin^2\alpha + A_{22}n^2}{A_{66}R_0^2(m+2)(m+1)} \tag{C.10}$$

$$G_{2,5} = -\frac{A_{22}n\cos\alpha}{A_{66}R_0^2(m+2)(m+1)} \tag{C.11}$$

$$G_{3,1} = \frac{A_{12}\cos\alpha}{D_{11}R_0(m+4)(m+3)(m+2)} \tag{C.12}$$

$$G_{3,2} = \frac{(3A_{12}m-A_{22})\sin\alpha\cos\alpha}{D_{11}R_0^2m_{41}} \tag{C.13}$$

$$G_{3,3} = \frac{[3A_{12}(m-1)+2A_{22}]\sin^2\alpha\cos\alpha}{D_{11}R_0^3m_{41}} \tag{C.14}$$

$$G_{3,4} = \frac{[A_{12}(m-2)+A_{22}]\sin^3\alpha\cos\alpha}{D_{11}R_0^4m_{41}} \tag{C.15}$$

$$G_{3,5} = \frac{A_{22}n\cos\alpha}{D_{11}R_0^2m_{41}} \tag{C.16}$$

$$G_{3,6} = \frac{A_{22} n \sin 2\alpha}{D_{11} R_0^3 m_{41}} \tag{C.17}$$

$$G_{3,7} = \frac{A_{22} n \sin^2 \alpha \cos \alpha}{D_{11} R_0^4 m_{41}} \tag{C.18}$$

$$G_{3,8} = -\frac{2(2m+1)\sin \alpha}{R_0 (m+4)} \tag{C.19}$$

$$G_{3,9} = \left[\frac{2(D_{12} + 2D_{66})n^2 + D_{22} \sin^2 \alpha}{D_{11} R_0^2} - \frac{P}{2\pi D_{11} \cos \alpha} - \frac{M \cos \phi}{\pi D_{11} R_0^2 \cos \alpha} - \frac{6m^2 \sin^2 \alpha}{R_0^2} \right] \Big/ (m+4)(m+3) \tag{C.20}$$

$$G_{3,10} = \left\{ -\frac{q(m+1)\tan \alpha}{D_{11}} - \frac{3Pm \sin \alpha}{2D_{11} R_0^2 \pi \cos \alpha} + \frac{M \cos \phi \sin \alpha (2m-1)}{\pi D_{11} R_0^3 \cos \alpha} - \frac{2m(m-1)(2m-1)\sin^3 \alpha}{R_0^3} + \frac{[2(D_{12} + 2D_{66})n^2 + D_{22} \sin^2 \alpha](2m-1)\sin \alpha}{D_{11} R_0^3} \right\} \Big/ (m+4)(m+3)(m+2) \tag{C.21}$$

$$G_{3,11} = \left\{ -[2(D_{12} + 2D_{66})n^2 + D_{22} \sin^2 \alpha] \sin^2 \alpha m(m-2) - A_{22} R_0^2 \cos^2 \alpha - D_{11} m(m-1)^2 (m-2) \sin^4 \alpha - D_{22} n^4 + \frac{qn^2 R_0^3}{\cos \alpha} + 2(D_{12} + D_{22} + 2D_{66}) n^2 \sin^2 \alpha - 4qR_0^3 m \tan \alpha \sin \alpha - \frac{3PR_0 m(m-1)\sin^2 \alpha}{2\pi \cos \alpha} - \frac{M \cos \phi \sin \alpha m(m-2)}{\pi \cos \alpha} - 3.5qR_0^3 m(m-1)\tan \alpha \sin^2 \alpha \right\} \Big/ (D_{11} R_0^4 m_{41}) \tag{C.22}$$

$$G_{3,12} = \left[-\left(\frac{P}{2\pi \cos \alpha} + \frac{4.5qR_0^2}{\cos \alpha} \right)(m-1)(m-2)\sin^3 \alpha - 6qR_0^2 (m-1)\tan \alpha \sin^2 \alpha - 2A_{22} R_0 \sin \alpha \cos^2 \alpha + \frac{3qR_0^2 n^2 \sin \alpha}{\cos \alpha} \right] \Big/ (D_{11} R_0^4 m_{41}) \tag{C.23}$$

$$G_{3,13} = [-0.5q \tan \alpha R_0 (m-2)(5m-7)\sin^3 \alpha + 3qn^2 R_0 \tan \alpha \sin \alpha - A_{22} \sin^2 \alpha \cos^2 \alpha] / (D_{11} R_0^4 m_{41}) \tag{C.24}$$

$$G_{3,14} = \left[-0.5q(m-2)(m-3)\tan \alpha \sin \alpha - \frac{qn^2}{\cos \alpha} \right] \sin^3 \alpha \Big/ (D_{11} R_0^4 m_{41}) \tag{C.25}$$

where $m_{41} = (m+4)(m+3)(m+2)(m+1)$.

$$G'_{3,9} = \left[\frac{2(D_{12}+2D_{66})n^2 + D_{22}\sin^2\alpha}{D_{11}R_0^2} - \frac{P}{2\pi D_{11}\cos\alpha} - \frac{6m^2\sin^2\alpha}{R_0^2} \right] \Big/ (m+4)(m+3) \qquad \text{(C.26)}$$

$$G''_{3,9} = \left[-\frac{1}{2}\frac{M}{\pi D_{11}R_0^2\cos\alpha} \right] \Big/ (m+4)(m+3) \qquad \text{(C.27)}$$

$$G'_{3,10} = \left\{ -\frac{q(m+1)\tan\alpha}{D_{11}} - \frac{3Pm\sin\alpha}{2D_{11}R_0^2\pi\cos\alpha} - \frac{2m(m-1)(2m-1)\sin^3\alpha}{R_0^3} + \frac{[2(D_{12}+2D_{66})n^2 + D_{22}\sin^2\alpha](2m-1)\sin\alpha}{D_{11}R_0^3} \right\} \Big/ (m+4)(m+3)(m+2) \qquad \text{(C.28)}$$

$$G''_{3,10} = \left\{ -\frac{1}{2}\frac{M\sin\alpha(2m-1)}{\pi D_{11}R_0^3\cos\alpha} \right\} \Big/ (m+4)(m+3)(m+2) \qquad \text{(C.29)}$$

$$G'_{3,11} = \{ -[2(D_{12}+2D_{66})n^2 + D_{22}\sin^2\alpha]\sin^2\alpha m(m-2) - A_{22}R_0^2\cos^2\alpha - D_{11}m(m-1)^2(m-2)\sin^4\alpha - D_{22}n^4 + \frac{qn^2R_0^3}{\cos\alpha} + 2(D_{12}+D_{22}+2D_{66})n^2\sin^2\alpha - 4qR_0^3m\tan\alpha\sin\alpha - \frac{3PR_0m(m-1)\sin^2\alpha}{2\pi\cos\alpha} - 3.5qR_0^3m(m-1)\tan\alpha\sin^2\alpha \} / (D_{11}R_0^4m_{41}) \qquad \text{(C.30)}$$

$$G''_{3,11} = \left\{ -\frac{1}{2}\frac{M\cos\phi\sin\alpha m(m-2)}{\pi\cos\alpha} \right\} \Big/ R_0^4m_{41} \qquad \text{(C.31)}$$

For multi layer :

The coefficients $G_{i,j}$ in Eqs.(4.17) and $G'_{i,j}$, $G''_{i,j}$ in Eqs.(4.25) are

$$G_{1,1} = -\frac{(3m+1)\sin\alpha}{(m+2)R_0} \qquad \text{(C.32)}$$

$$G_{1,2} = -\frac{m(3m-1)\sin^2\alpha}{(m+2)(m+1)R_0^2} + \frac{A_{22}\sin^2\alpha + A_{66}n^2}{A_{11}R_0^2(m+2)(m+1)} \qquad \text{(C.33)}$$

$$G_{1,3} = -\frac{(A_{22}\sin^2\alpha + A_{66}n^2)\sin\alpha - A_{11}(m-1)^2\sin^3\alpha}{A_{11}R_0^3(m+2)(m+1)} \qquad \text{(C.34)}$$

$$G_{1,4} = -\frac{(A_{12}+A_{66})n}{A_{11}R_0(m+2)} \qquad \text{(C.35)}$$

$$G_{1,5} = -\frac{[2(A_{12}+A_{66})m - (A_{22}+A_{66})]n\sin^2\alpha}{A_{11}R_0^2(m+2)(m+1)} \qquad \text{(C.36)}$$

$$G_{1,6} = -\frac{[(A_{12}+A_{66})(m-1)-(A_{22}+A_{66})]n\sin^2\alpha}{A_{11}R_0^3(m+2)(m+1)} \tag{C.37}$$

$$G_{1,7} = \frac{B_{11}(m+3)}{A_{11}} \tag{C.38}$$

$$G_{1,8} = \frac{B_{11}(3m+1)\sin\alpha}{A_{11}R_0} \tag{C.39}$$

$$G_{1,9} = [B_{11}m(3m-1)\sin^3\alpha - (B_{12}+2B_{66})n^2 - B_{22}\sin\alpha + A_{12}R_0\cos\alpha]/A_{11}R_0^2(m+2) \tag{C.40}$$

$$G_{1,10} = \{B_{11}m(m-1)^2\sin^3\alpha - [(B_{12}+2B_{66})n^2 + B_{22}\sin^2\alpha] \times m\sin\alpha + R_0(2A_{12}m - A_{22})\sin\alpha\cos\alpha + (B_{12}+B_{22}+2B_{66})n^2\sin\alpha\}/A_{11}R_0^3(m+2)(m+1) \tag{C.41}$$

$$G_{1,11} = \frac{[A_{12}(m-1)-A_{22}]\sin^2\alpha\cos\alpha}{A_{11}R_0^3(m+2)(m+1)} \tag{C.42}$$

$$G_{2,1} = \frac{(A_{12}+A_{66})n}{A_{66}R_0(m+2)} \tag{C.43}$$

$$G_{2,2} = \frac{[2(A_{12}+A_{66})m + A_{22}+A_{66}]n\sin\alpha}{A_{66}R_0^2(m+2)(m+1)} \tag{C.44}$$

$$G_{2,3} = \frac{[(A_{12}+A_{66})(m-1)+(A_{22}+A_{66})]n\sin^2\alpha}{A_{66}R_0^3(m+2)(m+1)} \tag{C.45}$$

$$G_{2,4} = -\frac{(3m+1)\sin\alpha}{(m+2)R_0} \tag{C.46}$$

$$G_{2,5} = \frac{A_{22}n^2 + A_{66}[1-m(3m-1)]\sin^2\alpha}{A_{66}R_0^2(m+2)(m+1)} \tag{C.47}$$

$$G_{2,6} = \frac{[A_{22}n^2 - A_{66}m(m-2)\sin^2\alpha]\sin\alpha}{A_{66}R_0^3(m+2)(m+1)} \tag{C.48}$$

$$G_{2,7} = -\frac{(B_{12}+2B_{66})n}{A_{66}R_0} \tag{C.49}$$

$$G_{2,8} = -\frac{[2(B_{12}+B_{66})m + B_{22}]\sin\alpha}{A_{66}R_0^2(m+2)} \tag{C.50}$$

$$G_{2,9} = \frac{[B_{22}(n^2 - m\sin^2\alpha) - A_{22}R_0\cos\alpha - (B_{12}+2B_{66})m(m-1)\sin^2\alpha]n}{A_{66}R_0^3(m+2)(m+1)} \tag{C.51}$$

$$G_{2,10} = -\frac{A_{22}n\sin\alpha\cos\alpha}{A_{66}R_0^3(m+2)(m+1)} \tag{C.52}$$

$$G_{3,1} = \frac{B_{11}}{D_{11}(m+4)} \tag{C.53}$$

$$G_{3,2} = \frac{2(2m+1)B_{11}\sin\alpha}{D_{11}R_0(m+4)(m+3)} \tag{C.54}$$

$$G_{3,3} = \frac{(6B_{11}m^2 - B_{22})\sin^2\alpha - (B_{12}+2B_{66})n^2 + A_{12}R_0\cos\alpha}{D_{11}R_0^2(m+4)(m+3)(m+2)} \tag{C.55}$$

$$\begin{aligned} G_{3,4} = \{&2B_{11}R_0m(m-1)(2m-1)\sin^3\alpha + 3A_{12}R_0^2m\sin\alpha\cos\alpha \\ &- 2(B_{12}+2B_{66})R_0mn^2\sin\alpha - B_{22}R_0[n^2+(2m-1)\sin^2\alpha]\sin\alpha \\ &+ A_{22}R_0^2\sin\alpha\cos\alpha\}/(D_{11}R_0^4m_{41}) \end{aligned} \tag{C.56}$$

$$\begin{aligned} G_{3,5} = \{&B_{11}(m-1)^2(m-2)\sin^4\alpha + 3A_{12}R_0(m-1)\sin^2\alpha\cos\alpha \\ &- (B_{12}+2B_{66})n^2(m-1)\sin^2\alpha - B_{22}[n^2+(m-2)\sin^2\alpha]\sin^2\alpha \\ &+ 2A_{22}R_0\sin^2\alpha\cos\alpha\}/(D_{11}R_0^4m_{41}) \end{aligned} \tag{C.57}$$

$$G_{3,6} = \frac{[A_{12}(m-2)+A_{22}]\sin^3\alpha\cos\alpha}{D_{11}R_0^4m_{41}} \tag{C.58}$$

$$G_{3,7} = \frac{(B_{12}+2B_{66})n}{D_{11}R_0(m+4)(m+3)} \tag{C.59}$$

$$G_{3,8} = -\frac{[3(B_{12}+2B_{66})m - B_{22}]n\sin\alpha}{D_{11}R_0^2(m+4)(m+3)(m+2)} \tag{C.60}$$

$$\begin{aligned} G_{3,9} = \{&3(B_{12}+2B_{66})nm(m-1)\sin^2\alpha + A_{22}R_0n\cos\alpha \\ &- B_{22}n[n^2+(2m-1)\sin^2\alpha]\}/(D_{11}R_0^3m_{41}) \end{aligned} \tag{C.61}$$

$$\begin{aligned} G_{3,10} = \{&(B_{12}+2B_{66})n(m-1)(m-2)\sin^3\alpha + 2A_{22}R_0n\sin\alpha\cos\alpha \\ &- B_{22}[n^2+(m-2)\sin^2\alpha]n\sin\alpha\}/(D_{11}R_0^4m_{41}) \end{aligned} \tag{C.62}$$

$$G_{3,11} = \frac{A_{22}n\sin^2\alpha\cos\alpha}{D_{11}R_0^4m_{41}} \tag{C.63}$$

$$G_{3,12} = -\frac{2(2m+1)\sin\alpha}{R_0(m+4)} \tag{C.64}$$

$$\begin{aligned} G_{3,13} = \Bigg[&\frac{2(D_{12}+2D_{66})n^2 + D_{22}\sin^2\alpha}{D_{11}R_0^2} - \frac{P}{2\pi D_{11}\cos\alpha} - \frac{M\cos\phi}{\pi D_{11}R_0^2\cos\alpha} \\ &- \frac{6m^2\sin^2\alpha}{R_0^2} - \frac{2B_{12}\cos\alpha}{D_{11}R_0}\Bigg]\Big/(m+4)(m+3) \end{aligned} \tag{C.65}$$

$$\begin{aligned} G_{3,14} = \Bigg\{&-\frac{q(m+1)\tan\alpha}{D_{11}} - \frac{3Pm\sin\alpha}{2D_{11}R_0^2\pi\cos\alpha} + \frac{M\cos\phi\sin\alpha(2m-1)}{\pi D_{11}R_0^3\cos\alpha} \\ &- \frac{2m(m-1)(2m-1)\sin^3\alpha}{R_0^3} - \frac{6B_{12}m\sin\alpha\cos\alpha}{D_{11}R_o^2} \\ &+ \frac{[2(D_{12}+2D_{66})n^2 + D_{22}\sin^2\alpha](2m-1)\sin\alpha}{D_{11}R_0^3}\Bigg\}\Big/(m+4)(m+3)(m+2) \end{aligned} \tag{C.66}$$

$$G_{3,15} = \{[2(D_{12}+2D_{66})n^2 + D_{22}\sin^2\alpha]\sin^2\alpha m(m-2) - A_{22}R_0^2\cos^2\alpha$$

$$- D_{11}m(m-1)^2(m-2)\sin^4\alpha - D_{22}n^4 + \frac{qn^2R_0^3}{\cos\alpha}$$
$$+ 2(D_{12}+D_{22}+2D_{66})n^2\sin^2\alpha - 4qR_0^3 m\tan\alpha\sin\alpha$$
$$- \frac{3PR_0m(m-1)\sin^2\alpha}{2\pi\cos\alpha} - 3.5qR_0^3m(m-1)\tan\alpha\sin^2\alpha$$
$$- \frac{M\cos\phi\sin\alpha m(m-2)}{\pi\cos\alpha} - 6B_{12}R_0m(m-1)\cos\alpha\sin^2\alpha$$
$$- B_{22}R_0\cos\alpha(\sin^2\alpha - 2n^2)\Big\}\Big/(D_{11}R_0^4m_{41}) \qquad \text{(C.67)}$$

$$G_{3,16} = \left[-\left(\frac{P}{2\pi\cos\alpha} + 2B_{12}\cos\alpha + \frac{4.5qR_0^2}{\cos\alpha}\right)(m-1)(m-2)\sin^3\alpha\right.$$
$$- 6qR_0^2(m-1)\tan\alpha\sin^2\alpha - 2A_{22}R_0\sin\alpha\cos^2\alpha$$
$$\left. - B_{22}(\sin^2 - 2n^2)\sin\alpha\cos\alpha + \frac{3qR_0^2n^2\sin\alpha}{\cos\alpha}\right]\Big/(D_{11}R_0^4m_{41}) \qquad \text{(C.68)}$$

$$G_{3,17} = [-0.5q\tan\alpha R_0(m-2)(5m-7)\sin^3\alpha + 3qn^2R_0\tan\alpha\sin\alpha$$
$$- A_{22}\sin^2\alpha\cos^2\alpha]/(D_{11}R_0^4m_{41}) \qquad \text{(C.69)}$$

$$G_{3,18} = \left[-0.5q(m-2)(m-3)\tan\alpha\sin\alpha - \frac{qn^2}{\cos\alpha}\right]\sin^3\alpha\Big/(D_{11}R_0^4m_{41}) \qquad \text{(C.70)}$$

where $m_{41} = (m+4)(m+3)(m+2)(m+1)$.

$$G_{3,13}^{'} = \left[\frac{2(D_{12}+2D_{66})n^2 + D_{22}\sin^2\alpha}{D_{11}R_0^2} - \frac{P}{2\pi D_{11}\cos\alpha}\right.$$
$$\left. - \frac{6m^2\sin^2\alpha}{R_0^2} - \frac{2B_{12}\cos\alpha}{D_{11}R_0}\right]\Big/(m+4)(m+3) \qquad \text{(C.71)}$$

$$G_{3,13}^{''} = \left[-\frac{1}{2}\frac{M\cos\phi}{\pi D_{11}R_0^2\cos\alpha}\right]\Big/(m+4)(m+3) \qquad \text{(C.72)}$$

$$G_{3,14}^{'} = \left\{-\frac{q(m+1)\tan\alpha}{D_{11}} - \frac{3Pm\sin\alpha}{2D_{11}R_0^2\pi\cos\alpha}\right.$$
$$- \frac{2m(m-1)(2m-1)\sin^3\alpha}{R_0^3} - \frac{6B_{12}m\sin\alpha\cos\alpha}{D_{11}R_o^2}$$
$$\left. + \frac{[2(D_{12}+2D_{66})n^2 + D_{22}\sin^2\alpha](2m-1)\sin\alpha}{D_{11}R_0^3}\right\}\Big/(m+4)(m+3)(m+2) \qquad \text{(C.73)}$$

$$G_{3,14}^{''} = \left\{-\frac{1}{2}\frac{M\cos\phi\sin\alpha(2m-1)}{\pi D_{11}R_0^3\cos\alpha}\right\}\Big/(m+4)(m+3)(m+2) \qquad \text{(C.74)}$$

$$G_{3,15}^{'} = \left\{[2(D_{12}+2D_{66})n^2 + D_{22}\sin^2\alpha]\sin^2\alpha m(m-2) - A_{22}R_0^2\cos^2\alpha\right.$$

$$
\begin{aligned}
&- D_{11}m(m-1)^2(m-2)\sin^4\alpha - D_{22}n^4 + \frac{qn^2R_0^3}{\cos\alpha} \\
&+ 2(D_{12} + D_{22} + 2D_{66})n^2\sin^2\alpha - 4qR_0^3 m\tan\alpha\sin\alpha \\
&- \frac{3PR_0m(m-1)\sin^2\alpha}{2\pi\cos\alpha} - 3.5qR_0^3m(m-1)\tan\alpha\sin^2\alpha \\
&- 6B_{12}R_0m(m-1)\cos\alpha\sin^2\alpha \\
&- B_{22}R_0\cos\alpha(\sin^2\alpha - 2n^2)\Big\}\Big/(D_{11}R_0^4m_{41})
\end{aligned}
\tag{C.75}
$$

$$
G''_{3,15} = \left\{-\frac{1}{2}\frac{M\cos\phi\sin\alpha m(m-2)}{\pi\cos\alpha}\right\}\Big/(D_{11}R_0^4m_{41}) \tag{C.76}
$$

APPENDIX D

PROGRAM LOGIC

Computer program (COMBINED1, COMBINED2) to determine critical load using C-language has been developed. For confidence of my program logic, some existing data is compared with my data in Appendix E (E.28).

Outline of Program

{

- Input geometry dimensions and material parameters.
- Determine a_m, b_m, c_m in terms of $a_0, a_1, b_0, b_1, c_0, c_1, c_2, c_3$ using recurrence relationships.
- Calculate $U, V, W, \partial W/\partial x, N_x, N_{x\phi}$ and M_x for applying boundary conditions.

for(repeat m until converging)

begin

- Make coefficients matrix after imposing each boundary condition.
- Set the determinant to zero.
- Obtain the critical buckling load.

end.

}

repeat program for axial compression, outer pressure, and pure bending.

repeat program for combined outer pressure and axial compression,

for combined axial compression and pure bending, and

for combined outer pressure and pure bending.

Some other outputs are obtained by changing parameters.

COMBINED2 is developed by changing $G_{i,j}$ Appendix (C.32 through C.70) from COMBINED1.

APPENDIX E

NUMERICAL SOLUTION DATA

E.1 Buckling Values of Single Layer Isotropic Conical Shell under Axial Compression (P_{cr})

SS1:

$R_1/h=100.0$ $\nu_{x\phi}=0.3$ $E=30x10^6$ psi

alpa \ L/R_1	0.2	0.5	0.8	1.0
0.0	5693.58 (0)	5852.35 (0)	5695.17 (0)	5704.19 (0)
1.0	5695.08 (0)	5851.72 (0)	5702.50 (0)	5697.78 (0)
5.0	5684.01 (0)	5816.32 (0)	5658.91 (0)	5661.15 (0)
10.0	5612.92 (0)	5693.76 (0)	5527.38 (0)	5532.77 (0)
20.0	5291.02 (0)	5195.94 (0)	5023.51 (0)	5042.77 (0)
30.0	4763.01 (0)	4396.63 (0)	4259.73 (0)	4280.68 (0)
40.0	4081.90 (0)	3373.90 (0)	3337.28 (0)	3344.74 (0)
45.0	3701.91 (0)	2819.85 (0)	2853.76 (0)	2844.99 (0)
50.0	3304.71 (0)	2268.52 (0)	2374.17 (0)	2347.80 (0)
60.0	2481.52 (0)	1279.54 (0)	1466.63 (0)	1427.55 (0)
70.0	1647.50 (0)	574.31 (0)	670.24 (0)	686.94 (0)
80.0	819.87 (0)	186.00 (0)	149.34 (0)	160.71 (0)

SS2:

$R_1/h=100.0$ $\nu_{x\phi}=0.3$ $E=30x10^6$ psi

alpa \ L/R_1	0.2	0.5	0.8	1.0
0.0	5723.26 (1)	5868.08 (1)	5721.70 (1)	5721.64 (1)
1.0	5726.86 (1)	5867.87 (1)	5719.45 (1)	5720.48 (1)
5.0	5715.63 (1)	5832.42 (1)	5676.29 (1)	5680.21 (1)
10.0	5644.25 (1)	5710.26 (1)	5546.10 (1)	5553.64 (1)
20.0	5321.44 (1)	5214.88 (1)	5049.08 (1)	5067.57 (1)
30.0	4791.70 (1)	4418.81 (1)	4291.79 (1)	4315.75 (1)
40.0	4107.67 (1)	3399.35 (1)	3372.43 (1)	3382.95 (1)
45.0	3725.75 (1)	2846.55 (1)	2888.32 (1)	2883.64 (1)
50.0	3326.34 (1)	2295.72 (1)	2406.59 (1)	2384.62 (1)
60.0	2498.09 (1)	1303.43 (1)	1491.28 (1)	1456.54 (1)
70.0	1658.58 (1)	589.21 (1)	686.97 (1)	704.04 (1)
80.0	825.37 (1)	191.78 (1)	156.85 (1)	168.83 (1)

SS3:

$R_1/h=100.0$ $\nu_{x\phi}=0.3$ $E=30x10^6$ psi

alpa \ L/R_1	0.2	0.5	0.8	1.0
0.0	5693.58 (0)	5852.35 (0)	5695.17 (0)	5704.19 (0)
1.0	5695.08 (0)	5851.72 (0)	5702.50 (0)	5697.78 (0)
5.0	5684.01 (0)	5816.32 (0)	5658.91 (0)	5661.15 (0)
10.0	5612.92 (0)	5693.76 (0)	5527.38 (0)	5532.77 (0)
20.0	5291.02 (0)	5195.94 (0)	5023.51 (0)	5042.77 (0)
30.0	4763.01 (0)	4396.63 (0)	4259.73 (0)	4280.68 (0)
40.0	4081.90 (0)	3373.90 (0)	3337.28 (0)	3344.74 (0)
45.0	3701.91 (0)	2819.85 (0)	2853.76 (0)	2844.99 (0)
50.0	3304.71 (0)	2268.52 (0)	2374.17 (0)	2347.80 (0)
60.0	2481.52 (0)	1279.54 (0)	1466.63 (0)	1427.55 (0)
70.0	1647.50 (0)	574.31 (0)	670.24 (0)	686.94 (0)
80.0	819.87 (0)	186.00 (0)	149.34 (0)	160.71 (0)

SS4:

$R_1/h=100.0$ $\nu_{x\phi}=0.3$ $E=30x10^6$ psi

alpa \ L/R_1	0.2	0.5	0.8	1.0
0.0	11467.88 (7)	11434.46 (8)	11417.15 (6)	11411.53 (6)
1.0	11465.41 (7)	11430.86 (8)	11413.10 (6)	11407.11 (6)
5.0	11388.56 (7)	11344.97 (8)	11328.68 (6)	11322.78 (6)
10.0	11145.10 (7)	11080.13 (8)	11076.16 (6)	11073.75 (6)
20.0	10174.14 (6)	10075.59 (8)	10081.32 (4)	10071.24 (8)
30.0	8703.41 (5)	8561.41 (7)	8556.18 (8)	8553.62 (7)
40.0	6899.04 (4)	6695.91 (6)	6691.24 (7)	6698.27 (5)
45.0	5940.34 (2)	5706.63 (5)	5699.51 (6)	5705.20 (4)
50.0	4982.36 (0)	4715.08 (4)	4715.78 (5)	4709.42 (0)
60.0	3263.36 (0)	2878.30 (0)	2869.82 (7)	2846.62 (5)
70.0	1895.93 (0)	1357.16 (5)	1333.61 (4)	1345.68 (6)
80.0	852.23 (0)	349.13 (3)	353.67 (4)	342.18 (0)

CC1:

$R_1/h=100.0$ $\nu_{x\phi}=0.3$ $E=30x10^6$ psi

alpa \ L/R_1	0.2	0.5	0.8	1.0
0.0	18947.95 (0)	11408.30 (2)	11410.63 (6)	11414.18 (6)
1.0	18969.21 (0)	11405.02 (2)	11407.73 (6)	11409.29 (6)
5.0	18991.13 (0)	11321.94 (1)	11328.87 (6)	11321.97 (6)
10.0	18861.19 (0)	11073.31 (1)	11068.05 (5)	11066.95 (6)
20.0	18086.18 (0)	10083.84 (7)	10073.76 (4)	10074.47 (4)
30.0	16667.75 (0)	8561.42 (7)	8560.29 (0)	8558.69 (1)
40.0	14688.34 (0)	6697.43 (6)	6743.36 (6)	6695.02 (5)
45.0	13520.16 (0)	5704.22 (5)	5707.42 (6)	5704.64 (4)
50.0	12251.30 (0)	4714.73 (4)	4715.93 (5)	4714.10 (1)
60.0	9466.04 (0)	2883.41 (0)	2852.07 (1)	2857.44 (6)
70.0	6436.40 (0)	1533.89 (0)	1334.57 (4)	1335.87 (1)
80.0	3254.42 (0)	636.56 (0)	370.92 (0)	344.15 (1)

CC2:

$R_1/h=100.0$ $\nu_{x\phi}=0.3$ $E=30x10^6$ psi

alpa \ L/R_1	0.2	0.5	0.8	1.0
0.0	18977.26 (1)	12179.75 (6)	11495.33 (8)	11436.14 (7)
1.0	18999.87 (1)	12187.73 (6)	11490.10 (8)	11434.61 (7)
5.0	19021.61 (1)	12123.01 (8)	11398.23 (8)	11352.21 (9)
10.0	18891.32 (1)	11678.67 (7)	11125.49 (8)	11093.05 (9)
20.0	18115.22 (1)	10531.30 (7)	10094.94 (8)	10126.28 (9)
30.0	16694.95 (1)	8823.48 (6)	8559.50 (8)	8638.31 (9)
40.0	14712.72 (1)	6805.77 (5)	6739.43 (7)	6719.69 (8)
45.0	13542.77 (1)	5762.76 (4)	5763.34 (7)	5717.47 (8)
50.0	12271.89 (1)	4737.05 (3)	4820.74 (7)	4724.47 (1)
60.0	9482.02 (1)	2896.27 (1)	3001.23 (5)	2883.90 (6)
70.0	6447.26 (1)	1544.26 (1)	1361.47 (4)	1399.77 (5)
80.0	3259.89 (1)	641.59 (1)	375.76 (1)	348.28 (1)

CC3:

$R_1/h=100.0$ $\nu_{x\phi}=0.3$ $E=30x10^6$ psi

alpa \ L/R_1	0.2	0.5	0.8	1.0
0.0	18947.95 (0)	11975.14 (8)	11566.08 (8)	11432.72 (7)
1.0	18969.21 (0)	11983.30 (8)	11547.98 (8)	11424.45 (7)
5.0	18991.13 (0)	11947.68 (8)	11414.98 (8)	11344.19 (9)
10.0	18861.19 (0)	11747.57 (8)	11116.10 (8)	11082.93 (9)
20.0	18086.18 (0)	10842.69 (9)	10086.09 (8)	10119.38 (9)

30.0	16667.75 (0)	9394.33 (8)	8559.45 (8)	8642.00 (9)
40.0	14688.34 (0)	7054.12 (0)	6733.88 (8)	6746.37 (8)
45.0	13520.16 (0)	5860.52 (0)	5787.64 (8)	5736.73 (0)
50.0	12251.30 (0)	4752.19 (0)	4835.57 (7)	4714.98 (0)
60.0	9466.04 (0)	2883.41 (0)	3016.04 (7)	2892.33 (7)
70.0	6436.40 (0)	1533.89 (0)	1395.10 (0)	1416.89 (6)
80.0	3254.42 (0)	636.56 (0)	370.92 (0)	344.47 (0)

CC4:

$R_1/h=100.0$ $\nu_{x\phi}=0.3$ $E=30x10^6$ psi

alpa \ L/R_1	0.2	0.5	0.8	1.0
0.0	22719.14 (5)	12945.84 (8)	11842.72 (9)	11968.78 (10)
1.0	22737.25 (5)	12947.86 (8)	11837.25 (9)	11971.44 (4)
5.0	22712.71 (5)	12885.55 (8)	11752.30 (9)	11906.71 (4)
10.0	22462.78 (5)	12638.61 (8)	11502.35 (9)	11376.21 (8)
20.0	21255.68 (4)	11612.95 (8)	10541.44 (9)	10607.96 (6)
30.0	19188.30 (3)	9991.12 (8)	9058.00 (8)	9031.32 (10)
40.0	16434.82 (0)	7991.24 (8)	7183.80 (8)	6979.55 (8)
45.0	14888.37 (0)	6935.53 (8)	6202.46 (8)	5976.36 (8)
50.0	13275.50 (0)	5828.30 (7)	5185.36 (7)	4985.18 (8)
60.0	9945.36 (0)	3764.01 (6)	3270.42 (6)	3102.24 (7)
70.0	6589.20 (0)	2013.03 (5)	1611.31 (6)	1535.33 (6)
80.0	3274.37 (0)	741.26 (2)	491.22 (4)	439.73 (4)

E.2 Buckling Values of Single Layer Isotropic Conical Shell under Outer Pressure (q_{cr})

SS1:

$R_1/h=100.0$ $\nu_{x\phi}=0.3$ $E=30x10^6$ psi

alpa \ L/R_1	0.2	0.5	0.8	1.0
0.0	2836.05 (17)	692.51 (11)	392.56 (9)	304.58 (8)
1.0	2830.18 (17)	687.93 (11)	388.37 (9)	300.78 (8)
5.0	2797.70 (17)	667.52 (11)	371.22 (9)	285.97 (8)
10.0	2737.88 (17)	637.93 (11)	348.98 (9)	267.70 (8)
20.0	2558.40 (17)	566.88 (11)	301.29 (9)	222.79 (9)
30.0	2308.17 (17)	483.78 (11)	247.91 (10)	180.25 (9)
40.0	1999.59 (17)	394.22 (11)	195.13 (10)	139.47 (9)
45.0	1827.50 (17)	348.90 (11)	169.23 (9)	120.03 (9)
50.0	1645.69 (17)	302.95 (10)	143.70 (9)	101.52 (9)
60.0	1258.89 (17)	214.06 (10)	97.17 (9)	67.76 (8)
70.0	850.06 (17)	132.72 (9)	56.44 (8)	38.50 (8)
80.0	428.06 (17)	61.81 (8)	23.75 (7)	15.27 (6)

SS2:

$R_1/h=100.0$ $\nu_{x\phi}=0.3$ $E=30x10^6$ psi

alpa \ L/R_1	0.2	0.5	0.8	1.0
0.0	2848.37 (17)	739.19 (11)	452.84 (9)	365.49 (9)
1.0	2842.42 (17)	734.34 (11)	448.48 (9)	360.23 (9)
5.0	2809.55 (17)	712.45 (11)	428.66 (10)	339.24 (9)
10.0	2749.04 (17)	680.19 (11)	399.40 (10)	313.56 (9)
20.0	2567.63 (17)	601.66 (11)	338.65 (10)	262.49 (9)
30.0	2315.08 (17)	509.64 (11)	276.00 (10)	208.81 (10)
40.0	2004.18 (17)	411.32 (11)	214.06 (10)	159.05 (10)
45.0	1831.04 (17)	362.07 (11)	184.45 (10)	135.99 (10)
50.0	1648.30 (17)	313.56 (10)	156.32 (10)	113.56 (9)
60.0	1260.09 (17)	218.89 (10)	103.33 (9)	73.71 (9)

70.0	850.43 (17)	134.31 (9)	58.75 (8)	40.75 (8)
80.0	428.11 (17)	62.02 (8)	24.10 (7)	15.70 (6)

SS3:

$R_1/h=100.0$ $\nu_{x\phi}=0.3$ $E=30x10^6$ psi

alpa \ L/R_1	0.2	0.5	0.8	1.0
0.0	2935.04 (18)	734.73 (11)	410.03 (9)	317.87 (8)
1.0	2928.88 (18)	730.83 (11)	406.43 (9)	314.68 (8)
5.0	2894.54 (18)	711.05 (12)	391.58 (9)	298.66 (9)
10.0	2830.91 (18)	679.21 (12)	366.84 (10)	275.66 (9)
20.0	2639.25 (18)	604.24 (12)	314.76 (10)	233.34 (9)
30.0	2372.24 (18)	517.04 (12)	261.50 (10)	192.20 (9)
40.0	2044.96 (18)	422.41 (12)	207.26 (10)	149.64 (10)
45.0	1863.77 (18)	374.14 (12)	180.41 (10)	129.52 (10)
50.0	1673.50 (18)	325.84 (11)	154.27 (10)	110.11 (9)
60.0	1272.89 (18)	229.34 (11)	105.71 (10)	73.22 (9)
70.0	855.30 (18)	140.88 (10)	61.45 (9)	42.01 (8)
80.0	428.77 (17)	63.84 (9)	25.38 (7)	16.63 (7)

SS4:

$R_1/h=100.0$ $\nu_{x\phi}=0.3$ $E=30x10^6$ psi

alpa \ L/R_1	0.2	0.5	0.8	1.0
0.0	2967.24 (18)	809.32 (12)	486.85 (10)	389.76 (9)
1.0	2960.95 (18)	804.16 (12)	481.88 (10)	385.16 (9)
5.0	2925.77 (18)	780.89 (12)	461.33 (10)	366.74 (10)
10.0	2860.49 (18)	746.54 (12)	434.42 (10)	337.12 (10)
20.0	2663.94 (18)	662.18 (12)	368.74 (11)	281.56 (10)
30.0	2390.82 (18)	561.68 (12)	301.99 (11)	227.84 (10)
40.0	2057.35 (18)	452.68 (12)	235.81 (11)	175.23 (10)
45.0	1873.34 (18)	397.67 (12)	203.84 (11)	149.91 (10)
50.0	1680.58 (18)	343.69 (12)	173.21 (11)	125.75 (10)
60.0	1276.12 (18)	239.00 (11)	114.93 (10)	82.45 (10)
70.0	856.31 (18)	144.39 (10)	65.27 (9)	45.72 (9)
80.0	428.90 (17)	64.34 (9)	26.15 (7)	17.37 (7)

CC1:

$R_1/h=100.0$ $\nu_{x\phi}=0.3$ $E=30x10^6$ psi

alpa \ L/R_1	0.2	0.5	0.8	1.0
0.0	4773.37 (24)	919.18 (12)	473.52 (10)	356.14 (9)
1.0	4764.39 (24)	914.30 (12)	468.38 (10)	351.19 (9)
5.0	4714.14 (24)	892.16 (12)	447.58 (10)	331.64 (9)
10.0	4619.72 (25)	859.21 (12)	421.24 (10)	308.65 (9)
20.0	4329.53 (25)	772.36 (13)	366.51 (10)	264.42 (9)
30.0	3924.58 (25)	670.81 (13)	307.73 (11)	215.89 (10)
40.0	3420.47 (26)	559.90 (13)	246.86 (11)	169.96 (10)
45.0	3134.97 (26)	502.48 (13)	217.24 (11)	148.07 (10)
50.0	2831.42 (26)	444.53 (13)	187.83 (10)	127.05 (10)
60.0	2178.52 (26)	329.04 (13)	131.88 (10)	87.72 (9)
70.0	1478.31 (26)	215.15 (12)	82.11 (9)	52.74 (9)
80.0	746.89 (26)	105.96 (12)	38.09 (9)	23.49 (8)

CC2:

$R_1/h=100.0$ $\nu_{x\phi}=0.3$ $E=30x10^6$ psi

alpa \ L/R_1	0.2	0.5	0.8	1.0
0.0	4786.88 (24)	971.90 (12)	529.08 (10)	412.07 (9)
1.0	4777.86 (24)	966.41 (13)	524.11 (10)	407.43 (9)

5.0	4727.32 (24)	939.38 (13)	503.40 (10)	387.02 (10)
10.0	4631.52 (25)	900.36 (13)	472.79 (11)	357.22 (10)
20.0	4339.56 (25)	806.93 (13)	405.40 (11)	300.59 (10)
30.0	3932.26 (25)	697.41 (13)	336.21 (11)	245.27 (10)
40.0	3425.38 (26)	577.99 (13)	266.85 (11)	190.96 (10)
45.0	3138.80 (26)	516.59 (13)	233.03 (11)	164.77 (10)
50.0	2834.28 (26)	455.05 (13)	200.35 (11)	139.71 (10)
60.0	2179.85 (26)	333.92 (13)	139.12 (10)	94.32 (10)
70.0	1478.73 (26)	216.94 (12)	84.58 (10)	55.34 (9)
80.0	746.95 (26)	106.20 (12)	38.47 (9)	23.94 (8)

CC3:

$R_1/h=100.0$ $\nu_{x\phi}=0.3$ $E=30x10^6$ psi

alpa \ L/R_1	0.2	0.5	0.8	1.0
0.0	4778.41 (24)	922.44 (12)	473.54 (10)	356.17 (9)
1.0	4769.48 (24)	917.71 (12)	468.41 (10)	351.19 (9)
5.0	4719.39 (24)	896.18 (12)	447.72 (10)	331.70 (9)
10.0	4623.39 (25)	861.63 (13)	421.64 (10)	308.81 (9)
20.0	4333.09 (25)	774.68 (13)	367.68 (10)	265.15 (10)
30.0	3927.65 (25)	673.49 (13)	308.41 (11)	216.51 (10)
40.0	3422.10 (26)	562.41 (13)	247.73 (11)	170.78 (10)
45.0	3136.31 (26)	504.71 (13)	218.10 (11)	148.90 (10)
50.0	2832.46 (26)	446.40 (13)	189.24 (11)	127.84 (10)
60.0	2179.05 (26)	330.08 (13)	132.95 (10)	88.81 (10)
70.0	1478.48 (26)	215.89 (12)	82.68 (10)	53.17 (9)
80.0	746.92 (26)	106.07 (12)	38.22 (9)	23.64 (8)

CC4:

$R_1/h=100.0$ $\nu_{x\phi}=0.3$ $E=30x10^6$ psi

alpa \ L/R_1	0.2	0.5	0.8	1.0
0.0	4799.15 (24)	983.83 (13)	537.16 (10)	418.16 (9)
1.0	4790.19 (24)	977.94 (13)	532.45 (10)	413.79 (9)
5.0	4739.32 (25)	951.61 (13)	510.21 (11)	390.07 (10)
10.0	4641.14 (25)	913.21 (13)	477.81 (11)	360.98 (10)
20.0	4348.38 (25)	820.01 (13)	411.39 (11)	305.53 (10)
30.0	3939.51 (25)	709.16 (13)	342.30 (11)	248.71 (11)
40.0	3429.50 (26)	587.11 (13)	272.03 (11)	193.64 (11)
45.0	3142.11 (26)	524.12 (13)	237.47 (11)	167.67 (11)
50.0	2836.81 (26)	460.95 (13)	203.94 (11)	142.97 (11)
60.0	2181.08 (26)	336.90 (13)	141.69 (11)	96.19 (10)
70.0	1479.13 (26)	218.55 (12)	85.72 (10)	56.54 (9)
80.0	747.00 (26)	106.41 (12)	3 8.75 (9)	24.25 (8)

E.3 Buckling Ratio of Single Layer Isotropic Conical Shell under Axial Compression ($P_{cr}/P_{classical}$)

SS1:

$R_1/h=100.0$ $\nu_{x\phi}=0.3$ $E=30x10^6$ psi

alpa \ L/R_1	0.2	0.5	0.8	1.0
0.0	0.4991 (0)	0.5130 (0)	0.4992 (0)	0.5000 (0)
1.0	0.4994 (0)	0.5131 (0)	0.5000 (0)	0.4996 (0)
5.0	0.5020 (0)	0.5137 (0)	0.4998 (0)	0.5000 (0)
10.0	0.5073 (0)	0.5146 (0)	0.4996 (0)	0.5001 (0)
20.0	0.5252 (0)	0.5158 (0)	0.4987 (0)	0.5006 (0)
30.0	0.5567 (0)	0.5139 (0)	0.4979 (0)	0.5003 (0)
40.0	0.6097 (0)	0.5040 (0)	0.4985 (0)	0.4996 (0)

45.0	0.6490 (0)	0.4944 (0)	0.5003 (0)	0.4988 (0)
50.0	0.7011 (0)	0.4813 (0)	0.5037 (0)	0.4981 (0)
60.0	0.8701 (0)	0.4486 (0)	0.5142 (0)	0.5005 (0)
70.0	1.2345 (0)	0.4303 (0)	0.5022 (0)	0.5147 (0)
80.0	2.3833 (0)	0.5407 (0)	0.4341 (0)	0.4672 (0)

SS2:

$R_1/h=100.0$ $\nu_{x\phi}=0.3$ $E=30x10^6$ psi

alpa \ L/R_1	0.2	0.5	0.8	1.0
0.0	0.5017 (1)	0.5144 (1)	0.5015 (1)	0.5015 (1)
1.0	0.5021 (1)	0.5145 (1)	0.5015 (1)	0.5016 (1)
5.0	0.5048 (1)	0.5152 (1)	0.5014 (1)	0.5017 (1)
10.0	0.5101 (1)	0.5161 (1)	0.5013 (1)	0.5019 (1)
20.0	0.5282 (1)	0.5177 (1)	0.5012 (1)	0.5030 (1)
30.0	0.5600 (1)	0.5164 (1)	0.5016 (1)	0.5044 (1)
40.0	0.6136 (1)	0.5078 (1)	0.5037 (1)	0.5053 (1)
45.0	0.6532 (1)	0.4990 (1)	0.5064 (1)	0.5055 (1)
50.0	0.7057 (1)	0.4870 (1)	0.5106 (1)	0.5059 (1)
60.0	0.8759 (1)	0.4570 (1)	0.5229 (1)	0.5107 (1)
70.0	1.2428 (1)	0.4415 (1)	0.5148 (1)	0.5276 (1)
80.0	2.3993 (1)	0.5575 (1)	0.4560 (1)	0.4908 (1)

SS3:

$R_1/h=100.0$ $\nu_{x\phi}=0.3$ $E=30x10^6$ psi

alpa \ L/R_1	0.2	0.5	0.8	1.0
0.0	0.4991 (0)	0.5130 (0)	0.4992 (0)	0.5000 (0)
1.0	0.4994 (0)	0.5131 (0)	0.5000 (0)	0.4996 (0)
5.0	0.5020 (0)	0.5137 (0)	0.4998 (0)	0.5000 (0)
10.0	0.5073 (0)	0.5146 (0)	0.4996 (0)	0.5001 (0)
20.0	0.5252 (0)	0.5158 (0)	0.4987 (0)	0.5006 (0)
30.0	0.5567 (0)	0.5139 (0)	0.4979 (0)	0.5003 (0)
40.0	0.6097 (0)	0.5040 (0)	0.4985 (0)	0.4996 (0)
45.0	0.6490 (0)	0.4944 (0)	0.5003 (0)	0.4988 (0)
50.0	0.7011 (0)	0.4813 (0)	0.5037 (0)	0.4981 (0)
60.0	0.8701 (0)	0.4486 (0)	0.5142 (0)	0.5005 (0)
70.0	1.2345 (0)	0.4303 (0)	0.5022 (0)	0.5147 (0)
80.0	2.3833 (0)	0.5407 (0)	0.4341 (0)	0.4672 (0)

SS4:

$R_1/h=100.0$ $\nu_{x\phi}=0.3$ $E=30x10^6$ psi

alpa \ L/R_1	0.2	0.5	0.8	1.0
0.0	1.0052 (7)	1.0023 (8)	1.0008 (6)	1.0003 (6)
1.0	1.0053 (7)	1.0023 (8)	1.0007 (6)	1.0002 (6)
5.0	1.0059 (7)	1.0021 (8)	1.0006 (6)	1.0001 (6)
10.0	1.0073 (7)	1.0014 (8)	1.0011 (6)	1.0009 (6)
20.0	1.0100 (6)	1.0002 (8)	1.0008 (4)	0.9998 (8)
30.0	1.0172 (5)	1.0006 (7)	1.0000 (8)	0.9997 (7)
40.0	1.0305 (4)	1.0002 (6)	0.9995 (7)	1.0005 (5)
45.0	1.0414 (2)	1.0004 (5)	0.9992 (6)	1.0002 (4)
50.0	1.0570 (0)	1.0003 (4)	1.0005 (5)	0.9991 (0)
60.0	1.1442 (0)	1.0092 (0)	1.0062 (7)	0.9981 (5)
70.0	1.4207 (0)	1.0170 (5)	0.9993 (4)	1.0084 (6)
80.0	2.4774 (0)	1.0149 (3)	1.0281 (4)	0.9947 (0)

CC1:

$R_1/h=100.0$ $\nu_{x\phi}=0.3$ $E=30x10^6$ psi

alpa \ L/R_1	0.2	0.5	0.8	1.0
0.0	1.6609 (0)	1.0000 (2)	1.0002 (6)	1.0005 (6)
1.0	1.6633 (0)	1.0000 (2)	1.0003 (6)	1.0004 (6)
5.0	1.6774 (0)	1.0000 (1)	1.0006 (6)	1.0000 (6)
10.0	1.7047 (0)	1.0008 (1)	1.0003 (5)	1.0002 (6)
20.0	1.7954 (0)	1.0010 (7)	1.0000 (4)	1.0001 (4)
30.0	1.9480 (0)	1.0006 (7)	1.0005 (0)	1.0003 (1)
40.0	2.1940 (0)	1.0004 (6)	1.0073 (6)	1.0001 (5)
45.0	2.3702 (0)	1.0000 (5)	1.0006 (6)	1.0001 (4)
50.0	2.5991 (0)	1.0002 (4)	1.0005 (5)	1.0001 (1)
60.0	3.3190 (0)	1.0110 (0)	1.0000 (1)	1.0019 (6)
70.0	4.8230 (0)	1.1494 (0)	1.0000 (4)	1.0010 (1)
80.0	9.4605 (0)	1.8505 (0)	1.0783 (0)	1.0004 (1)

CC2:

$R_1/h=100.0$ $\nu_{x\phi}=0.3$ $E=30x10^6$ psi

alpa \ L/R_1	0.2	0.5	0.8	1.0
0.0	1.6635 (1)	1.0676 (6)	1.0076 (8)	1.0024 (7)
1.0	1.6660 (1)	1.0686 (6)	1.0075 (8)	1.0026 (7)
5.0	1.6801 (1)	1.0708 (8)	1.0068 (8)	1.0027 (9)
10.0	1.7074 (1)	1.0555 (7)	1.0055 (8)	1.0026 (9)
20.0	1.7983 (1)	1.0454 (7)	1.0021 (8)	1.0052 (9)
30.0	1.9512 (1)	1.0312 (6)	1.0004 (8)	1.0096 (9)
40.0	2.1977 (1)	1.0166 (5)	1.0067 (7)	1.0037 (8)
45.0	2.3742 (1)	1.0103 (4)	1.0104 (7)	1.0023 (8)
50.0	2.6035 (1)	1.0050 (3)	1.0227 (7)	1.0023 (1)
60.0	3.3246 (1)	1.0155 (1)	1.0523 (5)	1.0112 (6)
70.0	4.8312 (1)	1.1572 (1)	1.0202 (4)	1.0489 (5)
80.0	9.4764 (1)	1.8651 (1)	1.0923 (1)	1.0124 (1)

CC3:

$R_1/h=100.0$ $\nu_{x\phi}=0.3$ $E=30x10^6$ psi

alpa \ L/R_1	0.2	0.5	0.8	1.0
0.0	1.6609 (0)	1.0497 (8)	1.0138 (8)	1.0021 (7)
1.0	1.6633 (0)	1.0507 (8)	1.0126 (8)	1.0017 (7)
5.0	1.6774 (0)	1.0553 (8)	1.0082 (8)	1.0020 (9)
10.0	1.7047 (0)	1.0618 (8)	1.0047 (8)	1.0017 (9)
20.0	1.7954 (0)	1.0763 (9)	1.0012 (8)	1.0045 (9)
30.0	1.9480 (0)	1.0980 (8)	1.0004 (8)	1.0100 (9)
40.0	2.1940 (0)	1.0537 (0)	1.0059 (8)	1.0077 (8)
45.0	2.3702 (0)	1.0274 (0)	1.0146 (8)	1.0057 (0)
50.0	2.5991 (0)	1.0082 (0)	1.0259 (7)	1.0003 (0)
60.0	3.3190 (0)	1.0110 (0)	1.0575 (7)	1.0141 (7)
70.0	4.8230 (0)	1.1494 (0)	1.0454 (0)	1.0617 (6)
80.0	9.4605 (0)	1.8505 (0)	1.0783 (0)	1.0013 (0)

CC4:

$R_1/h=100.0$ $\nu_{x\phi}=0.3$ $E=30x10^6$ psi

alpa \ L/R_1	0.2	0.5	0.8	1.0
0.0	1.9915 (5)	1.1348 (8)	1.0381 (9)	1.0491 (10)
1.0	1.9937 (5)	1.1353 (8)	1.0379 (9)	1.0497 (4)
5.0	2.0061 (5)	1.1381 (8)	1.0380 (9)	1.0517 (4)
10.0	2.0302 (5)	1.1423 (8)	1.0396 (9)	1.0282 (8)
20.0	2.1100 (4)	1.1528 (8)	1.0464 (9)	1.0530 (6)
30.0	2.2426 (3)	1.1677 (8)	1.0586 (8)	1.0555 (10)
40.0	2.4549 (0)	1.1937 (8)	1.0731 (8)	1.0426 (8)

45.0	2.6101 (0)	1.2159 (8)	1.0874 (8)	1.0477 (8)
50.0	2.8164 (0)	1.2365 (7)	1.1001 (7)	1.0576 (8)
60.0	3.4871 (0)	1.3197 (6)	1.1467 (6)	1.0877 (7)
70.0	4.9375 (0)	1.5084 (5)	1.2074 (6)	1.1505 (6)
80.0	9.5185 (0)	2.1548 (2)	1.4280 (4)	1.2783 (4)

E.4 Buckling Values of Single Layer Isotropic Conical Shell in Pure Bending (M_{cr})

SS1:

$R_1/h=100.0$ $\nu_{x\phi}=0.3$ $E=30x10^6$ psi

alpa \ L/R_1	0.2	0.5	0.8	1.0
0.0	2893.14 (2)	1364.16 (2)	1454.45 (2)	146.62 (6)
1.0	2900.01 (2)	1373.59 (2)	1427.46 (2)	157.37 (6)
5.0	2914.71 (2)	1403.66 (2)	1321.25 (2)	207.38 (6)
10.0	2903.47 (2)	1422.50 (2)	1194.69 (2)	288.80 (6)
20.0	2784.10 (2)	1397.11 (2)	981.82 (2)	532.45 (5)
30.0	2547.08 (2)	1293.79 (2)	807.03 (2)	835.46 (4)
40.0	2215.21 (2)	1124.15 (2)	653.51 (2)	1023.33 (4)
45.0	2022.46 (2)	1017.80 (2)	581.89 (2)	650.73 (2)
50.0	1816.60 (2)	898.36 (2)	512.61 (2)	472.50 (2)
60.0	1378.53 (2)	624.58 (2)	377.79 (2)	301.56 (2)
70.0	922.42 (2)	336.57 (2)	241.18 (2)	187.50 (2)
80.0	461.27 (2)	121.65 (2)	92.83 (2)	81.43 (2)

SS2:

$R_1/h=100.0$ $\nu_{x\phi}=0.3$ $E=30x10^6$ psi

alpa \ L/R_1	0.2	0.5	0.8	1.0
0.0	2893.20 (2)	1365.81 (2)	1457.97 (2)	175.06 (5)
1.0	2900.06 (2)	1375.34 (2)	1429.76 (2)	187.05 (5)
5.0	2914.88 (2)	1408.23 (2)	1314.99 (2)	242.80 (5)
10.0	2903.96 (2)	1435.56 (2)	1189.33 (2)	332.62 (5)
20.0	2785.61 (2)	1438.81 (2)	1007.60 (2)	608.81 (4)
30.0	2549.46 (2)	1365.91 (2)	869.27 (2)	959.48 (4)
40.0	2217.83 (2)	1211.12 (2)	738.93 (2)	1004.18 (2)
45.0	2024.90 (2)	1102.43 (2)	671.80 (2)	712.38 (2)
50.0	1818.72 (2)	973.53 (2)	601.92 (2)	555.69 (2)
60.0	1379.76 (2)	665.97 (2)	451.15 (2)	370.12 (2)
70.0	922.88 (2)	348.34 (2)	282.08 (2)	228.96 (2)
80.0	461.33 (2)	122.91 (2)	99.21 (2)	92.20 (2)

SS3:

$R_1/h=100.0$ $\nu_{x\phi}=0.3$ $E=30x10^6$ psi

alpa \ L/R_1	0.2	0.5	0.8	1.0
0.0	5690.33 (6)	3277.11 (2)	3068.43 (4)	230.35 (7)
1.0	5698.23 (6)	3293.35 (2)	3143.60 (4)	250.08 (7)
5.0	5694.61 (6)	3332.68 (2)	3499.10 (4)	345.03 (7)
10.0	5609.45 (6)	3328.36 (2)	3690.22 (3)	508.96 (7)
20.0	5163.17 (3)	3171.09 (2)	3324.35 (2)	1113.27 (7)
30.0	4286.38 (2)	2854.85 (2)	2781.57 (2)	2198.08 (4)
40.0	3318.32 (2)	2424.73 (2)	2317.57 (2)	2102.32 (4)
45.0	2853.07 (2)	2180.64 (2)	1862.99 (2)	2005.37 (4)
50.0	2415.04 (2)	1923.36 (2)	1460.38 (2)	1829.81 (4)
60.0	1640.06 (2)	1379.65 (2)	897.09 (2)	1221.55 (4)
70.0	1001.52 (2)	752.73 (2)	491.03 (2)	422.29 (2)
80.0	471.26 (2)	179.13 (2)	183.07 (2)	148.61 (2)

SS4:

$R_1/h=100.0$ $\nu_{x\phi}=0.3$ $E=30x10^6$ psi

alpa \ L/R_1	0.2	0.5	0.8	1.0
0.0	5717.47 (7)	3275.05 (2)	3289.93 (4)	406.71 (7)
1.0	5726.16 (7)	3291.54 (2)	3389.96 (4)	442.97 (7)
5.0	5727.16 (7)	3332.25 (2)	3650.53 (3)	619.77 (7)
10.0	5651.71 (7)	3330.36 (2)	3713.08 (3)	936.29 (7)
20.0	5241.83 (6)	3180.18 (2)	3354.95 (2)	2346.45 (4)
30.0	4548.09 (5)	2872.34 (2)	2818.61 (2)	2396.22 (4)
40.0	3650.04 (4)	2449.12 (2)	2471.07 (2)	2312.68 (3)
45.0	3159.24 (3)	2207.33 (2)	1877.85 (2)	2151.97 (3)
50.0	2678.13 (3)	1951.68 (2)	1464.95 (2)	2027.03 (2)
60.0	1792.78 (2)	1412.61 (2)	905.79 (2)	1270.21 (4)
70.0	1054.62 (2)	784.67 (5)	498.26 (2)	426.02 (2)
80.0	478.54 (2)	206.14 (3)	191.78 (2)	151.19 (2)

CC1:

$R_1/h=100.0$ $\nu_{x\phi}=0.3$ $E=30x10^6$ psi

alpa \ L/R_1	0.2	0.5	0.8	1.0
0.0	9536.94 (3)	2530.10 (2)	1466.79 (2)	530.86 (6)
1.0	9564.50 (3)	2550.75 (2)	1468.87 (2)	580.21 (6)
5.0	9640.68 (3)	2620.32 (2)	1470.12 (2)	824.80 (6)
10.0	9654.56 (3)	2674.86 (2)	1454.43 (2)	1274.59 (6)
20.0	9405.67 (3)	2676.79 (2)	1367.03 (2)	1650.36 (4)
30.0	8794.57 (3)	2550.66 (2)	1223.68 (2)	1643.59 (2)
40.0	7850.09 (3)	2322.39 (2)	1050.78 (2)	1011.36 (2)
45.0	7266.99 (3)	2179.34 (2)	959.06 (2)	820.90 (2)
50.0	6619.10 (3)	2024.36 (2)	865.47 (2)	683.28 (2)
60.0	5158.85 (3)	1735.20 (3)	674.16 (2)	484.24 (2)
70.0	3529.99 (3)	949.98 (3)	476.73 (2)	325.80 (2)
80.0	1791.74 (3)	405.73 (3)	257.65 (3)	178.15 (2)

CC2:

$R_1/h=100.0$ $\nu_{x\phi}=0.3$ $E=30x10^6$ psi

alpa \ L/R_1	0.2	0.5	0.8	1.0
0.0	9537.06 (3)	2533.81 (2)	1473.87 (2)	693.99 (6)
1.0	9564.62 (3)	2554.69 (2)	1475.90 (2)	757.86 (6)
5.0	9640.83 (3)	2629.83 (2)	1478.80 (2)	1070.46 (3)
10.0	9654.77 (3)	2701.27 (2)	1471.25 (2)	1385.02 (4)
20.0	9406.10 (3)	2760.17 (2)	1421.71 (2)	1756.11 (4)
30.0	8795.20 (3)	2697.36 (2)	1328.53 (2)	1597.94 (2)
40.0	7850.76 (3)	2513.09 (2)	1193.18 (2)	1098.85 (2)
45.0	7267.60 (3)	2382.30 (2)	1109.85 (2)	936.45 (2)
50.0	6619.63 (3)	2241.74 (2)	1016.20 (2)	807.08 (2)
60.0	5159.16 (3)	1743.64 (3)	799.62 (2)	592.52 (2)
70.0	3530.11 (3)	953.39 (3)	554.63 (2)	393.52 (2)
80.0	1791.75 (3)	406.22 (3)	259.67 (3)	211.18 (2)

CC3:

$R_1/h=100.0$ $\nu_{x\phi}=0.3$ $E=30x10^6$ psi

alpa \ L/R_1	0.2	0.5	0.8	1.0
0.0	11169.46 (3)	3873.60 (2)	3569.54 (2)	604.87 (7)
1.0	11196.94 (3)	3898.32 (2)	3450.74 (2)	666.07 (7)
5.0	11255.65 (3)	3975.60 (2)	3332.57 (2)	981.47 (7)
10.0	11210.46 (3)	4021.63 (2)	3279.35 (2)	1651.07 (7)

20.0	10737.17 (3)	3955.39 (2)	3162.88 (2)	2509.37 (4)
30.0	9810.64 (3)	3708.19 (2)	3005.26 (2)	2599.36 (4)
40.0	8531.24 (3)	3331.53 (2)	2267.68 (2)	2554.91 (4)
45.0	7793.70 (3)	3122.97 (2)	1931.46 (2)	2453.94 (4)
50.0	7008.15 (3)	2957.67 (2)	1632.79 (2)	2185.22 (4)
60.0	5336.32 (3)	2188.92 (7)	1115.04 (2)	996.26 (2)
70.0	3585.39 (3)	1188.83 (3)	697.99 (2)	530.88 (2)
80.0	1798.87 (3)	439.32 (3)	311.34 (3)	292.92 (4)

CC4:

$R_1/h=100.0$ $\nu_{x\phi}=0.3$ $E=30x10^6$ psi

alpa \ L/R_1	0.2	0.5	0.8	1.0
0.0	11278.93 (3)	3868.28 (2)	3592.89 (2)	1194.80 (7)
1.0	11306.68 (3)	3893.07 (2)	3458.55 (2)	1362.67 (7)
5.0	11367.94 (3)	3970.81 (2)	3340.42 (2)	2285.24 (4)
10.0	11328.65 (3)	4017.60 (2)	3292.55 (2)	2480.91 (4)
20.0	10870.42 (3)	3952.31 (2)	3194.29 (2)	2741.55 (4)
30.0	9949.80 (3)	3702.19 (2)	3593.59 (2)	2903.55 (4)
40.0	8655.61 (3)	3311.45 (2)	2264.80 (2)	2890.58 (2)
45.0	7902.75 (3)	3083.37 (2)	1929.69 (2)	2580.47 (2)
50.0	7098.27 (3)	2855.77 (2)	1633.00 (2)	2397.73 (2)
60.0	5385.69 (3)	2223.60 (6)	1115.36 (2)	992.96 (2)
70.0	3602.91 (3)	1203.03 (5)	692.52 (2)	530.48 (2)
80.0	1801.31 (3)	445.02 (3)	315.00 (3)	244.46 (2)

E.5

a) Buckling Ratio of Single Layer Isotropic Conical Shell under Axial Compression ($P_{cr}/P_{cylinder}$)

SS2:

$R_1/h=100.0$ $\nu_{x\phi}=0.3$ $E=30x10^6$ psi

alpa \ L/R_1	0.2	0.5	0.8	1.0
0.0	1.0000 (1)	1.0000 (1)	1.0000 (1)	1.0000 (1)
1.0	1.0006 (1)	1.0000 (1)	0.9996 (1)	0.9998 (1)
5.0	0.9987 (1)	0.9939 (1)	0.9921 (1)	0.9928 (1)
10.0	0.9862 (1)	0.9731 (1)	0.9693 (1)	0.9706 (1)
20.0	0.9298 (1)	0.8887 (1)	0.8824 (1)	0.8857 (1)
30.0	0.8372 (1)	0.7530 (1)	0.7501 (1)	0.7543 (1)
40.0	0.7177 (1)	0.5793 (1)	0.5894 (1)	0.5913 (1)
45.0	0.6510 (1)	0.4851 (1)	0.5048 (1)	0.5040 (1)
50.0	0.5812 (1)	0.3912 (1)	0.4206 (1)	0.4168 (1)
60.0	0.4365 (1)	0.2221 (1)	0.2606 (1)	0.2546 (1)
70.0	0.2898 (1)	0.1004 (1)	0.1201 (1)	0.1230 (1)
80.0	0.1442 (1)	0.0327 (1)	0.0274 (1)	0.0295 (1)

b) Buckling Ratio of Single Layer Isotropic Conical Shell under Outer Pressure ($q_{cr}/q_{cylinder}$)

SS2:

$R_1/h=100.0$ $\nu_{x\phi}=0.3$ $E=30x10^6$ psi

alpa \ L/R_1	0.2	0.5	0.8	1.0
0.0	1.0000 (17)	1.0000 (11)	1.0000 (9)	1.0000 (9)
1.0	0.9979 (17)	0.9934 (11)	0.9904 (9)	0.9856 (9)
5.0	0.9864 (17)	0.9638 (11)	0.9466 (10)	0.9282 (9)
10.0	0.9651 (17)	0.9202 (11)	0.8820 (10)	0.8579 (9)
20.0	0.9014 (17)	0.8140 (11)	0.7478 (10)	0.7182 (9)
30.0	0.8128 (17)	0.6895 (11)	0.6095 (10)	0.5713 (10)

40.0	0.7036 (17)	0.5564 (11)	0.4727 (10)	0.4352 (10)
45.0	0.6428 (17)	0.4898 (11)	0.4073 (10)	0.3721 (10)
50.0	0.5787 (17)	0.4242 (10)	0.3452 (10)	0.3107 (9)
60.0	0.4424 (17)	0.2961 (10)	0.2282 (9)	0.2017 (9)
70.0	0.2986 (17)	0.1817 (9)	0.1297 (8)	0.1115 (8)
80.0	0.1503 (17)	0.0839 (8)	0.0532 (7)	0.0429 (6)

c) Buckling Ratio of Single Layer Isotropic Conical Shell in Pure Bending ($M_{cr}/M_{cylinder}$)

SS2:
R_1/h=100.0 $\nu_{x\phi}$=0.3 E=30x10^6 psi

alpa \ L/R_1	0.2	0.5	0.8	1.0
0.0	1.0000 (2)	1.0000 (2)	1.0000 (2)	1.0000 (5)
1.0	1.0024 (2)	1.0070 (2)	0.9806 (2)	1.0685 (5)
5.0	1.0075 (2)	1.0311 (2)	0.9019 (2)	1.3869 (5)
10.0	1.0037 (2)	1.0511 (2)	0.8157 (2)	1.9000 (5)
20.0	0.9628 (2)	1.0534 (2)	0.6911 (2)	3.4777 (4)
30.0	0.8812 (2)	1.0001 (2)	0.5962 (2)	5.4809 (4)
40.0	0.7666 (2)	0.8867 (2)	0.5068 (2)	5.7362 (2)
45.0	0.6999 (2)	0.8072 (2)	0.4608 (2)	4.0693 (2)
50.0	0.6286 (2)	0.7128 (2)	0.4128 (2)	3.1743 (2)
60.0	0.4769 (2)	0.4876 (2)	0.3094 (2)	2.1142 (2)
70.0	0.3190 (2)	0.2550 (2)	0.1935 (2)	1.3079 (2)
80.0	0.1595 (2)	0.0900 (2)	0.0680 (2)	0.5267 (2)

E.6 Buckling Values of Single Layer Isotropic Conical Shell under Axial Compression (P_{cr}) with Outer Pre-Pressure

SS2:
R_1/h=100.0 $\nu_{x\phi}$=0.3 E=30x10^6 psi
L/R_1=0.2

Alpa \ Pre_q	0%	25%	50%	75%	100%
0.0	5723.3 (1)	5705.1 (1)	5625.5 (5)	3955.4 (12)	0.0 (17)
1.0	5726.9 (1)	5708.8 (1)	5629.6 (5)	3960.0 (12)	0.0 (17)
5.0	5715.6 (1)	5697.9 (1)	5621.1 (5)	3960.3 (13)	0.0 (17)
10.0	5644.2 (1)	5627.1 (1)	5555.0 (5)	3919.1 (13)	0.0 (17)
20.0	5321.4 (1)	5306.1 (1)	5247.2 (5)	3720.5 (13)	0.0 (17)
30.0	4791.7 (1)	4778.2 (1)	4735.5 (5)	3383.1 (13)	0.0 (17)
40.0	4107.7 (1)	4096.0 (1)	4068.1 (4)	2934.6 (13)	0.0 (17)
45.0	3725.7 (1)	3714.9 (1)	3692.3 (4)	2678.6 (13)	0.0 (17)
50.0	3326.3 (1)	3316.4 (1)	3298.7 (4)	2406.9 (13)	0.0 (17)
60.0	2498.1 (1)	2490.1 (1)	2478.5 (3)	1826.4 (12)	0.0 (17)
70.0	1658.6 (1)	1652.9 (1)	1645.4 (2)	1222.9 (12)	0.0 (17)
80.0	825.4 (1)	822.4 (1)	818.5 (1)	612.0 (12)	0.0 (17)

L/R_1=0.5

alpa \ Pre_q	0%	25%	50%	75%	100%
0.0	5868.1 (1)	5840.0 (3)	4991.1 (7)	2975.0 (9)	0.0 (11)
1.0	5867.9 (1)	5839.1 (3)	4989.0 (7)	2976.7 (9)	0.0 (11)
5.0	5832.4 (1)	5800.4 (3)	4935.0 (8)	2961.2 (9)	0.0 (11)
10.0	5710.3 (1)	5670.6 (4)	4798.3 (8)	2878.0 (10)	0.0 (11)
20.0	5214.9 (1)	5151.2 (4)	4316.1 (8)	2578.8 (10)	0.0 (11)
30.0	4418.8 (1)	4334.9 (4)	3614.5 (8)	2170.1 (10)	0.0 (11)
40.0	3399.4 (1)	3317.5 (4)	2761.5 (7)	1655.9 (9)	0.0 (11)
45.0	2846.5 (1)	2778.7 (4)	2321.5 (7)	1394.2 (9)	0.0 (11)

50.0	2295.7 (1)	2249.9 (3)	1897.7 (7)	1145.6 (9)	0.0 (10)
60.0	1303.4 (1)	1286.7 (2)	1128.0 (6)	700.8 (8)	0.0 (10)
70.0	589.2 (1)	580.7 (1)	542.3 (4)	353.9 (7)	0.0 (9)
80.0	191.8 (1)	188.7 (1)	183.9 (2)	129.7 (6)	0.0 (8)

L/R_1=0.8

alpa \ Pre_q	0%	25%	50%	75%	100%
0.0	5721.7 (1)	5704.8 (1)	5327.3 (6)	3406.2 (8)	0.2 (9)
1.0	5719.5 (1)	5702.7 (1)	5322.3 (6)	3400.5 (8)	0.3 (9)
5.0	5676.3 (1)	5660.5 (1)	5274.2 (6)	3375.7 (8)	0.0 (10)
10.0	5546.1 (1)	5531.9 (1)	5152.3 (6)	3284.2 (9)	0.0 (10)
20.0	5049.1 (1)	5035.9 (1)	4651.8 (7)	2903.2 (9)	0.0 (10)
30.0	4291.8 (1)	4275.3 (1)	3896.5 (7)	2390.7 (9)	0.0 (10)
40.0	3372.4 (1)	3350.5 (1)	2997.5 (7)	1815.5 (9)	0.0 (10)
45.0	2888.3 (1)	2864.0 (1)	2527.7 (7)	1527.3 (9)	0.0 (10)
50.0	2406.6 (1)	2380.6 (1)	2063.4 (7)	1233.2 (8)	0.0 (10)
60.0	1491.3 (1)	1459.7 (3)	1214.9 (6)	719.1 (8)	0.0 (9)
70.0	687.0 (1)	659.3 (3)	543.9 (5)	325.7 (7)	0.0 (8)
80.0	156.9 (1)	152.2 (1)	137.4 (3)	86.3 (5)	0.0 (7)

L/R_1=1.0

alpa \ Pre_q	0%	25%	50%	75%	100%
0.0	5721.6 (1)	5704.9 (1)	5444.0 (5)	3671.8 (8)	0.5 (9)
1.0	5720.5 (1)	5703.3 (1)	5442.9 (5)	3665.9 (8)	0.0 (9)
5.0	5680.2 (1)	5664.2 (1)	5405.3 (5)	3614.0 (8)	0.5 (9)
10.0	5553.6 (1)	5540.4 (1)	5258.7 (6)	3491.9 (8)	0.0 (9)
20.0	5067.6 (1)	5055.9 (1)	4735.3 (6)	3084.9 (8)	0.1 (9)
30.0	4315.7 (1)	4299.1 (1)	3976.0 (7)	2530.2 (9)	0.1 (10)
40.0	3382.9 (1)	3358.6 (1)	3049.4 (7)	1902.8 (9)	0.0 (10)
45.0	2883.6 (1)	2856.4 (1)	2569.2 (7)	1586.4 (8)	0.0 (10)
50.0	2384.6 (1)	2356.0 (1)	2106.0 (7)	1276.4 (8)	0.0 (9)
60.0	1456.5 (1)	1430.1 (1)	1241.0 (6)	741.1 (8)	0.0 (9)
70.0	704.0 (1)	681.4 (3)	562.9 (5)	330.6 (7)	0.0 (8)
80.0	168.8 (1)	161.8 (2)	136.4 (4)	82.5 (5)	0.0 (6)

E.7 Buckling Values of Single Layer Isotropic Conical Shell in Pure Bending (M_{cr}) with Axial Pre-Compressed

SS2:

R_1/h=100.0 $\nu_{x\phi}$=0.3 E=30x10^6 psi

L/R_1=0.2

alpa \ Pre_P	0%	25%	50%	75%	100%
0.0	2893.2 (2)	2184.7 (2)	1474.2 (2)	762.0 (2)	0.0 (1)
1.0	2900.1 (2)	2189.8 (2)	1477.6 (2)	763.6 (2)	0.0 (1)
5.0	2914.9 (2)	2200.7 (2)	1484.7 (2)	767.1 (2)	0.0 (1)
10.0	2904.0 (2)	2192.1 (2)	1478.6 (2)	763.8 (2)	0.0 (1)
20.0	2785.6 (2)	2101.9 (2)	1417.4 (2)	732.0 (2)	0.0 (1)
30.0	2549.5 (2)	1923.0 (2)	1296.4 (2)	669.6 (2)	0.0 (1)
40.0	2217.8 (2)	1672.3 (2)	1127.2 (2)	582.5 (2)	0.0 (1)
45.0	2024.9 (2)	1526.6 (2)	1029.0 (2)	531.9 (2)	0.0 (1)
50.0	1818.7 (2)	1371.0 (2)	924.1 (2)	477.9 (2)	0.0 (1)
60.0	1379.8 (2)	1040.0 (2)	701.0 (2)	362.9 (2)	0.0 (1)
70.0	922.9 (2)	695.5 (2)	468.9 (2)	243.0 (2)	0.0 (1)
80.0	461.3 (2)	347.7 (2)	234.4 (2)	121.5 (2)	0.0 (1)

L/R_1=0.5

alpa \ Pre_P	0%	25%	50%	75%	100%
0.0	1365.8 (2)	1219.1 (2)	990.3 (2)	631.7 (2)	22.7 (0)
1.0	1375.3 (2)	1226.7 (2)	995.5 (2)	634.3 (2)	23.3 (0)
5.0	1408.2 (2)	1251.8 (2)	1012.0 (2)	641.5 (2)	25.9 (0)
10.0	1435.6 (2)	1269.9 (2)	1020.9 (2)	642.6 (2)	26.7 (2)
20.0	1438.8 (2)	1257.7 (2)	997.4 (2)	616.8 (2)	22.9 (2)
30.0	1365.9 (2)	1176.2 (2)	916.5 (2)	553.4 (2)	18.5 (2)
40.0	1211.1 (2)	1023.3 (2)	778.7 (2)	455.3 (2)	15.3 (2)
45.0	1102.4 (2)	920.4 (2)	690.1 (2)	395.8 (2)	14.6 (2)
50.0	973.5 (2)	801.4 (2)	590.5 (2)	331.9 (2)	14.7 (2)
60.0	666.0 (2)	529.6 (2)	375.9 (2)	204.5 (2)	15.3 (2)
70.0	348.3 (2)	269.1 (2)	186.7 (2)	101.6 (2)	0.0 (1)
80.0	122.9 (2)	94.4 (2)	65.8 (2)	37.2 (2)	0.0 (1)

L/R_1=0.8

alpa \ Pre_P	0%	25%	50%	75%	100%
0.0	1438.0 (2)	1346.0 (4)	1011.4 (3)	523.5 (3)	0.0 (1)
1.0	1429.8 (2)	1377.7 (4)	1052.5 (3)	537.8 (3)	0.0 (1)
5.0	1315.0 (2)	1495.8 (4)	1179.2 (4)	595.9 (3)	0.0 (1)
10.0	1189.3 (2)	1617.8 (4)	1291.0 (4)	667.5 (3)	0.0 (1)
20.0	1007.6 (2)	1248.4 (2)	1428.3 (4)	796.5 (3)	0.0 (1)
30.0	869.3 (2)	942.5 (2)	964.2 (2)	761.8 (2)	0.0 (1)
40.0	738.9 (2)	741.8 (2)	685.5 (2)	494.9 (2)	0.0 (1)
45.0	671.8 (2)	655.0 (2)	586.3 (2)	414.3 (2)	0.0 (1)
50.0	601.9 (2)	571.7 (2)	498.1 (2)	344.9 (2)	17.5 (0)
60.0	451.2 (2)	408.4 (2)	338.6 (2)	223.5 (2)	8.6 (0)
70.0	282.1 (2)	242.4 (2)	188.8 (2)	114.6 (2)	6.7 (0)
80.0	99.2 (2)	78.5 (2)	56.1 (2)	32.1 (2)	0.0 (1)

L/R_1=1.0

alpa \ Pre_P	0%	25%	50%	75%	100%
0.0	175.1 (5)	184.0 (5)	187.0 (5)	157.7 (3)	0.0 (1)
1.0	187.0 (5)	195.1 (5)	196.5 (5)	162.5 (3)	0.0 (1)
5.0	242.8 (5)	245.3 (5)	238.5 (5)	183.6 (3)	0.0 (1)
10.0	332.6 (5)	323.2 (5)	301.1 (5)	213.0 (3)	0.0 (1)
20.0	608.8 (4)	523.0 (3)	430.3 (3)	280.6 (3)	0.0 (1)
30.0	959.5 (4)	835.8 (3)	595.6 (3)	358.3 (3)	0.0 (1)
40.0	1004.2 (2)	1050.3 (4)	847.2 (4)	441.5 (3)	0.0 (1)
45.0	712.4 (2)	948.7 (2)	873.1 (4)	481.3 (3)	0.0 (1)
50.0	555.7 (2)	635.9 (2)	716.3 (2)	517.5 (3)	0.0 (1)
60.0	370.1 (2)	366.2 (2)	334.8 (2)	244.2 (2)	0.0 (1)
70.0	229.0 (2)	209.4 (2)	176.4 (2)	120.2 (2)	3.1 (0)
80.0	92.2 (2)	77.0 (2)	58.1 (2)	34.4 (2)	3.2 (0)

E.8 Buckling Values of Single Layer Isotropic Conical Shell in Pure Bending (M_{cr}) with Outer Pre-Pressure

SS2:

R_1/h=100.0 $\nu_{x\phi}$=0.3 E=30x10^6 psi

L/R_1=0.2

alpa \ Pre_q	0%	25%	50%	75%	100%
0.0	2893.2 (2)	2859.9 (2)	2813.7 (6)	1975.2 (12)	0.0 (17)
1.0	2900.1 (2)	2866.8 (2)	2820.6 (6)	1980.9 (12)	0.0 (17)
5.0	2914.9 (2)	2881.8 (2)	2835.9 (6)	1993.3 (13)	0.0 (17)

10.0	2904.0 (2)	2871.5 (2)	2826.6 (5)	1989.5 (13)	0.0 (17)
20.0	2785.6 (2)	2755.3 (2)	2712.6 (5)	1919.6 (13)	0.0 (17)
30.0	2549.5 (2)	2522.2 (2)	2483.5 (5)	1771.5 (13)	0.0 (17)
40.0	2217.8 (2)	2194.2 (2)	2160.7 (4)	1556.7 (13)	0.0 (17)
45.0	2024.9 (2)	2003.2 (2)	1972.0 (4)	1429.1 (13)	0.0 (17)
50.0	1818.7 (2)	1799.1 (2)	1770.5 (4)	1290.8 (13)	0.0 (17)
60.0	1379.8 (2)	1364.5 (2)	1341.3 (3)	988.5 (12)	0.0 (17)
70.0	922.9 (2)	912.5 (2)	896.0 (3)	666.0 (12)	0.0 (17)
80.0	461.3 (2)	456.0 (2)	447.5 (3)	334.5 (12)	0.0 (17)

L/R_1=0.5

alpa \ Pre_q	0%	25%	50%	75%	100%
0.0	1365.8 (2)	1356.9 (2)	1347.9 (2)	1338.8 (2)	0.0 (11)
1.0	1375.3 (2)	1366.4 (2)	1357.3 (2)	1348.2 (2)	0.0 (11)
5.0	1408.2 (2)	1399.1 (2)	1389.9 (2)	1380.6 (2)	0.0 (11)
10.0	1453.6 (2)	1426.2 (2)	1416.8 (2)	1407.3 (2)	0.0 (11)
20.0	1438.8 (2)	1429.1 (2)	1419.2 (2)	1409.1 (2)	0.0 (11)
30.0	1365.9 (2)	1355.8 (2)	1345.2 (2)	1334.1 (2)	0.0 (11)
40.0	1211.1 (2)	1200.4 (2)	1188.8 (2)	1076.5 (9)	0.0 (11)
45.0	1102.4 (2)	1091.3 (2)	1079.1 (2)	893.4 (9)	0.0 (11)
50.0	973.5 (2)	961.9 (2)	949.1 (2)	724.0 (9)	0.0 (10)
60.0	666.0 (2)	654.0 (2)	640.5 (2)	435.2 (8)	0.0 (10)
70.0	348.3 (2)	338.4 (2)	327.2 (2)	217.4 (7)	0.0 (9)
80.0	122.9 (2)	117.8 (2)	112.0 (2)	79.2 (6)	0.0 (8)

L/R_1=0.8

alpa \ Pre_q	0%	25%	50%	75%	100%
0.0	1458.0 (2)	1452.9 (4)	1408.0 (4)	1361.6 (4)	108.9 (1)
1.0	1429.8 (2)	1425.7 (2)	1421.6 (2)	1394.8 (4)	113.9 (1)
5.0	1315.0 (2)	1310.1 (2)	1305.2 (2)	1300.4 (2)	137.9 (1)
10.0	1189.3 (2)	1183.2 (2)	1177.0 (2)	1170.8 (2)	180.0 (1)
20.0	1007.6 (2)	999.9 (2)	992.1 (2)	984.2 (2)	358.3 (1)
30.0	869.3 (2)	861.1 (2)	852.9 (2)	844.6 (2)	836.1 (2)
40.0	738.9 (2)	731.2 (2)	723.2 (2)	715.1 (2)	706.8 (2)
45.0	671.8 (2)	664.4 (2)	656.8 (2)	648.9 (2)	640.8 (2)
50.0	601.9 (2)	595.0 (2)	587.7 (2)	580.1 (2)	572.2 (2)
60.0	451.2 (2)	445.3 (2)	439.0 (2)	432.2 (2)	0.0 (9)
70.0	282.1 (2)	277.2 (2)	271.5 (2)	265.0 (2)	0.0 (8)
80.0	99.2 (2)	94.9 (2)	89.7 (2)	60.6 (5)	0.0 (7)

L/R_1=1.0

alpa \ Pre_q	0%	25%	50%	75%	100%
0.0	175.1 (5)	139.4 (6)	96.4 (7)	49.0 (8)	0.0 (9)
1.0	187.0 (5)	149.8 (6)	104.3 (7)	53.5 (8)	0.0 (9)
5.0	242.8 (5)	198.5 (6)	142.2 (7)	76.1 (8)	0.0 (9)
10.0	332.6 (5)	279.0 (6)	208.0 (7)	118.8 (8)	0.0 (9)
20.0	608.8 (4)	550.6 (5)	451.4 (6)	312.5 (7)	0.0 (9)
30.0	959.5 (4)	920.0 (4)	880.0 (4)	790.3 (6)	59.3 (1)
40.0	1004.2 (2)	973.8 (2)	943.6 (2)	913.5 (2)	113.2 (1)
45.0	712.4 (2)	694.2 (2)	676.3 (2)	658.8 (2)	189.5 (1)
50.0	555.7 (2)	544.2 (2)	532.7 (2)	521.2 (2)	406.5 (1)
60.0	370.1 (2)	363.8 (2)	357.2 (2)	350.5 (2)	343.5 (2)
70.0	229.0 (2)	225.1 (2)	220.7 (2)	216.0 (2)	124.0 (8)
80.0	92.2 (2)	89.3 (2)	85.7 (2)	70.4 (5)	0.0 (6)

E.9 Buckling Values of Single Layer Orthotropic Conical Shell under Axial Compression (P_{cr})

SS1:

R_1/h=100.0 $\nu_{x\phi}$=0.300 $\nu_{\phi x}$=0.30000 E_x=30x10^6 psi E_ϕ=30x10^6 psi $G_{x\phi}$=11.5x10^6 psi

alpa \ L/R_1	0.2	0.5	0.8	1.0
0.0	5693.58 (0)	5852.35 (0)	5695.17 (0)	5704.19 (0)
1.0	5695.08 (0)	5851.72 (0)	5702.50 (0)	5697.78 (0)
5.0	5684.01 (0)	5816.32 (0)	5658.91 (0)	5661.15 (0)
10.0	5612.92 (0)	5693.76 (0)	5527.38 (0)	5532.77 (0)
20.0	5291.02 (0)	5195.94 (0)	5023.51 (0)	5042.77 (0)
30.0	4763.01 (0)	4396.63 (0)	4259.73 (0)	4280.68 (0)
40.0	4081.90 (0)	3373.90 (0)	3337.28 (0)	3344.74 (0)
45.0	3701.91 (0)	2819.85 (0)	2853.76 (0)	2844.99 (0)
50.0	3304.71 (0)	2268.52 (0)	2374.17 (0)	2347.80 (0)
60.0	2481.52 (0)	1279.54 (0)	1466.63 (0)	1427.55 (0)
70.0	1647.50 (0)	574.31 (0)	670.24 (0)	686.94 (0)
80.0	819.87 (0)	186.00 (0)	149.34 (0)	160.71 (0)

SS1:

R_1/h=100.0 $\nu_{x\phi}$=0.300 $\nu_{\phi x}$=0.03000 E_x=30x10^6 psi E_ϕ=3x10^6 psi $G_{x\phi}$=11.5x10^5 psi

alpa \ L/R_1	0.2	0.5	0.8	1.0
0.0	4055.40 (0)	1363.41 (6)	1348.12 (6)	1396.47 (6)
1.0	4061.45 (0)	1363.96 (6)	1347.43 (6)	1395.16 (6)
5.0	4071.70 (0)	1358.78 (6)	1336.33 (6)	1382.04 (6)
10.0	4054.01 (0)	1335.99 (6)	1303.73 (6)	1347.63 (6)
20.0	3916.26 (0)	1237.54 (5)	1178.72 (7)	1219.74 (6)
30.0	3644.71 (0)	1081.72 (5)	993.90 (6)	1024.68 (6)
40.0	3248.04 (0)	887.89 (4)	773.33 (6)	788.72 (6)
45.0	3006.98 (0)	783.33 (3)	660.38 (6)	666.44 (6)
50.0	2740.26 (0)	677.08 (2)	550.90 (6)	547.58 (6)
60.0	2139.55 (0)	472.16 (0)	344.58 (5)	331.04 (5)
70.0	1467.06 (0)	292.49 (0)	179.14 (3)	161.50 (4)
80.0	745.83 (0)	138.49 (0)	67.39 (0)	52.90 (1)

SS1:

R_1/h=100.0 $\nu_{x\phi}$=0.300 $\nu_{\phi x}$=0.01500 E_x=30x10^6 psi E_ϕ=1.5x10^6 psi $G_{x\phi}$=5.77x10^5 psi

alpa \ L/R_1	0.2	0.5	0.8	1.0
0.0	3964.99 (0)	995.42 (6)	823.77 (6)	833.93 (6)
1.0	3971.66 (0)	996.95 (6)	824.06 (6)	833.69 (6)
5.0	3983.12 (0)	998.39 (6)	817.79 (7)	827.85 (6)
10.0	3968.45 (0)	989.58 (6)	799.56 (7)	805.92 (7)
20.0	3841.03 (0)	937.41 (5)	733.09 (7)	727.60 (7)
30.0	3583.78 (0)	843.89 (5)	633.56 (7)	617.08 (7)
40.0	3202.89 (0)	719.66 (4)	508.58 (6)	486.29 (6)
45.0	2969.52 (0)	649.42 (3)	443.15 (6)	416.03 (6)
50.0	2709.97 (0)	575.49 (2)	378.64 (6)	347.68 (6)
60.0	2121.43 (0)	423.82 (0)	253.68 (5)	222.32 (5)
70.0	1457.65 (0)	276.40 (0)	145.99 (3)	119.40 (4)
80.0	742.04 (0)	135.88 (0)	62.61 (0)	46.18 (1)

SS1:

R_1/h=100.0 $\nu_{x\phi}$=0.300 $\nu_{\phi x}$=0.01000 E_x=30x10^6 psi E_ϕ=1x10^6 psi $G_{x\phi}$=3.85x10^5 psi

alpa \ L/R_1	0.2	0.5	0.8	1.0
0.0	3935.80 (0)	871.12 (6)	635.94 (7)	620.46 (6)
1.0	3941.75 (0)	872.99 (6)	635.97 (7)	620.68 (6)
5.0	3953.62 (0)	876.72 (6)	632.99 (7)	616.97 (7)

10.0	3939.95 (0)	872.72 (6)	622.22 (7)	601.11 (7)
20.0	3815.97 (0)	836.14 (5)	577.94 (7)	548.34 (7)
30.0	3563.50 (0)	763.89 (5)	507.94 (7)	471.31 (7)
40.0	3187.87 (0)	663.16 (4)	417.56 (6)	378.99 (6)
45.0	2957.05 (0)	604.43 (3)	368.92 (6)	328.25 (6)
50.0	2699.90 (0)	541.38 (2)	320.11 (6)	278.37 (6)
60.0	2115.41 (0)	407.62 (0)	223.02 (5)	185.11 (5)
70.0	1454.53 (0)	271.03 (0)	134.86 (3)	105.19 (4)
80.0	740.78 (0)	135.01 (0)	61.01 (0)	43.93 (1)

SS1:

$R_1/h=100.0$ $\nu_{x\phi}=0.300$ $\nu_{\phi x}=0.00750$ $E_x=30\times10^6$ psi $E_\phi=7.5\times10^5$ psi $G_{x\phi}=2.88\times10^5$ psi

alpa \ L/R_1	0.2	0.5	0.8	1.0
0.0	3920.81 (0)	808.67 (6)	539.31 (7)	508.80 (6)
1.0	3926.80 (0)	810.72 (6)	539.73 (7)	509.27 (6)
5.0	3938.87 (0)	815.61 (6)	538.86 (7)	506.44 (7)
10.0	3925.71 (0)	814.05 (6)	531.95 (7)	495.44 (7)
20.0	3803.45 (0)	785.29 (5)	499.17 (7)	456.19 (7)
30.0	3553.36 (0)	723.77 (5)	444.35 (7)	396.77 (7)
40.0	3180.36 (0)	634.83 (4)	371.54 (6)	324.15 (7)
45.0	2950.82 (0)	581.88 (3)	331.48 (6)	283.59 (6)
50.0	2694.87 (0)	524.28 (2)	290.65 (6)	243.24 (6)
60.0	2112.40 (0)	399.50 (0)	207.62 (5)	166.32 (5)
70.0	1452.97 (0)	268.47 (1)	129.28 (3)	98.06 (4)
80.0	740.15 (0)	134.58 (0)	60.21 (0)	42.80 (1)

SS2:

$R_1/h=100.0$ $\nu_{x\phi}=0.300$ $\nu_{\phi x}=0.03000$ $E_x=30\times10^6$ psi $E_\phi=3\times10^6$ psi $G_{x\phi}=1.15\times10^6$ psi

alpa \ L/R_1	0.2	0.5	0.8	1.0
0.0	4058.62 (1)	1367.44 (6)	1371.58 (6)	1436.42 (6)
1.0	4064.46 (1)	1367.92 (6)	1370.49 (6)	1434.44 (6)
5.0	4074.69 (1)	1362.56 (6)	1357.92 (6)	1418.86 (6)
10.0	4056.99 (1)	1339.66 (6)	1323.81 (6)	1381.92 (6)
20.0	3919.15 (1)	1240.43 (5)	1197.77 (6)	1250.07 (6)
30.0	3647.44 (1)	1084.97 (5)	1009.19 (6)	1050.89 (6)
40.0	3250.49 (1)	891.15 (4)	785.42 (6)	809.42 (6)
45.0	3009.26 (1)	786.72 (3)	670.56 (6)	683.85 (6)
50.0	2742.33 (1)	680.43 (2)	559.07 (6)	561.53 (6)
60.0	2141.15 (1)	474.55 (1)	349.11 (5)	338.64 (5)
70.0	1468.13 (1)	293.86 (1)	181.45 (3)	164.67 (4)
80.0	746.37 (1)	139.03 (1)	68.09 (1)	53.87 (1)

E.10 Buckling Values of Single Layer Orthotropic Conical Shell under Outer Pressure (q_{cr})

SS1:

$R_1/h=100.0$ $\nu_{x\phi}=0.300$ $\nu_{\phi x}=0.30000$ $E_x=30\times10^6$ psi $E_\phi=30\times10^6$ psi $G_{x\phi}=11.5\times10^6$ psi

alpa \ L/R_1	0.2	0.5	0.8	1.0
0.0	2836.05 (17)	692.51 (11)	392.56 (9)	304.58 (8)
1.0	2830.18 (17)	687.93 (11)	388.37 (9)	300.78 (8)
5.0	2797.70 (17)	667.52 (11)	371.22 (9)	285.97 (8)
10.0	2737.88 (17)	637.93 (11)	348.98 (9)	267.70 (8)
20.0	2558.40 (17)	566.88 (11)	301.29 (9)	222.79 (9)
30.0	2308.17 (17)	483.78 (11)	247.91 (10)	180.25 (9)
40.0	1999.59 (17)	394.22 (11)	195.13 (10)	139.47 (9)
45.0	1827.50 (17)	348.90 (11)	169.23 (9)	120.03 (9)

50.0	1645.69 (17)	302.95 (10)	143.70 (9)	101.52 (9)
60.0	1258.89 (17)	214.06 (10)	97.17 (9)	67.76 (8)
70.0	850.06 (17)	132.72 (9)	56.44 (8)	38.50 (8)
80.0	428.06 (17)	61.81 (8)	23.75 (7)	15.27 (6)

SS1:

$R_1/h=100.0$ $\nu_{x\phi}=0.300$ $\nu_{\phi x}=0.03000$ $E_x=30x10^6$ psi $E_\phi=3x10^6$ psi $G_{x\phi}=1.15x10^6$ psi

alpa \ L/R_1	0.2	0.5	0.8	1.0
0.0	528.29 (28)	95.79 (13)	49.66 (10)	38.65 (9)
1.0	527.30 (28)	95.26 (13)	49.18 (10)	38.19 (9)
5.0	521.79 (28)	92.88 (13)	47.18 (10)	36.33 (9)
10.0	511.47 (29)	89.43 (13)	44.55 (10)	33.60 (10)
20.0	479.77 (29)	81.07 (14)	38.33 (11)	28.20 (10)
30.0	435.46 (29)	70.78 (14)	31.98 (11)	22.99 (10)
40.0	379.73 (30)	59.55 (14)	25.65 (11)	17.99 (10)
45.0	348.29 (30)	53.70 (14)	22.57 (11)	15.60 (10)
50.0	314.79 (30)	47.76 (14)	19.58 (11)	13.33 (10)
60.0	242.53 (30)	35.75 (14)	13.96 (11)	9.19 (10)
70.0	164.73 (31)	23.74 (14)	8.80 (10)	5.59 (9)
80.0	83.26 (31)	11.83 (14)	4.21 (10)	2.58 (9)

SS1:

$R_1/h=100.0$ $\nu_{x\phi}=0.300$ $\nu_{\phi x}=0.0.1500$ $E_x=30x10^6$ psi $E_\phi=1.5x10^6$ psi $G_{x\phi}=5.77x10^5$ psi

alpa \ L/R_1	0.2	0.5	0.8	1.0
0.0	343.86 (33)	58.65 (14)	28.09 (11)	21.28 (10)
1.0	343.23 (33)	58.37 (14)	27.80 (11)	20.99 (10)
5.0	339.63 (34)	57.12 (14)	26.62 (11)	19.82 (10)
10.0	332.82 (34)	55.05 (15)	25.12 (11)	18.42 (10)
20.0	312.46 (34)	50.12 (15)	21.99 (11)	15.71 (10)
30.0	283.57 (35)	44.25 (16)	18.57 (12)	12.90 (11)
40.0	247.51 (35)	37.56 (16)	15.13 (12)	10.23 (11)
45.0	227.10 (36)	34.05 (16)	13.44 (12)	8.97 (11)
50.0	205.28 (36)	30.45 (16)	11.79 (12)	7.76 (11)
60.0	158.19 (36)	23.03 (16)	8.59 (12)	5.51 (11)
70.0	107.49 (36)	15.43 (16)	5.59 (12)	3.46 (10)
80.0	54.35 (36)	7.73 (16)	2.74 (12)	1.66 (10)

SS1:

$R_1/h=100.0$ $\nu_{x\phi}=0.300$ $\nu_{\phi x}=0.01000$ $E_x=30x10^6$ psi $E_\phi=1x10^6$ psi $G_{x\phi}=3.85x10^5$ psi

alpa \ L/R_1	0.2	0.5	0.8	1.0
0.0	270.25 (37)	45.07 (15)	20.43 (11)	15.09 (10)
1.0	269.74 (37)	44.87 (15)	20.25 (11)	14.90 (10)
5.0	266.90 (37)	43.87 (16)	19.50 (11)	14.15 (10)
10.0	261.66 (37)	42.35 (16)	18.53 (12)	13.24 (10)
20.0	245.58 (38)	38.74 (16)	16.21 (12)	11.30 (11)
30.0	222.99 (39)	34.24 (17)	13.85 (12)	9.38 (11)
40.0	194.60 (39)	29.23 (17)	11.42 (13)	7.54 (11)
45.0	178.58 (39)	26.56 (18)	10.19 (13)	6.65 (11)
50.0	161.47 (40)	23.78 (18)	8.98 (13)	5.79 (11)
60.0	124.44 (40)	18.03 (18)	6.62 (13)	4.16 (11)
70.0	84.56 (40)	12.11 (18)	4.35 (13)	2.67 (11)
80.0	42.76 (40)	6.08 (18)	2.15 (13)	1.30 (11)

SS1:

$R_1/h=100.0$ $\nu_{x\phi}=0.300$ $\nu_{\phi x}=0.00750$ $E_x=30x10^6$ psi $E_\phi=7.5x10^5$ psi $G_{x\phi}=2.88x10^5$ psi

alpa \ L/R_1	0.2	0.5	0.8	1.0

0.0	228.74 (40)	37.69 (16)	16.58 (11)	11.97 (10)
1.0	228.30 (40)	37.52 (16)	16.45 (11)	11.83 (10)
5.0	225.86 (40)	36.71 (17)	15.84 (12)	11.28 (10)
10.0	221.39 (40)	35.46 (17)	15.00 (12)	10.58 (11)
20.0	207.84 (41)	32.48 (18)	13.28 (12)	9.05 (11)
30.0	188.74 (41)	28.77 (18)	11.36 (13)	7.60 (11)
40.0	164.71 (42)	24.62 (19)	9.42 (13)	6.14 (12)
45.0	151.16 (42)	22.37 (19)	8.45 (13)	5.44 (12)
50.0	136.69 (43)	20.05 (19)	7.48 (13)	4.75 (12)
60.0	105.34 (43)	15.24 (19)	5.56 (14)	3.46 (12)
70.0	71.59 (43)	10.25 (19)	3.67 (14)	2.24 (12)
80.0	36.20 (43)	5.15 (20)	1.82 (14)	1.10 (12)

SS2:

$R_1/h=100.0$ $\nu_{x\phi}=0.300$ $\nu_{\phi x}=0.03000$ $E_x=30\times10^6$ psi $E_\phi=3\times10^6$ psi $G_{x\phi}=1.15\times10^6$ psi

alpa \ L/R_1	0.2	0.5	0.8	1.0
0.0	528.40 (28)	96.41 (13)	50.87 (10)	40.21 (9)
1.0	527.41 (28)	95.87 (13)	50.37 (10)	39.73 (9)
5.0	521.90 (28)	93.47 (13)	48.31 (10)	37.68 (10)
10.0	511.57 (29)	89.98 (13)	45.52 (11)	34.74 (10)
20.0	479.85 (29)	81.49 (14)	39.08 (11)	29.11 (10)
30.0	435.52 (29)	71.09 (14)	32.53 (11)	23.67 (10)
40.0	379.77 (30)	59.76 (14)	26.02 (11)	18.43 (10)
45.0	348.32 (30)	53.86 (14)	22.86 (11)	15.95 (10)
50.0	314.82 (30)	47.88 (14)	19.79 (11)	13.59 (10)
60.0	242.54 (30)	35.81 (14)	14.06 (11)	9.31 (10)
70.0	164.74 (31)	23.76 (14)	8.83 (10)	5.63 (9)
80.0	83.26 (31)	11.83 (14)	4.22 (10)	2.59 (9)

E.11 Buckling Values of Single Layer Orthotropic Conical Shell in Pure Bending (M_{cr})

SS1:

$R_1/h=100.0$ $\nu_{x\phi}=0.300$ $\nu_{\phi x}=0.30000$ $E_x=30\times10^6$ psi $E_\phi=30\times10^6$ psi $G_{x\phi}=11.5\times10^6$ psi

alpa \ L/R_1	0.2	0.5	0.8	1.0
0.0	2893.14 (2)	1364.16 (2)	1454.45 (2)	146.62 (6)
1.0	2900.01 (2)	1373.59 (2)	1427.46 (2)	157.37 (6)
5.0	2914.71 (2)	1403.66 (2)	1321.25 (2)	207.38 (6)
10.0	2903.47 (2)	1422.50 (2)	1194.69 (2)	288.80 (6)
20.0	2784.10 (2)	1397.11 (2)	981.82 (2)	532.45 (5)
30.0	2547.08 (2)	1293.79 (2)	807.03 (2)	835.46 (4)
40.0	2215.21 (2)	1124.15 (2)	653.51 (2)	1023.33 (4)
45.0	2022.46 (2)	1017.80 (2)	581.89 (2)	650.73 (2)
50.0	1816.60 (2)	898.36 (2)	512.61 (2)	472.50 (2)
60.0	1378.53 (2)	624.58 (2)	377.79 (2)	301.56 (2)
70.0	922.42 (2)	336.57 (2)	241.18 (2)	187.50 (2)
80.0	461.27 (2)	121.65 (2)	92.83 (2)	81.43 (2)

SS1:

$R_1/h=100.0$ $\nu_{x\phi}=0.300$ $\nu_{\phi x}=0.03000$ $E_x=30\times10^6$ psi $E_\phi=3\times10^6$ psi $G_{x\phi}=1.15\times10^6$ psi

alpa \ L/R_1	0.2	0.5	0.8	1.0
0.0	2041.04 (3)	682.01 (2)	478.26 (2)	368.75 (2)
1.0	2047.47 (3)	685.26 (2)	483.22 (2)	372.95 (2)
5.0	2066.64 (3)	694.11 (2)	499.76 (2)	386.99 (2)
10.0	2074.77 (3)	695.32 (2)	512.30 (2)	397.80 (2)
20.0	2035.85 (3)	665.33 (2)	510.21 (2)	397.99 (2)

30.0	1921.62 (3)	596.96 (2)	474.11 (2)	373.31 (2)
40.0	1733.73 (3)	500.91 (2)	407.78 (2)	328.17 (2)
45.0	1613.79 (3)	446.76 (2)	364.69 (2)	299.03 (2)
50.0	1477.88 (3)	390.89 (2)	316.17 (2)	265.92 (2)
60.0	1163.38 (3)	280.02 (2)	210.31 (2)	188.74 (2)
70.0	802.45 (3)	177.19 (2)	113.08 (2)	103.19 (2)
80.0	409.42 (3)	85.02 (2)	44.54 (2)	35.84 (2)

SS1:

$R_1/h=100.0$ $\nu_{x\phi}=0.300$ $\nu_{\phi x}=0.01500$ $E_x=30x10^6$ psi $E_\phi=1.5x10^6$ psi $G_{x\phi}=5.77x10^5$ psi

alpa \ L/R_1	0.2	0.5	0.8	1.0
0.0	1989.32 (3)	501.77 (6)	409.13 (2)	325.80 (2)
1.0	1995.73 (3)	504.61 (6)	412.94 (2)	329.67 (2)
5.0	2015.22 (3)	513.54 (6)	425.26 (2)	342.67 (2)
10.0	2024.57 (3)	518.74 (6)	433.47 (2)	352.84 (2)
20.0	1990.54 (3)	508.23 (5)	425.60 (2)	353.56 (2)
30.0	1883.69 (3)	471.05 (5)	387.15 (2)	330.40 (2)
40.0	1704.40 (3)	411.55 (4)	323.40 (2)	286.12 (2)
45.0	1588.80 (3)	374.99 (2)	283.97 (6)	256.96 (2)
50.0	1457.07 (3)	335.55 (2)	242.28 (5)	223.80 (2)
60.0	1149.99 (3)	252.24 (2)	163.16 (4)	150.11 (2)
70.0	794.84 (3)	167.15 (2)	93.96 (2)	80.71 (2)
80.0	406.07 (3)	82.98 (2)	41.25 (2)	31.49 (2)

SS1:

$R_1/h=100.0$ $\nu_{x\phi}=0.300$ $\nu_{\phi x}=0.01000$ $E_x=30x10^6$ psi $E_\phi=1x10^6$ psi $G_{x\phi}=3.85x10^5$ psi

alpa \ L/R_1	0.2	0.5	0.8	1.0
0.0	1972.10 (3)	437.90 (6)	358.55 (2)	300.68 (2)
1.0	1978.51 (3)	440.67 (6)	361.55 (2)	304.15 (2)
5.0	1998.10 (3)	449.85 (6)	371.00 (2)	315.74 (2)
10.0	2007.86 (3)	456.51 (6)	376.51 (2)	324.51 (2)
20.0	1975.46 (3)	452.70 (5)	355.94 (6)	323.42 (2)
30.0	1871.07 (3)	426.02 (5)	315.42 (6)	299.19 (2)
40.0	1694.64 (3)	379.09 (4)	262.35 (6)	254.61 (2)
45.0	1580.49 (3)	349.19 (3)	233.23 (6)	226.07 (2)
50.0	1450.15 (3)	315.78 (3)	203.18 (5)	194.64 (2)
60.0	1145.53 (3)	242.37 (3)	142.98 (5)	127.12 (5)
70.0	792.32 (3)	163.55 (3)	87.18 (3)	71.50 (4)
80.0	404.96 (3)	82.21 (3)	40.14 (2)	30.00 (2)

SS1:

$R_1/h=100.0$ $\nu_{x\phi}=0.300$ $\nu_{\phi x}=0.00750$ $E_x=30x10^6$ psi $E_\phi=7.5x10^5$ psi $G_{x\phi}=2.88x10^5$ psi

alpa \ L/R_1	0.2	0.5	0.8	1.0
0.0	1963.49 (3)	405.95 (6)	310.04 (6)	280.56 (2)
1.0	1969.90 (3)	408.69 (6)	311.03 (6)	283.66 (2)
5.0	1989.55 (3)	417.99 (6)	313.67 (6)	293.87 (2)
10.0	1999.50 (3)	425.38 (6)	313.53 (6)	301.27 (2)
20.0	1967.92 (3)	424.88 (5)	300.72 (6)	298.38 (2)
30.0	1864.76 (3)	403.48 (5)	272.09 (6)	273.51 (2)
40.0	1689.76 (3)	362.82 (4)	231.40 (6)	230.11 (2)
45.0	1576.34 (3)	336.11 (3)	208.17 (6)	199.26 (6)
50.0	1446.69 (3)	305.76 (3)	183.72 (5)	169.09 (5)
60.0	1143.31 (3)	237.33 (3)	132.86 (5)	113.19 (5)
70.0	791.06 (3)	161.64 (3)	83.55 (3)	66.48 (4)
80.0	404.41 (3)	81.75 (3)	39.59 (2)	29.24 (2)

SS2:

R_1/h=100.0 $\nu_{x\phi}$=0.300 $\nu_{\phi x}$=0.03000 E_x=30x10^6 psi E_ϕ=3x10^6 psi $G_{x\phi}$=1.15x10^6 psi

alpa \ L/R_1	0.2	0.5	0.8	1.0
0.0	2041.04 (3)	682.08 (2)	478.48 (2)	369.02 (2)
1.0	2047.47 (3)	685.33 (2)	483.48 (2)	373.27 (2)
5.0	2066.65 (3)	694.44 (2)	501.23 (2)	388.66 (2)
10.0	2074.79 (3)	696.38 (2)	517.28 (2)	403.42 (2)
20.0	2035.92 (3)	668.45 (2)	525.87 (2)	415.98 (2)
30.0	1921.73 (3)	601.64 (2)	499.13 (2)	403.42 (2)
40.0	1733.84 (3)	505.73 (2)	434.93 (2)	364.27 (2)
45.0	1613.90 (3)	451.13 (2)	389.55 (2)	334.66 (2)
50.0	1477.97 (3)	394.56 (2)	336.95 (2)	298.57 (2)
60.0	1163.44 (3)	282.05 (2)	220.98 (2)	209.15 (2)
70.0	802.47 (3)	177.91 (2)	116.41 (2)	110.04 (2)
80.0	409.42 (3)	85.11 (2)	44.96 (2)	36.64 (2)

E.12 Buckling Values of Multil Layer Orthotropic Conical Shell under Axial Compression (P_{cr})

SS1:

R_1/h=100.0 $\nu_{x\phi}$=0.250 $\nu_{\phi x}$=0.00625 E_x=30x10^6 psi E_ϕ=7.5x10^5 psi $G_{x\phi}$=3.75x10^5 psi

alpa	N \ L/R_1	0.2	0.5	0.8	1.0
	2	953.81 (8)	670.79 (7)	697.80 (8)	704.39 (7)
	4	2022.10 (7)	1010.58 (6)	1119.19 (6)	1067.23 (6)
0.0	6	2217.45 (7)	1067.01 (6)	1168.52 (5)	1123.93 (6)
	16	2351.42 (7)	1105.71 (6)	1200.71 (5)	1162.78 (6)
	2	942.66 (8)	668.08 (7)	693.82 (8)	729.93 (7)
	4	2009.98 (7)	993.62 (6)	1104.29 (7)	1071.04 (7)
10.0	6	2205.35 (7)	1046.72 (6)	1175.30 (7)	1117.39 (6)
	16	2339.44 (7)	1083.05 (6)	1223.79 (7)	1148.11 (6)
	2	802.45 (8)	535.13 (7)	569.65 (9)	613.91 (7)
	4	1761.49 (7)	801.46 (6)	919.79 (7)	842.48 (7)
30.0	6	1937.13 (6)	846.21 (6)	972.87 (7)	891.89 (7)
	16	2057.55 (6)	877.03 (6)	1009.18 (7)	925.72 (7)
	2	618.67 (7)	347.09 (7)	385.52 (8)	366.66 (8)
	4	1405.92 (6)	552.01 (6)	596.57 (5)	588.25 (7)
45.0	6	1551.27 (6)	588.60 (6)	614.61 (5)	628.86 (7)
	16	1651.51 (6)	613.93 (6)	627.22 (5)	650.72 (6)
	2	405.87 (6)	173.42 (6)	184.18 (6)	186.84 (7)
	4	962.89 (5)	301.32 (5)	270.48 (5)	287.41 (5)
60.0	6	1066.09 (5)	323.49 (5)	285.19 (5)	301.08 (5)
	16	1137.19 (5)	338.88 (5)	295.35 (5)	310.51 (5)

SS2:

R_1/h=100.0 $\nu_{x\phi}$=0.250 $\nu_{\phi x}$=0.00625 E_x=30x10^6 psi E_ϕ=7.5x10^5 psi $G_{x\phi}$=3.75x10^5 psi

alpa	N \ L/R_1	0.2	0.5	0.8	1.0
	2	1772.24 (8)	824.50 (8)	706.55 (7)	717.03 (7)
	4	2314.60 (7)	1102.63 (6)	1119.38 (6)	1067.31 (6)
0.0	6	2355.74 (7)	1119.90 (6)	1184.30 (6)	1124.01 (6)
	16	2375.17 (7)	1124.32 (6)	1229.94 (6)	1163.71 (6)
	2	1759.21 (8)	835.33 (9)	709.95 (8)	822.41 (6)

	4	2300.87 (7)	1070.42 (6)	1096.43 (7)	1051.20 (6)
10.0	6	2342.07 (7)	1085.11 (6)	1169.52 (7)	1101.92 (6)
	16	2361.74 (7)	1088.12 (6)	1181.34 (5)	1137.88 (6)
	2	1530.98 (8)	735.36 (10)	601.89 (9)	750.37 (9)
	4	2019.01 (6)	841.96 (6)	888.99 (5)	830.41 (7)
30.0	6	2055.10 (6)	853.97 (6)	891.28 (5)	881.17 (7)
	16	2073.16 (6)	856.91 (6)	887.69 (5)	918.33 (6)
	2	1216.54 (7)	471.44 (7)	396.35 (8)	392.00 (8)
	4	1616.81 (6)	589.34 (6)	566.24 (5)	582.58 (7)
45.0	6	1648.33 (6)	599.96 (6)	571.40 (5)	609.33 (5)
	16	1664.88 (6)	603.65 (6)	571.36 (5)	606.57 (5)
	2	826.47 (6)	260.31 (6)	211.29 (7)	191.83 (7)
	4	1111.11 (5)	331.12 (5)	278.74 (5)	285.11 (5)
60.0	6	1134.19 (5)	335.89 (5)	283.89 (5)	291.58 (5)
	16	1146.96 (5)	337.35 (5)	285.63 (5)	294.26 (5)

SS3:

R_1/h=100.0 $\nu_{x\phi}$=0.250 $\nu_{\phi x}$=0.00625 E_x=30x10^6 psi E_ϕ=7.5x10^5 psi $G_{x\phi}$=3.75x10^5 psi

alpa	N \L/R_1	0.2	0.5	0.8	1.0
	2	1049.19 (9)	759.12 (7)	737.26 (8)	755.11 (8)
	4	2160.78 (8)	1142.68 (6)	1178.56 (7)	1142.68 (6)
0.0	6	2361.37 (8)	1198.26 (6)	1255.84 (7)	1198.26 (6)
	16	2498.86 (8)	1236.46 (6)	1308.90 (7)	1236.45 (6)
	2	1033.94 (9)	743.29 (7)	729.00 (8)	797.41 (10)
	4	2141.06 (8)	1115.01 (6)	1158.20 (7)	1118.78 (7)
10.0	6	2341.16 (8)	1167.79 (6)	1230.95 (7)	1184.05 (6)
	16	2478.34 (8)	1203.97 (6)	1280.89 (7)	1218.36 (6)
	2	869.88 (9)	572.95 (7)	591.74 (8)	609.58 (7)
	4	1852.55 (8)	862.97 (6)	957.62 (6)	880.87 (7)
30.0	6	2032.72 (8)	907.07 (6)	992.70 (6)	932.84 (7)
	16	2155.89 (7)	937.10 (6)	1017.69 (6)	968.55 (7)
	2	667.92 (8)	375.53 (7)	405.98 (8)	387.90 (8)
	4	1466.59 (7)	587.74 (6)	611.88 (5)	618.88 (7)
45.0	6	1612.53 (7)	623.17 (6)	632.38 (5)	660.11 (7)
	16	1712.62 (7)	647.24 (6)	645.77 (5)	688.31 (7)
	2	434.48 (7)	194.13 (6)	197.95 (6)	201.86 (7)
	4	994.88 (6)	326.93 (5)	288.60 (5)	301.32 (5)
60.0	6	1096.24 (1)	348.08 (5)	302.54 (5)	315.02 (5)
	16	1164.78 (1)	362.42 (5)	311.81 (5)	323.98 (5)

SS4:

R_1/h=100.0 $\nu_{x\phi}$=0.250 $\nu_{\phi x}$=0.00625 E_x=30x10^6 psi E_ϕ=7.5x10^5 psi $G_{x\phi}$=3.75x10^5 psi

alpa	N \L/R_1	0.2	0.5	0.8	1.0
	2	1851.46 (9)	884.53 (9)	756.87 (8)	775.67 (7)
	4	2465.50 (8)	1238.02 (6)	1183.89 (7)	1147.67 (6)
0.0	6	2509.68 (8)	1257.24 (6)	1258.81 (7)	1201.28 (6)
	16	2527.43 (8)	1260.84 (6)	1309.88 (7)	1237.68 (6)
	2	1837.41 (9)	904.36 (10)	780.72 (8)	900.96 (9)

	4	2448.13 (8)	1211.29 (6)	1164.25 (7)	1126.58 (7)
10.0	6	2492.02 (8)	1227.39 (6)	1233.71 (7)	1189.35 (7)
	16	2509.83 (8)	1229.19 (6)	1281.39 (7)	1221.54 (6)
	2	1595.38 (9)	800.00 (10)	904.17 (7)	791.79 (10)
	4	2133.86 (8)	953.30 (6)	965.38 (7)	890.39 (7)
30.0	6	2174.18 (8)	965.27 (6)	1019.14 (7)	935.89 (7)
	16	2191.81 (8)	966.30 (6)	1010.82 (6)	968.06 (7)
	2	1255.66 (8)	510.93 (7)	435.59 (9)	605.75 (9)
	4	1698.69 (7)	655.56 (6)	641.77 (6)	621.40 (7)
45.0	6	1730.44 (7)	665.80 (6)	655.38 (6)	659.82 (7)
	16	1745.02 (7)	667.90 (6)	658.37 (5)	685.15 (5)
	2	854.03 (7)	281.04 (7)	233.10 (8)	212.38 (7)
	4	1154.82 (6)	368.98 (6)	312.71 (5)	317.41 (5)
60.0	6	1177.56 (6)	376.94 (5)	317.67 (5)	323.32 (5)
	16	1188.96 (6)	377.38 (5)	318.63 (5)	325.05 (5)

E.13 Buckling Values of Multi Layer Orthotropic Conical Shell under Outer Pressure (q_{cr})

SS1:

R_1/h=100.0 $\nu_{x\phi}$=0.250 $\nu_{\phi x}$=0.00625 E_x=30x10^6 psi E_ϕ=7.5x10^5 psi $G_{x\phi}$=3.75x10^5 psi

alpa	N \L/R_1	0.2	0.5	0.8	1.0
	2	247.85 (16)	64.86 (9)	41.35 (8)	34.61 (7)
	4	574.36 (16)	129.11 (8)	79.39 (7)	65.96 (6)
0.0	6	634.83 (16)	139.94 (8)	85.99 (7)	70.72 (6)
	16	676.40 (16)	147.40 (8)	90.54 (7)	74.01 (6)
	2	239.14 (17)	59.78 (10)	37.61 (8)	30.86 (8)
	4	555.65 (16)	120.14 (9)	70.96 (7)	57.98 (7)
10.0	6	614.14 (16)	130.63 (8)	76.34 (7)	62.72 (7)
	16	654.35 (16)	137.40 (8)	80.03 (7)	65.96 (7)
	2	201.51 (17)	45.27 (10)	26.87 (9)	21.74 (9)
	4	471.00 (17)	91.42 (9)	50.76 (8)	39.82 (7)
30.0	6	520.91 (17)	99.70 (9)	55.01 (8)	42.54 (7)
	16	555.23 (17)	105.39 (9)	57.43 (7)	44.37 (7)
	2	159.57 (17)	31.92 (10)	17.51 (9)	13.60 (9)
	4	374.96 (17)	66.14 (9)	33.85 (8)	25.33 (7)
45.0	6	414.85 (17)	72.39 (9)	36.43 (7)	27.18 (7)
	16	442.28 (17)	76.68 (9)	38.14 (7)	28.44 (7)
	2	109.98 (17)	19.08 (9)	9.35 (8)	6.91 (8)
	4	259.99 (17)	41.47 (8)	18.61 (7)	13.43 (7)
60.0	6	287.77 (17)	45.45 (8)	20.23 (7)	14.60 (7)
	16	306.87 (17)	48.20 (8)	21.34 (7)	15.40 (7)

SS2:

R_1/h=100.0 $\nu_{x\phi}$=0.250 $\nu_{\phi x}$=0.00625 E_x=30x10^6 psi E_ϕ=7.5x10^5 psi $G_{x\phi}$=3.75x10^5 psi

alpa	N \L/R_1	0.2	0.5	0.8	1.0
	2	352.98 (20)	78.66 (10)	47.43 (8)	39.11 (8)
	4	620.70 (17)	138.10 (8)	83.53 (7)	69.92 (6)

0.0	6	657.70 (16)	145.25 (8)	88.89 (7)	73.71 (6)
	16	680.64 (16)	149.36 (8)	92.17 (7)	75.95 (6)
	2	340.89 (20)	72.89 (10)	41.88 (9)	33.27 (8)
	4	599.50 (17)	126.69 (9)	73.50 (7)	59.13 (7)
10.0	6	636.53 (17)	134.80 (9)	77.78 (7)	63.34 (7)
	16	658.49 (16)	138.62 (8)	80.39 (7)	66.04 (7)
	2	288.44 (21)	54.70 (11)	28.31 (9)	21.51 (9)
	4	508.23 (17)	95.74 (9)	50.59 (8)	38.09 (7)
30.0	6	538.60 (17)	101.64 (9)	53.73 (7)	40.60 (7)
	16	558.30 (17)	105.30 (9)	55.47 (7)	42.28 (7)
	2	229.06 (21)	39.65 (11)	18.83 (9)	13.76 (9)
	4	404.66 (18)	69.63 (9)	33.94 (7)	24.58 (7)
45.0	6	429.13 (17)	73.97 (9)	35.86 (7)	26.23 (7)
	16	444.67 (17)	76.69 (9)	37.07 (7)	27.33 (7)
	2	158.44 (21)	25.09 (10)	10.94 (8)	7.57 (8)
	4	280.18 (18)	44.20 (9)	19.26 (7)	13.61 (7)
60.0	6	297.67 (17)	46.99 (8)	20.46 (7)	14.60 (7)
	16	308.46 (17)	48.41 (8)	21.22 (7)	15.09 (6)

SS3:

$R_1/h=100.0$ $\nu_{x\phi}=0.250$ $\nu_{\phi x}=0.00625$ $E_x=30\times10^6$ psi $E_\phi=7.5\times10^5$ psi $G_{x\phi}=3.75\times10^5$ psi

alpa	N \L/R_1	0.2	0.5	0.8	1.0
	2	249.84 (17)	66.64 (10)	42.58 (8)	35.87 (7)
	4	576.88 (16)	133.95 (9)	81.83 (7)	68.72 (6)
0.0	6	637.35 (16)	145.16 (8)	88.42 (7)	73.46 (6)
	16	678.92 (16)	152.61 (8)	92.97 (7)	76.74 (6)
	2	241.02 (17)	61.47 (10)	38.75 (9)	31.37 (8)
	4	558.14 (16)	123.01 (9)	73.46 (7)	59.29 (7)
10.0	6	616.61 (16)	134.00 (9)	78.85 (7)	64.06 (7)
	16	656.81 (16)	141.55 (9)	82.55 (7)	67.33 (7)
	2	203.12 (17)	46.68 (10)	27.57 (9)	22.21 (9)
	4	472.38 (17)	93.49 (9)	51.95 (8)	41.03 (7)
30.0	6	522.24 (17)	101.71 (9)	56.19 (8)	43.78 (7)
	16	556.51 (17)	107.34 (9)	59.06 (8)	45.60 (7)
	2	160.71 (17)	32.94 (10)	18.12 (9)	14.06 (9)
	4	375.81 (17)	67.45 (9)	34.67 (8)	26.23 (7)
45.0	6	415.64 (17)	73.62 (9)	37.60 (8)	28.06 (7)
	16	443.01 (17)	77.84 (9)	39.27 (7)	29.27 (7)
	2	110.57 (17)	19.84 (9)	9.82 (8)	7.25 (8)
	4	260.35 (17)	42.23 (9)	19.23 (7)	13.88 (7)
60.0	6	288.08 (17)	46.36 (9)	20.81 (7)	15.02 (7)
	16	307.14 (17)	49.04 (8)	21.87 (7)	15.79 (7)

SS4:

$R_1/h=100.0$ $\nu_{x\phi}=0.250$ $\nu_{\phi x}=0.00625$ $E_x=30\times10^6$ psi $E_\phi=7.5\times10^5$ psi $G_{x\phi}=3.75\times10^5$ psi

alpa	N \L/R_1	0.2	0.5	0.8	1.0
	2	354.56 (20)	80.14 (10)	48.37 (8)	39.50 (8)
	4	623.81 (17)	141.69 (9)	86.29 (7)	72.53 (7)

0.0	6	661.25 (16)	150.96 (9)	91.69 (7)	76.82 (6)
	16	683.61 (16)	155.05 (8)	94.95 (7)	79.09 (6)
	2	342.46 (20)	74.12 (11)	42.58 (9)	33.95 (8)
	4	602.57 (17)	130.22 (9)	76.63 (7)	60.86 (7)
10.0	6	639.24 (17)	138.27 (9)	80.92 (7)	65.07 (7)
	16	661.42 (16)	143.12 (9)	83.48 (7)	67.75 (7)
	2	289.55 (21)	55.76 (11)	29.24 (9)	22.20 (9)
	4	510.57 (17)	98.67 (9)	52.23 (8)	39.97 (7)
30.0	6	540.64 (17)	104.47 (9)	55.95 (8)	42.42 (7)
	16	559.92 (17)	107.97 (9)	58.26 (7)	44.01 (7)
	2	229.85 (21)	40.38 (11)	19.48 (9)	14.25 (9)
	4	405.86 (18)	71.46 (9)	35.10 (8)	25.84 (7)
45.0	6	430.38 (17)	75.72 (9)	37.62 (8)	27.44 (7)
	16	445.62 (17)	78.31 (9)	38.84 (7)	28.48 (7)
	2	158.88 (21)	25.57 (10)	11.25 (9)	7.87 (8)
	4	280.75 (18)	44.96 (9)	20.05 (7)	14.14 (7)
60.0	6	298.21 (17)	47.78 (9)	21.22 (7)	15.11 (7)
	16	308.84 (17)	49.50 (8)	21.93 (7)	15.71 (7)

E.14 Buckling Values of Multi Layer Orthotropic Conical Shell in Bending (M_{cr})

SS1:

R_1/h=50.0 $\nu_{x\phi}$=0.250 $\nu_{\phi x}$=0.02500 E_x=30x10^6 psi E_ϕ=3x10^6 psi $G_{x\phi}$=1.5x10^6 psi

alpa	N \L/R_1	0.2	0.5	0.8	1.0
	2	5147.99 (2)	2553.72 (2)	4297.71 (10)	4570.22 (3)
	4	8391.61 (2)	3913.48 (2)	3013.42 (2)	8593.28 (2)
0.0	6	8986.91 (2)	4135.36 (2)	3225.34 (2)	7855.96 (4)
	16	9390.57 (2)	4292.86 (2)	3380.73 (2)	8019.53 (4)
	2	5195.49 (2)	2782.84 (2)	4874.75 (2)	5412.17 (3)
	4	8509.87 (2)	4160.70 (2)	3212.69 (2)	7986.86 (4)
10.0	6	9119.86 (3)	4382.90 (2)	3432.97 (2)	8256.11 (4)
	16	9532.69 (3)	4542.06 (2)	3595.87 (2)	8430.89 (4)
	2	4667.17 (2)	2665.66 (2)	4612.91 (4)	4466.33 (9)
	4	7769.88 (3)	3744.77 (2)	3127.93 (2)	2960.09 (2)
30.0	6	8342.68 (3)	3920.87 (2)	3331.45 (2)	3133.97 (2)
	16	8736.10 (3)	4040.65 (4)	3484.61 (2)	3266.38 (2)
	2	3805.93 (2)	1908.00 (2)	1532.56 (2)	1414.37 (2)
	4	6431.85 (2)	2551.53 (4)	2373.34 (2)	2149.93 (2)
45.0	6	6917.78 (2)	2667.81 (4)	2529.07 (2)	2291.33 (2)
	16	7251.60 (2)	2758.22 (4)	2647.94 (2)	2399.04 (2)
	2	2667.98 (2)	1003.93 (2)	884.84 (2)	787.47 (2)
	4	4573.39 (2)	1419.52 (3)	1337.44 (2)	1248.36 (2)
60.0	6	4926.09 (2)	1496.26 (3)	1417.98 (2)	1338.50 (2)
	16	5168.42 (2)	1552.07 (3)	1482.29 (2)	1411.28 (2)

SS2:

$R_1/h=50.0$ $\nu_{x\phi}=0.250$ $\nu_{\phi x}=0.02500$ $E_x=30x10^6$ psi $E_\phi=3x10^6$ psi $G_{x\phi}=1.5x10^6$ psi

alpa	N \L/R_1	0.2	0.5	0.8	1.0
	2	8223.04 (3)	2972.27 (2)	1979.64 (2)	4885.07 (3)
	4	9286.85 (2)	4078.36 (2)	3053.70 (2)	8393.59 (2)
0.0	6	9392.03 (2)	4220.82 (2)	3249.54 (2)	3267.01 (2)
	16	9449.51 (2)	4312.98 (2)	3389.89 (2)	3399.42 (2)
	2	8321.07 (3)	3103.33 (2)	2019.62 (2)	5697.70 (3)
	4	9413.34 (2)	4188.42 (2)	3110.48 (2)	3050.05 (2)
10.0	6	9521.29 (2)	4321.81 (2)	3306.43 (2)	3233.40 (2)
	16	9580.59 (2)	4406.64 (2)	4336.40 (2)	3367.40 (2)
	2	7563.37 (3)	2883.92 (2)	1820.50 (2)	1723.95 (2)
	4	8612.55 (2)	3651.28 (2)	2787.23 (2)	2583.45 (2)
30.0	6	8716.90 (2)	3731.20 (2)	2955.96 (2)	2748.23 (2)
	16	8775.75 (2)	3779.75 (2)	3077.01 (2)	2868.04 (2)
	2	6232.77 (3)	2266.77 (2)	1456.00 (2)	1280.43 (2)
	4	7143.99 (3)	2663.98 (2)	2184.95 (2)	1977.70 (2)
45.0	6	7236.46 (2)	2699.67 (2)	2307.60 (2)	2106.24 (2)
	16	7289.39 (2)	2720.35 (2)	2396.67 (2)	2201.97 (2)
	2	4409.12 (3)	1374.45 (2)	951.22 (2)	805.44 (2)
	4	5088.56 (3)	1523.71 (2)	1326.76 (2)	1229.03 (2)
60.0	6	5158.75 (2)	1537.59 (2)	1381.90 (2)	1307.18 (2)
	16	5199.66 (2)	1545.29 (2)	1423.40 (2)	1369.26 (2)

SS3:

$R_1/h=50.0$ $\nu_{x\phi}=0.250$ $\nu_{\phi x}=0.02500$ $E_x=30x10^6$ psi $E_\phi=3x10^6$ psi $G_{x\phi}=1.5x10^6$ psi

alpa	N \L/R_1	0.2	0.5	0.8	1.0
	2	6537.08 (7)	4905.11 (2)	2997.32 (2)	2836.98 (2)
	4	9883.18 (6)	7344.39 (5)	4476.11 (2)	3871.11 (2)
0.0	6	10480.06 (6)	7512.63 (5)	4733.54 (2)	4107.44 (2)
	16	10877.88 (6)	7724.65 (5)	4916.79 (2)	4286.60 (2)
	2	6567.57 (7)	5069.77 (2)	3196.21 (2)	2885.88 (2)
	4	9960.83 (6)	6876.62 (5)	4691.53 (2)	4079.88 (2)
10.0	6	10568.17 (6)	7042.16 (5)	4953.50 (2)	4319.77 (2)
	16	10973.23 (6)	7225.76 (5)	5139.60 (2)	4499.34 (2)
	2	5757.20 (6)	4058.10 (6)	2773.27 (2)	2498.25 (2)
	4	8868.04 (6)	4941.54 (5)	4027.28 (2)	3547.70 (2)
30.0	6	9436.14 (6)	5100.28 (5)	4254.55 (2)	3738.44 (2)
	16	9809.36 (5)	5241.56 (5)	4417.21 (2)	3880.57 (2)
	2	4357.56 (2)	2506.29 (6)	2007.24 (2)	1775.88 (2)
	4	6927.20 (2)	3242.94 (5)	2979.97 (2)	2555.39 (2)
45.0	6	7395.73 (2)	3371.80 (5)	3156.56 (2)	2700.04 (2)
	16	7708.67 (2)	3474.65 (5)	3283.89 (2)	2807.79 (2)
	2	2848.43 (2)	1309.82 (5)	1173.99 (2)	984.39 (2)
	4	4723.94 (2)	1767.90 (5)	1756.90 (2)	1481.51 (2)
60.0	6	5067.82 (2)	1855.37 (5)	1856.53 (2)	1575.04 (2)
	16	5299.97 (2)	1919.86 (5)	1928.69 (2)	1646.09 (2)

SS4:

$R_1/h=50.0$ $\nu_{x\phi}=0.250$ $\nu_{\phi x}=0.02500$ $E_x=30x10^6$ psi $E_\phi=3x10^6$ psi $G_{x\phi}=1.5x10^6$ psi

alpa	N \L/R_1	0.2	0.5	0.8	1.0
	2	9746.28 (6)	5188.64 (2)	3129.31 (2)	2777.94 (2)
	4	10883.61 (6)	7695.75 (2)	5368.18 (10)	3932.55 (2)
0.0	6	10964.60 (6)	7855.46 (5)	4790.36 (2)	4162.97 (2)
	16	10971.90 (6)	8374.07 (2)	4948.53 (2)	4329.02 (2)
	2	9823.26 (6)	5430.84 (2)	3338.61 (2)	2877.23 (2)
	4	10982.05 (6)	7436.62 (5)	4794.70 (2)	4140.56 (2)
10.0	6	11066.41 (6)	7441.34 (5)	5036.26 (2)	4371.58 (2)
	16	11076.79 (6)	7456.36 (5)	5198.10 (2)	4535.16 (2)
	2	8738.85 (6)	5003.42 (2)	2960.81 (2)	2515.89 (2)
	4	9831.65 (6)	5492.68 (6)	4257.31 (2)	3638.41 (2)
30.0	6	9918.56 (6)	5503.89 (5)	4476.08 (2)	3829.26 (2)
	16	9939.65 (6)	5493.02 (5)	4620.80 (2)	3962.28 (2)
	2	6988.75 (5)	3279.24 (6)	2232.48 (2)	1862.39 (2)
	4	7910.96 (5)	3626.95 (5)	3263.43 (2)	2708.70 (2)
45.0	6	7992.74 (5)	3636.27 (5)	3436.16 (2)	2853.46 (2)
	16	8024.08 (5)	3627.73 (5)	3549.28 (2)	2953.38 (2)
	2	4719.45 (3)	1783.83 (5)	1376.42 (2)	1094.22 (2)
	4	5400.35 (3)	1966.95 (5)	2026.61 (2)	1623.78 (2)
60.0	6	5469.59 (3)	1978.42 (5)	2129.01 (2)	1715.50 (2)
	16	5506.45 (3)	1976.34 (5)	2194.49 (2)	1779.36 (2)

E.15 Buckling Values of Multi Layer Orthotropic Conical Shell under Axial Compression (P_{cr}) with Outer Pre-Pressure

SS2:

$R_1/h=100.0$ $\nu_{x\phi}=0.250$ $\nu_{\phi x}=0.00625$ $E_x=30x10^6$ psi $E_\phi=7.5x10^5$ psi $G_{x\phi}=3.75x10^5$ psi

$L/R_1=0.2$

N= 2

alpa \ Pre_q	0%	25%	50%	75%	100%
0.0	1772.24 (8)	1579.33 (11)	1253.38 (14)	735.94 (17)	0.00 (20)
10.0	1759.21 (8)	1570.57 (11)	1248.56 (14)	734.75 (17)	0.00 (20)
30.0	1530.98 (8)	1381.01 (11)	1105.07 (14)	653.31 (18)	0.00 (21)
45.0	1216.54 (7)	1111.35 (10)	898.02 (14)	532.80 (18)	0.00 (21)
60.0	826.47 (6)	769.65 (10)	628.46 (14)	374.44 (18)	0.00 (21)

N= 4

alpa \ Pre_q	0%	25%	50%	75%	100%
0.0	2314.60 (7)	2066.34 (9)	1632.23 (12)	952.82 (14)	0.00 (17)
10.0	2300.87 (7)	2058.71 (9)	1628.16 (12)	953.81 (15)	0.00 (17)
30.0	2019.01 (6)	1821.49 (9)	1449.29 (12)	846.61 (15)	0.00 (17)
45.0	1616.81 (6)	1477.14 (9)	1183.70 (12)	693.71 (15)	0.00 (18)
60.0	1111.11 (5)	1032.55 (9)	833.51 (12)	491.14 (15)	0.00 (18)

N= 6

alpa \ Pre_q	0%	25%	50%	75%	100%
0.0	2355.74 (7)	2101.00 (9)	1660.99 (12)	964.93 (14)	0.00 (16)
10.0	2342.07 (7)	2092.58 (9)	1653.47 (12)	962.39 (14)	0.00 (17)
30.0	2055.10 (6)	1853.71 (9)	1473.63 (12)	864.38 (15)	0.00 (17)
45.0	1648.33 (6)	1505.00 (9)	1204.02 (12)	706.30 (15)	0.00 (17)

60.0	1134.19 (5)	1052.76 (8)	847.93 (12)	498.04 (15)	0.00 (17)

N=16

alpa \ Pre_q	0%	25%	50%	75%	100%
0.0	2375.17 (7)	2116.43 (9)	1672.00 (11)	971.77 (14)	0.00 (16)
10.0	2361.74 (7)	2108.21 (9)	1667.06 (12)	968.37 (14)	0.00 (16)
30.0	2073.16 (6)	1868.68 (9)	1484.19 (12)	869.92 (14)	0.00 (17)
45.0	1664.88 (6)	1519.01 (9)	1214.15 (12)	714.08 (15)	0.00 (17)
60.0	1146.96 (5)	1063.37 (8)	856.30 (12)	504.16 (15)	0.00 (17)

L/R_1=0.5

N= 2

alpa \ Pre_q	0%	25%	50%	75%	100%
0.0	824.50 (8)	723.86 (8)	529.83 (8)	288.79 (9)	0.00 (10)
10.0	835.33 (9)	739.44 (7)	517.04 (9)	284.76 (10)	0.01 (10)
30.0	735.36 (10)	563.84 (8)	406.96 (9)	223.40 (10)	0.01 (11)
45.0	471.44 (7)	386.83 (8)	285.53 (9)	158.55 (10)	0.00 (11)
60.0	260.31 (6)	218.16 (7)	163.63 (8)	92.09 (9)	0.00 (10)

N= 4

alpa \ Pre_q	0%	25%	50%	75%	100%
0.0	1102.63 (6)	904.92 (6)	647.56 (7)	351.47 (8)	0.00 (8)
10.0	1070.42 (6)	883.46 (7)	636.06 (7)	345.15 (8)	0.01 (9)
30.0	841.96 (6)	696.97 (7)	508.73 (7)	278.48 (8)	0.00 (9)
45.0	589.34 (6)	488.31 (6)	359.11 (7)	199.00 (8)	0.00 (9)
60.0	331.12 (5)	279.32 (6)	210.55 (7)	118.69 (8)	0.00 (9)

N= 6

alpa \ Pre_q	0%	25%	50%	75%	100%
0.0	1119.90 (6)	912.10 (6)	659.11 (7)	369.74 (8)	0.00 (8)
10.0	1085.11 (6)	891.94 (6)	638.73 (7)	346.32 (8)	0.00 (9)
30.0	853.97 (6)	707.40 (6)	512.07 (7)	280.24 (8)	0.00 (9)
45.0	599.96 (6)	493.02 (6)	362.85 (7)	201.03 (8)	0.00 (9)
60.0	335.89 (5)	283.90 (6)	214.34 (7)	121.24 (8)	0.00 (8)

N=16

alpa \ Pre_q	0%	25%	50%	75%	100%
0.0	1124.32 (6)	910.76 (6)	662.48 (7)	371.44 (7)	0.00 (8)
10.0	1088.12 (6)	889.75 (6)	640.14 (7)	353.12 (8)	0.00 (8)
30.0	856.91 (6)	705.60 (6)	510.70 (7)	279.29 (8)	0.00 (9)
45.0	603.65 (6)	493.14 (6)	362.94 (7)	200.96 (8)	0.00 (9)
60.0	337.35 (5)	285.87 (6)	215.63 (6)	121.27 (7)	0.00 (8)

E.16 Buckling Values of Multi Layer Orthotropic Conical Shell in Pure Bending (M_{cr}) with Axial Pre-Compressed

SS2:

R_1/h=50.0 $\nu_{x\phi}$=0.250 $\nu_{\phi x}$=0.02500 $E_x=30\times10^6$ psi $E_\phi=3\times10^6$ psi $G_{x\phi}=1.5\times10^6$ psi

L/R_1=0.2

N= 2

alpa \ Pre_P	0%	25%	50%	75%	100%
0.0	8223.04 (3)	6189.68 (3)	4127.31 (2)	2071.75 (2)	0.00 (1)
10.0	8321.07 (3)	6263.72 (3)	4177.68 (2)	2096.96 (2)	0.00 (1)
30.0	7563.37 (3)	5695.87 (3)	3800.67 (2)	1908.57 (2)	0.00 (1)
45.0	6232.77 (3)	4695.98 (3)	3134.35 (2)	1574.80 (2)	0.00 (1)
60.0	4409.12 (3)	3323.31 (3)	2218.67 (2)	1115.21 (2)	0.00 (1)

Nb= 4

alpa \ Pre_P	0%	25%	50%	75%	100%

0.0	9286.85 (2)	6962.23 (2)	4645.35 (2)	2334.76 (2)	0.00 (1)
10.0	9413.34 (2)	7056.86 (2)	4708.14 (2)	2366.39 (2)	0.00 (1)
30.0	8612.55 (2)	6456.22 (2)	4307.80 (2)	2166.49 (2)	0.00 (1)
45.0	7143.99 (3)	5355.97 (2)	3574.13 (2)	1798.73 (2)	0.00 (1)
60.0	5088.56 (3)	3815.32 (2)	2546.30 (2)	1282.23 (2)	0.00 (1)

N= 6

alpa \ Pre_P	0%	25%	50%	75%	100%
0.0	9392.03 (2)	7042.01 (2)	4698.76 (2)	2361.12 (2)	0.00 (1)
10.0	9521.29 (2)	7138.79 (2)	4763.10 (2)	2393.55 (2)	0.00 (1)
30.0	8716.90 (2)	6535.58 (2)	4361.18 (2)	2193.06 (2)	0.00 (1)
45.0	7236.46 (2)	5425.66 (2)	3621.13 (2)	1822.26 (2)	0.00 (1)
60.0	5158.75 (2)	3867.93 (2)	2581.88 (2)	1300.16 (2)	0.00 (1)

Nb=16

alpa \ Pre_P	0%	25%	50%	75%	100%
0.0	9449.51 (2)	7085.31 (2)	4727.22 (2)	2374.44 (2)	0.00 (1)
10.0	9580.59 (2)	7183.49 (2)	4792.64 (2)	2407.50 (2)	0.00 (1)
30.0	8775.75 (2)	6580.12 (2)	4390.80 (2)	2207.29 (2)	0.00 (1)
45.0	7289.39 (2)	5465.81 (2)	3647.98 (2)	1835.36 (2)	0.00 (1)
60.0	5199.66 (2)	3899.00 (2)	2602.78 (2)	1310.50 (2)	0.00 (1)

L/R_1=0.5

N= 2

alpa \ Pre_P	0%	25%	50%	75%	100%
0.0	2972.27 (2)	2671.57 (2)	2270.26 (2)	1725.98 (2)	668.32 (7)
10.0	3103.33 (2)	2764.63 (2)	2320.20 (2)	1728.62 (2)	638.29 (3)
30.0	2883.92 (2)	2486.79 (2)	1987.41 (2)	1037.12 (5)	0.00 (5)
45.0	2266.77 (2)	1861.41 (2)	1342.08 (4)	672.37 (4)	0.00 (4)
60.0	1374.45 (2)	1061.65 (2)	727.18 (3)	364.00 (3)	0.00 (3)

N= 4

alpa \ Pre_P	0%	25%	50%	75%	100%
0.0	4078.36 (2)	3482.45 (2)	2776.31 (2)	1494.90 (4)	0.00 (5)
10.0	4188.42 (2)	3541.56 (2)	2764.20 (4)	1420.23 (4)	0.00 (5)
30.0	3651.28 (2)	2977.32 (2)	2037.23 (4)	1019.84 (4)	0.00 (4)
45.0	2663.98 (2)	2069.68 (4)	1381.37 (4)	691.42 (4)	0.00 (4)
60.0	1523.71 (2)	1157.02 (2)	773.41 (3)	387.01 (3)	0.00 (3)

N= 6

alpa \ Pre_P	0%	25%	50%	75%	100%
0.0	4220.82 (2)	3581.28 (2)	2834.82 (2)	1462.93 (4)	0.00 (5)
10.0	4321.81 (2)	3631.95 (2)	2732.79 (4)	1395.63 (4)	0.00 (5)
30.0	3731.20 (2)	3028.23 (2)	2031.07 (4)	1016.64 (4)	0.00 (4)
45.0	2699.67 (2)	2073.06 (4)	1383.44 (4)	692.37 (4)	0.00 (4)
60.0	1537.59 (2)	1165.22 (3)	777.34 (3)	388.98 (3)	0.00 (3)

N=16

alpa \ Pre_P	0%	25%	50%	75%	100%
0.0	4312.98 (2)	3648.71 (2)	2864.82 (4)	1452.61 (4)	0.00 (5)
10.0	4406.64 (2)	3693.06 (2)	2719.59 (4)	1386.83 (4)	0.00 (5)
30.0	3779.75 (2)	3034.55 (4)	2025.52 (4)	1013.86 (4)	0.00 (4)
45.0	2720.35 (2)	2071.71 (4)	1382.49 (4)	691.87 (4)	0.00 (4)
60.0	1545.29 (2)	1167.08 (3)	778.55 (3)	389.57 (3)	0.00 (3)

E.17 Buckling Values of Multi Layer Orthotropic Conical Shell in Pure Bending (M_{cr}) with Outer Pre-Pressure

SS2:

R_1/h=50.0 $\nu_{x\phi}$=0.250 $\nu_{\phi x}$=0.02500 $E_x=30\times10^6$ psi $E_\phi=3\times10^6$ psi $G_{x\phi}=1.5\times10^6$ psi

L/R_1=0.2

N= 2

alpa \ Pre_q	0%	25%	50%	75%	100%
0.0	8223.04 (3)	8057.07 (5)	6950.90 (11)	4297.05 (15)	0.00 (18)
10.0	8321.07 (3)	8161.53 (5)	7053.44 (11)	4365.24 (15)	0.00 (19)
30.0	7563.37 (3)	7441.67 (5)	6486.55 (11)	4037.87 (16)	0.00 (19)
45.0	6232.77 (3)	6140.89 (3)	5399.81 (11)	3366.26 (16)	0.00 (19)
60.0	4409.12 (3)	4345.28 (3)	3854.49 (11)	2410.92 (16)	0.00 (20)

N= 4

alpa \ Pre_q	0%	25%	50%	75%	100%
0.0	9286.85 (2)	9018.69 (6)	7606.87 (10)	4614.39 (14)	0.00 (16)
10.0	9413.34 (2)	9150.11 (6)	7732.12 (11)	4683.39 (14)	0.00 (17)
30.0	8612.55 (2)	8402.18 (6)	7129.62 (11)	4344.76 (14)	0.00 (17)
45.0	7143.99 (3)	6989.74 (5)	5958.88 (11)	3645.71 (14)	0.00 (17)
60.0	5088.56 (3)	4989.14 (5)	4275.54 (11)	2617.79 (15)	0.00 (18)

N= 6

alpa \ Pre_q	0%	25%	50%	75%	100%
0.0	9392.03 (2)	9104.95 (6)	7651.36 (10)	4652.79 (13)	0.00 (16)
10.0	9521.29 (2)	9238.93 (6)	7776.14 (10)	4705.87 (14)	0.00 (16)
30.0	8716.90 (2)	8491.26 (6)	7180.52 (11)	4357.01 (14)	0.00 (17)
45.0	7236.46 (2)	7073.89 (6)	6008.51 (11)	3661.35 (14)	0.00 (17)
60.0	5158.75 (2)	5054.00 (5)	4314.14 (11)	2637.52 (14)	0.00 (17)

N=16

alpa \ Pre_q	0%	25%	50%	75%	100%
0.0	9449.51 (2)	9141.03 (6)	7656.60 (10)	4638.99 (13)	0.00 (16)
10.0	9580.59 (2)	9277.92 (6)	7784.64 (10)	4721.48 (14)	0.00 (16)
30.0	8775.75 (2)	8533.18 (6)	7194.14 (11)	4351.33 (14)	0.00 (17)
45.0	7289.39 (2)	7115.17 (6)	6027.03 (11)	3661.83 (14)	0.00 (17)
60.0	5199.66 (2)	5090.47 (5)	4333.14 (11)	2641.84 (14)	0.00 (17)

L/R_1=0.5

N= 2

alpa \ Pre_q	0%	25%	50%	75%	100%
0.0	2972.27 (2)	2950.70 (2)	2928.95 (2)	2907.03 (2)	1536.06 (18)
10.0	3103.33 (2)	3080.05 (2)	3056.46 (2)	3032.57 (2)	0.01 (9)
30.0	2883.92 (2)	2856.02 (2)	2826.85 (2)	1742.77 (8)	0.00 (10)
45.0	2266.77 (2)	2236.15 (2)	1833.76 (7)	1063.56 (8)	0.00 (10)
60.0	1374.45 (2)	1305.97 (5)	1048.27 (6)	605.77 (8)	0.00 (9)

N= 4

alpa \ Pre_q	0%	25%	50%	75%	100%
0.0	4078.36 (2)	4029.80 (2)	3980.72 (2)	3265.40 (6)	0.00 (8)
10.0	4188.42 (2)	4137.44 (2)	4085.75 (2)	2852.39 (6)	0.00 (8)
30.0	3651.28 (2)	3592.95 (5)	2863.09 (6)	1744.38 (7)	0.00 (9)
45.0	2663.98 (2)	2441.38 (5)	1925.65 (6)	1140.39 (7)	0.00 (9)
60.0	1523.71 (2)	1404.94 (4)	1121.11 (6)	659.27 (7)	0.00 (8)

N= 6

alpa \ Pre_q	0%	25%	50%	75%	100%
0.0	4220.82 (2)	4167.13 (2)	4112.84 (2)	3202.99 (6)	0.02 (8)
10.0	4321.81 (2)	4265.97 (2)	4075.34 (5)	2799.34 (6)	0.00 (8)
30.0	3731.20 (2)	3585.02 (5)	2863.01 (6)	1748.85 (7)	0.00 (8)
45.0	2699.67 (2)	2447.11 (5)	1932.67 (6)	1145.16 (7)	0.00 (8)
60.0	1537.59 (2)	1410.61 (4)	1130.74 (6)	666.40 (7)	0.00 (8)

N=16

alpa \ Pre_q	0%	25%	50%	75%	100%
0.0	4312.98 (2)	4255.90 (2)	4198.21 (2)	3245.53 (6)	489.89 (7)

10.0	4406.64 (2)	4347.74 (2)	4057.40 (5)	2804.29 (6)	0.00 (8)
30.0	3779.75 (2)	3584.26 (5)	2881.90 (6)	1786.78 (7)	0.00 (8)
45.0	2720.35 (2)	2449.59 (5)	1942.51 (6)	1160.50 (7)	0.00 (8)
60.0	1545.29 (2)	1411.29 (4)	1136.56 (6)	672.53 (7)	0.00 (8)

E.18 Buckling Values of Long Single Layer Isotropic Conical Shell under Axial Compression (P_{cr})

SS2:

R_1/h=100.0 $\nu_{x\phi}$=0.3 E=30x10^6 psi

alpa \ L/R_1	0.2	0.5	0.8	1.0	1.5	2.0	3.0	4.0
0.0	5723.26	5868.08	5721.70	5721.64	5704.14	197.08	0.17	3.00
1.0	5726.86	5867.87	5719.45	5720.48	5703.98	699.19	1.57	0.06
5.0	5715.63	5832.42	5676.29	5680.21	5674.95	3976.78	0.00	1.42
10.0	5644.25	5710.26	5546.10	5553.64	5537.76	4481.79	0.15	0.14
20.0	5321.44	5214.88	5049.08	5067.57	5064.87	4688.94	0.01	0.13
30.0	4791.70	4418.81	4291.79	4315.75	4315.10	4257.70	0.00	0.00
40.0	4107.67	3399.35	3372.43	3382.95	3391.76	3391.02	0.00	0.00
45.0	3725.75	2846.55	2888.32	2883.64	2896.27	2898.56	0.00	0.00
50.0	3326.34	2295.72	2406.59	2384.62	2399.72	2399.34	0.00	1.31
60.0	2498.09	1303.43	1491.28	1456.54	1461.01	1462.04	1430.76	0.04
70.0	1658.58	589.21	686.97	704.04	686.39	690.28	689.27	654.11
80.0	825.37	191.78	156.85	168.83	184.92	180.77	181.05	180.60

SS2:

R_1/h=50.0 $\nu_{x\phi}$=0.3 E=30x10^6 psi

alpa \ L/R_1	0.2	0.5	0.8	1.0	1.5	2.0	3.0	4.0
0.0	37231.45	21580.48	23120.75	22878.01	22957.68	22988.23	166.24	0.01
1.0	37278.38	21547.93	23124.03	22867.67	22949.20	22913.42	1741.55	6.35
5.0	37336.97	21274.90	23006.79	22693.36	22784.11	22759.84	4647.60	0.62
10.0	37113.03	20625.69	22567.72	22184.07	22288.95	22279.00	21022.17	0.00
20.0	35683.27	18417.49	20752.96	20267.06	20364.49	20370.66	21116.77	2.52
30.0	33005.79	15307.58	17812.53	17363.87	17379.03	17384.07	17587.29	60.71
40.0	29210.11	11771.55	13973.30	13802.03	13653.86	13681.88	13724.40	2391.66
45.0	26946.24	10001.25	11828.62	11878.66	11653.04	11699.71	11751.37	9592.26
50.0	24470.38	8305.55	9631.32	9908.87	9648.70	9704.64	9710.07	8955.16
60.0	18983.29	5308.75	5505.61	5983.86	5912.00	5910.78	5920.95	5862.32
70.0	12949.39	2985.95	2428.74	2612.92	2865.03	2800.30	2805.72	2798.56
80.0	6561.29	1301.12	737.73	658.02	697.08	754.26	742.66	738.44

SS2:

R_1/h=33.3 $\nu_{x\phi}$=0.3 E=30x10^6 psi

alpa \ L/R_1	0.2	0.5	0.8	1.0	1.5	2.0	3.0	4.0
0.0	120259.80	44901.04	53340.29	52063.54	51874.97	51831.88	52646.35	3.85
1.0	120429.83	44866.64	53316.20	52071.44	51851.21	51811.65	52617.44	133.57
5.0	120722.23	44463.02	52887.96	51816.98	51466.88	51433.91	51670.07	12.93
10.0	120187.16	43383.99	51601.78	50852.57	50316.96	50312.15	50253.77	10987.29
20.0	116092.84	39526.87	46606.04	46832.93	45901.36	46014.92	46125.18	29709.66
30.0	108043.57	33942.64	38845.78	40261.84	39116.36	39332.24	39350.00	37242.27
40.0	96291.06	27409.11	29411.35	31615.76	30838.27	30977.74	30999.13	30961.92
45.0	89148.93	24034.18	24541.17	26771.11	26465.67	26467.22	26516.05	26334.34
50.0	81245.34	20704.54	19840.54	21808.80	22100.88	21931.18	22007.78	22006.72
60.0	63441.45	14444.61	11639.10	12510.73	13741.76	13427.20	13458.41	13416.71
70.0	43504.52	8959.51	5734.86	5574.69	6356.54	6515.23	6372.14	6380.65
80.0	22067.67	4244.38	2148.67	1726.33	1515.48	1629.64	1732.20	1696.72

SS2:
$R_1/h=25.0$ $\nu_{x\phi}=0.3$ $E=30x10^6$ psi

alpa \ L/R_1	0.2	0.5	0.8	1.0	1.5	2.0	3.0	4.0
0.0	280574.75	80687.13	92145.07	94716.27	92296.80	92498.30	92013.12	23660.78
1.0	280987.56	80705.48	91983.05	94723.23	92235.93	92449.30	92174.45	45670.82
5.0	281759.47	80357.61	90737.52	94191.71	91481.96	91775.30	91706.13	75635.12
10.0	280674.88	78996.58	87878.27	92247.90	89402.34	89795.55	89671.34	86555.76
20.0	271578.19	73461.57	78240.48	84116.55	81715.68	82143.52	82089.75	82606.87
30.0	253319.56	64886.08	64645.75	70859.92	70124.24	70135.77	70262.02	70333.74
40.0	226341.20	54318.60	49166.00	54093.19	55882.97	55185.50	55431.69	55326.77
45.0	209825.88	48628.34	41430.63	45220.38	48165.97	47224.01	47458.43	47365.76
50.0	191467.28	42832.36	34049.37	36546.22	40236.09	39296.39	39413.62	39324.25
60.0	149859.22	31313.30	21152.25	21232.20	24387.48	24421.70	24076.03	24082.93
70.0	102956.12	20303.30	11455.46	10195.37	10789.43	11683.90	11501.09	11440.98
80.0	52186.37	9938.65	4807.04	3671.23	2806.63	2816.27	3097.73	3099.22

E.19 Buckling Values of Long Single Layer Isotropic Conical Shell under Outer Pressure (q_{cr})

SS2:
$R_1/h=100.0$ $\nu_{x\phi}=0.3$ $E=30x10^6$ psi

alpa \ L/R_1	0.2	0.5	0.8	1.0	1.5	2.0	3.0	4.0
0.0	2848.37	739.19	452.84	365.49	252.06	28.52	0.01	0.16
1.0	2842.42	734.34	448.48	360.23	245.54	85.54	0.00	0.00
5.0	2809.55	712.45	428.66	339.24	225.44	149.66	1.43	0.01
10.0	2749.04	680.19	399.40	313.56	202.49	144.27	0.01	0.03
20.0	2567.63	601.66	338.65	262.49	161.34	108.92	0.01	0.00
30.0	2315.08	509.64	276.00	208.81	123.58	84.50	0.01	0.03
40.0	2004.18	411.32	214.06	159.05	91.15	60.26	0.08	0.00
45.0	1831.04	362.07	184.45	135.99	76.51	50.00	0.00	0.23
50.0	1648.30	313.56	156.32	113.56	63.02	40.84	0.00	0.00
60.0	1260.09	218.89	103.33	73.71	39.81	25.28	11.15	0.00
70.0	850.43	134.31	58.75	40.75	21.11	13.10	6.52	1.50
80.0	428.11	62.02	24.10	15.70	7.49	4.47	2.15	1.24

SS2:
$R_1/h=50.0$ $\nu_{x\phi}=0.3$ $E=30x10^6$ psi

alpa \ L/R_1	0.2	0.5	0.8	1.0	1.5	2.0	3.0	4.0
0.0	21983.89	4565.41	2590.31	2042.61	1377.09	1080.99	3.45	0.00
1.0	21941.62	4536.71	2566.50	2015.04	1350.50	1052.11	1.57	0.00
5.0	21706.01	4408.08	2458.78	1904.20	1251.21	926.70	464.42	0.00
10.0	21269.05	4220.53	2294.88	1765.60	1134.49	807.77	471.36	0.61
20.0	19947.16	3769.25	1954.29	1483.92	885.53	620.59	352.59	0.05
30.0	18056.98	3242.49	1604.77	1186.29	680.79	456.14	256.69	0.00
40.0	15713.43	2674.18	1260.95	911.42	502.38	327.14	174.40	39.84
45.0	14397.02	2384.69	1096.42	782.64	422.23	271.63	142.63	0.89
50.0	12997.91	2096.36	939.34	657.36	348.65	221.54	114.43	43.47
60.0	9992.20	1529.23	638.74	436.19	222.98	137.82	68.45	28.04
70.0	6775.18	987.01	385.56	251.68	121.07	72.55	35.02	20.38
80.0	3421.17	482.14	172.98	107.11	46.53	26.34	11.82	6.70

SS2:
$R_1/h=33.3$ $\nu_{x\phi}=0.3$ $E=30x10^6$ psi

alpa \ L/R_1	0.2	0.5	0.8	1.0	1.5	2.0	3.0	4.0
0.0	73660.57	13787.58	7345.70	5670.21	3784.97	2881.34	1929.28	1.36
1.0	73518.37	13707.19	7281.43	5597.72	3720.94	2798.32	1878.40	6.42

5.0	72729.82	13346.22	6972.80	5303.56	3475.21	2505.81	1667.63	292.97
10.0	71274.00	12818.45	6523.40	4931.29	3076.98	2217.13	1359.69	0.00
20.0	66882.63	11541.80	5587.05	4160.27	2420.19	1670.56	975.55	96.32
30.0	60651.84	10036.47	4624.64	3344.07	1868.09	1234.41	676.30	194.63
40.0	52832.45	8386.34	3674.65	2591.09	1383.30	886.67	466.43	280.21
45.0	48432.62	7532.22	3217.30	2239.73	1165.57	736.92	381.05	201.67
50.0	43749.96	6670.48	2777.73	1894.27	965.86	602.17	305.60	158.57
60.0	33668.31	4950.91	1944.12	1279.10	624.54	377.55	183.44	108.77
70.0	22848.56	3264.00	1204.05	771.11	347.99	202.56	95.14	54.69
80.0	11544.13	1618.44	570.93	344.22	141.28	76.42	33.01	18.40

SS2:
R_1/h=25.0 $\nu_{x\phi}$=0.3 E=30x10^6 psi

alpa \ L/R_1	0.2	0.5	0.8	1.0	1.5	2.0	3.0	4.0
0.0	174158.64	30836.39	15487.84	11964.90	7741.49	5943.78	4041.27	2555.68
1.0	173821.92	30682.94	15332.27	11837.50	7576.52	5824.88	3857.10	2235.84
5.0	171958.33	29982.16	14681.61	11197.94	6958.89	5212.29	3292.56	2185.75
10.0	168523.14	28928.51	13821.49	10329.48	6272.02	4479.21	2848.16	1799.69
20.0	158170.95	26175.82	11969.25	8642.31	5060.32	3402.55	1941.66	1289.44
30.0	143526.25	22866.06	10002.38	7015.22	3866.56	2552.30	1384.66	866.10
40.0	125066.20	19241.56	8016.86	5475.75	2867.45	1820.01	937.25	573.20
45.0	114672.70	17354.24	7048.40	4753.25	2431.71	1517.40	763.83	459.76
50.0	103605.73	15436.97	6110.38	4069.49	2035.53	1249.56	615.07	366.74
60.0	79760.43	11560.13	4353.72	2831.31	1315.93	780.20	375.16	217.44
70.0	54144.89	7681.01	2772.38	1718.65	754.30	429.65	194.00	110.02
80.0	27361.94	3829.01	1342.04	801.49	316.95	167.93	69.90	37.67

E.20 Buckling Values of Long Single Layer Isotropic Conical Shell in Pure Bending (M_{cr})

SS2:
R_1/h=100.0 $\nu_{x\phi}$=0.3 E=30x10^6 psi

alpa \ L/R_1	0.2	0.5	0.8	1.0	1.2	1.5	1.8	2.0
0.0	2893.20	1365.81	1457.97	175.06	30.11	19.24	135.33	0.07
1.0	2900.06	1375.34	1429.76	187.05	31.89	19.23	174.04	0.16
5.0	2914.88	1408.23	1314.99	242.80	39.80	19.49	212.85	0.19
10.0	2903.96	1435.56	1189.33	332.62	51.51	20.09	224.38	0.45
20.0	2785.61	1438.81	1007.60	608.81	85.12	21.03	67.39	146.90
30.0	2549.46	1365.91	869.27	959.48	148.79	23.88	227.60	50.84
40.0	2217.83	1211.12	738.93	1004.18	302.56	32.73	13.43	155.49
45.0	2024.90	1102.43	671.80	712.38	449.57	42.00	12.72	9.78
50.0	1818.72	973.53	601.92	555.69	592.19	59.62	13.64	8.41
60.0	1379.76	665.97	451.15	370.12	375.58	176.66	24.15	9.98
70.0	922.88	348.34	282.08	228.96	196.52	191.53	111.93	33.69
80.0	461.33	122.91	99.21	92.20	81.83	68.69	60.45	57.07

SS2:
R_1/h=50.0 $\nu_{x\phi}$=0.3 E=30x10^6 psi

alpa \ L/R_1	0.2	0.5	0.8	1.0	1.2	1.5	1.8	2.0
0.0	19078.85	8533.91	4934.25	4143.98	3615.09	176.60	40.36	71.17
1.0	19134.79	8580.39	4982.47	4174.84	3936.19	193.88	43.24	68.47
5.0	19293.42	8721.75	5155.18	4281.65	5013.94	275.73	56.28	37.31
10.0	19335.12	8786.78	5316.78	4371.78	6103.62	411.86	75.69	43.63
20.0	18881.38	8513.34	5435.75	4394.42	4653.90	885.07	130.47	60.85
30.0	17713.43	7691.60	5253.01	4198.44	3924.54	2000.10	237.89	95.01
40.0	15872.55	6398.68	4749.94	3788.15	3325.77	4055.95	527.91	168.30

45.0	14723.07	5632.50	4377.25	3506.51	3022.70	3287.41	862.07	255.81
50.0	13437.04	4829.87	3925.44	3176.50	2706.74	2544.84	1560.21	422.42
60.0	10511.14	3255.58	2804.46	2380.07	2023.02	1713.91	1688.38	1731.11
70.0	7213.57	1904.24	1530.01	1423.24	1263.61	1060.05	931.78	878.01
80.0	3668.41	851.33	533.08	481.39	461.19	428.96	388.46	364.38

SS2:

$R_1/h=33.3$ $\nu_{x\phi}=0.3$ $E=30x10^6$ psi

alpa \ L/R_1	0.2	0.5	0.8	1.0	1.2	1.5	1.8	2.0
0.0	61771.54	21715.86	15034.42	11669.86	10078.27	4313.35	327.39	113.70
1.0	61961.43	21813.51	15182.19	11796.56	10182.38	4943.62	367.19	126.62
5.0	62524.48	22084.08	15705.04	12250.64	10545.53	8953.56	562.60	187.25
10.0	62751.53	22133.46	16175.92	12678.73	10868.24	13850.06	905.01	285.28
20.0	61545.17	21256.17	16423.47	13021.22	11064.88	10905.22	2205.68	619.45
30.0	58073.18	19177.71	15631.80	12616.78	10655.32	9527.47	6034.70	1466.61
40.0	52383.84	16186.38	13735.09	11427.60	9652.82	8227.67	8736.40	4092.79
45.0	48756.51	14476.50	12388.20	10538.46	8939.41	7518.14	7170.41	8340.56
50.0	44647.72	12698.20	10815.55	9458.79	8092.32	6754.04	6138.21	6307.08
60.0	35143.91	9136.07	7282.16	6783.80	6027.72	5053.36	4434.51	4166.02
70.0	24239.62	5800.30	3977.09	3749.06	3560.90	3146.43	2776.55	2587.57
80.0	12366.99	2788.83	1599.57	1346.39	1232.70	1161.37	1106.60	1063.25

SS2:

$R_1/h=25.0$ $\nu_{x\phi}=0.3$ $E=30x10^6$ psi

alpa \ L/R_1	0.2	0.5	0.8	1.0	1.2	1.5	1.8	2.0
0.0	144235.73	41789.32	32496.10	25726.21	21595.33	18398.37	3269.59	675.96
1.0	144686.94	41987.26	32788.95	26008.39	21839.41	18646.31	3938.98	777.94
5.0	146044.92	42567.06	33791.35	27013.81	22700.35	19449.18	7477.41	1301.39
10.0	146655.55	42781.86	34602.48	27945.12	23490.71	20084.11	15018.38	2298.96
20.0	144068.27	41497.94	34573.21	28604.74	24086.74	20358.69	20217.09	6881.74
30.0	136231.17	38092.43	32163.70	27495.61	23308.04	19480.80	17864.68	20271.36
40.0	123182.34	32990.95	27462.76	24503.70	21111.87	17558.55	15588.67	14992.60
45.0	114794.37	29984.49	24422.20	22308.40	19485.74	16233.78	14290.31	13492.60
50.0	105247.86	26776.86	21092.48	19687.52	17520.09	14683.89	12863.41	12037.88
60.0	83028.98	20037.38	14255.64	13537.43	12668.55	10977.10	9633.31	8970.09
70.0	57368.74	13218.52	8239.64	7427.78	7113.89	6623.92	6001.87	5630.53
80.0	29302.80	6540.21	3620.98	2940.31	2591.94	2349.90	2246.17	2196.08

E.21 Buckling Values of Single Layer Isotropic Conical Shell under Axial Compression (P_{cr}) with Different Young's modulus

SS2:

$R_1/h=100.0$ $\nu_{x\phi}=0.3$ $E=30x10^6$ psi

alpa \ L/R_1	0.2	0.5	0.8	1.0	1.2	1.5	1.8	2.0
0.0	5723.26	5868.08	5721.70	5721.64	5722.67	5704.14	6163.03	197.08
1.0	5726.86	5867.87	5719.45	5720.48	5719.58	5703.98	6014.76	699.19
5.0	5715.63	5832.42	5676.29	5680.21	5677.83	5674.95	5945.43	3976.78
10.0	5644.25	5710.26	5546.10	5553.64	5553.15	5537.76	5619.64	4481.79
20.0	5321.44	5214.88	5049.08	5067.57	5065.26	5064.87	5038.14	4688.94
30.0	4791.70	4418.81	4291.79	4315.75	4315.87	4315.10	4299.42	4257.70
40.0	4107.67	3399.35	3372.43	3382.95	3391.05	3391.76	3397.53	3391.02
45.0	3725.75	2846.55	2888.32	2883.64	2895.71	2896.27	2896.56	2898.56
50.0	3326.34	2295.72	2406.59	2384.62	2397.04	2399.72	2399.62	2399.34
60.0	2498.09	1303.43	1491.28	1456.54	1452.99	1461.01	1461.37	1462.04
70.0	1658.58	589.21	686.97	704.04	691.10	686.39	689.58	690.28

80.0	825.37	191.78	156.85	168.83	180.80	184.92	182.01	180.77

SS2:

$R_1/h=100.0$ $\nu_{x\phi}=0.3$ $E=30x10^7$ psi

alpa \ L/R_1	0.2	0.5	0.8	1.0	1.2	1.5	1.8	2.0
0.0	57232.59	58680.80	57218.21	57217.85	57212.94	57193.24	61747.40	18132.10
1.0	57268.57	58678.69	57193.98	57197.04	57182.31	57042.04	59361.93	26057.77
5.0	57156.29	58324.14	56762.59	56789.14	56793.41	56894.04	55864.98	38396.61
10.0	56442.47	57102.68	55460.64	55539.48	55517.77	55516.65	57395.94	45655.61
20.0	53214.39	52148.72	50491.23	50676.14	50655.09	50592.53	49996.02	47441.76
30.0	47917.03	44188.14	42917.92	43158.07	43156.43	43161.69	43209.91	43005.70
40.0	41076.68	33993.50	33724.32	33829.30	33910.54	33910.40	33917.58	33994.83
45.0	37257.45	28465.44	28883.25	28836.37	28956.41	28963.33	28974.11	29091.09
50.0	33263.38	22957.16	24066.02	23846.08	23970.14	23998.24	23996.17	24046.08
60.0	24980.90	13034.26	14912.83	14565.40	14529.66	14609.84	14616.85	14618.44
70.0	16585.76	5892.14	6869.67	7040.41	6911.04	6863.96	6895.85	6903.05
80.0	8253.71	1917.76	1568.55	1688.28	1808.05	1849.20	1820.11	1807.73

SS2:

$R_1/h=100.0$ $\nu_{x\phi}=0.3$ $E=60x10^7$ psi

alpa \ L/R_1	0.2	0.5	0.8	1.0	1.2	1.5	1.8	2.0
0.0	114465.19	117361.59	114436.41	114435.70	114425.88	114386.48	123494.80	36264.21
1.0	114537.14	117357.38	114387.95	114394.09	114364.62	114084.08	118723.86	52115.54
5.0	114312.59	116648.29	113525.17	113578.29	113586.81	113788.07	111729.96	76793.23
10.0	112884.95	114205.35	110921.29	111078.96	111035.55	111033.30	114791.88	91311.21
20.0	106428.78	104297.45	100982.46	101352.28	101310.18	101185.05	99992.04	94883.52
30.0	95834.05	88376.28	85835.84	86316.14	86312.87	86323.38	86419.83	86011.41
40.0	82153.35	67987.00	67448.65	67658.59	67821.08	67820.80	67835.16	67989.66
45.0	74514.90	56930.88	57766.49	57672.74	57912.81	57926.66	57948.22	58182.18
50.0	66526.75	45914.32	48132.04	47692.17	47940.28	47996.48	47992.34	48092.16
60.0	49961.80	26068.53	29825.65	29130.79	29059.32	29219.69	29233.71	29236.87
70.0	33171.53	11784.27	13739.34	14080.82	13822.09	13727.92	13791.69	13806.09
80.0	16507.42	3835.51	3137.10	3376.56	3616.09	3698.40	3640.22	3615.46

SS2:

$R_1/h=100.0$ $\nu_{x\phi}=0.3$ $E=90x10^7$ psi

alpa \ L/R_1	0.2	0.5	0.8	1.0	1.2	1.5	1.8	2.0
0.0	171697.78	176042.59	171650.16	171657.42	171680.13	169400.73	180110.95	35639.80
1.0	171805.67	176036.08	171583.58	171591.47	171585.95	171122.03	183084.25	5375.77
5.0	171468.88	174972.34	170286.48	170386.22	170344.84	169898.89	174541.50	76938.69
10.0	169327.41	171307.88	166381.31	166614.63	166549.70	166466.16	166454.00	129979.42
20.0	159643.16	156446.09	151473.45	152028.23	151952.48	151870.48	149223.81	143932.88
30.0	143751.08	132564.50	128753.19	129476.13	129479.88	129500.40	129626.53	128348.83
40.0	123230.05	101980.53	101172.91	101487.98	101728.01	101735.51	101740.42	101484.59
45.0	111772.39	85396.30	86649.62	86509.08	86870.05	86888.45	86931.16	86941.70
50.0	99790.15	68871.54	72197.92	71538.73	71911.65	71996.66	72000.49	72118.61
60.0	74942.68	39102.79	44738.57	43696.17	43588.76	43832.39	43850.70	43853.08
70.0	49757.29	17676.40	20609.00	21121.25	20733.17	20591.84	20687.24	20709.91
80.0	24761.13	5753.27	4705.65	5064.85	5424.15	5547.60	5460.33	5423.17

SS2:

$R_1/h=100.0$ $\nu_{x\phi}=0.3$ $E=120x10^7$ psi

alpa \ L/R_1	0.2	0.5	0.8	1.0	1.2	1.5	1.8	2.0
0.0	228930.38	234723.19	228872.83	228871.41	228851.75	228772.97	246989.59	72528.41
1.0	229074.28	234714.77	228775.91	228788.17	228729.23	228168.16	237447.72	104231.09
5.0	228625.17	233296.58	227050.34	227156.58	227173.63	227576.14	223459.92	153586.45

10.0	225769.89	228410.70	221842.58	222157.92	222071.09	222066.61	229583.75	182622.42
20.0	212857.56	208594.89	201964.92	202704.56	202620.36	202370.11	199984.08	189767.03
30.0	191668.11	176752.56	171671.69	172632.28	172625.73	172646.77	172839.66	172022.81
40.0	164306.70	135974.00	134897.30	135317.19	135642.16	135641.59	135670.31	135979.31
45.0	149029.80	113861.76	115532.98	115345.48	115825.63	115853.32	115896.44	116364.37
50.0	133053.50	91828.64	96264.08	95384.34	95880.55	95992.96	95984.68	96184.33
60.0	99923.60	52137.05	59651.30	58261.59	58118.64	58439.38	58467.41	58473.74
70.0	66343.05	23568.55	27478.67	28161.65	27644.18	27455.84	27583.38	27612.19
80.0	33014.84	7671.03	6274.20	6753.13	7232.19	7396.81	7280.44	7230.93

E.22 Buckling Values of Single Layer Isotropic Conical Shell under Outer Pressure (q_{cr}) with Different Young's modulus

SS2:

R_1/h=100.0 $\nu_{x\phi}$=0.3 E=30x10^6 psi

alpa \ L/R_1	0.2	0.5	0.8	1.0	1.2	1.5	1.8	2.0
0.0	2848.37	739.19	452.84	365.49	307.17	252.06	215.49	28.52
1.0	2842.42	734.34	448.48	360.23	302.44	245.54	194.76	85.54
5.0	2809.55	712.45	428.66	339.24	284.61	225.44	184.15	149.66
10.0	2749.04	680.19	399.40	313.56	258.73	202.49	163.23	144.27
20.0	2567.63	601.66	338.65	262.49	210.20	161.34	128.59	108.92
30.0	2315.08	509.64	276.00	208.81	165.80	123.58	96.59	84.50
40.0	2004.18	411.32	214.06	159.05	124.44	91.15	70.30	60.26
45.0	1831.04	362.07	184.45	135.99	105.22	76.51	58.64	50.00
50.0	1648.30	313.56	156.32	113.56	87.26	63.02	48.03	40.84
60.0	1260.09	218.89	103.33	73.71	55.99	39.81	29.93	25.28
70.0	850.43	134.31	58.75	40.75	30.34	21.11	15.62	13.10
80.0	428.11	62.02	24.10	15.70	11.21	7.49	5.40	4.47

SS2:

R_1/h=100.0 $\nu_{x\phi}$=0.3 E=30x10^7 psi

alpa \ L/R_1	0.2	0.5	0.8	1.0	1.2	1.5	1.8	2.0
0.0	28483.67	7391.87	4528.42	3655.07	3070.27	2524.08	2281.80	308.46
1.0	28424.16	7343.40	4484.95	3601.69	3024.98	2454.73	2039.34	1237.87
5.0	28095.53	7124.52	4286.67	3392.33	2845.98	2250.50	1753.58	1586.73
10.0	27490.40	6801.87	3993.95	3135.61	2587.66	2027.68	1658.29	1317.91
20.0	25676.33	6016.63	3386.49	2624.93	2101.92	1614.32	1290.85	1145.91
30.0	23150.77	5096.40	2759.96	2087.99	1658.08	1236.49	971.25	836.52
40.0	20041.75	4113.16	2140.66	1590.47	1244.46	911.32	703.12	603.45
45.0	18310.40	3620.71	1844.55	1359.88	1052.20	765.15	586.26	499.30
50.0	16483.03	3135.59	1563.18	1135.63	872.56	630.15	480.24	409.61
60.0	12600.88	2188.92	1033.35	737.10	559.94	398.16	299.20	252.73
70.0	8504.31	1343.12	587.55	407.49	303.42	211.11	156.22	130.94
80.0	4281.08	620.18	240.95	156.98	112.11	74.90	53.99	44.68

SS2:

R_1/h=100.0 $\nu_{x\phi}$=0.3 E=60x10^7 psi

alpa \ L/R_1	0.2	0.5	0.8	1.0	1.2	1.5	1.8	2.0
0.0	56967.33	14783.74	9056.83	7310.14	6140.53	5048.16	4563.59	616.92
1.0	56848.32	14686.79	8969.90	7203.38	6049.97	4909.46	4078.67	2475.74
5.0	56191.07	14249.04	8573.34	6784.66	5691.96	4500.99	3507.15	3173.45
10.0	54980.81	13603.75	7987.90	6271.23	5175.31	4055.36	3316.57	2635.82
20.0	51352.66	12033.27	6772.97	5249.87	4203.84	3228.64	2581.70	2291.81
30.0	46301.53	10192.81	5519.92	4175.98	3316.15	2472.98	1942.49	1673.04
40.0	40083.50	8226.32	4281.32	3180.93	2488.92	1822.63	1406.23	1206.89

45.0	36620.80	7241.42	3689.10	2719.75	2104.40	1530.29	1172.53	998.61
50.0	32966.05	6271.19	3126.36	2271.27	1745.12	1260.31	960.47	819.23
60.0	25201.75	4377.84	2066.69	1474.20	1119.87	796.33	598.41	505.47
70.0	17008.63	2686.24	1175.10	814.99	606.83	422.22	312.45	261.87
80.0	8562.15	1240.36	481.91	313.95	224.21	149.80	107.99	89.37

SS2:

$R_1/h=100.0$ $\nu_{x\phi}=0.3$ $E=90x10^7$ psi

alpa \ L/R_1	0.2	0.5	0.8	1.0	1.2	1.5	1.8	2.0
0.0	85451.01	22175.62	13585.30	10964.90	9212.04	7582.65	6845.00	769.91
1.0	85272.49	22030.23	13454.87	10805.88	9072.78	7378.48	6069.93	1282.71
5.0	84286.60	21373.55	12859.97	10176.93	8538.67	6756.17	5190.19	4544.62
10.0	82471.22	20405.61	11982.04	9406.84	7761.75	6099.30	4991.37	4194.84
20.0	77028.99	18049.91	10159.49	7874.43	6304.99	4847.11	3857.75	3401.03
30.0	69452.30	15289.22	8279.83	6264.07	4974.25	3709.47	2898.76	2534.77
40.0	60125.26	12339.48	6421.94	4771.45	3733.40	2733.93	2111.63	1810.33
45.0	54931.20	10862.12	5533.64	4079.63	3156.45	2295.43	1760.65	1505.16
50.0	49449.09	9406.77	4689.57	3406.88	2617.63	1890.30	1441.34	1227.47
60.0	37802.62	6566.76	3100.04	2211.30	1679.82	1194.46	897.70	758.61
70.0	25512.94	4029.37	1762.65	1222.47	910.26	633.31	468.67	392.85
80.0	12843.23	1860.54	722.87	470.93	336.32	224.71	161.98	134.05

SS2:

$R_1/h=100.0$ $\nu_{x\phi}=0.3$ $E=120x10^7$ psi

alpa \ L/R_1	0.2	0.5	0.8	1.0	1.2	1.5	1.8	2.0
0.0	113934.66	29567.48	18113.66	14620.27	12281.06	10096.32	9127.18	1233.83
1.0	113696.65	29373.58	17939.80	14406.75	12099.93	9818.93	8157.35	4951.48
5.0	112382.13	28498.09	17146.68	13569.32	11383.92	9001.99	7014.31	6346.91
10.0	109961.62	27207.50	15975.80	12542.46	10350.62	8110.72	6633.15	5271.64
20.0	102705.32	24066.54	13545.95	10499.74	8407.68	6457.28	5163.41	4583.62
30.0	92603.06	20385.61	11039.84	8351.96	6632.31	4945.96	3884.99	3346.09
40.0	80167.01	16452.64	8562.63	6361.87	4977.84	3645.27	2812.47	2413.79
45.0	73241.59	14482.83	7378.19	5439.50	4208.80	3060.58	2345.05	1997.21
50.0	65932.11	12542.37	6252.72	4542.53	3490.25	2520.62	1920.94	1638.46
60.0	50403.50	8755.68	4133.39	2948.39	2239.75	1592.66	1196.81	1010.94
70.0	34017.25	5372.49	2350.20	1629.97	1213.67	844.43	624.89	523.75
80.0	17124.31	2480.72	963.82	627.90	448.43	299.61	215.97	178.74

E.23 Buckling Values of Single Layer Isotropic Conical Shell in Pure Bending (M_{cr}) with Different Young's modulus

SS2:

$R_1/h=100.0$ $\nu_{x\phi}=0.3$ $E=30x10^6$ psi

alpa \ L/R_1	0.2	0.5	0.8	1.0	1.2	1.5	1.8	2.0
0.0	2893.20	1365.81	1457.97	175.06	30.11	19.24	135.33	0.07
1.0	2900.06	1375.34	1429.76	187.05	31.89	19.23	174.04	0.16
5.0	2914.88	1408.23	1314.99	242.80	39.80	19.49	212.85	0.19
10.0	2903.96	1435.56	1189.33	332.62	51.51	20.09	224.38	0.45
20.0	2785.61	1438.81	1007.60	608.81	85.12	21.03	67.39	146.90
30.0	2549.46	1365.91	869.27	959.48	148.79	23.88	227.60	50.84
40.0	2217.83	1211.12	738.93	1004.18	302.56	32.73	13.43	155.49
45.0	2024.90	1102.43	671.80	712.38	449.57	42.00	12.72	9.78
50.0	1818.72	973.53	601.92	555.69	592.19	59.62	13.64	8.41
60.0	1379.76	665.97	451.15	370.12	375.58	176.66	24.15	9.98
70.0	922.88	348.34	282.08	228.96	196.52	191.53	111.93	33.69

80.0	461.33	122.91	99.21	92.20	81.83	68.69	60.45	57.07

SS2:
$R_1/h=100.0$ $\nu_{x\phi}=0.3$ $E=30x10^7$ psi

alpa \ L/R_1	0.2	0.5	0.8	1.0	1.2	1.5	1.8	2.0
0.0	28932.02	13658.08	14579.61	1750.63	301.04	192.17	1350.60	0.94
1.0	29000.63	13753.47	14297.50	1870.67	318.67	192.22	1736.06	0.91
5.0	29148.81	14082.25	13149.79	2427.96	397.93	194.85	2127.34	1.72
10.0	29039.63	14355.63	11893.41	3326.07	515.15	200.95	2242.54	4.45
20.0	27856.06	14388.08	10076.00	6087.75	851.08	210.24	674.74	1468.98
30.0	25494.65	13659.06	8692.67	9594.95	1487.85	238.66	2275.79	509.97
40.0	22178.29	12111.18	7389.31	10041.82	3025.71	327.37	134.43	1554.64
45.0	20249.00	11024.26	6718.02	7123.79	4495.79	419.95	127.35	97.67
50.0	18187.15	9735.25	6019.23	5556.93	5921.92	596.24	136.43	84.08
60.0	13797.57	6659.67	4511.55	3701.18	3755.79	1766.52	241.46	99.77
70.0	9228.76	3483.37	2820.84	2289.64	1965.24	1915.28	1119.27	336.87
80.0	4613.32	1229.06	992.08	922.05	818.33	686.88	604.46	570.65

SS2:
$R_1/h=100.0$ $\nu_{x\phi}=0.3$ $E=60x10^7$ psi

alpa \ L/R_1	0.2	0.5	0.8	1.0	1.2	1.5	1.8	2.0
0.0	57864.04	27316.17	29159.23	3501.26	602.09	384.33	2701.20	1.88
1.0	58001.27	27506.94	28595.01	3741.35	637.34	384.43	3472.12	1.82
5.0	58297.62	28164.50	26299.57	4855.92	795.87	389.69	4254.67	3.43
10.0	58079.25	28711.25	23786.81	6652.14	1030.31	401.90	4485.08	8.90
20.0	55712.13	28776.16	20152.01	12175.50	1702.15	420.48	1349.49	2937.96
30.0	50989.30	27318.11	17385.33	19189.90	2975.70	477.32	4551.59	1019.93
40.0	44356.57	24222.35	14778.61	20083.64	6051.43	654.74	268.86	3109.29
45.0	40498.00	22048.53	13436.03	14247.57	8991.57	839.90	254.70	195.34
50.0	36374.30	19470.51	12038.45	11113.85	11843.84	1192.47	272.86	168.17
60.0	27595.15	13319.34	9023.09	7402.35	7511.58	3533.04	482.92	199.54
70.0	18457.53	6966.75	5641.68	4579.28	3930.48	3830.57	2238.54	673.73
80.0	9226.64	2458.11	1984.16	1844.09	1636.66	1373.77	1208.92	1141.31

SS2:
$R_1/h=100.0$ $\nu_{x\phi}=0.3$ $E=90x10^7$ psi

alpa \ L/R_1	0.2	0.5	0.8	1.0	1.2	1.5	1.8	2.0
0.0	86796.06	40974.22	43738.85	5251.59	903.03	576.51	4066.12	2.61
1.0	87001.87	41260.41	42892.41	5612.03	956.64	576.79	5215.02	2.05
5.0	87446.41	42246.71	39449.56	7283.27	1193.83	585.69	6380.65	6.13
10.0	87118.88	43066.82	35680.17	9978.77	1545.20	602.85	6731.52	13.31
20.0	83568.16	43164.20	30227.81	18263.44	2553.27	631.03	2021.98	4400.90
30.0	76483.95	40977.21	26078.04	28783.65	4463.78	715.95	6827.85	1521.07
40.0	66534.86	36333.50	22167.92	30125.44	9076.82	981.70	402.86	4668.31
45.0	60747.01	33072.80	20154.07	21371.36	13488.00	1259.85	382.37	292.96
50.0	54561.46	29205.76	18057.71	16670.81	17766.62	1788.60	409.29	252.30
60.0	41392.73	19979.00	13534.64	11103.53	11267.30	5299.63	724.37	299.47
70.0	27686.29	10450.12	8462.52	6868.91	5895.72	5745.84	3357.80	1010.66
80.0	13839.96	3687.17	2976.24	2766.14	2454.99	2060.66	1813.38	1711.95

SS2:
$R_1/h=100.0$ $\nu_{x\phi}=0.3$ $E=120x10^7$ psi

alpa \ L/R_1	0.2	0.5	0.8	1.0	1.2	1.5	1.8	2.0
0.0	115728.08	54632.34	58318.45	7002.51	1204.17	768.66	5402.41	3.75
1.0	116002.54	55013.88	57190.02	7482.70	1274.69	768.86	6944.24	3.65
5.0	116595.24	56328.99	52599.14	9711.85	1591.74	779.38	8509.35	6.87

10.0	116158.50	57422.51	47573.62	13304.29	2060.62	803.81	8970.15	17.80
20.0	111424.25	57552.33	40304.02	24351.01	3404.31	840.97	2698.98	5875.92
30.0	101978.61	54636.22	34770.66	38379.80	5951.40	954.63	9103.18	2039.87
40.0	88713.15	48444.70	29557.23	40167.28	12102.85	1309.47	537.72	6218.57
45.0	80996.00	44097.05	26872.06	28495.15	17983.14	1679.79	509.40	390.69
50.0	72748.61	38941.02	24076.90	22227.70	23687.68	2384.95	545.73	336.33
60.0	55190.29	26638.67	18046.19	14804.71	15023.16	7066.08	965.85	399.09
70.0	36915.06	13933.50	11283.37	9158.55	7860.97	7661.14	4477.09	1347.47
80.0	18453.28	4916.23	3968.32	3688.18	3273.32	2747.54	2417.84	2282.61

E-24 Buckling Values of Single Layer Isotropic Conical Shell under Axial Compression to Decide Circumferential wave number n and Critical Value (P_{cr})

SS4:

R_1/h=100.0 $\nu_{x\phi}$=0.3 E=30x10^6 psi alpa=30 ° L/R_1=0.5

n= 0	9051.51
n= 1	9063.76
n= 2	9100.89
n= 3	9154.57
n= 4	9014.10
n= 5	8812.92
n= 6	8648.79
n= 7	8561.41
n= 8	8585.75
n= 9	8747.12
n=10	9060.05
n=11	9544.86
n=12	10221.47

E.25 Buckling Values of Single Layer Isotropic Conical Shell under Outer Pressure To Decide Circumferential wave number n and Critical Value (q_{cr})

SS1:

R_1/h=100.0 $\nu_{x\phi}$=0.3 E=30x10^6 psi alpa=30 ° L/R_1=0.2

n= 4	12308.01
n= 5	8460.25
n= 6	6282.47
n= 7	4957.64
n= 8	4103.99
n= 9	3530.16
n=10	3133.01
n=11	2853.27
n=12	2655.05
n=13	2515.59
n=14	2419.93
n=15	2357.88
n=16	2322.32
n=17	2308.17
n=18	2311.70
n=19	2330.11
n=20	2361.32
n=21	2403.68
n=22	2455.94
n=23	2517.10

n=24	2586.36
n=25	2663.08
n=26	2746.73
n=27	2836.89
n=28	2933.20

E.26 Buckling Values of Single Layer Isotropic Conical Shell under Axial Compression (P_{cr}) with same $R_1/h=100$ ratio of different radius R_1.

SS2:
R_1=1.0 in. h=0.010 in. R_1/h=100.0 $\nu_{x\phi}$=0.3 E=30x10^6 psi

alpa \ L/R_1	0.2	0.5	0.8	1.0
0.0	5723.26	5868.08	5721.70	5721.64
1.0	5726.86	5867.87	5719.45	5720.48
5.0	5715.63	5832.42	5676.29	5680.21
10.0	5644.25	5710.26	5546.10	5553.64
20.0	5321.44	5214.88	5049.08	5067.57
30.0	4791.70	4418.81	4291.79	4315.75
40.0	4107.67	3399.35	3372.43	3382.95
45.0	3725.75	2846.55	2888.32	2883.64
50.0	3326.34	2295.72	2406.59	2384.62
60.0	2498.09	1303.43	1491.28	1456.54
70.0	1658.58	589.21	686.97	704.04
80.0	825.37	191.78	156.85	168.83

SS2:
R_1=0.8 in. h=0.0080 in. R_1/h=100.0 $\nu_{x\phi}$=0.3 E=30x10^6 psi

alpa \ L/R_1	0.2	0.5	0.8	1.0
0.0	3172.40	3651.29	3661.76	3661.09
1.0	3172.39	3650.68	3660.78	3661.02
5.0	3154.77	3627.02	3634.99	3632.96
10.0	3094.11	3550.64	3554.45	3552.07
20.0	2856.05	3252.82	3243.27	3242.21
30.0	2494.20	2792.52	2762.09	2762.39
40.0	2056.50	2216.13	2165.09	2170.22
45.0	1824.83	1899.47	1845.52	1853.44
50.0	1592.15	1572.09	1526.14	1535.04
60.0	1141.10	923.59	932.18	931.00
70.0	726.33	395.54	450.59	440.86
80.0	350.81	103.79	108.05	116.88

SS2:
R_1=0.6 in. h=0.0060 in. R_1/h=100.0 $\nu_{x\phi}$=0.3 E=30x10^6 psi

alpa \ L/R_1	0.2	0.5	0.8	1.0
0.0	1877.11	2061.02	2057.10	2053.49
1.0	1875.09	2060.30	2059.77	1997.39
5.0	1854.50	2045.08	2041.86	2043.71
10.0	1801.63	1998.60	1998.22	2009.27
20.0	1615.46	1820.05	1824.15	1828.89
30.0	1349.04	1546.46	1554.08	1553.38
40.0	1043.59	1212.93	1220.72	1221.29
45.0	889.87	1037.21	1042.52	1042.60
50.0	742.10	862.80	863.84	864.04
60.0	479.23	534.71	524.76	526.15

70.0	272.86	250.18	247.18	247.79
80.0	120.24	56.94	66.42	66.00

SS2:

R_1=0.4 in. h=0.0040 in. R_1/h=100.0 $\nu_{x\phi}$=0.3 E=30x10^6 psi

alpa \ L/R_1	0.2	0.5	0.8	1.0
0.0	938.90	914.96	128.61	0.05
1.0	938.86	914.69	162.60	0.29
5.0	933.19	908.50	626.78	0.00
10.0	913.64	888.34	716.97	0.00
20.0	834.38	810.38	753.06	0.00
30.0	707.01	690.50	689.07	136.43
40.0	543.90	542.55	543.43	477.59
45.0	455.45	463.36	463.94	438.42
50.0	367.32	383.76	384.65	383.55
60.0	208.55	232.75	233.87	233.50
70.0	94.27	110.21	110.45	110.43
80.0	30.68	29.22	28.92	28.91

E.27 Check Convergence of Buckling Value and Ratio of Single Isotropic Conical Shell under Axial Compression (P_{cr}) and ratio ($P_{cr}/P_{classical}$)

SS1:

R_1/h=100.0 $\nu_{x\phi}$=0.3 E=30x10^6 psi

alpa=30 ° R_1=1 in. L/R_1=1.0

m= 8	P=12438.393554688	P/Pcl= 1.453728506942
m= 9	P= 4042.139892578	P/Pcl= 0.472422259760
m=10	P=10553.707031250	P/Pcl= 1.233457093779
m=11	P= 1865.910766602	P/Pcl= 0.218077009776
m=12	P= 1039.457641602	P/Pcl= 0.121485881494
m=13	P= 7245.083984375	P/Pcl= 0.846764099959
m=14	P= 1802.084716797	P/Pcl= 0.210617385052
m=15	P= 804.417785645	P/Pcl= 0.094015763478
m=16	P= 4320.635253906	P/Pcl= 0.504971209432
m=17	P= 423.044281006	P/Pcl= 0.049443003093
m=18	P= 4251.342773438	P/Pcl= 0.496872699465
m=19	P= 4871.424316406	P/Pcl= 0.569344294103
m=20	P= 4238.031738281	P/Pcl= 0.495316981584
m=21	P= 4067.008789063	P/Pcl= 0.475328794563
m=22	P= 4285.567871094	P/Pcl= 0.500872733706
m=23	P= 4245.341796875	P/Pcl= 0.496171339546
m=24	P= 4281.925781250	P/Pcl= 0.500447067014
m=25	P= 4287.156250000	P/Pcl= 0.501058374374
m=26	P= 4280.682128906	P/Pcl= 0.500301716021
m=27	P= 4281.925781250	P/Pcl= 0.500447067014
m=28	P= 4280.683593750	P/Pcl= 0.500301887223
m=29	P= 4280.682128906	P/Pcl= 0.500301716021
m=30	P= 4280.683593750	P/Pcl= 0.500301887223
m=31	P= 4280.683593750	P/Pcl= 0.500301887223
m=32	P= 4280.683593750	P/Pcl= 0.500301887223
m=33	P= 4280.683593750	P/Pcl= 0.500301887223
m=34	P= 4280.683593750	P/Pcl= 0.500301887223
m=35	P= 4280.683593750	P/Pcl= 0.500301887223

E.28 Buckling Ratio of Single Layer Isotropic Conical Shell under Axial Compression ($P_{cr}/P_{classical}$) Compare with Existing Data

SS1:

$R_1/h=100.0$ $\nu_{x\phi}=0.3$ $E=30x10^6$ psi

					Ref. [31]	
alpa \ L/R_1	0.2	0.5	0.8	1.0	0.2	0.5
0.0	0.4991 (0)	0.5130 (0)	0.4992 (0)	0.5000 (0)	/	/
1.0	0.4994 (0)	0.5131 (0)	0.5000 (0)	0.4996 (0)	0.5032 (0)	0.5131 (0)
5.0	0.5020 (0)	0.5137 (0)	0.4998 (0)	0.5000 (0)	0.5057 (0)	0.5142 (0)
10.0	0.5073 (0)	0.5146 (0)	0.4996 (0)	0.5001 (0)	0.5106 (0)	0.5151 (0)
20.0	0.5252 (0)	0.5158 (0)	0.4987 (0)	0.5006 (0)	0.5280 (0)	0.5163 (0)
30.0	0.5567 (0)	0.5139 (0)	0.4979 (0)	0.5003 (0)	0.5616 (0)	0.5140 (0)
40.0	0.6097 (0)	0.5040 (0)	0.4985 (0)	0.4996 (0)	/	/
45.0	0.6490 (0)	0.4944 (0)	0.5003 (0)	0.4988 (0)	0.6491 (0)	0.4947 (0)
50.0	0.7011 (0)	0.4813 (0)	0.5037 (0)	0.4981 (0)	/	/
60.0	0.8701 (0)	0.4486 (0)	0.5142 (0)	0.5005 (0)	0.8715 (0)	0.4486 (0)
70.0	1.2345 (0)	0.4303 (0)	0.5022 (0)	0.5147 (0)	1.2346 (0)	0.4303 (0)
80.0	2.3833 (0)	0.5407 (0)	0.4341 (0)	0.4672 (0)	2.3832 (0)	0.5405 (0)

SS2:

$R_1/h=100.0$ $\nu_{x\phi}=0.3$ $E=30x10^6$ psi

					Ref. [31]	
alpa \ L/R_1	0.2	0.5	0.8	1.0	0.2	0.5
0.0	0.5017 (1)	0.5144 (1)	0.5015 (1)	0.5015 (1)	/	/
1.0	0.5021 (1)	0.5145 (1)	0.5015 (1)	0.5016 (1)	0.5081 (1)	0.5147 (1)
5.0	0.5048 (1)	0.5152 (1)	0.5014 (1)	0.5017 (1)	0.5098 (1)	0.5163 (1)
10.0	0.5101 (1)	0.5161 (1)	0.5013 (1)	0.5019 (1)	0.5102 (1)	0.5163 (1)
20.0	0.5282 (1)	0.5177 (1)	0.5012 (1)	0.5030 (1)	0.5284 (1)	0.5179 (1)
30.0	0.5600 (1)	0.5164 (1)	0.5016 (1)	0.5044 (1)	0.5604 (1)	0.5166 (1)
40.0	0.6136 (1)	0.5078 (1)	0.5037 (1)	0.5053 (1)	/	/
45.0	0.6532 (1)	0.4990 (1)	0.5064 (1)	0.5055 (1)	0.6534 (1)	0.4992 (1)
50.0	0.7057 (1)	0.4870 (1)	0.5106 (1)	0.5059 (1)	/	/
60.0	0.8759 (1)	0.4570 (1)	0.5229 (1)	0.5107 (1)	0.8759 (1)	0.4596 (1)
70.0	1.2428 (1)	0.4415 (1)	0.5148 (1)	0.5276 (1)	1.2428 (1)	0.4423 (1)
80.0	2.3993 (1)	0.5575 (1)	0.4560 (1)	0.4908 (1)	2.3997 (1)	0.5572 (1)

SS3:

$R_1/h=100.0$ $\nu_{x\phi}=0.3$ $E=30x10^6$ psi

					Ref. [31]	
alpa \ L/R_1	0.2	0.5	0.8	1.0	0.2	0.5
0.0	0.4991 (0)	0.5130 (0)	0.4992 (0)	0.5000 (0)	/	/
1.0	0.4994 (0)	0.5131 (0)	0.5000 (0)	0.4996 (0)	0.5032 (0)	0.5131 (0)
5.0	0.5020 (0)	0.5137 (0)	0.4998 (0)	0.5000 (0)	0.5057 (0)	0.5142 (0)
10.0	0.5073 (0)	0.5146 (0)	0.4996 (0)	0.5001 (0)	0.5106 (0)	0.5151 (0)
20.0	0.5252 (0)	0.5158 (0)	0.4987 (0)	0.5006 (0)	0.5280 (0)	0.5163 (0)
30.0	0.5567 (0)	0.5139 (0)	0.4979 (0)	0.5003 (0)	0.5616 (0)	0.5140 (0)
40.0	0.6097 (0)	0.5040 (0)	0.4985 (0)	0.4996 (0)	/	/
45.0	0.6490 (0)	0.4944 (0)	0.5003 (0)	0.4988 (0)	0.6491 (0)	0.4947 (0)
50.0	0.7011 (0)	0.4813 (0)	0.5037 (0)	0.4981 (0)	/	/
60.0	0.8701 (0)	0.4486 (0)	0.5142 (0)	0.5005 (0)	0.8715 (0)	0.4486 (0)
70.0	1.2345 (0)	0.4303 (0)	0.5022 (0)	0.5147 (0)	1.2346 (0)	0.4303 (0)
80.0	2.3833 (0)	0.5407 (0)	0.4341 (0)	0.4672 (0)	2.3832 (0)	0.5405 (0)

SS4:

$R_1/h=100.0$ $\nu_{x\phi}=0.3$ $E=30x10^6$ psi

					Ref. [31]	
alpa \ L/R_1	0.2	0.5	0.8	1.0	0.2	0.5
0.0	1.0052 (7)	1.0023 (8)	1.0008 (6)	1.0003 (6)	/	/
1.0	1.0053 (7)	1.0023 (8)	1.0007 (6)	1.0002 (6)	1.0051 (7)	1.0020 (8)

5.0	1.0059 (7)	1.0021 (8)	1.0006 (6)	1.0001 (6)	1.0057 (7)	1.0018 (8)
10.0	1.0073 (7)	1.0014 (8)	1.0011 (6)	1.0009 (6)	1.0071 (7)	1.0012 (8)
20.0	1.0100 (6)	1.0002 (8)	1.0008 (4)	0.9998 (8)	1.0097 (6)	1.0000 (8)
30.0	1.0172 (5)	1.0006 (7)	1.0000 (8)	0.9997 (7)	1.0171 (5)	1.0006 (7)
40.0	1.0305 (4)	1.0002 (6)	0.9995 (7)	1.0005 (5)	/	/
45.0	1.0414 (2)	1.0004 (5)	0.9992 (6)	1.0002 (4)	1.0415 (2)	1.0110 (5)
50.0	1.0570 (0)	1.0003 (4)	1.0005 (5)	0.9991 (0)	/	/
60.0	1.1442 (0)	1.0092 (0)	1.0062 (7)	0.9981 (5)	1.1443 (0)	1.0032 (5)
70.0	1.4207 (0)	1.0170 (5)	0.9993 (4)	1.0084 (6)	1.4207 (0)	1.1015 (5)
80.0	2.4774 (0)	1.0149 (3)	1.0281 (4)	0.9947 (0)	2.4774 (0)	1.0111 (3)

APPENDIX F

PROCEDURE FOR BUCKLING ANALYSIS

The steps are from reference [3].

Step 1: Build the model

Specify the jobname and analysis title and then use PREP7 to define the element types, element real constants, material properties, and the model geometry.

Points to Remember

- Only linear behavior is valid.
- Young's modulus(EX) (or stiffness in some form) must be defined

Step 2: Obtain the static solution:

The procedure to obtain a static solution with the following exceptions:

- Prestress effect [**PSTRES**] must be activated.
- Unit load are usually sufficient (that is, actual load values need not be specified). All loads are scaled. (Also, the maximum permissible eigenvalue is 1,000,000 - you must use larger applied loads if your eigenvalue exceeds this limit.)
- You can apply a non-zero constraint in the prestressing pass as the static load. The eigenvalues found in the buckling solution will be the load factors applied to these non-zero constraint values.
- At end of the solution, leave SOLUTION [**FINISH**]

Step 3: Obtain the eigenvalue buckling solution

This step requires files Jobname.EMAT and Jobname.ESAV from the static analysis. The following tasks are involved in obtaining the eigenvalue buckling solution:

1. Enter the ANSYS solution processor.

   GUI Path: **Main Menu>Solution**

2. Define the analysis type and analysis options.

   Option: New Analysis [**ANTYPE**]

   Choose New Analysis. Restarts are not valid in an eigenvalue buckling analysis.

   Option: Analysis Type: Eigen Buckling [**ANTYPE**]

   Choose Eigen Buckling analysis type.

   Option: Eigenvalue Extraction Method [**BUCOPT**]

   Choose one of the following solution methods. The space iteration method is generally recommended for eigenvalue buckling because it uses the full system matrices. (If you choose the reduced method, you will need to define master degrees of freedom before initiating the solution.)

- Reduced (Householder) method
- Subspace iteration method

   Option: Number of Eigenvalues to be Extracted [**BUCOPT**]

   Default to one, which is usually sufficient for eigenvalue buckling.

   Option: Shift Point for Eigenvalues Calculation [**BUCOPT**]

   This option represents the point (load factor) about which eigenvalues are calculated. The shift point is helpful when numerical problems are encountered (due to negative eigenvalues, for example). Defaults to 0.0.

Option: Number of Reduced Eigenvectors to Print [**BUCOPT**]

This option is valid only for the reduced method. This option allows you to get a listing of the reduced eigenvectors (buckled mode shapes) on the printed output file (Jobname.OUT).

3. Specify load step options.

The only load step options valid for eigenvalue buckling are expansion pass options and output controls. Expansion pass option are explained next in step 4. You can request buckled mode shapes from the reduced method to be included in the printed output. No other output control is applicable.

GUI Path: Main Menu>Solution>-Load Step Opts- Output Ctrls>Solu Printout

4. Save a back-up copy of the database to a named file.

GUI Path: Utility Menu>File>Save As

5. Start solution calculations.

GUI: Main Menu>Solution>-Solve-Current LS

The output from the solution mainly consists of the eigenvalues, which are printed as part of the printed output (Jobname.OUT). The eigenvalues represent the buckling load factors; if unit load were applied in the static analysis, they are the buckling loads. No buckling mode shapes are written to the data base or the result file, so you cannot postprocess the results yet. To do this, you need to expand the solution (explained next).

Sometimes you may see both positive and negative eigenvalues calculated. Negative eigenvalues indicate that buckling occurs when the loads are applied in an opposite sense.

6. Leave the SOLUTION processor.

GUI: Close the Solution menu.

Step 4. Expand the solution.

To review the buckled mode shape(s), the solution must be expanded regardless of which eigenvalue extraction method is used. In the case of the subspace iteration method, which uses full system matrices, you may think of "expansion" to simple mean writing buckled mode shapes to the results file.

Step 5. Review the results.

Results from a buckling expansion pass are written to the structural results file, Jobname.RST. They consist of buckling load factors, buckling mode shapes, and relative stress distributions in POST1, the general postprocessor. To review results in POST1, the database must contain the same model for which the buckling solution was calculated (issue **RESUME** if necessary). Also, the results file (Jobname.RST) from the expansion pass must be available.

1. List all buckling load factors.

GUI: Main Menu>General Postproc>Results Summary

2. Read in data for the desired mode to display buckling mode shapes. (Each mode is stored on the results file as a separate substep.)

GUI: Main Menu>General Postproc>-Read Results-loadstep

3. Display the mode shape.

GUI: Main Menu>General Postproc>Plot Results>Deformed Shape

4. Contour the relative stress distributions.

GUI: Main Menu>General Postproc>Plot Results>-Contour Plot-Nodal Solution or

Main Menu>General Postproc>Plot Results>-Contour Plot-Element Solution

REFERENCES

[1] B. D. Agarwal and L. J. *Broutman, Analysis and Performanced of Fiber Composites*, John Wiley & Sons, 1980.

[2] *ANSYS Elements Reference*. 000853. Ninth Edition. SAS IP, Inc.

[3] *ANSYS Structural Analysis Guide*. 000857. 3rd Edition. SAS IP

[4] *ANSYS Theory Reference*. 000855. Eighth Edition. SAS IP

[5] M. Baruch and O. Harari and J. Singer, "Low buckling loads of axially compressed conical shells," Journal of Applied Mechanics, pp. 384-392, June 1970.

[6] D. O. Brush and B. O. Almroth, *Buckling of Bars, Plates, and Shells*, McGraw-Hill, New York, 1975.

[7] Chin-Hao Chang and Lester Katz, "Buckling of axially compressed conical shells," Journal of The Engineering Mechanics Division, Proceedings of American Society of Civil Engineers, vol. 106, No. EM3, pp. 501-516, June 1980.

[8] Stewart Cowley, *Space Flight*, A Gateway Fact Book Warwick Press, New York, 1983.

[9] L. H. Donnell, "A new theory for the buckling of thin cylinders under axial compression and bending," Trans. ASME vol.17 No.1, pp. 795-806, 1934.

[10] L. H. Donnell, *Beams, Plates, and Shells*, McGraw-Hill, New York, 1976.

[11] W. Flügge, *Stresses in Shells*, 2nd ed., Springer, Berlin, 1990.

[12] Robert M. Jones, *Mechanics of Composite Materials*, Scripta Book Company, Washington, D.C. 1975.

[13] W. T. Kotter, "A consistent first approximation in general theory of thin elastic shells, in the theory of thin elastic shells," North-Holland, Amsterdam, pp. 12-33, 1960.

[14] W. T. Kotter, "On the nonlinear theory of thin elastic shells," Proc. K. Ned. Akad, Wet., ser., B69, 1966.

[15] Dinah L. Moché, *The Astronauts*, Random House, New York, 1987.

[16] R. L. Norton, *Machine Design; An Integrated Approach*, Prentice-Hall Inc., Upper Saddle River, New Jersey, 1996.

[17] Robert O. Parmley, *Standard Handbook of Fastening and Joining*, McGraw-Hill, New York, 1977.

[18] J. N. Reddy, *An Introduction to The Finite Element Method*, McGraw-Hill, Inc., New York, 1984.

[19] C. T. F. Ross, *Finite Element Programs For Axisymmetric Programs in Engineering*, John Wiley & Sons, New York, 1984.

[20] J. L. Sanders, "Nonlinear theories for thin shells," Q. Appl., Math., vol. 21, 1, pp. 21-36, 1963.

[21] M. M. Schwartz, *Composite Materials Handbook*, McGraw-Hill, New York, 1984.

[22] P. Seide, "A Donnell-type theory for asymmetrical bending and buckling of thin conical shells," Journal of Applied Mechanics vol. 24, pp. 547-552, 1957.

[23] P. Seide, "Axisymmetrical buckling of circular cones under axial compression," Journal of Applied Mechanics vol. 23, pp. 626-628, 1956.

[24] P. Seide, "Buckling of circular cones under axial compression," Journal of Applied Mechanics, vol. 28, p. 315, 1961.

[25] P. Seide and V. I. Weingarten, "On the buckling of circular cylindrical shells under pure bending," ASME Journal of Applied Mechanics, pp. 112-116, March 1961.

[26] J. Singer, "Donnell-type equations for bending and buckling of orthotropic conical shells," ASME Journal of Applied Mechanics vol. 30, pp. 303-305, 1963.

[27] B. S. K. Sundarasivarao and N. Ganesan, "deformation of varying thickness of conical shells subjected to axisymmetric loading with various end conditions," Engineering Fracture Mechanics, vol. 39, No. 6 pp. 1003-1010, 1991.

[28] S. P. Timoshenko, *Theory of Elastic Stability*, McGraw-Hill, New York, 1961.

[29] Liyong Tong, "Buckling load of composite conical shells under axial compression," Journal of Applied Mechanics, vol 61, pp. 718-719, September, 1994.

[30] Liyong Tong and B. Tabarrok and T. K. Wang, "Bending analysis of orthotropic conical shells," Int. J. Solids Structures, vol.17, No.2, pp. 215-227, 1993.

[31] Liyong Tong and B. Tabarrok and T. K. Wang, "Simple solutions for buckling of orthotropic conical shells," Int. J. Solids Structures vol. 29, No.8, pp. 933-946, 1992.

[32] Liyong Tong and T. K. Wang, "Simple solutions for buckling of laminated conical shells," Int. J. Mech. Sci. vol. 34, No.2, pp. 93-111, 1992.

[33] A. C. Ugural, Buckling of Anisotropic "Cylindrical shells under axial compression and bending," Ph.D. thesis, University of Wisconsin, September, 1966.

[34] A. C. Ugural, *Mechanical Design; An Integrated Approach*, McGraw-Hill (in press), New York, 2002.

[35] A. C. Ugural, *Stresses in plates and shells*, McGraw-Hill, New York, 1999.

[36] A. C. Ugural and S. Cheng, "Buckling of composite cylindrical shells under pure bending," AIAA Journal, vol. 6, No. 2, Feb. pp. 349-354, 1968.

[37] A. C. Ugural and Saul K. Fenster, *Advanced Strength and Applied Elasticity*, third edition, Prentice-Hall, Englewood Cliffs, New Jersey, 1995.